U.S. Department
of Transportation

**National Highway
Traffic Safety
Administration**

Design Requirements and Specifications: Thorax - Abdomen Development Task

Interim Report: Trauma Assessment Device Development Program

Technical Report Documentation Page

1. Report No.	2. Government Accession No.	3. Recipient's Catalog No.
DOT HS 807 511		

4. Title and Subtitle	5. Report Date
DESIGN REQUIREMENTS AND SPECIFICATIONS: THORAX-ABDOMEN DEVELOPMENT TASK. INTERIM REPORT. TRAUMA ASSESSMENT DEVICE DEVELOPMENT PROGRAM	November 1989
	6. Performing Organization Code
7. Author(s)	8. Performing Organization Report No.
L.W. Schneider, A.I. King,* and M.S. Beebe**	UMTRI-89-20
9. Performing Organization Name and Address	10. Work Unit No. (TRAIS)
University of Michigan Transportation Research Institute 2901 Baxter Road Ann Arbor, Michigan 48109-2150	11. Contract or Grant No. DTNH22-83-C-07005
	13. Type of Report and Period Covered
12. Sponsoring Agency Name and Address	SUBTASK 1-2 REPORT
U.S. Department of Transportation National Highway Traffic Safety Administration Washington, D.C. 20590	14. Sponsoring Agency Code

15. Supplementary Notes

*Wayne State University, Detroit, Michigan
**Humanetics, Inc., Carson, California
Mark Haffner, NHTSA COTR

16. Abstract

While the thorax (i.e., ribcage) of the Hybrid III ATD is significantly improved over that of its predecessor, Hybrid II, additional design changes are needed to achieve improved interaction with, and injury assessment from, the variety of restraint/vehicle environments that are encountered in vehicle impact testing. The scope of these modifications includes not only the ribcage and thorax, but also the shoulder, spine, and abdomen components.

In preparation for design and development of new and improved ATD torso components, it was considered important to define the performance requirements and specifications of the new system. This document sets forth design goals and specifications for an improved thorax/spine/shoulder/abdomen system of a frontal impact test dummy and presents the data and rationale upon which these requirements are based. As new biomechanical response and injury data are collected, and as additional analyses of old data increase our understanding of human response and injury tolerance for impact environments, the design requirements set forth in this document may require updating and modification.

17. Key Words	18. Distribution Statement
Anthropomorphic Test Device Dummy Design Thorax Abdomen	Document is available to the public from the National Technical Information Service, Springfield, Virginia 22161

19. Security Classif. (of this report)	20. Security Classif. (of this page)	21. No. of Pages	22. Price
None	None	200	

ACKNOWLEDGEMENTS

The authors would like to express appreciation to Richard Chandler, Roger Daniel, Charles Kroell, John Melvin, Raymond Neathery, Priya Prasad, and David Viano for taking the time to review an earlier draft of this document and for providing written comments and input. The collective experience and insight of these researchers has been most helpful in formulating the design goals and specifications contained in this report.

The authors would also like to acknowledge Dr. John Cavanaugh for collecting and analyzing static regional load-deflection characteristics of the human ribcage and Hybrid III and for the shoulder dissections conducted for the purpose of determining shoulder mass distribution.

Special appreciation and recognition is also given to Leda Ricci for assisting with the literature review and compilation of biomechanical data and for preparing and editing multiple versions of this document.

PREFACE

While the Hybrid III ATD is the most advanced anthropomorphic crash dummy for automotive frontal impact testing, improvements are needed in the biofidelity and injury assessment capability of the thorax and abdomen, particularly with regard to interaction with and injuries from restraint systems. These needed improvements have been the subject of much discussion within automotive industry user groups and at meetings of the SAE Mechanical Human Simulation Subcommittee of the Human Biomechanics Simulation Standards Committee. While near-term modifications to the Hybrid III thorax can and are being made to address these limitations, it is believed that a complete redesign will offer the greater performance benefit and injury assessment potential over the long run.

In preparation for such a design effort, it was considered important to the NHTSA and to the project principals to define the design goals and performance specifications for the new hardware before beginning serious prototype development. This report was prepared to document these requirements and specifications and to provide rationale for them. It addresses both general design objectives such as durability, repeatability, and temperature sensitivity, as well as more specific biomechanical performance requirements, instrumentation needs, and anthropometric specifications. The need to modify and update these design goals and specifications as new biomechanical data become available is expected.

CONTENTS

ACKNOWLEDGEMENTS iii

PREFACE v

LIST OF TABLES xi

LIST OF FIGURES xiii

INTRODUCTION 1

PART A. DESIGN GOALS AND REQUIREMENTS 3

A1.0 Priority of Thorax/Abdomen Use Modes 3

A1.1 Retrofit Subcomponent for Hybrid III 3
A1.2 Subcomponent Test Device 3
A1.3 Component for Future ATDs 4

A2.0 Crash Vectors 4

A3.0 Restraint/Vehicle Environments 4

A3.1 The Unrestrained Front Seat Occupant 5

A3.1.1 Injury Patterns 5
A3.1.2 Loading Patterns 5

A3.2 Occupants Restrained by Two- or Three-Point Belts 7

A3.2.1 Injury Patterns 7
A3.2.2 Loading Patterns 9

A3.3 Airbags and Belt/Bag Combinations 11

A3.3.1 Injury Patterns 11
A3.3.2 Loading Patterns 11

A4.0 Maximum Crash Severity by Restraint/Vehicle Environment 12

A5.0 Injury Assessment Range 13

A6.0 Temperature Sensitivity 17

A6.1 Operating Temperature Range 17
A6.2 Durability Temperature Range 19

A7.0 Durability Requirements 19

A8.0 Repeatability and Reproducibility 20

PART B. DESIGN AND PERFORMANCE SPECIFICATIONS 23

B1.0 Biomechanical Impact Response 23

B1.1 Thoracic Response 24

B1.1.1 Sternal Response to Pendulum Impacts 24
B1.1.2 Kroell Corridors for Restrained-Back Conditions 29
B1.1.3 Skeletal Versus Total Deflection 32
B1.1.4 Kroell Impact Response Characteristics at Other Regions ... 32
B1.1.5 Other Response Data to Pendulum Impacts 38
B1.1.6 Impact into a Steering System 39
B1.1.7 Impact Response to Two- and Three-Point-Belt Loading 44
B1.1.8 Impact Response to Airbag Loading 50
B1.1.9 Impact Response to Large Flat Surfaces 50
B1.1.10 Static Response Data 50
B1.1.11 Other Frontal Impact Response Criteria 62
B1.1.12 Ribcage Coupling 62

B1.2 Abdominal Impact Response 77

B1.2.1 Rigid Bar Impacts 77
B1.2.2 Steering Wheel Impacts 79
B1.2.3 Kroell Impacts to Upper Abdomen 79

B2.0 Instrumentation 79

B2.1 A Review of Thoraco-Abdominal Injury Mechanisms 79

B2.1.1 Injury Mechanisms of the Flail Chest (Rib Fractures) 84
B2.1.2 Mechanisms of Lung Contusion 86
B2.1.3 Mechanisms of Hemothorax and Pneumothorax 86
B2.1.4 Mechanisms of Contusion and Rupture of the Heart and Great Vessels 86
B2.1.5 Mechanisms of Injury to the Liver 86
B2.1.6 Mechanisms of Injury to the Spleen 87
B2.1.7 Mechanisms of Injury to the Kidneys 87
B2.1.8 Mechanisms of Injury to the Intestines 87
B2.1.9 Mechanisms of Injury to the Urogenital Organs 87
B2.1.10 Spinal Injuries 87

B2.2 Thorax/Abdomen Injury Criteria 88
B2.3 Instrumentation for the Thorax and Abdomen 94

B3.0 Anthropometric Specifications 95

B3.1 Thorax/Abdomen 95
B3.2 Ribcage 95
B3.3 Thoracic and Lumbar Spines 101
B3.4 Shoulder Mass and Distribution 101
B3.5 Shoulder Kinematics 104
B3.6 Shoulder Design Criteria 109

PART C. SUMMARY OF KEY DESIGN REQUIREMENTS AND PERFORMANCE SPECIFICATIONS 113

C.1 Primary Priorities 113

C1.1 General Requirements 113
C1.2 Thorax/Abdomen Response Biofidelity 113
C1.3 Shoulder/Spine 114
C1.4 Instrumentation 114
C1.5 Anthropometry 114
C1.6 Repeatability and Durability 115

C.2 Secondary Priorities 115

C2.1 General Requirements 115
C2.2 Response Biofidelity 115
C2.3 Instrumentation 115

REFERENCES 117

APPENDIX A: REVIEW OF HYBRID III ENHANCEMENT NEEDS 125

APPENDIX B: QUASI-STATIC FRONTAL LOADING OF THE THORAX OF HUMAN CADAVERS AND THE HYBRID III DUMMY ... 133

APPENDIX C: FORCE-TIME AND FORCE-DEFLECTION CURVES, Kroell et al. 1971, 1974 151

LIST OF TABLES

		Page
1.	Distribution of Thorax/Abdomen AIS≥3 Injuries and Harm for Unrestrained Drivers and Right-Front Passengers in Frontal Collisions (Haffner 1987)	6
2.	Comparison of Thorax/Abdomen Injuries Before and After Introduction of U.K. Belt-Use Law (Haffner 1987 from Rutherford 1985)	10
3.	UMIVOR Thorax/Abdomen Injuries to Front-Seat Belted Occupants	10
4.	Closing Speed Between the Thorax/Abdomen and Interior Components (Haffner 1987)	13
5.	Chest Compression and External Deflection for Different AIS and Age Values (based on analysis of Kroell data by Neathery et al. 1975)	15
6.	Summary of Elastic, Viscous, and Mass Parameter Values from Melvin et al. (1988a) Modeling of Kroell Data (Impactor mass=23.4 kg or 51.5 lbs)	25
7.	Preliminary Results from GM/WSU Kroell Impact Tests 6.5 cm (3 in) Below the Xiphoid Process On the Midline (Viano, May 1989)	39
8.	Peak Deflection for Quasi-Static Chest Loading with Airbag and Shoulder Belt (Kallieris 1987)	63
9.	Static Load-Deflection Coupling between Regions: Rib Loading (Cavanaugh et al. 1988)	75
10.	Static Load-Deflection Coupling between Regions: Sternum Loading (Cavanaugh et al. 1988)	76
11.	Regional Static Stiffness for 25 mm (1 in) Deflection with 5 cm x 10 cm (2"x4") Loading Surface (Cavanaugh et al. 1988)	76
12.	AATD Idealized Abdominal Impact Response Parameters (Rigid bar impactor, 4 cm by 35 cm, 10.0 kg) (Melvin et al. 1988a)	77
13.	Variables Associated with Injury Criteria (Nusholtz et al. 1988)	82
14.	Impact Mode and Identifying Symbols for Various Thoracic Impact Series (Melvin et al. 1988a)	91
15.	Anthropometric Specifications for Thorax and Abdomen (Schneider et al. 1985 and Robbins 1985)	97
16.	Means and S.D. of Rib Shape and Orientation Measurements (Dansereau and Stokes 1988)	98
17.	Asymmetry of Rib Shape Measurements (Dansereau and Stokes 1988)	99

18. Distribution of Shoulder Mass (Cavanaugh, August 1988) 102

19. Average Mass Distribution of Individual Shoulder Tissues (Cavanaugh, August 1988) 103

LIST OF FIGURES

		Page
1.	Comparison of steering wheel deformations for cadavers and dummies (Begeman 1988)	8
2.	AIS injury rating versus maximum plateau force; AIS injury rating versus normalized chest deflection (Kroell et al. l974)	16
3.	Dummy component-test peak chest accelerations and peak sternal deflections versus temperature (Saul 1984)	18
4.	Force versus total deflection; nominal 23.1-kg (51-lb) striker at various velocities (Kroell et al. 1974)	24
5.	AATD frontal thoracic impact response—loading only (15.2-cm rigid disc, 23.4-kg impact mass) (Melvin et al. 1988a)	26
6.	Apparent initial stiffness of the load-deflection response of the chest to frontal impact with a flat, circular impactor (Melvin et al. 1988a)	27
7.	Plateau force versus impactor velocity for frontal chest impacts with a flat, circular impactor (Melvin et al. 1988a)	28
8.	Composite of Kroell et al. force-time response curves, nominal 19.5-kg (43-lb) and 23.6-kg (52-lb) impactor masses (Kroell et al. 1971)	30
9a.	Force versus total deflection; restrained back experiments 10.43-kg (23–lb) striker at nominal 7.2 ms (16 mph) (Kroell et al. 1974)	31
9b.	Comparison of restrained-back response corridor with corridor from unrestrained data (Kroell et al. 1974)	31
10.	Averaged adjusted skeletal force-deflection corridors for 4.3- and 6.7-m/s impacts (Neathery 1974)	32
11.	Abdominal and thoracic impact areas for new Kroell tests conducted at Wayne State University for GM (Viano and Lau 1988).	33
12.	Results from 6.7 m/s Kroell frontal impact tests to sternum. Data reanalyzed by Viano and Lau (1988)	34
13.	Results for Kroell-type impacts at 6.7 m/s to *lateral thorax*, 60°-to-frontal (Viano and Lau 1988)	35
14.	Results for Kroell-type impacts at 6.7 m/s to *lateral abdomen*, 60°-to-frontal, 15.3 cm (6 in) below sternum (Viano and Lau 1988)	36
15.	Initial stiffness and plateau force for 6.7 m/s Kroell-type impacts to different regions of the thorax (Viano and Lau 1988)	37

16. F-δ corridors for 6.7 m/s tests at the sternum and lateral thorax at the level of the xiphoid process (Kroell data reanalyzed by Viano and Lau 1988) 38

17. Response for low-mass impactor resulting in lower total deflections (Lobdell et al. 1973) 40

18. Load-deflection of thorax, human volunteer, mid-sternum impact with a 10-kg, 15.3-cm- (6-in-) diameter padded striker at 2.4 to 4.6 m/sec (Patrick 1981) 41

19. Maximum force as a function of impact velocity for human volunteer (Patrick 1981) 41

20. Chest acceleration versus time for unrestrained cadaver impacts into steering wheel—CIRA sled tests (Morgan et al. 1987) 42

21. Column force versus time for unrestrained cadaver impacts into steering wheel —CIRA sled tests (Morgan et al. 1987) 43

22. Wayne State University test setup for cadaver impacts into non-collapsible steering columns at 40 km/hr (Begeman 1988) 45

23. Normalized force-deflection curves for the rigid-column Wayne State University tests (Begeman 1988) 46

24. Test setup and chest deflection measurement sites for L'Abbe et al. tests (1982) 47

25a. Maximum force versus maximum deflection for Hybrid III and human volunteers—*relaxed* state (L'Abbe et al. 1982) 48

25b. Maximum force versus maximum deflection for Hybrid III and human volunteers—*tensed* state (L'Abbe et al. 1982) 49

26. Test configuration for WSU two-point-belt/knee-bolster restraint loading of the human thorax/abdomen system (Cheng et al. 1984) 51

27. Time traces of upper and lower shoulder belt loads for Wayne State University two-point-belt/knee-bolster sled tests (Cheng et al. 1984) 52

28. Test configuration of WSU airbag sled tests (Cheng et al. 1982) 53

29. Steering column loads and T12 accelerations versus time for WSU cadaver/airbag sled tests (Cheng et al. 1982) 54

30. Left and right knee bolster load for WSU cadaver/airbag sled tests (Cheng et al. 1982) 55

31. Test setup for Calspan variable-area impact tests 56

32. Force-deflection curves for Calspan variable-area impact tests to sternal area 57

33. Comparison of static chest load-deflection curves, A-P (Stalnaker et al. 1973) 59

34. Static loading corridors for relaxed and tensed volunteers, back fully supported (Lobdell et al. 1973) 59

35. Sternal force-displacement diagrams for CPR compression-release cycles in a single subject at three levels of peak force (Weisfeldt 1979) 60

36. Force-deflection diagrams for compression release cycles in a single subject with large and small sternal pad (Weisfeldt 1979) 61

37. Locations of deflection measurement for quasi-static belt and airbag loading tests (Kallieris 1987) 63

38. Locations of accelerometers for thorax impact tests by Robbins et al. (1976) 64

39. Thoracic response in frontal pendulum impactor tests (4.5 m/s) (Melvin et al. 1988a) 65

40. Thoracic response in frontal sled three-point-belt tests (13.4 m/s) (Melvin et al. 1988a) 66

41. Thoracic response in frontal sled airbag tests (13.4 m/s) (Melvin et al. 1988a) 68

42. Regions of static loading with 5 cm x 10 cm (2"x4") surface and deflection measurement used by Cavanaugh et al. (1988) 70

43. End view of test setup for static loading tests on a cadaveric thorax (Cavanaugh et al. 1988) 71

44. Side view of test setup for static loading tests on a cadaveric thorax (Cavanaugh 1988) 72

45a. Schematic chest cross-section showing spine support only (Cavanaugh et al. 1988) 73

45b. Schematic chest cross-section showing rib plus spine support (Cavanaugh et al. 1988) 73

46. AATD abdominal impact response, frontal and lateral (rigid bar impactor 4-cm by 35-cm and 10-kg mass) (Melvin et al. 1988a) 78

47. Force-penetration corridors for low and high velocity impacts to abdomen with 25-mm- (1-in-) diameter rigid bar (Cavanaugh et al. 1986) 80

48. Test setup for thoraco-abdominal impacts to unembalmed cadavers using a rigid lower rim representation of a steering wheel (Nusholtz et al. 1988) 81

49. Comparison of force-deflection curves for rigid lower-rim impacts to abdomen (Nusholtz et al. 1988) 83

50. Illustration of thorax/abdomen anatomy showing primary visceral organs (*Stedman's Medical Dictionary, 2nd ed.*) 85

51. Various cadaver and volunteer impacts with revised AIS values using force, mass, area, and absorbed energy as injury predictors (unrestrained steering wheel impacts excluded) (Melvin et al. 1988a) 89

52. Various cadaver and volunteer impacts with revised AIS values using force, mass, area, and absorbed energy as an injury predictor (unrestrained steering wheel impacts excluded) (Melvin et al. 1988a) 90

53. Relation of velocity of deformation to injury criteria (Lau and Viano 1986) 92

54. UCSD cadaver/pendulum and GM pig/pendulum impacts, with revised AIS values, using two versions of the viscous criteria as injury predictors (Melvin et al. 1988a) 93

55. Side view of mid-size-male reference form (Schneider et al. 1985) 96

56. Intrinsic and extrinsic rib shape measures (Dansereau and Stokes 1988) . 100

57. Ogle/MIRA dummy ribcage (Searle and Haslegrave 1970; Warner and Ogle 1974) 100

58. Kinematic response to two- and three-point belts (Backaitis 1987) 105

59. The three joints of the shoulder girdle (Dempster 1965) 106

60. Bones and joints of the shoulder complex sequence (Dempster 1965) 106

61. Sternoclavicular articulation (Dempster 1965) 107

62. Joint sinus of sternoclavicular joint (Dempster 1965) 108

63. Range of motion at shoulder joint as a function of degrees of freedom (Robbins 1985a) 110

64. Upper limb and shoulder movement (Dempster 1965) 111

65. Shoulder girdle and glenohumeral joint movement (Dempster 1965) 112

A-1. Difference in ribcage between human and Hybrid III dummy (Matsuoka et al. 1989) 128

A-2. Chest deflection as a result of different belt positioning (Matsuoka et al. 1989) 130

B-1A. Force-deflection curve of AATD5, Run 1A, Cadaver #115, loaded at mid-sternum with a 25 mm (1 in) stroke at 1.7 mm/s (0.067 in/s) 136

B-1B. Deflection-time history at mid-sternal load arm, second, fifth, and seventh ribs and left clavicle 137

B-2A. Force-deflection curve of AATD3, Run 2, Hybrid III, loaded at mid-sternum with 25 mm (1 in) stroke at 1.7 mm/s (0.067 in/s) 138

B-2B. Deflection-time history at first, third, and sixth right ribs, anteriorly 139

B-3A. Force-deflection curve of AATD5, Run 5, cadaver #114, loaded at upper sternum with 25 mm (1 in) stroke at 1.7 mm/s (0.067 in/s) 140

B-3B. Deflection-time history at fourth, seventh, and ninth left ribs, posteriorly 141

B-4A. Force-deflection curve of AATD3, Run 7, Hybrid III, loaded at upper sternum with 50 mm (2 in) stroke at 1.7 mm/s (0.067 in/s) 142

B-4B. Deflection-time history at first, third, and sixth left ribs, posteriorly 143

B-5A. Force-deflection curve of AATD5, Run 17, Cadaver #115, loaded at right seventh rib with 25 mm (1 in) stroke at 1.7 mm/s (0.067 in/s) 144

B-5B. Deflection-time history at load arm (right seventh rib), right second rib, right fifth rib, and left second, fifth and seventh ribs, anteriorly 145

B-6A. Force-deflection curve of AATD4, Run 5, Hybrid III, loaded at right sixth rib with 25 mm (1 in) stroke at 1.7 mm/s (0.067 in/s) 146

B-6B. Deflection-time history of load arm and Instron actuator 147

B-6C. Deflection-time history of first, third, and sixth left ribs, anteriorly 148

B-6D. Deflection-time history of first and third right ribs, posteriorly 149

INTRODUCTION

The Thorax/Abdomen Development Project is an outgrowth of the NHTSA Advanced Anthropomorphic Test Device (AATD) Development Program. In the initial project, the anthropometric specifications for a family of future anthropomorphic test devices (ATDs) were determined. The results are contained in a three-volume final report by Schneider et al. (1985) and Robbins (1985a, 1985b) as well as eleven full-size engineering drawings of the three dummy sizes (DOT-HS-806–715, 716, 717 available from NTIS, accession no. PB-86–105046). The second part of the program, which has been referred to as Phase I, studied and compiled the latest available information on human biomechanical response and patterns of motor vehicle injuries. The result of the Phase I effort is a series of task reports (Carsten and O'Day 1988, Melvin and Weber, ed. 1988, Arendt et al. 1988, Melvin et al. 1988a, Melvin et al. 1988b) that are published in a single bound volume (DOT-HS-807–224 available from NTIS, accession no. PB-88–174495), and which provide the basis for the next generation of ATDs. Included are recommendations for new instrumentation technology and calibration procedures. In the final document of this series, the Task E–F report (Melvin et al. 1988a), design specifications and concepts are discussed and presented for the different body regions of an advanced, omnidirectional trauma assessment device for the 50th percentile male (TAD-50).

The focus of the current effort is to design and develop new thorax and abdomen subcomponents for future ATDs. It has been well established that motor-vehicle-related injuries to the thorax and abdomen comprise a major portion of the total injury problem. Measured by percent Harm, Malliaris et al. (1982) have found that injuries to the chest of motor vehicle occupants comprise 26.7 percent of total Harm, second only to that of the head. Using the Injury Priority Rating (IPR) system developed in Phase I of the AATD effort, the percent IPR was found by Carsten and O'Day (1988) to be 21.0 percent for the chest. The lower percent for IPR compared to Harm is due to the fact that persons suffering injuries to the thorax tend to experience total recovery more frequently than injuries of similar severities to the head. Similarly, injuries to the abdomen comprise 18.2 percent of the Harm and 7.9 percent of the total IPR. Combined then, injuries to the thorax and abdomen comprise 44.9 percent of the Harm and 28.9 percent of the IPR.

In the current ATD standard, the Part 572 or Hybrid II test dummy, the response of the thorax to dynamic loading is significantly different than that of the human (i.e., much stiffer) and the only injury-related measurement parameter is spinal acceleration, which has been shown to correlate poorly with the level or likelihood of soft-tissue thoracic injuries. In addition, the abdomen of the Part 572 dummy is a rubber-coated foam component that has neither humanlike response nor measurement capability.

Compared to the Part 572 test dummy, the latest and state-of-the-art ATD for frontal impacts, Hybrid III, has significantly improved dynamic stiffness for blunt impacts to the midline of the chest at the level of the mid-sternum and also measures sternal deflection and sternal velocity (through differentiation of deflection), which have been shown to have higher correlation to soft-tissue injuries than spinal accelerations. However, as documented in Appendix A, additional improvements in the Hybrid III torso are needed.

Accurate evaluation of vehicle design and restraint systems with regard to occupant protection requires that the ATD do a better job of providing humanlike response to impact loading and assessment for trauma-induced injuries, not only for interactions with steering wheels, instrument panels, and other vehicle components, but for a variety of active and passive restraint systems. With the variety of structures and geometries that can load the thorax during frontal impacts, injuries to the thorax and abdomen can occur to regions other than the sternum, thereby increasing the importance of biomechanical response fidelity and

injury assessment capability at multiple regions of the thorax/abdomen complex. The current project is an attempt to meet this need through design of an improved Hybrid III torso. Since the design and performance of spine and shoulder components play an important role in determining the interaction of the thorax and abdomen with vehicle components and restraint systems, these components are necessarily included in the redesign effort. For convenience, the term *thorax/abdomen design* will be used when referring to the general design effort with the understanding that the spine and shoulders are included.

Before setting out to design and develop a new and improved subcomponent for an anthropomorphic test device (ATD), however, it is important to document both the overall design goals for the subcomponent and the design and performance specifications that should guide the design process. In a general sense, this has already been accomplished by the Phase I task reports (DOT-HS-807–224) of the AATD program. The current effort attempts to incorporate the design-related information contained in these reports, supplement it with additional information, and bring all this information into better focus on the problem of developing a new thorax/abdomen subcomponent. In addition, discussions of the rationale and bases for the design guidelines are presented.

This document is divided into two main parts. Part A presents and discusses the overall *Design Goals and Requirements* while Part B presents the *Design and Performance Specifications*. The design goals and requirements are the more general issues that must be considered for the thorax/abdomen system to be a useful and functional test device and research tool and include such issues as durability, temperature sensitivity, repeatability and reproducibility, impact vectors and severities, performance range, impact environments, regional response and injury measurement requirements. The design specifications provide more specific details about the actual design and performance features of the new torso and include the areas of (1) dynamic and static mechanical response characteristics, (2) instrumentation, and (3) anthropometric specifications. Where possible and appropriate, test procedures are included so that the designer can evaluate prototype systems and components. Part C of this document provides a brief summary of the design goals and requirements presented in Parts A and B.

PART A. DESIGN GOALS AND REQUIREMENTS

The following sections present and discuss the general requirements and goals for the new thorax/abdomen subcomponent. The foundation for the discussion and material presented was a preliminary statement of goals and requirements provided to the authors by the NHTSA (Haffner 1987). The areas addressed include:

1. Priority of Thorax/Abdomen Use Modes
2. Crash Vectors
3. Restraint/Vehicle Environments
4. Maximum Crash Severity by Restraint/Vehicle Environment
5. Injury Assessment Range
6. Temperature Sensitivity
7. Durability Requirements
8. Repeatability and Reproducibility
9. Summary of Design Requirements

A1.0 PRIORITY OF THORAX/ABDOMEN USE MODES

A1.1 Retrofit Subcomponent for Hybrid III

The primary goal of this design effort is to develop an improved dummy thorax/abdomen to replace the thorax/abdomen of the Hybrid III anthropomorphic test dummy (ATD). The Hybrid III ATD is the state-of-the-art ATD for frontal impacts and provides more humanlike impact responses of the head, neck, chest, and lower extremities, as well as more advanced instrumentation capabilities, than its predecessor, the Part 572 ATD. There is, however, a need to improve the design and performance of Hybrid III, and particularly with regard to the impact response and injury assessment capabilities of the thorax/abdomen region. The new thorax/abdomen must, as a first priority, be designed as a retrofit subcomponent for the Hybrid III ATD.

Since the impact performance of the thorax and abdomen can also depend on the impact responses of other parts of the ATD torso, such as the shoulders and spine, the new thorax/abdomen must also address these parts of the Hybrid III. There is concern, for example, that the Hybrid III shoulders are too rigid and heavy and do not, therefore, represent the mobility, compliance, and mass properties of the human shoulder under impact conditions, especially during shoulder belt loading. There is also concern that the rigid thoracic spine of the Hybrid III inhibits realistic interaction of the thorax/abdomen with steering wheels, shoulder belts, and interior components of vehicles. Thus, along with replacement of the Hybrid III thorax and abdomen, the new design must incorporate improved shoulder and thoracic spine components. Obviously, in order to meet this Hybrid–III–retrofit requirement, the new components must be designed to interface and match up with existing Hybrid III components at the cervical and lumbar spines as well as the glenohumeral junction of the arms.

A1.2 Subcomponent Test Device

Secondary to the goal of upgrading the Hybrid III dummy is the goal of developing a subcomponent test device for evaluating the injury potential of vehicle components without

the need for whole-body impact testing. The existing subcomponent test device for steering wheel/column testing is a rigid torso block (SAE J944 "Black Tuffy") which has major deficiencies in representing the interaction and loading of the human occupant with a steering assembly. There is a need to improve upon these procedures. Therefore, in developing the Hybrid III replacement components, the potential for adapting the thorax/abdomen assembly to a stand-alone test device for vehicle component evaluations should be considered.

A1.3 Component for Future ATDs

Finally, the new thorax/abdomen should ideally be designed with the long-range potential for incorporation into a future advanced anthropomorphic test device (AATD or TAD-50). Any design and/or instrumentation concepts considered in developing the new subcomponent should therefore also be evaluated with regard to long-term ATD design potential, such as adaptability to a lateral and/or omnidirectional-response dummy and measurement of response parameters that may be used in future injury criteria.

A2.0 CRASH VECTORS

Since the Hybrid III ATD is a frontal impact device, the primary goal of this program is to develop a thorax/abdomen system for performance and measurement during frontal impacts, including impacts at angles within about 30 degrees to frontal. However, since lateral impact devices and standards are a near-term reality, and an omnidirectional or convertible (lateral/frontal) dummy is a foreseeable device of the future, the design should also offer the potential to provide response and injury assessment capability for impacts other than frontal, including lateral and oblique impacts. Thus, the design priorities for impact directions are:

1. Frontal (12 o'clock) ± 30 degrees (11 and 1 o'clock)
2. Side impact (8 to 10 o'clock and 2 through 4 o'clock)
3. Omnidirectional or convertible (8 o'clock to 12 o'clock to 4 o'clock)

A3.0 RESTRAINT/VEHICLE ENVIRONMENTS

The restraint environments to be encountered by the thorax/abdomen involve exposure of the driver and front-seat passenger while unrestrained, or restrained by a three-point belt, a two-point belt/knee bolster system, or an air cushion restraint with and without a belt restraint system. The thorax/abdomen should be designed to provide humanlike response (i.e., biofidelity in response) and meaningful injury assessment for impact loading imposed by the following types of restraints and vehicle components:

1. Steering assembly (by unrestrained driver)
2. Instrument panel (by unrestrained passenger)
3. Shoulder/lap belt—i.e., three-point belt
4. Shoulder belt only—i.e., shoulder belt and knee bolster
5. Airbag
6. Belts plus airbag

In order to understand the implications of these environments in terms of dummy design requirements, it is instructive to examine what is known about the injuries and injury patterns due to each condition and also to look at observed differences in thorax/abdomen loading patterns between humans (i.e., cadavers) and the Hybrid III ATD.

A3.1 The Unrestrained Front Seat Occupant

A3.1.1 Injury Patterns. For the unrestrained driver and passenger, the NASS database from 1979 to 1984 was interrogated by Haffner (1987) for frequency of system/lesion pairs for the thoracic region. This region was defined as containing the NASS body regions of chest, back (thoraco-lumbar spine), shoulder, and the abdominal organs liver and spleen. The following filters were applied:

a. Passenger cars
b. General area of damage—frontal
c. No rollover or ejection
d. Weighted file

Weighted distribution of injuries rated at AIS=3 or greater and of Harm for the unrestrained driver and right-front passenger are shown in Table 1. The Harm estimates for arterial and liver injuries were considerably higher than the fraction of injuries rated at AIS≥3 for both the driver and right-front passenger. The relative frequencies of heart and lung injuries are seen to be higher for the driver than the right-front passenger.

It should also be noted that 75% of whole-body Harm was for drivers compared with 25% for the right-front passenger. It can be expected that a primary factor contributing to this difference is a significantly higher exposure rate for drivers but other factors, such as steering wheel, seat position, and side of vehicle, cannot be ruled out. Cohen (1987) reported that, for the thorax/abdomen, most of the frontal contacts for the driver are to the steering assembly. On the passenger side, the instrument panel is the primary contact for both serious and minor/moderate injuries to the chest and abdomen.

Other observations from Table 1 are that:

- Arterial injuries, although representing less than 10% of AIS≥3 injuries, constitute close to 30% of estimated Harm.

- Liver injuries similarly represent approximately 10% of AIS≥3 counts, but account for 20% of Harm.

While shoulder contact with both the steering wheel and the instrument panel undoubtedly occurs in the real world, the automated NASS data do not distinguish clavicle fractures within the general category of skeletal injuries. In a recent study at CIRA by Schneider et al. (1987), unrestrained cadaveric subjects frequently sustained dislocations at the sterno-clavicular junction, but no clavicle fractures were found upon interaction with the steering assembly during frontal impact simulations. In a similar, as yet unpublished study by Wayne State University (Begeman 1988), there were also no clavicle injuries in the ten cadavers tested, some of which experienced high chest loads from impacts with a rigid (non-collapsible) steering assembly.

Perhaps the most significant observation, with regard to the design of a new thorax subcomponent for frontal type impacts, is the fact that soft-tissue injuries occur to organs such as the liver and spleen that are located under the lower, lateral ribcage region (i.e., the upper lateral abdomen region). Apparently, the rim of the steering wheel and/or the instrument panel produces soft-tissue injuries to these areas of the thorax/abdomen system of unrestrained drivers involved in frontal crashes. It would seem obvious that such injuries can only be accurately assessed by a test device that has good biofidelity and deflection/velocity instrumentation in these regions.

A3.1.2 Loading Patterns. In the unpublished Wayne State cadaver/steering wheel sled tests mentioned above, the measured steering wheel rim load was approximately 50% of the total steering column load and the cadaver thorax was able to completely invert a dished

TABLE 1

DISTRIBUTION OF THORAX/ABDOMEN AIS≥3 INJURIES AND HARM FOR UNRESTRAINED DRIVERS AND RIGHT-FRONT PASSENGERS IN FRONTAL COLLISIONS (Haffner 1987)

Injury	Driv AIS≥3 Injuries	Pass AIS≥3 Injuries	Driv Harm	Pass Harm
ARTERIAL Severance Laceration Puncture Rupture	8%	6%	27%	30%
HEART Contusion Laceration Puncture	10	4	18	4
JOINTS Dislocation Fract/Disloc	7	6	1	1
LIVER Laceration Contusion Abrasion	10	11	20	21
PULMONARY/LUNG Contusion Laceration	21	9	9	7
SPLEEN Contusion Laceration Rupture	6	8	3	9
SKELETAL Fracture	25	30	10	10
VERTEBRAL Dislocation	3	6	1	4
OTHER & UNKNOWN	10	20	11	14
TOTAL Percent	100%	100%	100%	100%

steering wheel, similar to the patterns seen in the field for severe frontal impacts. On the other hand, neither the Hybrid III dummy nor the Part 572 dummy was able to reproduce the inversion phenomenon. Figure 1 illustrates these differences in steering wheel deformation for cadavers, Part 572, and Hybrid III. As shown, the cadaver impact caused the wheel of the rim to turn inside out, the Hybrid III impact resulted in the rim flattening into a plane with the hub, while the Part 572 impact deformed the rim only partially.

Achievement of steering-rim deformation patterns similar to those produced by humans (i.e., cadavers) under the severe impact and rigid-column conditions of these tests does not, of course, guarantee response biofidelity or better injury assessment potential. The lack of humanlike deformation patterns, however, implies the need for ATD improvements with regard to the mass and mobility of the thorax/shoulder complex, thoracic spine flexibility, anthropometry of the chest and ribcage, and biofidelity throughout the thorax/abdomen.

A3.2 Occupants Restrained by Two- or Three-Point Belts

A3.2.1 Injury Patterns. The use of three-point belt restraint systems by front-seat occupants in the U.S. and worldwide is expected to continue for the foreseeable future. The belted and belt/bag restraint environment is expected to predominate in the 1990s and the thorax/abdomen subcomponent should therefore be able to discriminate between, and predict injury from, the variety of belt loading configurations encountered in the field.

Because of the brief period of time in which belt laws have been in effect in the U.S., the NASS database contains (as of December 1987[1]) insufficient information on injuries due to three-point-belt systems to be of value at the present time. Some data are available, however, from Canada and Europe although only the Canadian data can be considered to have been derived from a similar traffic mix and vehicular distribution. Dalmotas (1980) has provided some insight on the injury pattern of Canadian front seat occupants. For frontal impact, the Canadian database contains information on 121 belted occupants—91 drivers and 30 right-front passengers. The findings as summarized in Haffner (1987) from these frontal data are as follows:

- Shoulder/chest injuries constitute 22% of the AIS>2 counts on the driver side and 23% of AIS>2 counts on the passenger side.

- Abdominal/pelvic injuries are, relatively speaking, much more prevalent on the passenger side. These injuries represent only 4.5% of AIS>2 counts on the driver side but 22% of passenger AIS>2 counts.

- Whereas the few abdominal injuries on the driver side are attributed to wheel rim contact, all abdominal injuries on the passenger side are attributed to local belt intrusion. Concurrent loading of the seat back by a rear seat occupant is cited as a contributing factor in some of the cases.

- Those drivers who were assessed as *not having contacted the steering assembly*, but who were presumed to have been injured by the belt assembly itself, *experienced only skeletal fractures in the shoulder/chest region*, usually following the path of the belt on the torso. Fractures of the clavicle, sternum, and ribs were experienced. It is of interest that *no intra-thoracic injuries* were sustained in this group. As noted above, *no abdominal injuries in drivers were attributed to the belt assembly*.

---

[1]Date of original drafting of this document.

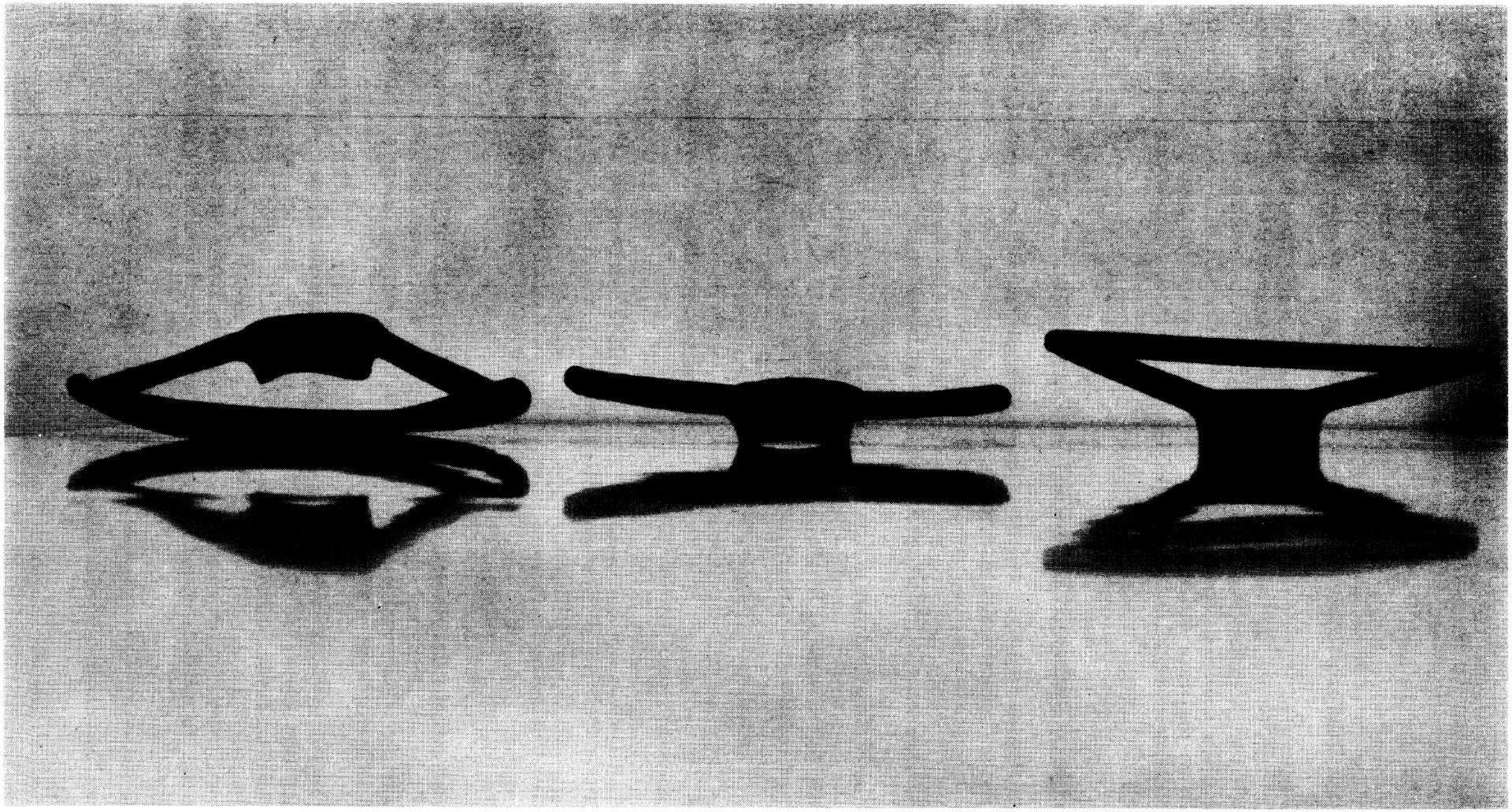

CADAVER HYBRID III PART 572

FIGURE 1. Comparison of steering wheel deformations for cadavers and dummies (Begeman 1988).

- Of the drivers judged to have contacted the wheel, intra–thoracic injuries *were* frequently associated with occurrence of multiple rib fractures. Abdominal injuries, though infrequent, were observed with steering wheel interaction.

- On the passenger side, *thoracic skeletal fractures also followed the path of the shoulder belt.* Internal injuries were apparently infrequent, but one case of myocardial contusion was observed. Abdominal injuries were relatively frequent, and were associated with local belt loading.

Rutherford et al. (1985) discusses the influence of the introduction of compulsory seat belt wearing in the U.K. upon injury patterns observed. It is not possible to specifically extract frontal accident exposures from the general data presented. Nevertheless, the findings of this study provide guidance with respect to the overall shift of thorax/abdomen injury patterns as indicated in Table 2.

The results of the studies by Dalmotas and Rutherford are seen to be consistent. A reduction of severe intrathoracic injuries appears to occur with three-point-belt restraint systems, offset to some degree by increased incidence of certain skeletal fractures and of abdominal injuries, especially on the passenger side. Also of interest is the relatively high frequency of observed contact of the belted driver with the steering assembly noted by Dalmotas.

In addition to these major studies of seat-belt-related injuries in Canada and England, some anecdotal information on injuries to front-seat restrained occupants in the U.S. is available in the UMIVOR data file maintained at UMTRI. Interrogation of this file for injuries to belted front-seat occupants revealed fifteen cases of thorax or abdomen injuries of AIS 2 or greater for frontal impacts (11 to 1 o'clock). As shown in Table 3, in three cases there were soft-tissue injuries to the spleen or liver when there was no apparent contact with the vehicle interior. Whether these injuries were caused by the lap or shoulder portion of the belt cannot be determined, but these limited observations provide further support for the need to assess for injuries in the areas of the spleen and liver (i.e, in the regions of the lower ribcage lateral to the mid-sagittal plane), not only for steering wheel impacts to the unrestrained occupant but also for seat-belt-induced injuries.

Injury data from a two-point shoulder belt with knee bolster are extremely sparse. Cheng et al. (1984) performed eleven cadaver tests with a VW two-point-belt/knee-bolster system for the right-front-passenger position. There were no reported liver injuries because of the fact that the shoulder belt crossed over from the right shoulder to the left side. However, the injury data showed that in seven cadavers there were more rib fractures on the left side than on the right.

A3.2.2 Loading Patterns. The manner in which belt restraint systems interact with the human body during impact loading is significantly different than for steering wheels and instrument panels, both in terms of the loading velocities and the load distributions. Since the belt restraint is already in contact (or close to contacting) the torso/abdomen, the impact velocity is lower for a belt system for a given crash severity. Also, the loads are concentrated along the length of webbing material in contact with the body. Since the Hybrid III thorax has been designed solely on the basis of thoracic impact response to sternal loading by a 15.3-cm- (6-in-) diameter rigid pendulum (see Section B1.1), the response of the Hybrid III thorax to lower velocity loads of belt webbing applied along a diagonal from the shoulder to the lower ribcage must be questioned. L'Abbe et al. (1982) have compared the thoracic response to dynamic shoulder belt loading of the thorax of human volunteers to that of Hybrid III and found significant differences, particularly in the regions of the shoulder and lower rib cage contacted by the belt (see Section B1.1.7).

Backaitis and St.-Laurent (1986), extending upon the work of L'Abbe et al., have also demonstrated significant differences in the deflection response of the Hybrid III thorax to

TABLE 2
COMPARISON OF THORAX/ABDOMEN INJURIES BEFORE AND AFTER INTRODUCTION OF U.K. BELT-USE LAW
(Haffner 1987 from Rutherford 1985)

Injuries REDUCED Post-Belt Law	Injuries INCREASED Post-Belt Law
Lung and pleura injuries	Sternum fractures
Kidney injuries	Thorax contusions, including cardiac contusions
Severe intra-thoracic injuries	Contusions of abdominal wall (passenger) and associated injuries to GI tract, mesentery, and pancreas
Rib fractures (driver)	
Contusions of abdominal wall (driver)	

TABLE 3
UMIVOR THORAX/ABDOMEN INJURIES TO FRONT-SEAT BELTED OCCUPANTS

Case No.	Occupant Position	Impact Direction	Restraint	Probable Veh Contact	Injury	Level	Body Region
1.	Left	01	3 Pt	No	Skeletal	2	Chest
2.	Left	01	3 Pt	No	Heart	3	Chest
3.	Left	01	3 Pt	No	Skeletal Contusion	2	Shoulder
4.	Right	12	3 Pt	No	Liver—Crushing	5	Abdomen
5.	Right	12	3 Pt	No	Digestive—Laceration	3	Abdomen
6.	Right	12	3 Pt	No	Spleen—Crushing	3	Abdomen
7.	Left	11	3 Pt	No	Skeletal	2	Shoulder
8.	Right	11	3 Pt	No	Skeletal	2	Chest
9.	Right	11	3 Pt	No	Skeletal	2	Shoulder
10.	Left	12	3 Pt	No	Liver—Contusion	2	Abdomen
11.	Left	12	3 Pt	No	Skeletal	2	Chest
12.	Right	12	3 Pt	No	Skeletal	2	Pelvic/Hip
13.	Left	12	3 Pt	No	Skeletal	2	Shoulder
14.	Right	12	3 Pt	No	Digestive—Laceration	5	Abdomen
15.	Left	12	3 Pt	No	Joints	2	Shoulder

belt loading compared to the response of the human chest at sub-injury levels of loading. For human volunteers, the deflections were smallest at the shoulder and greatest at the level of the seventh rib. For Hybrid III, maximum deflections were at the 7th rib and clavicle and the minimum deflections were at the sternum. In all regions under the belt except the shoulder (i.e., clavicle), the dummy demonstrated an overall stiffer chest than even the tensed volunteers. The study further showed that the single deflection sensor at the Hybrid III sternum significantly underestimated deflections due to forces applied at other locations.

Recently, the nearly rigid shoulder of the Hybrid III dummy has been identified as a possible problem in producing inappropriately low chest loads during three-point-belt tests. When the torso flexes forward around the lap belt, the rigid Hybrid III shoulder may take an inappropriately high proportion of the load, thereby resulting in unrealistically small chest deflections that are highly dependent on the amount of torso angulation. For the two-point-belt/knee-bolster system, this forward torso rotation does not take place since the body translates forward until the knees strike the knee bolster (see Figures 26 and 27, Section B1.1.7). Thus, the Hybrid III dummy has been found to produce higher chest deflections with two-point-belt systems than with three-point-belt systems, but it is difficult to know how much of this is representative of the human and how much is due to the effects of an overly rigid shoulder structure in the dummy.

In the two-point-belt/knee-bolster tests conducted by Cheng et al. (1984), the ratio of the lower belt load to that at the upper anchor point for ten of the eleven runs was 92%. In comparison, an analysis of three-point-belt loads from cadaver tests conducted at Wayne State University indicates a ratio of about 60% for lower belt load compared to upper belt load. These differences in lower shoulder belt loads between two- and three-point systems may indicate that two-point shoulder belts tend to exert more force on the lower thorax and upper abdomen than three-point belts. For the driver, this could result in a higher probability of liver injury. Again, the implication for ATD thorax design is the need for biofidelity and injury assessment (i.e., response parameter measurement) in these regions.

A3.3 AIRBAGS AND BELT/BAG COMBINATIONS

A3.3.1 Injury Patterns. The airbag can be a source for thoracic injuries for the out-of-position occupant. During deployment, bag slap resulting from the high velocity (15 m/s and greater) impact of the bag against the chest wall can cause injury to the lungs as well as the heart. It is hypothesized that the injuries would be due to stress waves transmitted from the outside of the chest wall to the organs within, although there are no known documented cases of such injuries. In terms of ATD thorax design, these high-velocity, low-mass types of impacts require that consideration be given to a measurement system that can detect the potential for injury under these conditions. The combined effect of a shoulder belt and airbag is also unknown since such restraint combinations have only recently been installed in a few models.

A3.3.2 Loading Patterns. Little is known about the response of the human thorax to the distributed loading due to airbag interaction. Since, under normal occupant position conditions, the air cushion itself is unlikely to be a cause of injury to the thorax, the value of such data to the present effort is primarily to ensure biofidelity in response so that other dummy components such as the head and neck will experience appropriate kinematics and interaction with other vehicle components. Response biofidelity for the out-of-position occupant will require correct biofidelity and measurement capability for high-velocity, low-mass loading, probably including sensing elements at the anterior chest wall.

For normal airbag loading to the seated occupant, impact velocities are probably less than for the unrestrained occupant into the steering wheel but greater than for the restrained occupant into the shoulder belt. The forces, however, will tend to be distributed

over a larger area of the thorax than for steering wheel impact. Designing to achieve the impact response force-deflection characteristics obtained by Calspan for large area loading (see Section B1.1.9, Figure 32) may be useful toward achieving airbag response biofidelity until better data are available. For quasi-static loading with a foam-filled airbag, Kallieris (1987) has demonstrated a uniform chest deflection pattern at six locations on the third, fourth, and fifth ribs in contrast to the asymmetric deflection pattern due to shoulder belts (see Section B1.1.10, Figure 37).

A4.0 MAXIMUM CRASH SEVERITY BY RESTRAINT/VEHICLE ENVIRONMENT

In addition to designing for biofidelity and injury assessment for the range of loading and injury patterns, the thorax/abdomen system must be designed to deal with severe impact conditions that may produce forces beyond the level of injury tolerance or required injury severity assessment. The local test environment to which the ATD thorax/abdomen will be exposed depends, of course, on vehicle structural and interior component design, as well as upon the test speed. One way of characterizing crash severity for design purposes is to utilize estimates of expected closing speed between the thorax/abdomen and major interior components. In terms of barrier equivalent velocity (BEV) in a full-up vehicle crash test environment, the following upper bounds on test speeds have been suggested by NHTSA (Haffner 1987):

Restraint Environment	Vehicle BEV
Unrestrained	48 km/h (30 mph)
Belted	56 km/h (35 mph)
Bag/Belt	56–64 km/h (35–40 mph)

Estimates have been obtained from several sources of the likely range of closing speed between the thorax/abdomen and interior components, as shown in Table 4. The estimated closing speed between the thorax/abdomen and vehicle interior components for unrestrained drivers and passengers in frontal collisions is seen to range up to 100% of barrier speed, depending upon the test or model chosen and upon assumptions employed. Based on this evidence, the new test device should be able to withstand crash severities which produce impact velocities in excess of 35 to 40 mph to the unrestrained ATD.

For designing the subcomponent thorax/abdomen system, it is more useful to translate these impact velocities of the vehicle (or sled) into expected loading forces due to the various restraints and vehicle components. Assuming improved biofidelity in the new thorax, such forces need to be based on cadaveric tests which represent severe frontal impacts and not on current dummy tests which can produce unrealistic forces.

A search was carried out to determine the maximum forces that can be expected for unrestrained-, belted-, and airbag-type impacts. The peak column load for cadaveric tests at Wayne State University simulating the unrestrained driver impacting a non-collapsible steering system was 13,000 N (2,923 lb), while that for a pre-deployed airbag was 16,000 N (3,597 lb). The highest shoulder belt load at the upper anchor point for the three-point restraint system was found to be 8,007 N (1,800 lb). For a two-point belt with knee bolster, the peak upper anchor load was 8,585 N (1,930 lb). These latter values are considered to be too low for upper dummy design limits (personal communication with R. Daniel and P. Prasad 1988). A value in the range of about 13 kN (3,000 lb) is recommended as an upper limit for dummy shoulder-belt loading.

TABLE 4

CLOSING SPEED BETWEEN THE THORAX/ABDOMEN AND INTERIOR COMPONENTS (Haffner 1987)

Source of Data	BEV (km/h)	BEV (mph)	Closing Speed (km/h)	Closing Speed (mph)	Remarks
Backaitis (1982)	48	30	43	27	MVMA2D 18-in. spacing
	56	35	50	31	
Simione (1987)	48	30	27	17	MVMA2D passenger simulation 24-in. spacing
	56	35	39	24	
Stucki (1987)	48	30	34 avg. (16–48)	21 avg. (10–30)	Half-offset with intrusion (PADS model)
	48	30	27 avg. (16–37)	17 avg. (10–23)	No intrusion (PADS model)
Morgan (1987)	43	27	27	17	Cadaver sled data; driver configuration

A5.0 INJURY ASSESSMENT RANGE

As an injury assessment tool, an ATD should provide information about the probabilities of injuries of different levels or severities that would result from each test/impact situation. The standard way of classifying the level of injury to a body organ or region is by use of the Abbreviated Injury Scale or AIS. According to this rating system, which has been established and periodically updated by the Committee on Injury Scaling, the numerical AIS ratings correspond to the following general levels of severity:

AIS	Severity Level
1	Minor
2	Moderate
3	Serious
4	Severe
5	Critical
6	Maximum (unsurvivable)
9	Unknown

As indicated by the severity level descriptions, the AIS rating system is based on mortality or threat to life and does not consider long-term disability resulting from injury. Nevertheless, the AIS has become the most common and popular rating system for standardizing injury data.

The type of injury corresponding to the different AIS ratings will, of course, depend on the particular body tissue and organ involved. For example, laceration (tearing) of the aorta is rated as an AIS 5 since it obviously represents a critical threat to life. However, fractures to multiple ribs resulting in a flail chest (i.e., loss of elasticity and strength in ribcage to the

extent that it remains in a collapsed condition) is rated as AIS 4, a severe injury with possibility of mortality less probable than aortic laceration.

Since an anthropomorphic test device must be able to evaluate and indicate improvements to automotive environments and restraints with regard to ability to reduce severity of injury and death, the ATD must be able to evaluate a system's performance over the range from *moderate* to *severe* levels of injury. With regard to the Hybrid III ATD measurement range, Wiechel et al. (1985) have noted:

> The current Hybrid III thorax can accommodate a maximum deflection of slightly over 76 mm (3 inches). Thus, the Hybrid III is designed to differentiate between the non-serious injuries (AIS 1–3) and to identify the presence of a serious injury (AIS>3).
>
> This limited injury measurement capability of the Hybrid III has left a void in the ability to evaluate automotive crash environments. Certainly, it is of paramount importance to be able to differentiate between serious and non-serious injuries and qualitatively determine an improvement in the design of a vehicle or vehicle component. However, the inability to quantitatively measure serious injuries is a handicap. Absent this ability, the assumption must be made that all injuries above AIS 3 are equally serious and life threatening. Any assumption of this is guesswork. It would be advantageous to be able to differentiate between a life threatening AIS 5 injury and a serious but not critical AIS 4 injury. This is especially the case in establishing the survivability of several crash environments as in unrestrained occupant or high-speed collisions.

Thus, each ATD subcomponent should be designed to provide maximal performance and injury assessment in the AIS 2–3–4 range, and it would be very desirable for the ATD subcomponent to provide useful information for higher severities of injuries without simply "bottoming out." For example, if impact conditions are severe enough to produce injury severities higher than AIS 4, it would be useful if the response transducers would continue to generate useful information that would indicate how much above AIS 4 the injury severity might be.

For purposes of designing a dummy component, however, the AIS numbers are of little value. What is needed are ranges of ATD impact response parameter values that correspond to the range of injury severities that the ATD should assess. Response parameters may be deflections, velocities, accelerations, forces, or various functions and combinations of these. To know the range of response parameters, however, requires that we know the relationships of impact response parameters to injury severities. In other words, we need to know both the *injury criteria* (i.e., what response parameters or combination of response parameters correlate with level of injury) and the *injury tolerance* levels (magnitudes of these parameters) for the different AIS ratings. Furthermore, as Lau and Viano (1986) and Horsch (1987) have suggested, the relation between injury criteria values and injury severities needs to be expressed as probabilities of injury severity, for maximum utility in vehicle design problems.

In any case, the ability to use impact response parameters of an ATD to predict injury levels, or the probability of injury levels, requires that the response parameters be somehow correlated with levels of injury (and the likelihood of these levels). This requires, first of all, that the ATD subcomponent reproduce the impact response characteristics of the human (i.e, the response of the human cadaver surrogate after appropriate adjustments) for the range of loading conditions that may be encountered and over the injury tolerance range of interest (i.e., AIS 2 through 4 and above). Assuming that this can be accomplished, relationships between these response parameters and the probabilities of AIS ratings must also be established.

Considering our limited understanding of thorax/abdomen injury criteria and injury tolerance, and the different thoracic and abdominal organs that may be injured by a variety of different mechanisms (see Section B2.1), the idea of specifying a single range of response parameters that must be designed in order to cover AIS 2 through 4 injuries is a gross simplification of a complex issue. Nevertheless, some guidelines can be established with the limited information available. The frontal 15.3-cm- (6-in-) diameter rigid-pendulum tests to the sternum of unembalmed cadavers, conducted and analyzed by Kroell et al. (1971, 1974), Neathery and Lobdell (1973), and Neathery et al. (1975), provide the best information available. Sections B1.1.1 and B1.1.2 of this document present the impact response requirements described by these test results.

Figure 2 shows relationships of AIS with the plateau force and the normalized chest deflection for these tests. The AIS values ranged from 2 through 6, and the better correlation to injury level was for the chest deflection response measure. In terms of designing the ATD thorax for prediction of AIS injuries in the range of 2 through 4 and above, it seems reasonable that, for injuries to the lower-sternal region of the thorax, if the impact response requirements of the Kroell corridors are met, the design will be responding and providing output over the desired injury range. More specifically, the relationship between AIS and chest compression (expressed as a percent of external chest depth) is given by Neathery et al. (1975) as:

$$AIS = -5.15 + 17.4\,(C) + 0.031\,(AGE) \qquad r^2=0.7613$$

where C = penetration/chest depth and AGE = years.

Solving for C gives:

$$C = 0.29545 + 0.05736\,AIS - 0.00179\,AGE$$

Based on this relationship, Table 5 gives the values of C and external deflection for AIS ratings from 2 to 5 and AGE values of 45 and 60 years. Values for external deflection are based on a chest depth at the lower sternum of 23 cm (9.1 in) reported by Melvin et al. (1988a) for the TAD-50.

TABLE 5

CHEST COMPRESSION AND EXTERNAL DEFLECTION FOR DIFFERENT AIS AND AGE VALUES
(Based on analysis of Kroell data by Neathery et al. 1975)

AIS	45 Years			60 Years		
	C (%)	External Deflection (mm)	External Deflection (in.)	C (%)	External Deflection (mm)	External Deflection (in.)
2	0.33	76	3.0	0.30	69	2.7
3	0.39	89	3.5	0.36	84	3.3
4	0.44	102	4.0	0.42	97	3.8
5	0.50	114	4.5	0.47	109	4.3

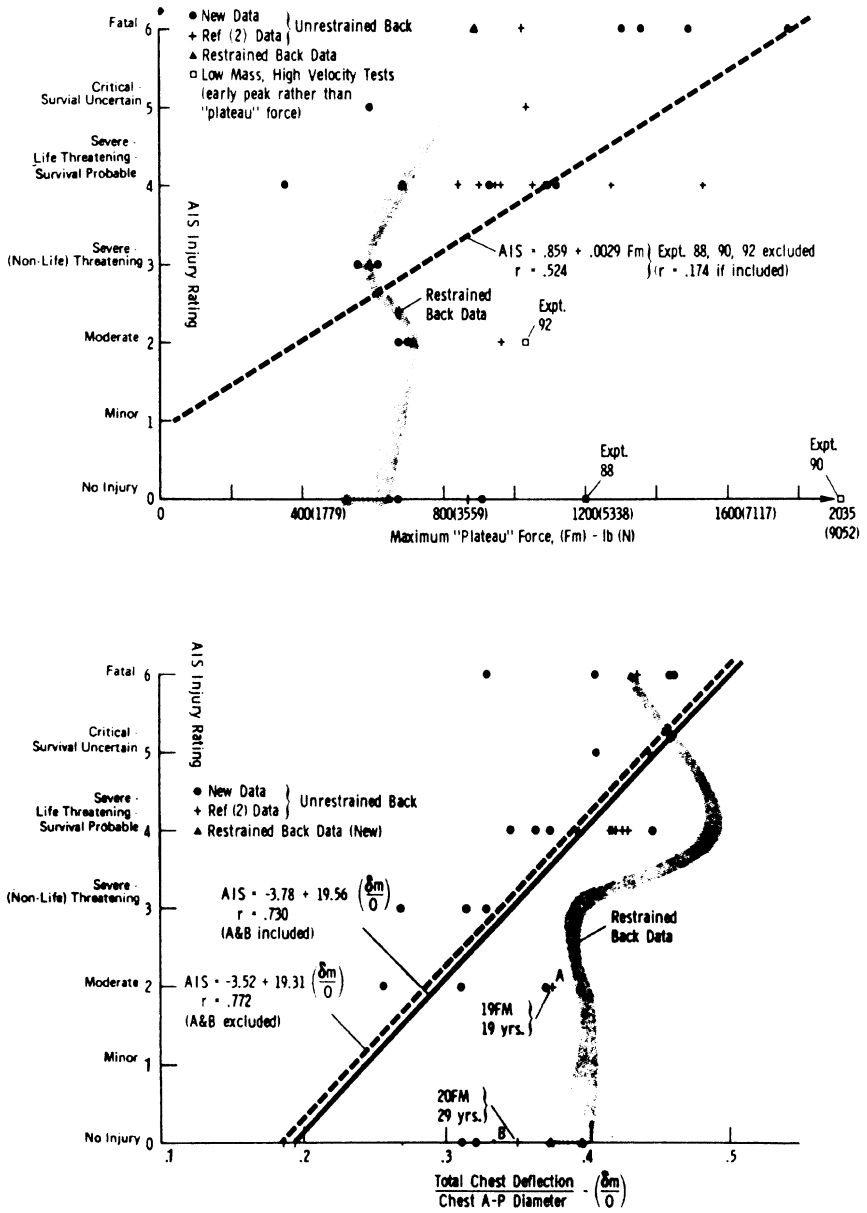

FIGURE 2. AIS injury rating versus maximum plateau force (top); AIS injury rating versus normalized chest deflection (bottom) (Kroell et al. 1974).

For internal deflections which are measured by dummy transducers, Neathery et al. (1975) have recommended subtracting 12.7 mm (0.5 inch) from external deflection. Applied to the values in Table 5, it is seen that internal chest deflections at the lower sternum of about 90 mm (3.5 in) are needed for biofidelity up to AIS 4, and deflections up to 100 mm (4.0 in) are needed for biofidelity up to AIS 5. Weichel et al. (1985) have suggested the use of acceleration-based criteria for injury levels above AIS 4 since, in the human chest, the sternum is essentially bottomed-out on the vertebrae at about 100 mm (4 in) of deflection (Verriest and Chapon 1985). Chandler (personal communication, May 1988) has suggested that spinal load cells can provide important injury assessment information beyond AIS 4.

Recent studies by Viano and Lau (1985) and others have suggested that the use of deflection alone as a soft-tissue injury criteria should be limited to conditions where chest loading rates are less than 3 m/s. These researchers have demonstrated that, for impact velocities greater than 3 m/s, the velocity of chest deflection can play an important role in injury causation to soft tissues. In the Kroell impact data, this velocity effect is reflected in the rate dependency of the initial stiffness and plateau force of the force-deflection curves. Achievement of appropriate response rate sensitivity is therefore important for measurement of the viscous injury criteria (*VC*) and is an important design consideration. With regard to AIS levels, Lau and Viano (1986) have used Logist analysis on the Kroell et al. data to estimate that $[VC]_{max}$=1.0 and 1.2 correspond to a 25% chance of sustaining an injury of AIS 4 or greater dummy frontal impact to the thorax and abdomen, respectively.

Injuries at AIS level 2 or greater can also occur to the thorax due to shoulder belt loading, where the distribution of forces and loading velocities are different from those in the Kroell impact tests. Unfortunately, good response and injury data do not exist for these types of loading conditions and therefore correlations of AIS levels with impact-response parameters under these conditions are not possible at this time.

A6.0 TEMPERATURE SENSITIVITY

A6.1 Operating Temperature Range

The ideal ATD would, of course, show no variation in response characteristics over the expected operating range. According to Seiffert and Leyer (1976), an ATD may be used in ambient temperatures ranging from 32°F to 104°F. Since material properties vary with temperature, there will be effects of temperature on response and response parameters.

Saul (1984) has compared the temperature sensitivities of thoracic response for the Hybrid III and Part 572 ATDs over the range of 65°F to 80°F. The results are shown in Figure 3. For peak resultant accelerations (measured at the spine), it is seen that the absolute changes for the two dummies are about the same going from 72° to 80° and 72° to 65°, but the percentage changes are more than double for the Hybrid III since the actual values are nearly half of those for the Part 572. For sternal deflection, both the absolute and percentage changes are significantly greater for the Hybrid III, being only 3% from 72°F to 80°F and 6% from 72°F to 65°F for the Part 572. In contrast, the Hybrid III showed a 27% increase from 72°F to 85°F and a 15% decrease from 72°F to 65°F.

Although corrections in response are possible for different temperatures, the larger temperature-related variability of the Hybrid III dummy thorax is a source of concern to users. Not only is the work of correcting the response measures an added burden and source of potential error, but the change in total dummy response (e.g., head/neck kinematics) due to the variability is not easily compensated for or predicted.

In the new thorax/abdomen, the goal should be to strive for the low temperature sensitivity of the Part 572 thorax while achieving a more compliant and humanlike

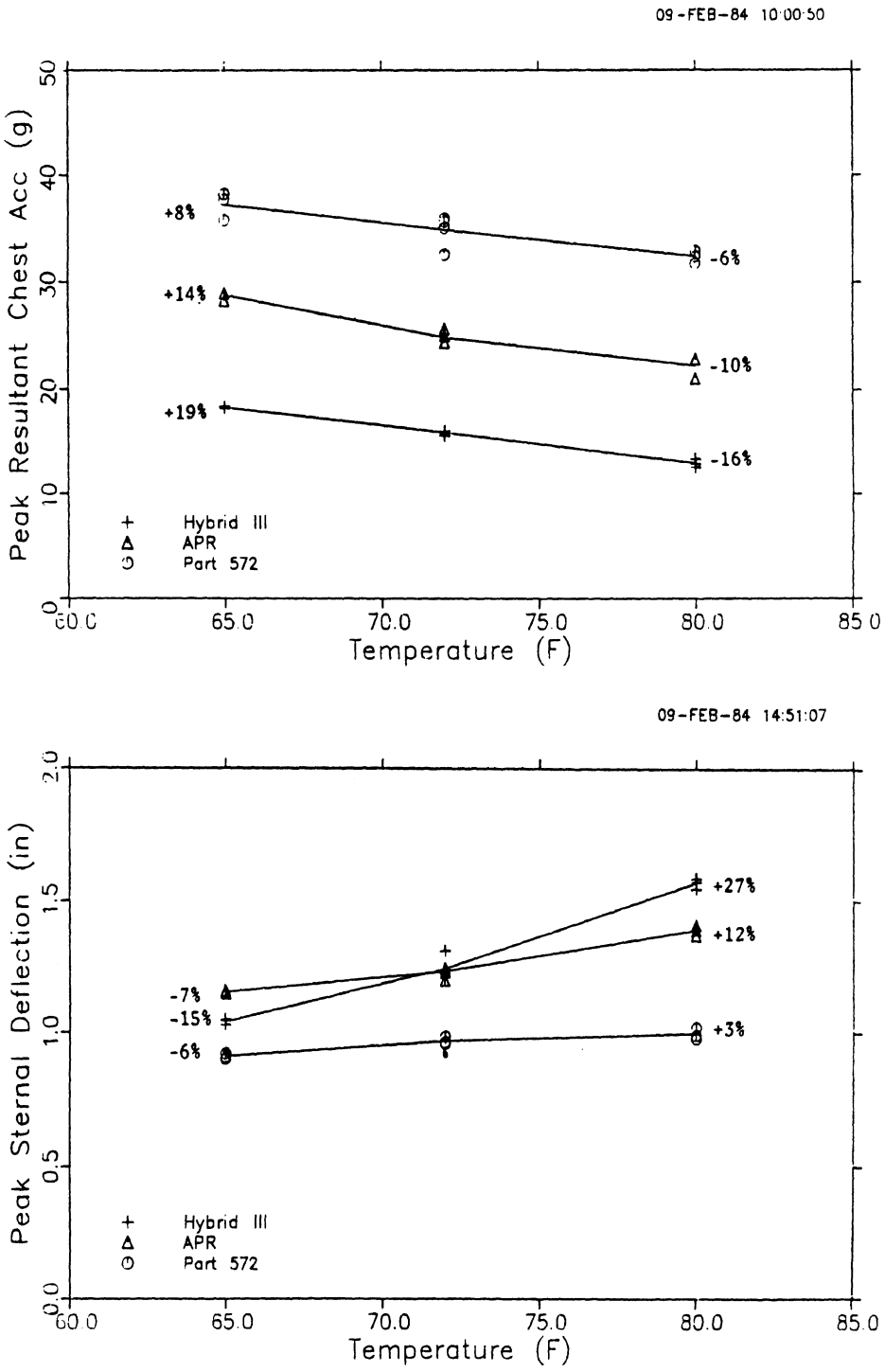

FIGURE 3. Dummy component-test peak chest accelerations (top) and peak sternal deflections (bottom) versus temperature (Saul 1984).

responding thorax. Since the new thorax/abdomen system will measure response variables that enable calculation of deflection-, viscous-, and acceleration-based injury criteria, meeting this requirement will require achieving low temperature-related variability in all of these response variables. An initial goal would be to attain 5% or less variability in the measures of chest/abdomen deflection, velocities, and spinal accelerations over the temperature range from 65°F to 80°F. Obviously, a design that allows for reducing the temperature sensitivity of response variables even more would be highly desirable.

A6.2 Durability Temperature Range

Because of a wide range of conditions under which ATDs may be stored during shipping, as well as the wide range of climates to which they may be exposed (e.g., the sunny, hot temperatures of Arizona and the cold winters of Michigan), the new thorax/abdomen design must be able to experience temperatures from -20°F to 140°F without breakdown or failure of parts and components and without significant changes in performance within the normal test temperature range (i.e., 65–80°F).

A7.0 DURABILITY REQUIREMENTS

A survey of industry ATD users conducted in Phase I of the AATD study (Melvin et al. 1988b) provided a variety of responses with regard to the durability requirements of an ATD and its subcomponents. Obviously, users would like the device to last through as many tests as possible without the need to replace parts and check calibration. With regard to the thorax, it is generally accepted that the standard pendulum calibration test is as destructive as most application testing and therefore many industry users tend to describe the durability in terms of the number of calibration tests that can be run. The test itself is similar to the tests performed by Kroell (1971, 1974) on unembalmed cadavers and requires that the thorax be impacted at the level of the lower sternum by a 15.3-cm- (6-in-) diameter cylinder having a mass of 23.4 kg (51.5 lbs) and impacting at a velocity of 6.7 m/s (22 ft/s).

Under these conditions, one hundred calibration-type tests is often mentioned as desirable since the Part 572 thorax was good for about this number. The Hybrid III thorax, on the other hand, has been found to need recalibration (i.e., replacement of parts) after about thirty tests or less, due in large part to separation of rib damping material and/or permanent deformation of the rib steel. Wiechel et al. (1985), for example, found that Hybrid III dummy #42 degraded after about 15 to 20 impacts using normal testing and calibration procedures. It has also been found that the thorax of Hybrid III may only be good for about 17 unrestrained driver tests due to twisting of the ribs that occurs during steering wheel impacts, and which tends to "pop" the damping material off the ribs with fewer tests than for anterior-posterior loading of the sternum. More recently, however, the use of a new damping material manufactured by E.A.R., Inc. has improved the durability of the Hybrid III ribs to thirty or more calibration tests (personal communication with J. Balser of GM Proving Grounds, 1987).[2]

---

[2]Further improvements in the Hybrid III rib durability may also be attained by development of a new damping material specifically for this purpose (the current damping material was designed for low-amplitude vibration damping in structures such as ship hulls) or by use of new composite rib materials which would eliminate the need for bonding polymer to steel.

From a durability standpoint, then, users clearly favor the more durable Part 572 thorax compared to the Hybrid III thorax. A reasonable durability design goal would therefore be:

> The thorax/abdomen system should sustain 50 to 100 impact exposures to the front of the thorax with a six-inch-diameter rigid impactor mass of 51.5 kg at impact velocities of 6.7 m/s (about 15 mph) without calibration shift.

Some further comments regarding durability issues of Part 572 and Hybrid III dummies are contained in the Phase I Task D report (Melvin et al. 1988b) and provide additional insight into the concerns of the users that should be considered in the new thorax/abdomen design.

> The skin/flesh jacket was particularly susceptible to tearing at the under arms and the abdominal flap. The zipper bonding to the jacket also regularly failed under normal use and, less frequently, the zipper itself. The sternum was also considered to have inadequate durability in that the leather would deteriorate and tear and the metal strips would break. The padding was also said to break down and shift, due to a lack of underlying structure, leaving a cavity and changing the shoulder belt location. The bending and permanent set of the ribs under severe impact conditions and the cracking and separation of the damping material were cited by several respondents. Problems with screw heads popping off and hexagonal socket holes rounding were also mentioned. Rib bending and damping material separation were also problems on the Hybrid III.

With regard to the zipper problems the following summary of the respondent comments was made:

> The majority responded that zipper failure was a frequent occurrence. Some pointed out that it was not the zipper itself as much as the bonding between the zipper and the skin jacket. Several suggested that both problems could be solved by using heavier zippers with reinforcing strips on the skin, and by making a skin jacket that fit better. Lacing was not considered desirable due to the time involved and the potential for variability. Approximately a third of the respondents suggested Velcro or zipper/Velcro combination. Others said that innovative closure methods, perhaps unknown in the dummy industry, should be investigated. The space program was suggested as a source of ideas.

A8.0 REPEATABILITY AND REPRODUCIBILITY

In order for an ATD or subcomponent test device to function as an effective industry and government standard, or even as a useful research tool, it must not only provide response biofidelity and meaningful injury assessment parameters, but it must also demonstrate that it can give the same results in repeated tests of the same ATD (repeatability) and in repeated tests with different ATDs of the same type (reproducibility). There is, of course, the question of what constitutes sameness in results or what percent of variability between tests is considered "good enough."

In the Phase I Task D report, Melvin et al. (1988b) have summarized the results of a user survey in which the issue of repeatability and reproducibility was one of the questions. The tolerable coefficient of variation for primary response characteristics and injury criteria from industry representatives ranged from 3% to 10%, with a preference for the 3% to 5% range. In a 1977 survey (SAE paper no. 770263), a 30% variation in injury criteria and calibration measures between two Part 572 dummies of different manufacturers was found, prompting one survey respondent to suggest a goal of reducing the current variation by 50%.

Among the sources of inter-test variability, both the level of expertise of technicians and problems in repeating dummy initial position were mentioned. The latter is clearly recognized as an area of difficulty in conducting impact tests with dummies, and needs to be addressed in future ATD designs. For example, Matsuoka et al. (1989) of Toyota have indicated that a large difference in chest deflection will result from a small difference in shoulder belt positioning. As shown in Figure A–2 of Appendix A, with the belt placed in one position it will "catch" on the bottom rib and result in larger sternal deflection than if the belt is placed slightly higher where it will slide up under the arm and produce smaller sternal deflection. Consideration should also be given to ways of improving targeting of the torso to more easily check for and establish repeatability in initial positioning. Most importantly, the new design should seek to achieve as good or better repeatability during component testing as that offered by the current Hybrid III thorax. In comparison testing between the APR, Part 572, and Hybrid III dummies, Saul (1984) found that Hybrid III had the best repeatability in both the component evaluation and in the three-point-belt restraint tests. He also noted, however, that temperature was controlled at 72°F for these tests, and that repeatability of the Hybrid III may require tightly controlled temperatures.

Finally, it should be noted that the goal of designing for humanlike response characteristics (i.e., biofidelity) and the goal of designing for repeatability and reproducibility may not be completely compatible. That is, a design that accurately represents the human in response characteristics may, by its very nature, be so sensitive to small changes in test conditions or manufacturing variations that it has inherent repeatability and reproducibility problems. For the industry user and for the government standard, the features of repeatability and reproducibility, as well as the features of durability, temperature sensitivity, and ease of use, should not be sacrificed in the effort to achieve improved biofidelity and injury assessment capability.

PART B. DESIGN AND PERFORMANCE SPECIFICATIONS

The previous section describes the overall design goals for the new thorax/abdomen subcomponent. In this section, the specifications for performance and design of the subcomponents, including the spine and shoulder, are presented and discussed. These specifications are divided into the three general categories of biomechanical response, instrumentation, and anthropometry.

It is a basic premise of this development effort that a successful injury assessment tool (i.e., ATD or subcomponent) must, first of all, reproduce human biomechanical response characteristics for the different types of loading conditions that it will encounter. This requires both impact response biofidelity and anthropometric specifications representative of the motor vehicle occupant. Furthermore, as Neathery et al. (1975) have suggested, assessment of injury should be by means of injury criteria based on parameters that are *included in—or predictably dependent upon—the parameters used to specify biomechanical fidelity*. This requires that adequate instrumentation be provided to produce response parameter measures necessary to calculate the injury criteria. Before beginning the prototype design work, it is necessary that the design and performance specifications in these three areas be clearly defined, so that potential design concepts can be evaluated with regard to the desired end product.

B1.0 BIOMECHANICAL IMPACT RESPONSE

As indicated in Part A of this document, the ATD thorax/abdomen should give humanlike responses for a range of impact environments including interactions of the unrestrained driver and passenger with steering wheels and instrument panels, as well as interactions with active or passive restraints including three-point lap/shoulder belts, two-point shoulder belts with knee bolsters, air bags, and various combinations of these. Since the loading conditions associated with different restraint/environment scenarios are different, it may be expected that the biomechanical responses of the human thorax/abdomen will also be different. For example, interaction of the thorax/abdomen of unrestrained drivers with steering wheel hubs and rims will involve more concentrated loading patterns and higher loading velocities than will interaction of drivers with three-point-belt systems where the velocities of loading are low and the impact forces are distributed over the thorax, abdomen, and the shoulder by a long length of webbing material.

In order to design response biofidelity into the new thorax/abdomen, information is needed that quantifies the mechanical responses to the range of restraint/environments and conditions that produce injuries and injury severities in the AIS 2 through 4 range (and higher). Unfortunately, all the data required to adequately describe the thorax/abdomen system (including the shoulder) are not available, and, even for those conditions where data do exist, the information is often not as complete as one would like. Even so, there are more data available than ever before for application to the design of a frontal impact thorax/abdomen subcomponent. The following sections summarize test results considered to be most pertinent to the design problem at hand. Most of the data pertain to the design of the thorax and include results from:

- Pendulum impacts to the sternum
- Impacts with a steering system
- Impacts with an airbag (driver and passenger)
- Impact loading due to a three-point-belt restraint
- Impact loading due to a two-point-belt restraint
- Impacts with large flat surfaces
- Static loading responses
- Mechanical compliance and deflection coupling between thoracic and abdominal regions of the ribcage

B1.1 Thoracic Response

B1.1.1 Sternal Response to Pendulum Impacts. The most complete thoracic impact response data available are those obtained by Kroell et al. (1971, 1974) using a 15.3-cm- (6-in) diameter rigid pendulum impactor. The results of tests with different pendulum masses and different impact velocities have been used to develop force/deflection response corridors for sternal loading of the human thorax. In addition, the data, that were obtained from unembalmed cadavers, have been adjusted to correct for estimated effects of muscle tension in the living human.

The Kroell thoracic response data clearly demonstrate that the human chest behaves as a viscoelastic structure with a consequent large amount of hysteresis or energy loss during dynamic loading to the sternum. The impact response of the thorax at the level of the 4th interspace between the 4th and 5th ribs[3] is illustrated in Figure 4 which shows the Kroell force-deflection corridor for 6.7 m/s impacts with a 23.4 kg (51.5 lb) impactor (shaded area) as well as individual curves derived from the Kroell force-time and deflection-time data.

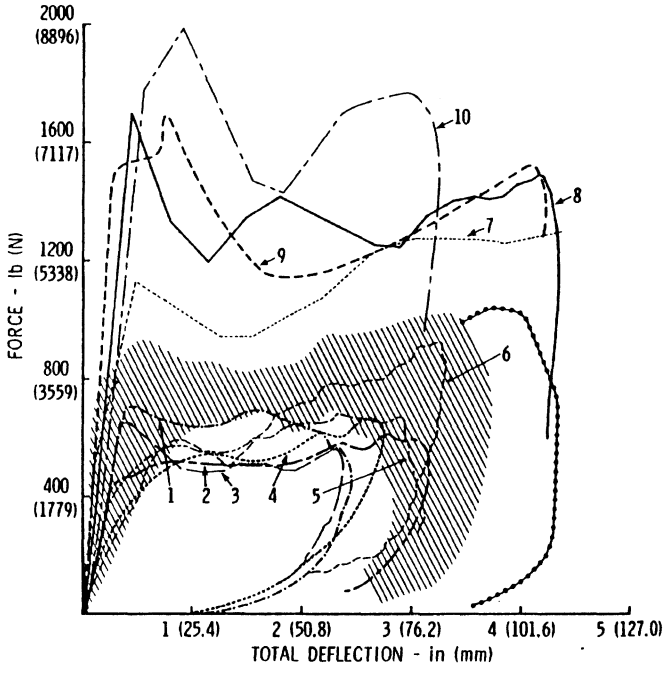

FIGURE 4. Force versus total deflection; nominal 23.1-kg (51–lb) striker at various velocities (Kroell et al. 1974).

---

[3]It has generally been assumed that the impactor in the Kroell test is centered at mid-sternal level. The 4th interspace is, however, closer to the bottom of the sternum, just above or at the xiphoid process.

The force developed during impact of the thorax is a result of viscous, elastic, and inertial factors. The initially high stiffness of the thorax and the plateau force following this rapid rise in force with minimal deflection are due, in large part, to its viscous nature and are therefore also rate dependent. For a freely moving impactor mass, as is the case in the original Kroell tests, the maximum deflection is determined by the amount of energy in the pendulum prior to impact and the response characteristics of the thorax. At maximum deflection, the velocity (relative to the spine) is obviously zero and the force is due only to the elastic forces generated by the compressed tissues plus any inertial forces due to acceleration of the whole torso. The unloading curve then follows the static nonlinear elastic force-deflection properties of the thorax (see Section B1.1.10 below) which are thought to be largely due to compression of internal organs against the spine as well as structural properties of the ribcage and its connective tissue.

Melvin et al. (1988a) have used the Kroell force-time and deflection-time impact response data to determine constants for the equation:

$$F(t) = K * D^2(t) + C * V(t) + m * A(t)$$

where K is the elastic spring constant, C is the viscous damping coefficient, m is the average effective mass, and F(t) is the force resulting from the deflection D, the velocity V, and the acceleration A, at any moment in time. The nonlinear elastic component was based on evidence of progressive stiffening behavior of soft tissues upon compression and has been demonstrated in static loading experiments by a number of researchers (see section below on static load-deflection properties). Applying this equation to the Kroell data produced values for the constants given in Table 6. It should be noted that the effective mass of the front of the thorax during dynamic loading was determined to be less than 0.4 kg (0.88 lb) in each case.

TABLE 6

SUMMARY OF ELASTIC, VISCOUS, AND MASS PARAMETER VALUES
FROM MELVIN ET AL. (1988a) MODELING OF KROELL DATA
(Impactor mass=23.4 kg or 51.5 lbs)

Impact Velocity (m/sec)	K		C		m	
	(N/cm^2)	(lb/in^2)	(N-s/cm)	(lb-s/in)	(kg)	(lb)
4.2	52.4	76.0	5.52	3.15	0.392	0.862
6.7	40.5	58.7	4.89	2.79	0.318	0.699
10.2	48.1	69.8	5.95	3.40	0.148	0.326
Average	47.0	68.2	5.45	3.11	0.286	0.630

Using this model, Melvin determined the "idealized" thoracic response corridors for impact conditions corresponding to the Kroell tests at three impact velocities. Figure 5 shows these idealized force-deflection corridors, which should be considered as the primary dynamic response design criteria for the thorax. Melvin also used the Kroell data along with some volunteer dynamic loading data from Patrick (1981) to determine the relationships of impactor velocity with initial stiffness and plateau force. The results are contained in Figures 3–2 and 3–3 of the Task B report (Melvin and Weber, ed. 1988) and are reproduced in Figures 6 and 7 to provide additional information for dynamic response design specifications.

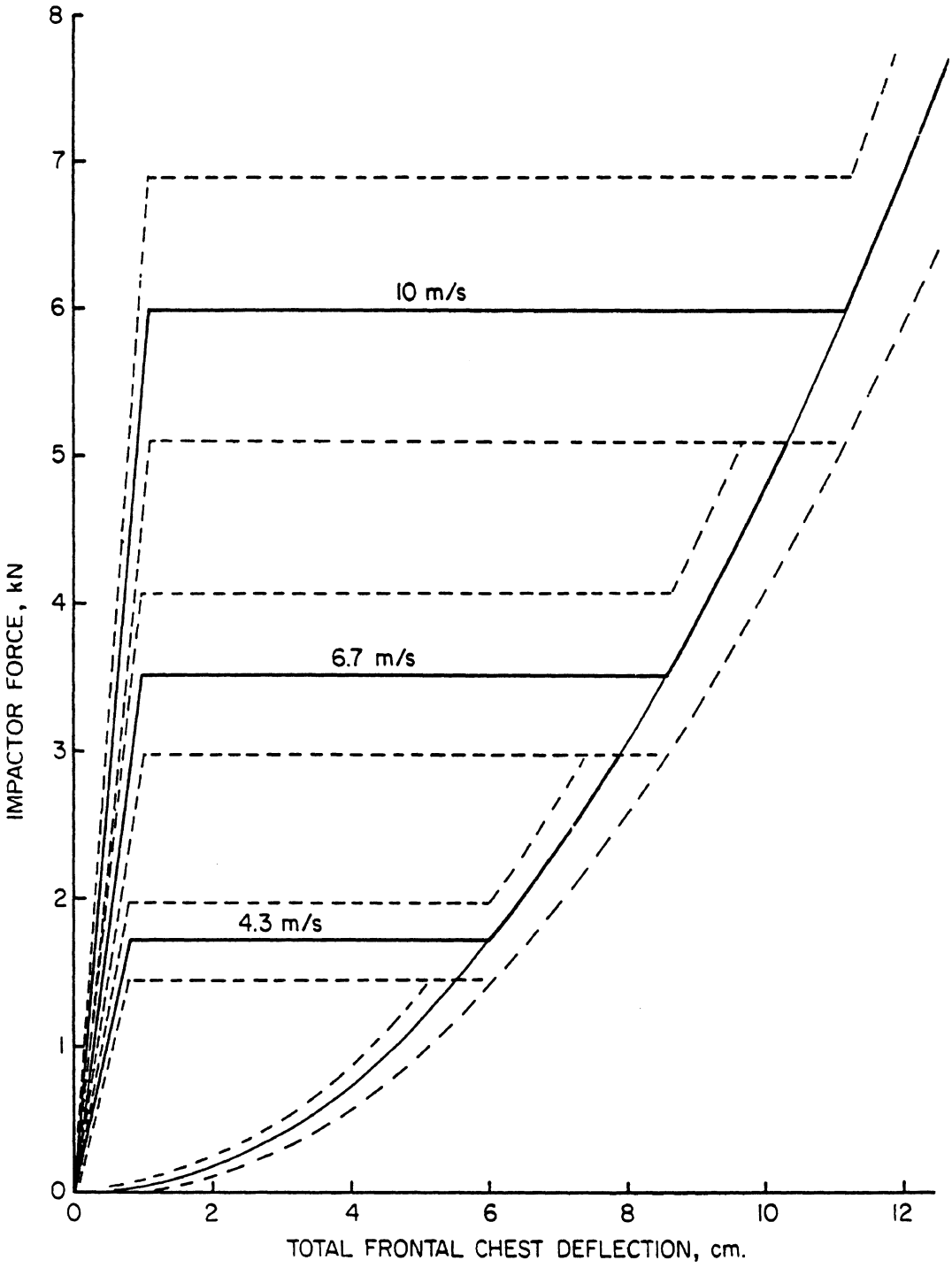

FIGURE 5. AATD frontal thoracic impact response—loading only (15.2-cm rigid disc, 23.4-kg impact mass) (Melvin et al. 1988a).

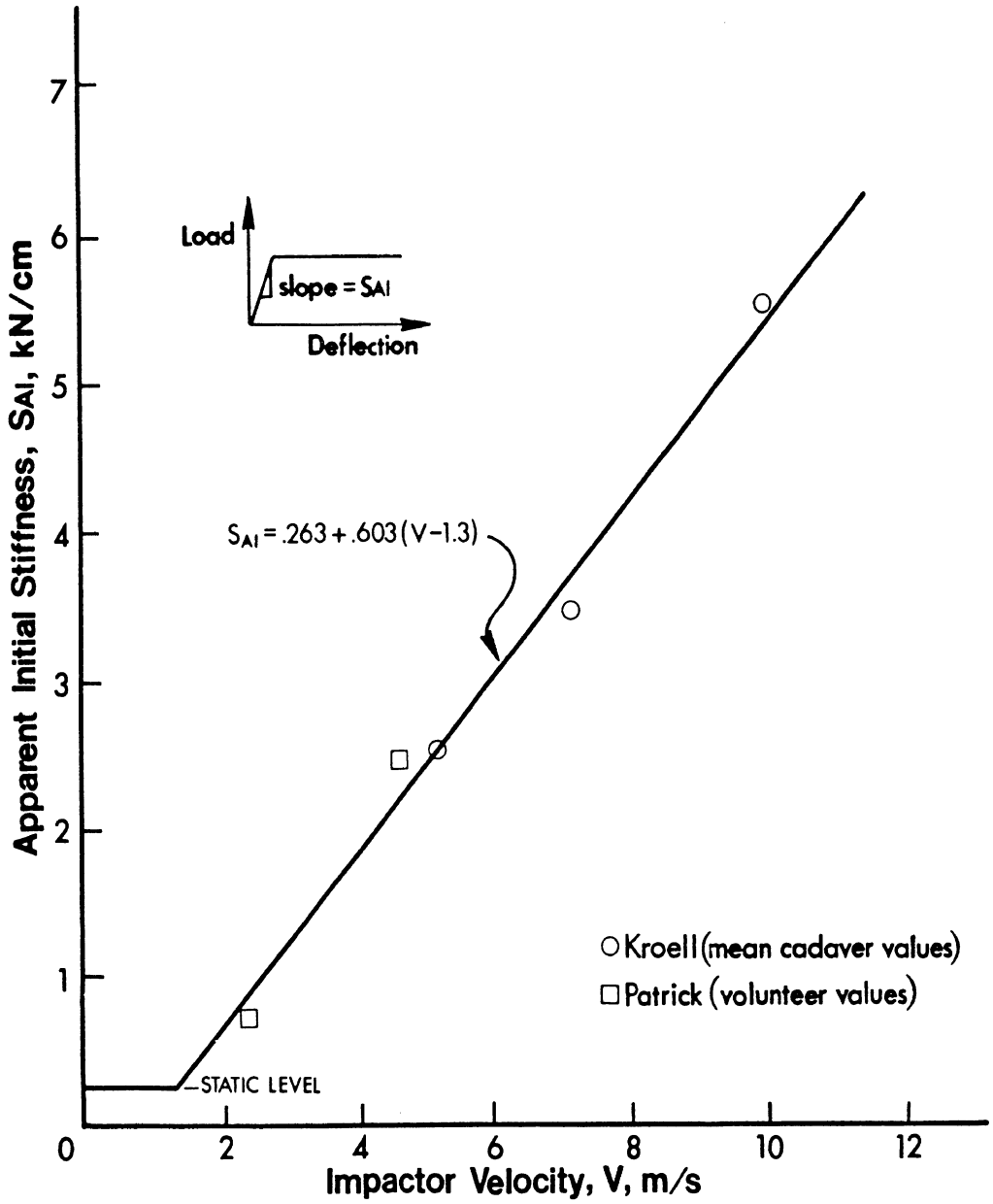

FIGURE 6. Apparent initial stiffness of the load-deflection response of the chest to frontal impact with a flat, circular impactor (Melvin et al. 1988a).

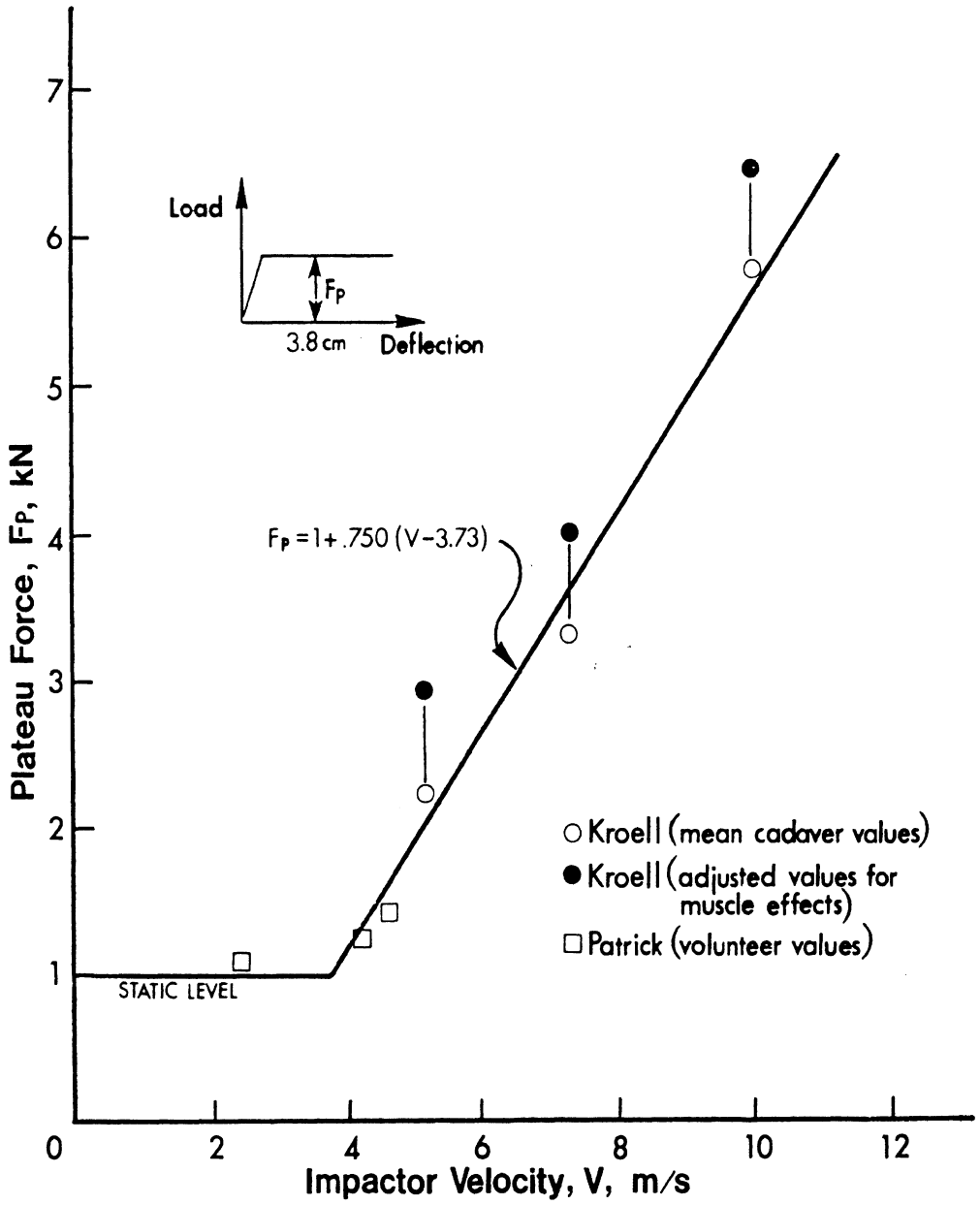

FIGURE 7. Plateau force versus impactor velocity for frontal chest impacts with a flat, circular impactor (Melvin et al. 1988a).

In order to evaluate a prototype thorax design with regard to the response specifications described above, the impact conditions used in collecting the data must be replicated. As illustrated in Figure 4, the Kroell force-deflection response corridor (hashed area) is based on force-time and deflection-time data obtained from impacts to the chests of seated unrestrained cadavers (with outstretched arms) with an unpadded, 15.3-cm- (6-in-) diameter striker plate having a mass of 23.4 kg (51.5 lb). The corner radius of the contact surface is 1.3 cm (0.5 in) to prevent edge loading effects. Impact velocities ranged from 6.7 to 7.4 m/s (15–16.6 mph). Additional response curves are also provided for higher impact velocities up to about 10 m/s (22.4 mph).

While the force-deflection curves and corridors provide the best characterization of thoracic response, some manipulation of force-time and deflection-time data is required to determine these curves. During preliminary testing of design concepts, it will be useful to compare force-time and deflection-time response curves directly to Kroell time-response curves. Figure 8 shows a composite of force-time response curves for the Kroell impacts. Additional curves are provided along with corresponding deflection-time curves and test conditions in Appendix C of this document.

It will be noted that a typical force pulse lasts about 24 to 40 ms for tests with 19.5 to 23.6 kg (43 to 52 lb) impactors at about 7.2 m/s (16 mph) and that the peak deflection is reached in about 20 to 30 ms. Also, in some of the tests a force spike occurs in the first few milliseconds prior to the development of the plateau force. Kroell et al. (1974) have indicated that this spike is a function of the "squareness of impact" and thus due to an "interface inertial loading" factor. Since these spikes occur at low values of chest deflection and there is no indication that they are related to injuries, they were eliminated in preparing the force-deflection corridors described above.

B1.1.2 Kroell Corridors for Restrained-Back Conditions. Since these response data were obtained from impacts to unrestrained cadaver chests, inertial effects of the torso as well as effects of spinal curvature and coupling to the body are factors that influence the response curves. Tests to evaluate a new thorax design should be conducted under similar circumstances with the thorax installed in a test dummy. In other words, the Kroell test is a whole-body component test which evaluates the biofidelity of the intact dummy thorax system. While such a test is necessary for final checkout of the new thorax within Hybrid III, it is not an appropriate test for evaluating pre-dummy prototype systems.

Recognizing this fact, Neathery (1974) used a mathematical model of the thorax to estimate the impact conditions that would produce the Kroell force-deflection response corridor for loading of the isolated thorax with a rigidly-supported cadaver spine. The results indicate that, at impact velocities of 7.2 m/s, reducing the impactor mass from 23.4 kg (51.5 lb) to 10.5 kg (23 lb) should produce the same response corridors for the restrained-back condition. Actual tests conducted under these conditions, however, are reported by Kroell et al. (1974) to have produced "lower average force levels and greater maximum deflections" than for the unrestrained back conditions, indicating that the thorax is "less stiff" when the back is restrained.

Figure 9a shows the force-deflection curves obtained from six tests under the restrained-back conditions and Figure 9b compares the corresponding response corridor with that of the unrestrained data at 7.2 m/s. The reason for the reduced stiffness with back support is unknown, but it has been hypothesized by Kroell that the presence of spinal curvature in the unrestrained case may be a contributing factor. In any case, these differences in response for full system testing and isolated-thorax testing should be kept in mind when evaluating interim prototype designs.

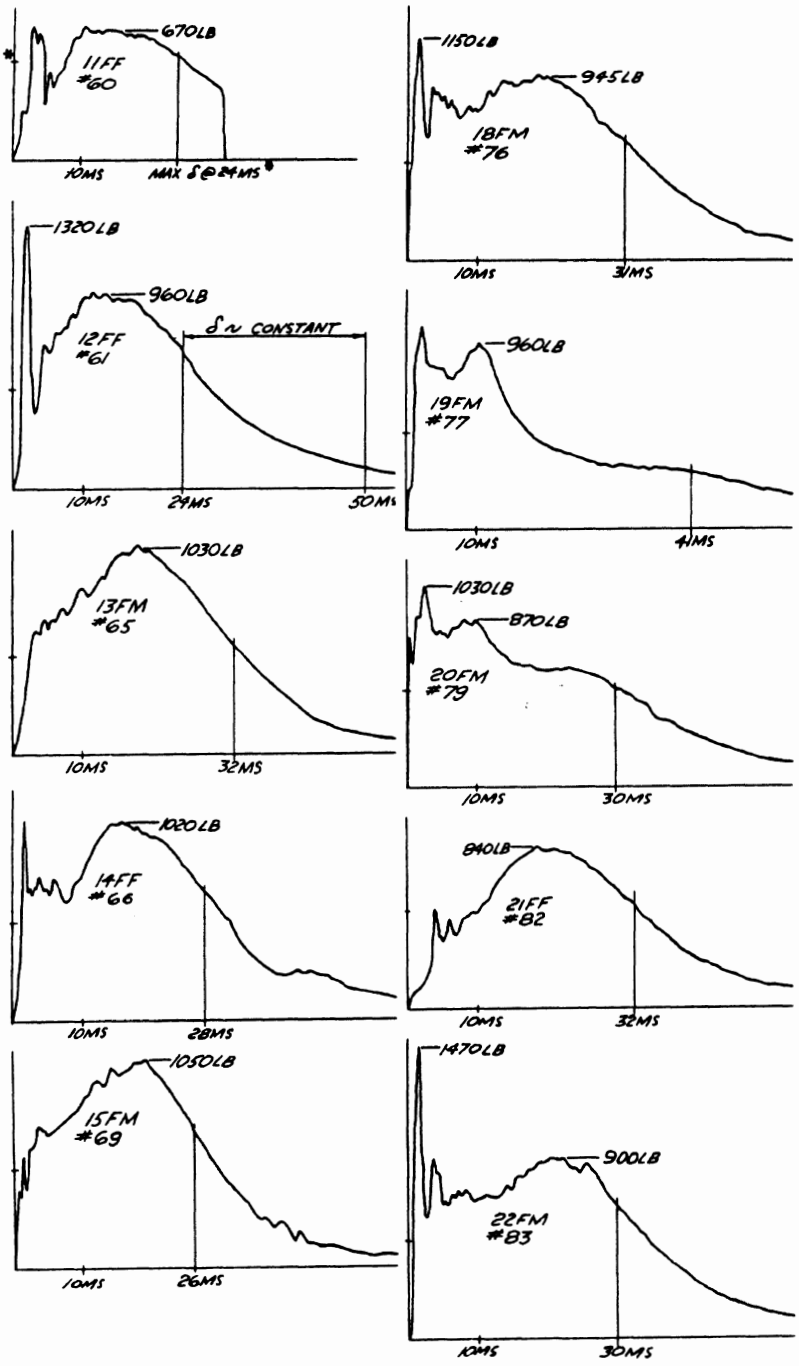

FIGURE 8. Composite of Kroell et al. force-time response curves, nominal 19.5-kg (43-lb) and 23.6-kg (52-lb) impactor masses (Kroell et al. 1971).

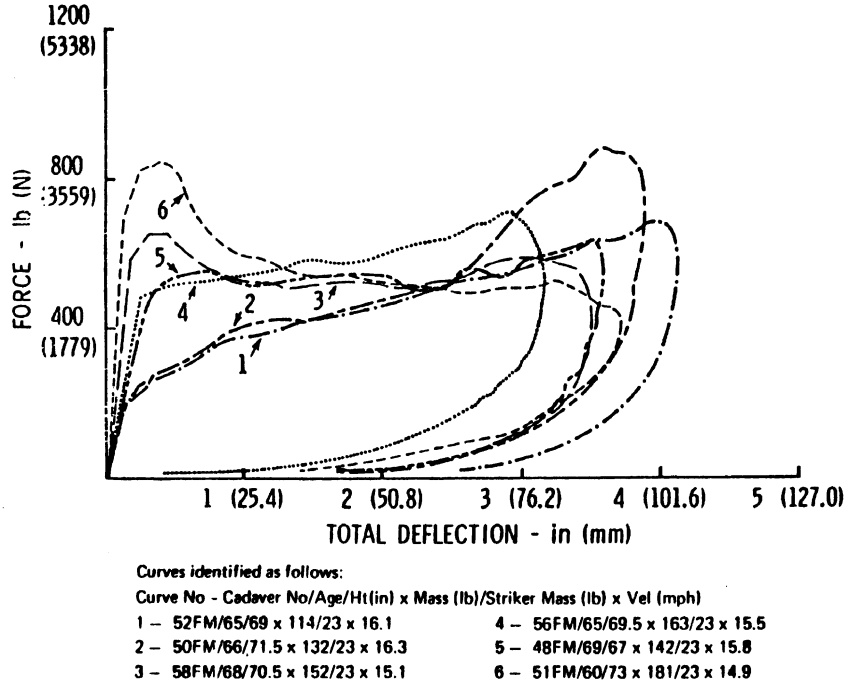

FIGURE 9a. Force versus total deflection; restrained back experiments 10.43–kg (23–lb) striker at nominal 7.2 ms (16 mph) (Kroell et al. 1974).

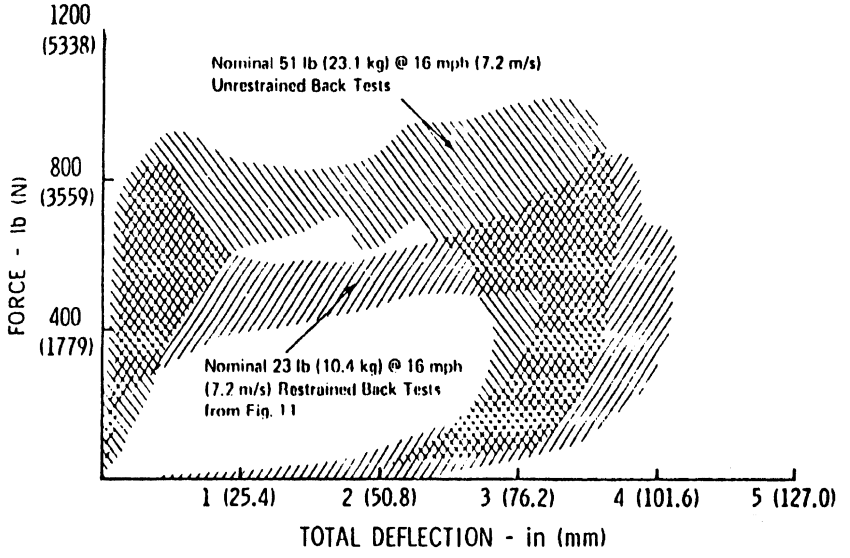

FIGURE 9b. Comparison of restrained-back response corridor with corridor from unrestrained data (Kroell et al. 1974).

B1.1.3 Skeletal Versus Total Deflection. In all thorax response plots presented so far, the deflection used is that of "total chest deflection" measured as the change in distance from the surface of the rigid impactor to the back of the cadaver. In a test device such as Hybrid III, the chest deflection measured by the transducer is an "internal" deflection of the ribs and does not include the deflection of the skin and any padding which represent the soft tissues external to the cadaver ribcage which are included in "total deflection." In the evaluation of internal response elements (e.g., dampers) or ribs, where padding is not provided or is not included in the deflection measurement, the deflection portion of the response curves must be modified to reflect the "internal" or "skeletal" deflection that is being measured. Lobdell et al. (1972) have recommended that 1.3 cm (0.5 in) be subtracted from the total deflections obtained at 6.7-m/s impacts. Figure 10 shows the recommended corridors developed by Neathery (1974) for 4.3- and 6.7-m/s impacts.

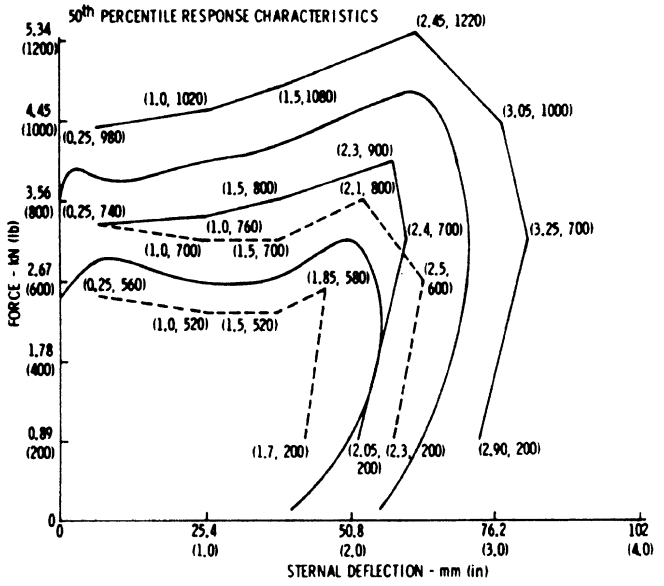

FIGURE 10. Averaged adjusted skeletal force-deflection corridors for 4.3- and 6.7-m/s impacts (Neathery 1974).

B1.1.4 Kroell Impact Response Characteristics at Other Regions. The Kroell impact conditions and results described above have become the standard for characterizing the dynamic response of the human chest. Until recently, however, data were only available for impacts to the lower sternal region (i.e., level of 4th interspace) on the midline. Over the past year, additional Kroell-type tests have been conducted at Wayne State University for General Motors Research Labs in which the thorax and abdomen were impacted lateral to the midline at two different levels as well as on the midline below the sternum (Viano 1988, unpublished; preliminary results of data subsequently published in Viano 1989b). The impact sites are illustrated in Figure 11 and include:

1. Impact at an angle of 60° to frontal 7.6 cm (3 in) below the xiphoid process and in the region of the lower ribcage (i.e., ribs 7 through 10).

2. Impact at the midline at about 7.6 cm (3 in) below the xiphoid process.

3. Impact at an angle of 60° to frontal at the level of the xiphoid process.

Impact at an angle of 60° to frontal 7.6 cm (3 in) below xiphoid process and in region of lower ribcage (i.e., ribs 7–10).

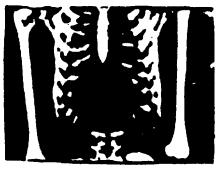

Impact at the midline at 7.6 cm (3 in) below xiphoid process.

Impact at an angle of 60° to frontal at the level of xiphoid process.

FIGURE 11. Abdominal and thoracic impact areas for new Kroell-type tests conducted at Wayne State University for GM (Viano and Lau 1988).

Results from the 60°-angle tests, along with the original Kroell data, have been reanalyzed and normalized for body weight (Viano and Lau, personal communication). Figures 12 through 14 show and compare the results for the three regions for tests with a 23.4-kg impactor at 6.7 m/s. It should be noted that these curves have *not* been adjusted for muscle tension or internal deflection. The increased dynamic compliance, both in terms of initial stiffness and plateau force, at the lateral thorax and lateral abdomen are readily apparent.

While the angle of these tests is more lateral than desired for definition of a frontal dummy, they offer the best available data for characterizing the impact response of the lower thoracic cage lateral to the midline. It will be noted that the initial stiffness and plateau values are similar for the lateral thorax and lateral abdomen regions. As shown in Figure 15, Viano and Lau have extrapolated from the lower ribcage data and suggest that results at 30-degrees-to-frontal would be similar to those obtained at 60-degrees-to-frontal. In the absence of other data, these will be used to define preliminary the dynamic response characteristics of the new thorax in the regions of the liver and spleen.

Figure 16 compares the impact response F-δ corridors for the sternum and lateral thorax where deflection at the impacted site is measured relative to a point on the opposite side of the ribcage taken along the direction of the impact. Since the lateral impacts were not aimed at the spine, the deflections achieved may be larger than those that would result from frontal impacts to the lower ribcage. In the latter, the tissues would compress against the spine and thereby limit peak deflection. Thus, some reduction in the deflection portions of the lateral response curves may be appropriate for a frontal impact dummy.

To date, four impact tests have been conducted three inches below the xiphoid process on the midline, including two at about 4.3 m/s and two at approximately 6.7 m/s. Complete results from these tests are not yet available. Preliminary analysis of the data, however, produced the peak values shown in Table 7 (Viano, personal communication, May 1989). In test #49, peak spinal accelerations of 6.14 Gs and 4.5 Gs were obtained at T8 and T12, respectively, while in test #53 the peak spinal accelerations were only 2.2 Gs and 1.92 Gs. Apparently, the impactor did not pick up much, if any, of the ribcage, and the low dynamic stiffness (i.e., low force, high deflection) indicated by the values of Table 7 result from compression of soft abdominal tissue.

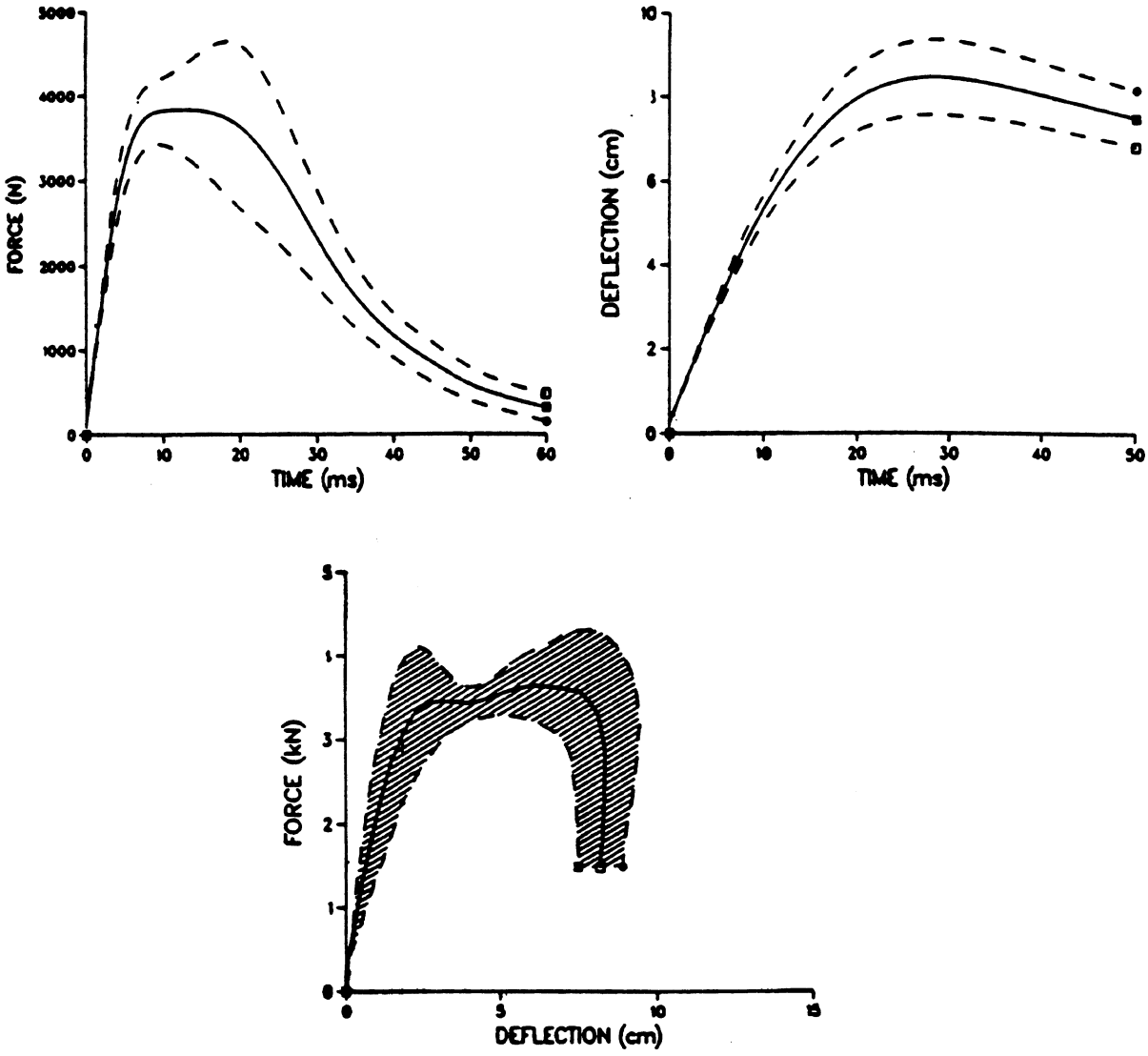

FIGURE 12. Results from 6.7 m/s Kroell frontal impact tests to sternum. Data reanalyzed by Viano and Lau (1988).

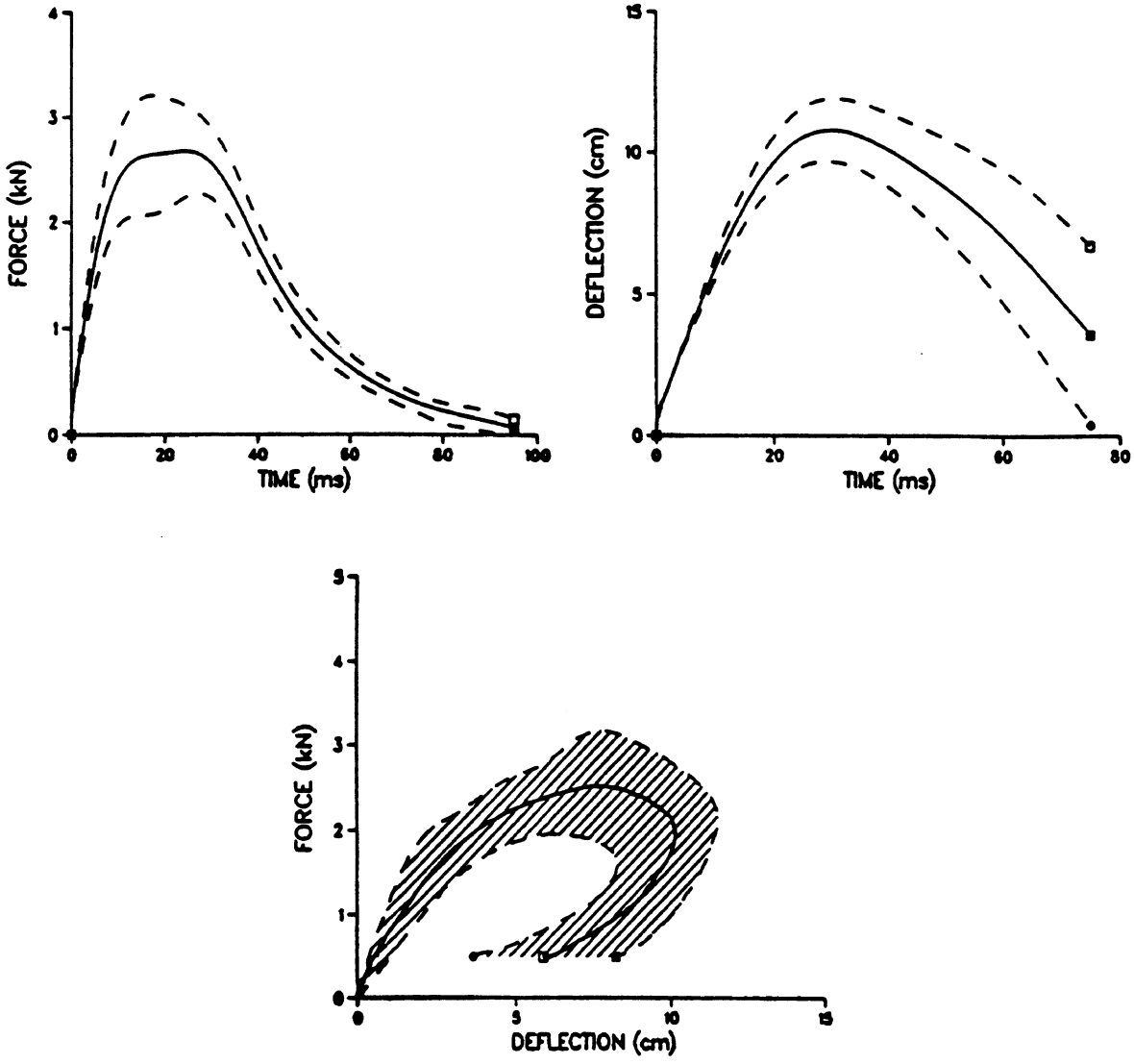

FIGURE 13. Results for Kroell-type impacts at 6.7 m/s to *lateral thorax* (configuration #1), 60°-to-frontal (Viano and Lau 1988).

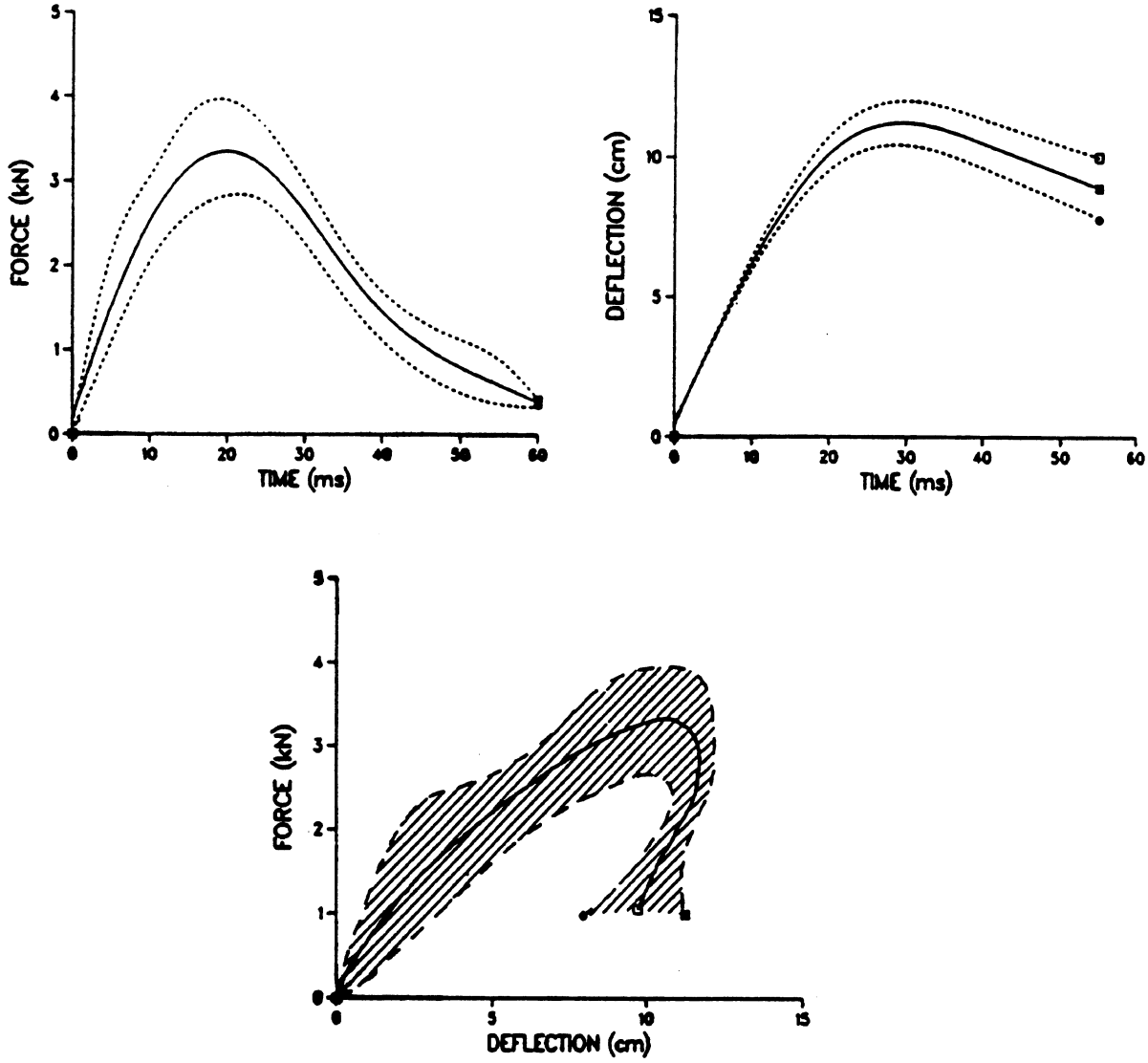

FIGURE 14. Results for Kroell-type impacts at 6.7 m/s to *lateral abdomen* (configuration #2), 60°-to-frontal, 15.3 cm (6 in) below mid-sternum (Viano and Lau 1988).

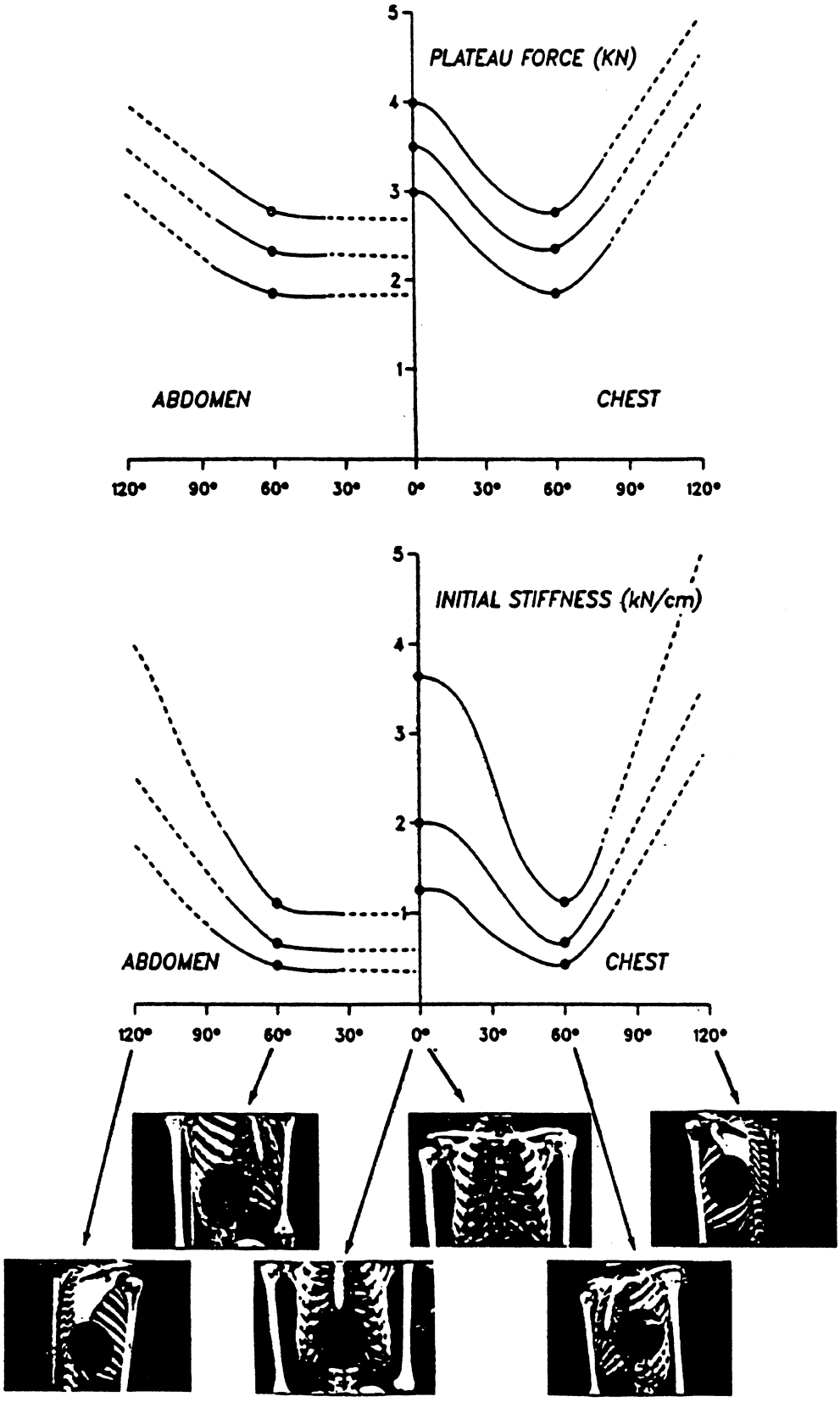

NOTE: Dashed lines indicate regions where no data are available. Center curves indicate mean values. Upper and lower curves indicate mean values ± one standard deviation.

FIGURE 15. Initial stiffness and plateau force for 6.7 m/s Kroell-type impacts to different regions of the thorax (Viano and Lau 1988).

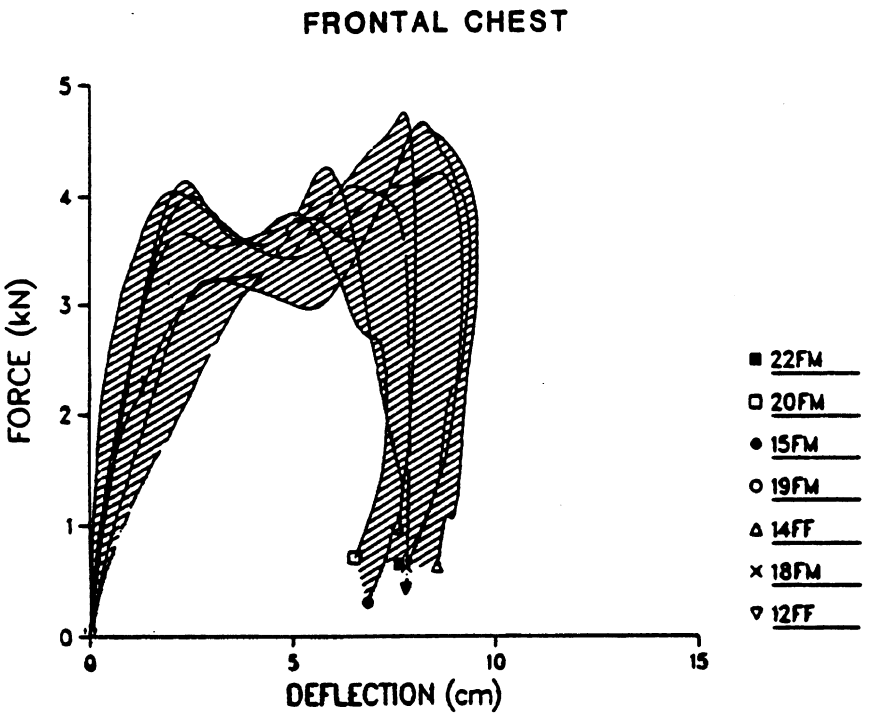

Results from reanalyzed Kroell (1974) impact data from frontal impact to the sternum.

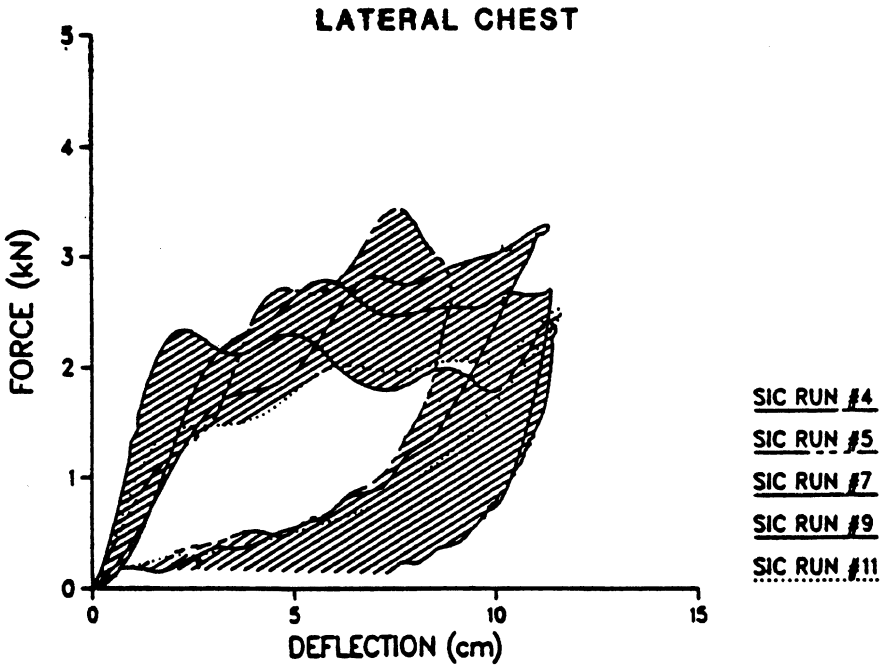

Results from new impact data for 60° impacts to the lateral thorax at the level of the xiphoid process.

FIGURE 16. F-δ corridors for 6.7 m/s tests at the sternum and lateral thorax at the level of the xiphoid process (Kroell 1974 data reanalyzed by Viano and Lau 1988). The latter may be used as an estimate for the frontal F-δ response corridor of the lower cage.

TABLE 7

PRELIMINARY RESULTS FROM GM/WSU KROELL IMPACT TESTS
6.5 CM (3 IN) BELOW THE XIPHOID PROCESS
ON THE MIDLINE (Viano, May 1989)

Test No.	Impact Velocity	Peak Force	Peak Deflection	Outside Dimension	Percent Deflection
49	4.3 m/s	1.99kN	11.0 cm	29.4 cm	37.2%
53	4.5 m/s	1.75kN	15.6 cm	35.5 cm	43.9%
56	6.7 m/s	5.6 kN	9.5 cm	24.7 cm	38.3%
59	6.7 m/s	3.4 kN	12.9 cm	26.4 cm	48.8%

B1.1.5 Other Response Data to Pendulum Impacts. In addition to the thoracic response data described above for an impactor mass of 23 kg (51 lb), it is important to be able to evaluate the thorax response for other impactor mass and velocity combinations. While no response corridors have been developed for these other test conditions, some force-deflection data do exist that demonstrate the types of response changes one should design for under different loading conditions.

Figure 17 is taken from Lobdell et al. (1973) and shows the different responses obtained for lower impactor masses which result in lower total deflections. As indicated by curves 26FM and 28FM, in which the impactor masses were 1.86 kg (4.1 lb) and 1.64 kg (3.6 lb), and the velocities were 11.2 and 14.5 m/s (25 and 32.4 mph), respectively, the responses show an initial peak in force, followed by decreasing force with increasing deflection to about two inches of total deflection. Apparently, with the lower deflections, the elastic stiffness component does not come significantly into play, since there is no "bottoming out" and the viscous nature dominates, resulting in decreasing load with decreasing velocity.

Figure 18 shows force-deflection curves obtained by Patrick (1981) from impacts to a volunteer with a 10 kg (22.1 lb), 15.3-cm- (6-in-) diameter padded striker (2.4 cm of Rubatex R310V padding) at impact velocities from 2.4 to 4.6 m/s. The data were generated under similar conditions as the Kroell unrestrained-back tests, except for the lower impactor mass and the presence of padding, and demonstrate similar force-deflection response curves. The initial dynamic stiffness ranges from 56.9 N/mm (325 lb/in) at 2.4 m/s for a relaxed subject to 245.2 N/mm (1400 lb/in) at 4.6 m/s for a tensed subject. Figure 19 shows the relationship between maximum impact force and impactor velocity under these conditions. These volunteer data provide additional guidance for thoracic response definition at sub-injury levels of dynamic loading.

B1.1.6 Impact into a Steering System. Cadaveric response data for thoracic impact into a steering wheel were published recently by Morgan et al. (1987), who performed eleven cadaveric impacts, three at 24 km/hr, one at 34 km/hr, and seven at 40 km/hr. Details of the test configuration were not given in the paper. Time traces of column force and resultant chest acceleration were provided but chest deflection data were not available. Figures 20 and 21 show plots of time traces of column force and resultant chest acceleration for cadaver tests made at 24, 34, and 40 km/hr, including a corridor for the 40 km/hr test velocity. The data had been scaled using the constant-velocity scaling method. The test configuration simulated the driver's compartment of a Chevrolet Citation.

Unpublished data of thoracic response to steering wheel impact are also available from Wayne State University (Begeman 1988). Tests were conducted with both collapsible and

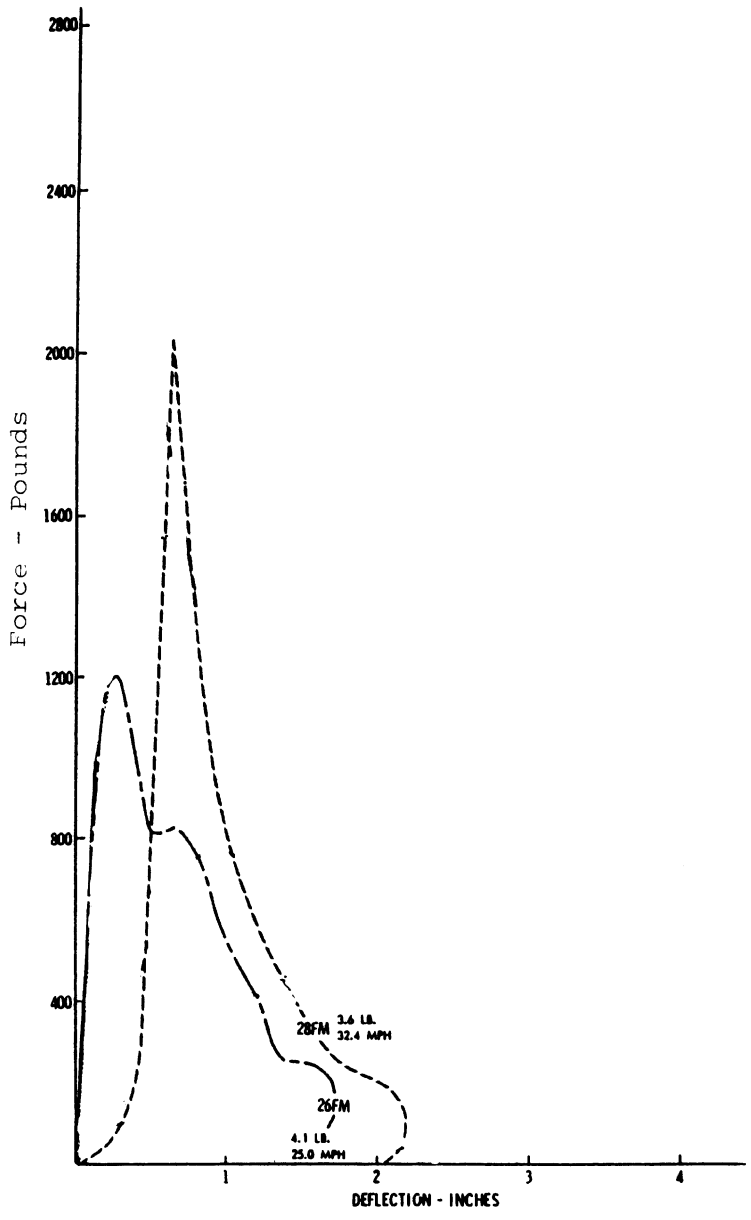

FIGURE 17. Response for low-mass impactor resulting in lower total deflections (Lobdell et al. 1973).

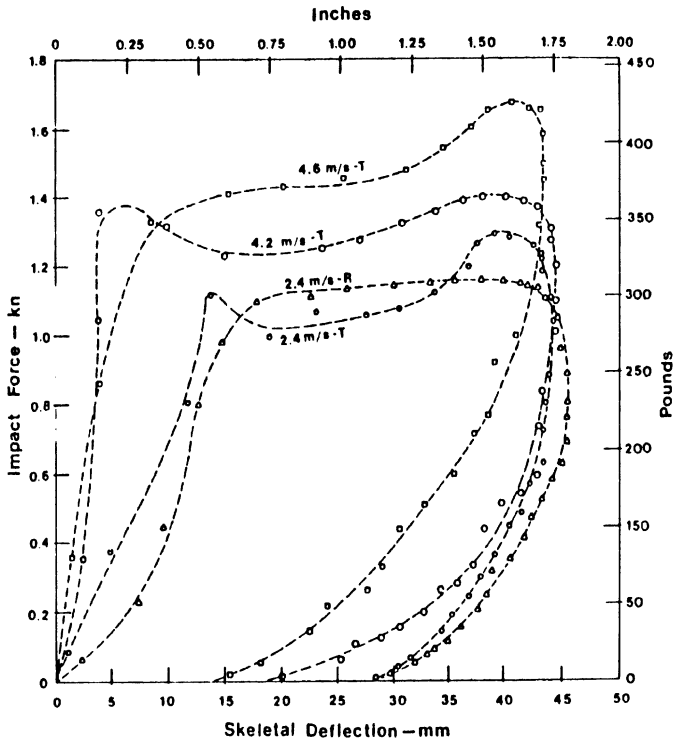

FIGURE 18. Load-deflection of thorax, human volunteer, mid-sternum impact with a 10-kg, 15.3-cm- (6-in-) diameter padded striker at 2.4 to 4.6 m/sec (Patrick 1981).

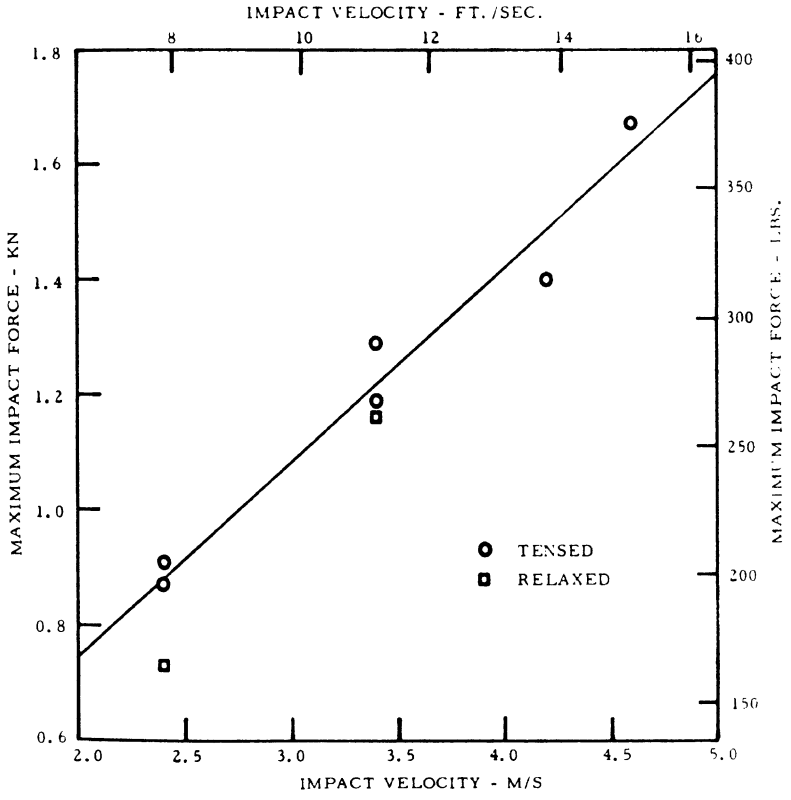

FIGURE 19. Maximum force as a function of impact velocity for human volunteer (Patrick 1981).

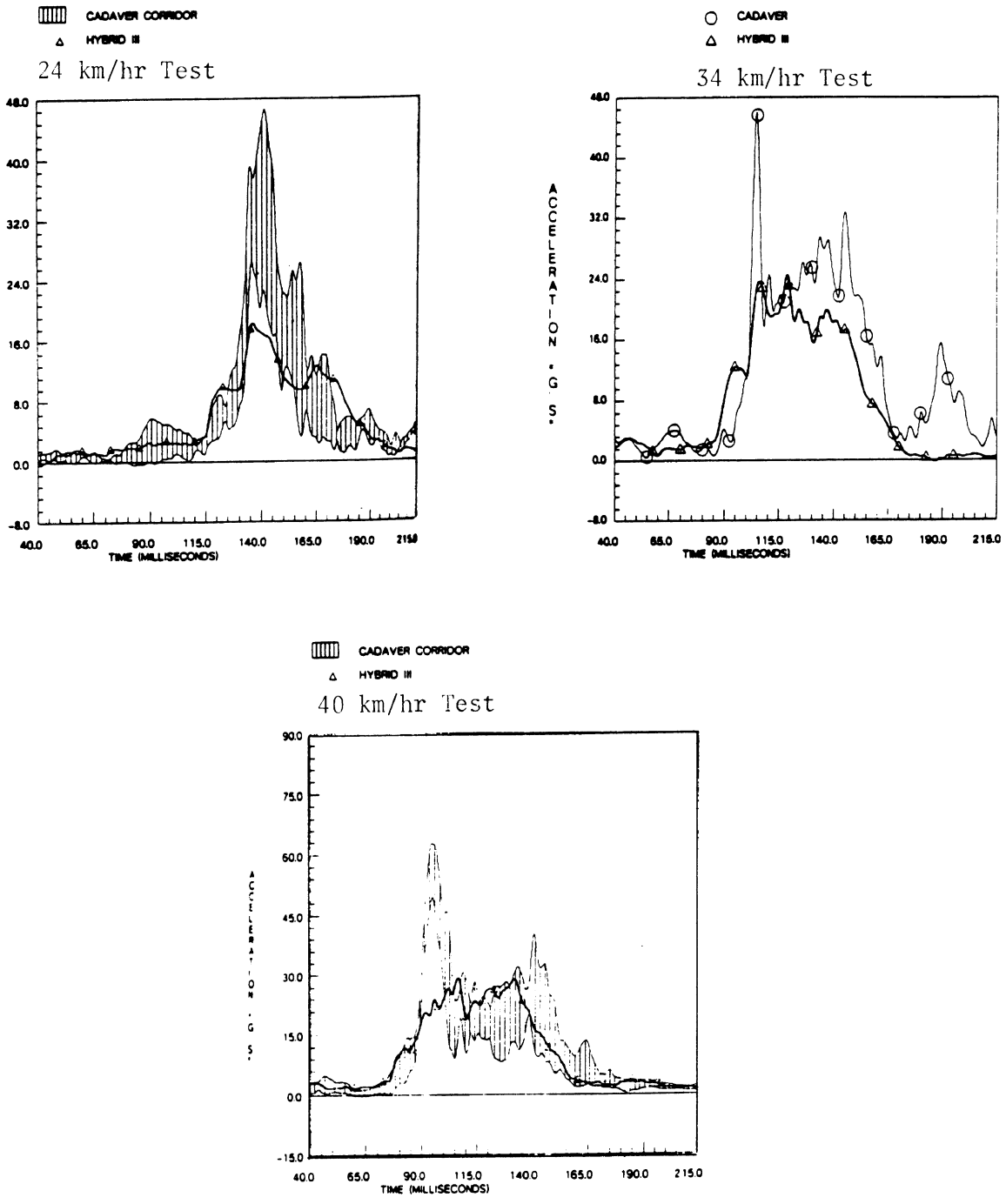

FIGURE 20. Chest acceleration versus time for unrestrained cadaver impacts into steering wheel—CIRA sled tests (Morgan et al. 1987).

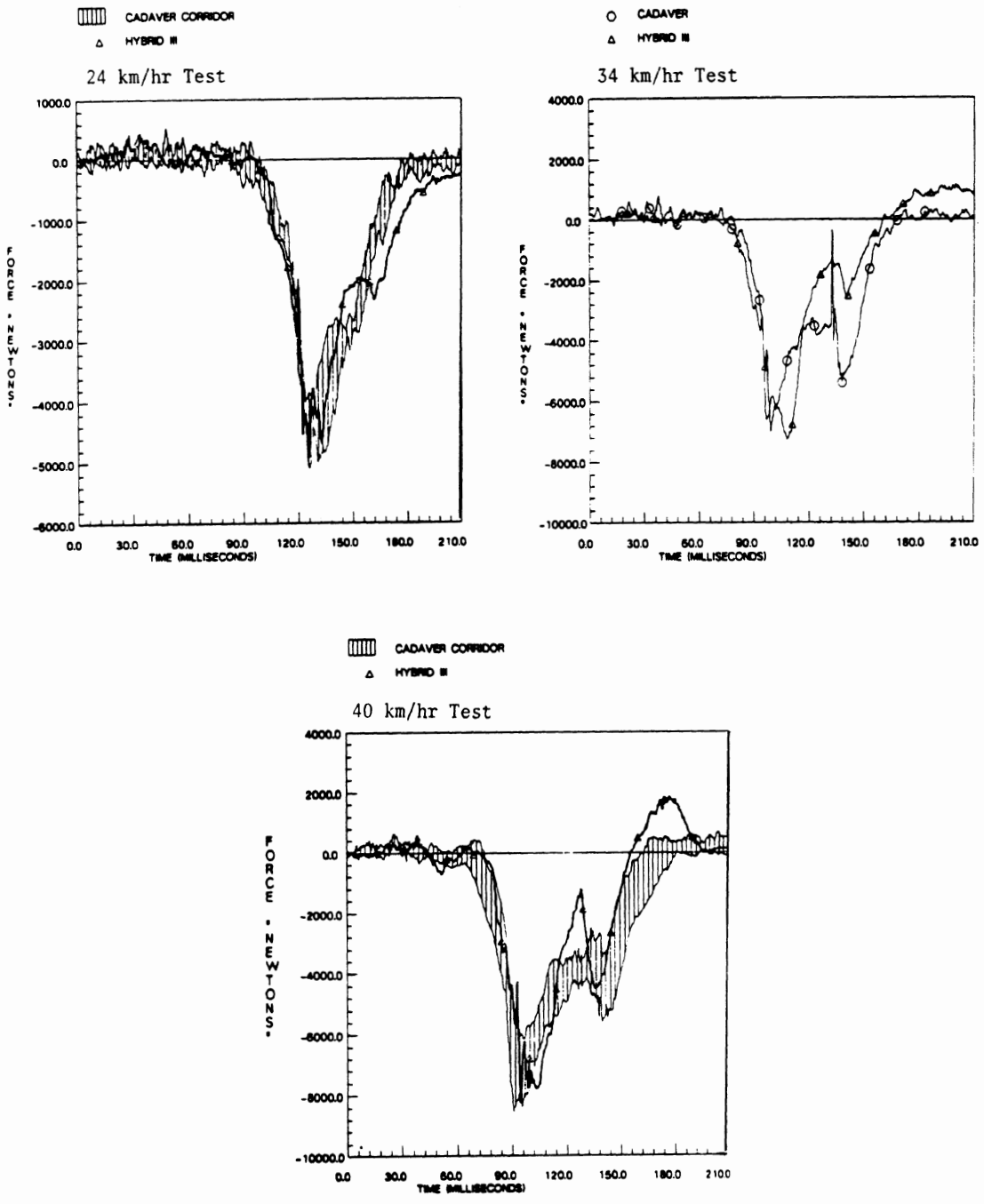

FIGURE 21. Column force versus time for unrestrained cadaver impacts into steering wheel—CIRA sled tests (Morgan et al. 1987).

non-collapsible steering columns at approximately 40 km/hr (11 m/s). The test configuration is shown in Figure 22. For the rigid-column tests, rim load was computed from the measured hub and column load.

Figure 23 shows a series of normalized force-deflection curves for the rigid-column impacts. The loads and deflections are higher than those of the Kroell corridor but the chest accelerations, as measured at the level of T8 on the spine, were within the 60-G, 3-ms FMVSS limit. The chest AIS for all four cadavers was between 2 and 4. Rim load was approximately 50% of the total column load. An attempt was made to cross plot force-time and deflection-time traces to obtain force-deflection curves for the collapsible column tests, but the curves were unrealistic and were not considered reliable or accurate enough to be used in this specification package.

B1.1.7 Impact Response to Two- and Three-Point-Belt Loading. While the importance of ATD interaction with two- and three-point-belt systems and inflatable airbags will be increasing in the years ahead, data describing the biomechanical response of the thorax to these types of loading are sparse. Thus, at the present time, the primary dynamic response requirements for impact loading of the thorax must necessarily be the Kroell-type data described in the previous sections. Nevertheless, it is useful to examine the limited data that are currently available for shoulder belt loading.

Dynamic belt-response data have been summarized by Melvin and Weber, ed. (1988). For a 43.5-km/h (27-mph) sled impact test, Fayon et al. (1975) found a sternal thoracic stiffness of 166.4 N/mm (951 lb/in) by calculating the resultant normal force from the geometry and tensions in the belt ends. Walfisch et al. (1982) report similar dynamic stiffness measures of the sternum due to sled test belt loading of five cadavers. Stiffnesses between 70 N/mm to 161.1 N/mm (400 to 920 lb/in) for deflections up to 5 cm (2 in) were estimated, with a mean stiffness of 119.4 N/mm (682 lb/in).

Recognizing the need for more information about the response of the thorax to belt loading for use in ATD design, L'Abbe et al. (1982) conducted a series of static and dynamic experiments with belt loading of the chests of volunteers in the supine, seated position. Chest deflections were measured at eleven different sites on the thorax as illustrated in Figure 24. Tests included both static point loading using a 3-cm- (1.2-in-) diameter steel pad as well as static and dynamic belt loading (see Section B1.1.10 for static results). Summarizing the results of L'Abbe et al. tests, Melvin and Weber, ed. (1988) report that dynamic loads were applied up to 3600 N (810 lb) and produced "apparent" stiffnesses (i.e., deflection versus maximum total belt load) of 137 N/mm (785 lb/in) at the mid-sternum, 123 N/mm (703 lb/in) at the right 7th rib, and 200 N/mm (1142 lb/in) at the left clavicle.

Figures 25(a) and 25(b) show scatter plots of maximum total belt force versus maximum deflections at the eleven measurement sites in the L'Abbe et al. tests and compare the results with the Hybrid III ATD. The authors note good agreement between the Hybrid III and the tensed subjects at the mid-sternum, but indicate the need for an ATD surrogate that would provide better agreement to the human at many of the other sites. In particular, the Hybrid III shoulder with soft tissue covering appears to be too soft and the stiffness at the lower ribs is to high. Also, the human torso demonstrates elastic expansion on the unloaded side while the Hybrid III shows inward deflection (i.e., compression). The authors point out the importance of achieving improvements to the dummy in these regions to accurately assess the possibility of clavicle fractures and reliably simulate whole-body kinematics and belt loading during crash testing. Additional data from similar experiments using unembalmed cadavers in which higher loading rates were used and larger deflections were produced have recently been collected at INRETS and will be available soon.

The only data available on two-point/knee-bolster restraint loading of the human thorax/abdomen system are from a series of eleven cadaveric tests carried out at Wayne State University using a Volkswagen passive-belt and knee-bolster system. The results were

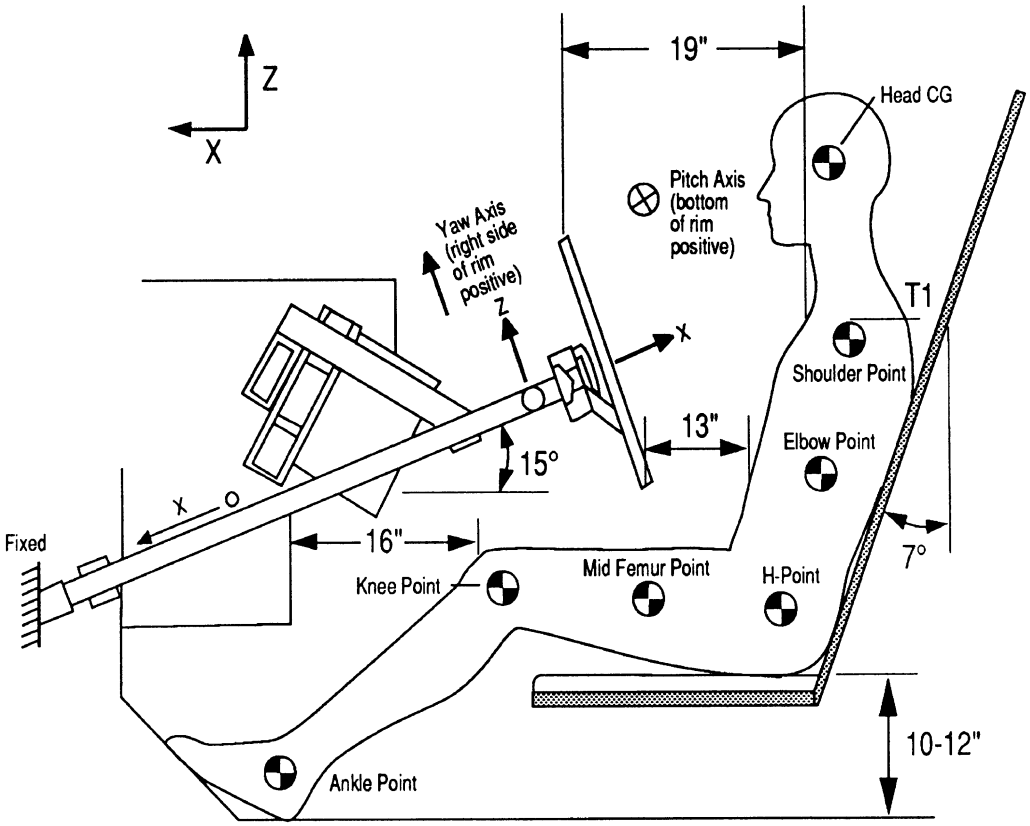

FIGURE 22. Wayne State University test setup for cadaver impacts into non-collapsible steering columns at 40 km/hr. (Begeman 1988).

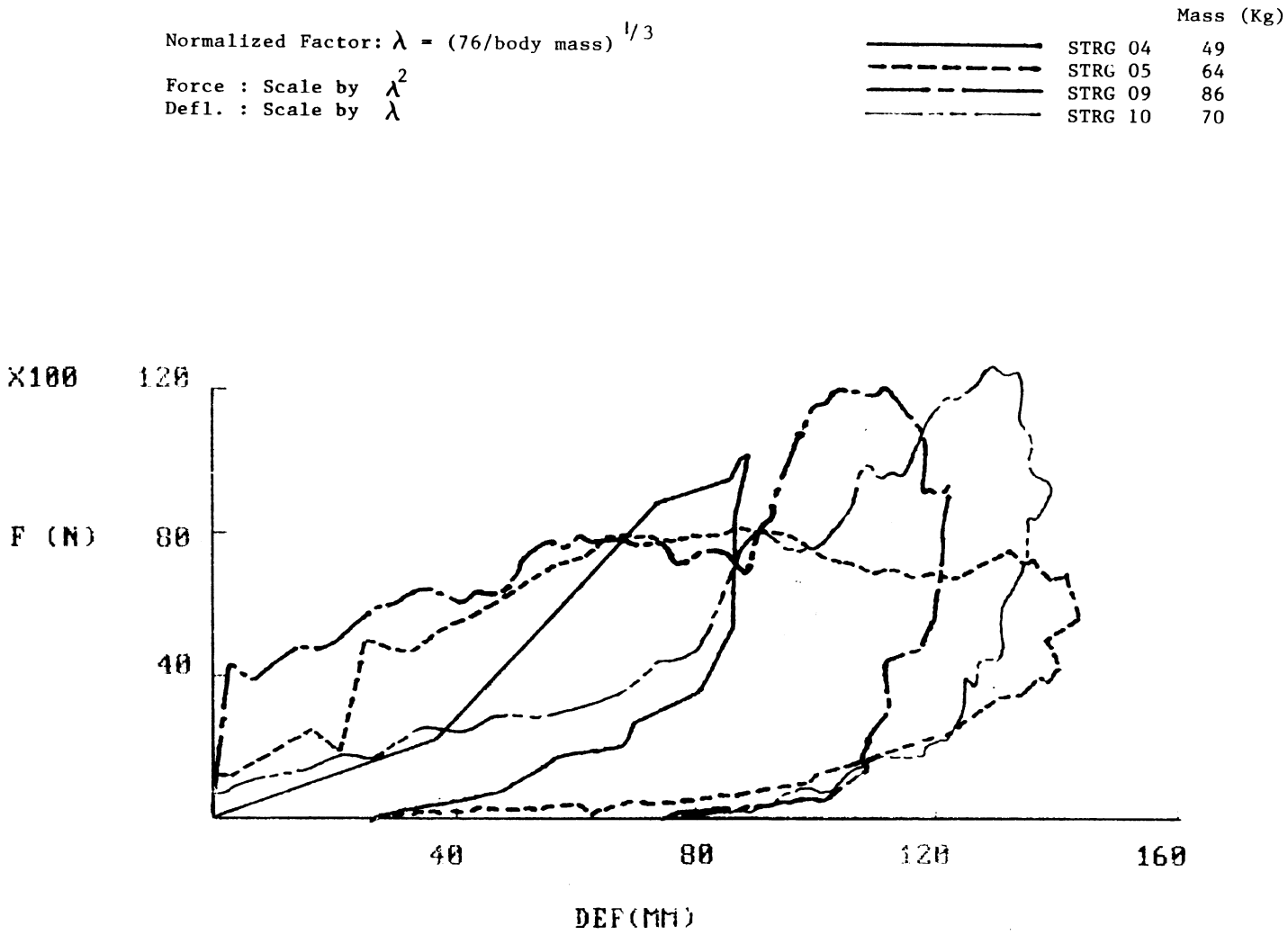

FIGURE 23. Normalized force-deflection curves for the rigid-column Wayne State University tests (Begeman 1988).

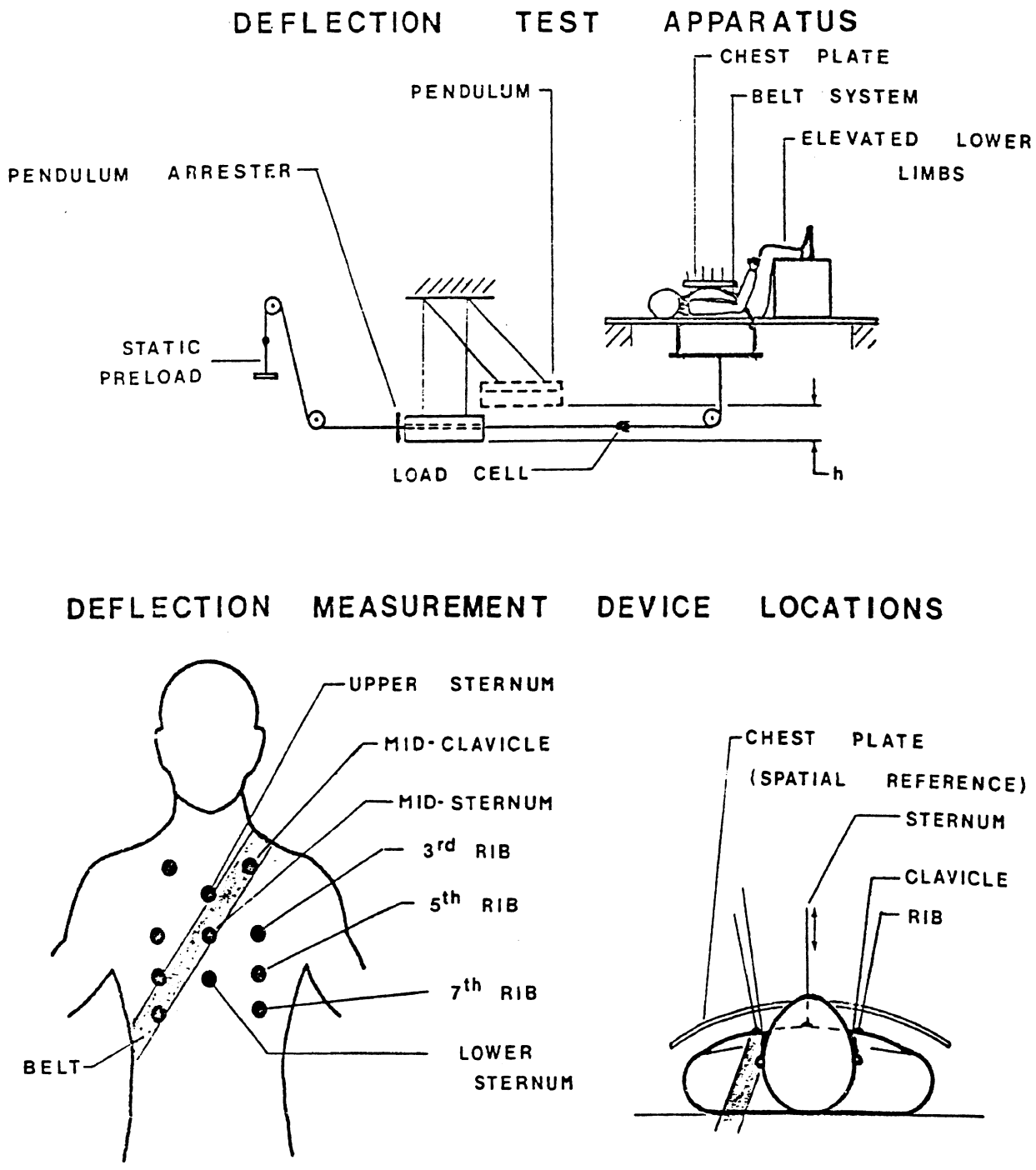

FIGURE 24. Test setup and chest deflection measurement sites for L'Abbe et al. tests (1982).

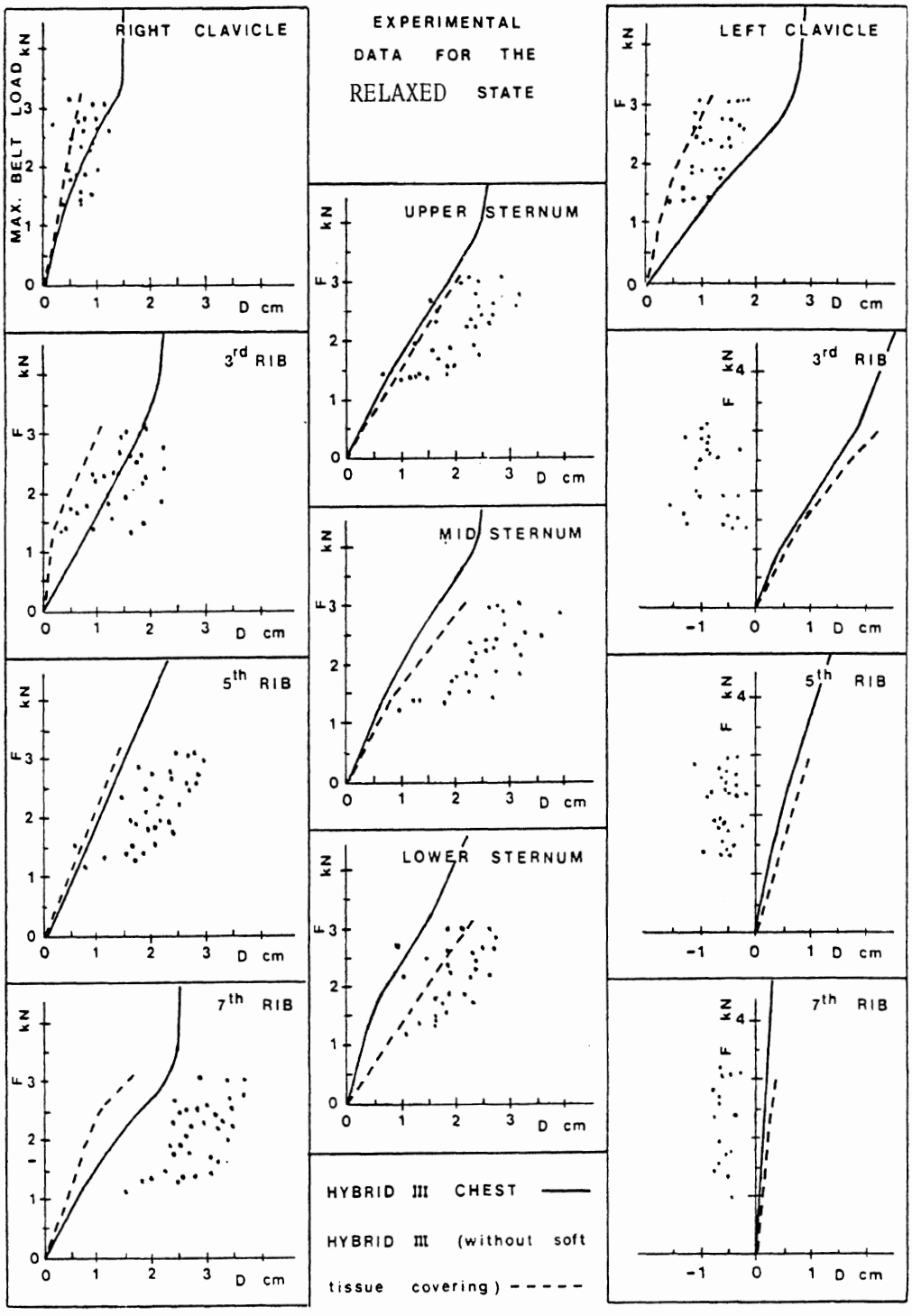

FIGURE 25(a). Maximum force versus maximum deflection for Hybrid III and human volunteers—*relaxed* state (L'Abbe et al. 1982).

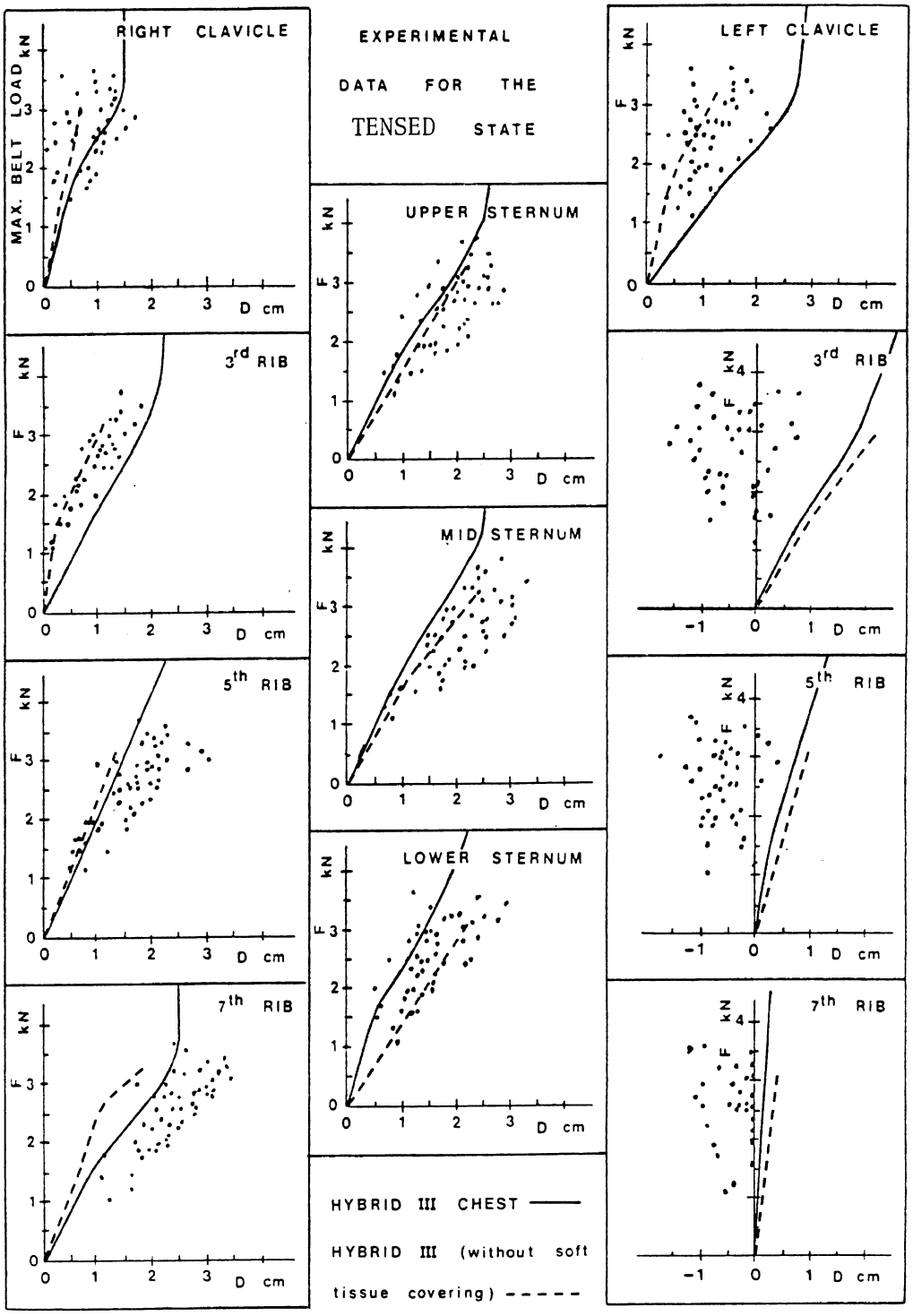

FIGURE 25(b). Maximum force versus maximum deflection for Hybrid III and human volunteers—*tensed* state (L'Abbe et al. 1982).

reported by Cheng et al. (1984). The test configuration is shown in Figure 26. The belt geometry was based on the anchorage location in a 1983 VW Rabbit equipped with a passive belt system. There were no force-deflection data because chest deflection was not measured. Time traces of upper and lower shoulder-belt anchor loads are shown in Figure 27. The peak upper shoulder-belt anchor load was in the range of 5.1 to 7.6 kN (1,146 to 1,708 lb) for 48 km/hr (30 mph) BEV impacts with a peak deceleration of 22 G. The peak belt loads ranged from 3.6 to 9.7 kN (809 to 2,181 lb) for four runs made at a peak deceleration of 35 G. The ratio of lower belt load to upper belt load was approximately 90%.

B1.1.8 Impact Response to Airbag Loading. Force-deflection data of the thorax for cadaveric impact with an airbag are not available. In a series of tests of a predeployed driver airbag performed at Wayne State University and reported by Cheng et al. (1982), the peak steering column force was found to be in the range of 8.5 to 16.0 kN (1,910 to 3,600 lb) for peak sled decelerations of 32 to 39 G. The peak airbag pressure ranged from 93 to 139 kPa (13.5 to 20.2 psi). The column was rigid and horizontal and the steering wheel was mounted normal to the column. The test configuration is shown in Figure 28. These data represent a severe impact with a driver airbag which resulted in injuries with a rated maximum AIS of 2 to 6. However, the chest AIS range was from 0 to 2. Figure 29 shows time traces of the resultant steering column load and A-P spinal acceleration, respectively, at the level of T12. It should be noted that column load will be influenced by the magnitude of knee loads. Figure 30 shows the left and right knee loads, respectively, for the same tests.

B1.1.9 Impact Response to Large Flat Surfaces. Recent results from cadaver tests at Calspan (unpublished) provide some information about the effect of area of loading on the force-deflection response at the sternum. Unfortunately, the tests were only conducted for larger areas of loading than used in the Kroell tests and not smaller areas. Figure 31 shows the test setup which is similar to that used by Kroell. Two of the tests were for impacts with a rigid 20 cm by 25 cm plate (500 cm^2) and three were for a 17 cm by 20 cm wood plate with an area of 340 cm^2. The impactor mass in all tests was about 25 kg (55 lbs) and the impactor velocities were about 6.7 m/s (22 ft/s) for the large plate and about 10.1 m/s (33 ft/s) for the small plate. Preliminary results are shown in Figure 32 which shows the force-deflection curves for five tests. The higher stiffnesses and lower total deflections obtained with the larger surface area is readily apparent.

B1.1.10 Static Response Data. The Hybrid III ATD thorax was designed primarily as an injury assessment tool for chest/steering wheel and chest/instrument panel interactions. Its ribcage was therefore appropriately constructed to reproduce the force-deflection loading corridor determined from Kroell tests conducted at 6.7 m/s with the secondary goal of meeting the 4.3 m/s loading corridor. At lower loading velocities and under static loading conditions, however, the Hybrid III chest is considerably stiffer than that of the human.

With the increased use of seat belts that has come about since the development of Hybrid III through state legislation, and the Federal requirement for passive restraint systems in all vehicles of the 1990s (i.e., FMVSS 208), it can be expected that higher loading rates will become less important and lower loading rates, resulting from interaction with shoulder belts and airbags, will become increasingly important. For example, a preliminary analysis of chest loading rates to shoulder-belted cadavers and test dummies during 48–km/hr (30–mph) frontal impacts indicates that peak rates of chest deflection in the range of 1 to 4 m/s can be expected under these conditions. In the new thorax, designing to achieve humanlike biofidelity in response to low loading rates, and even quasi-static loading conditions, may be of equal or greater importance than designing to achieve biofidelity at higher loading rates.

A number of studies have determined the static force-deflection properties of the human chest using both cadavers and living volunteers in relaxed and tensed conditions. Figure 33 shows the results determined by Stalnaker et al. (1973), who applied forces to the

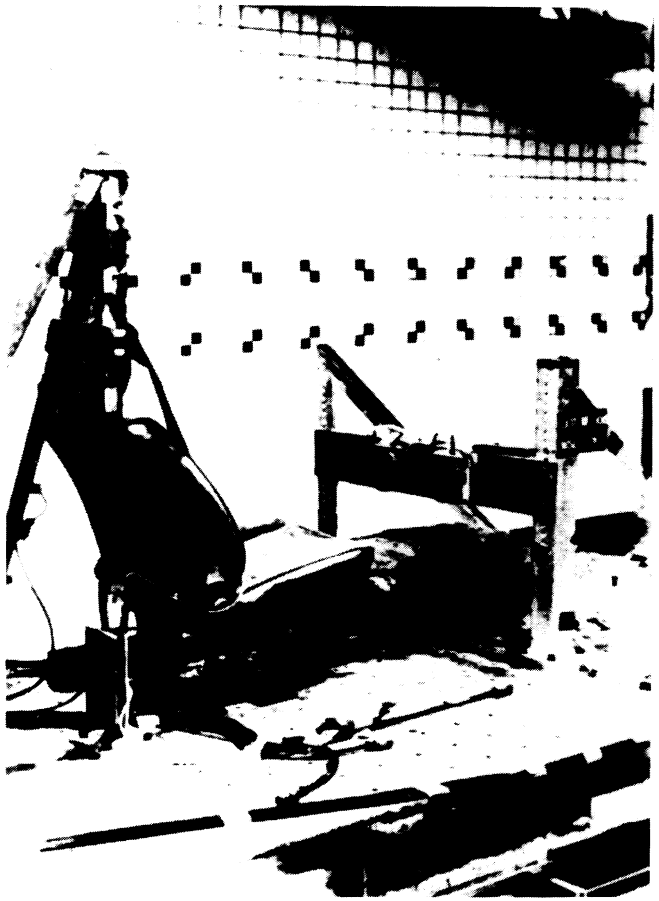

Test set-up for knee bar restraint

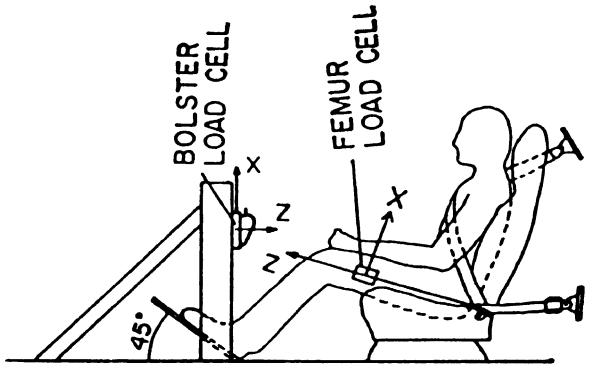

Schematic of test set-up

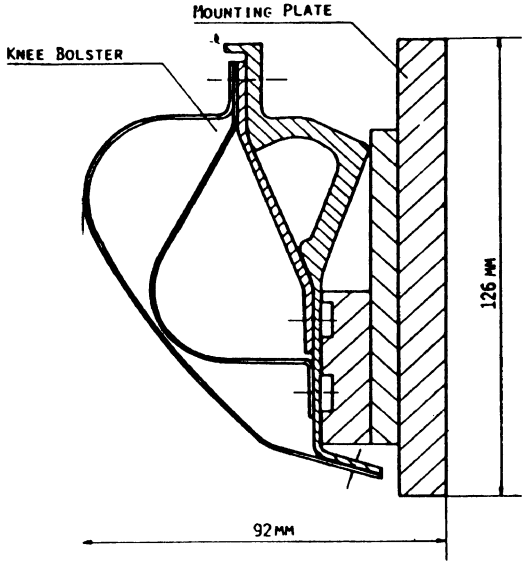

Cross-section of a VW knee bolster

FIGURE 26. Test configuration for WSU two-point-belt/knee-bolster restraint loading of the human thorax/abdomen system (Cheng et al. 1984).

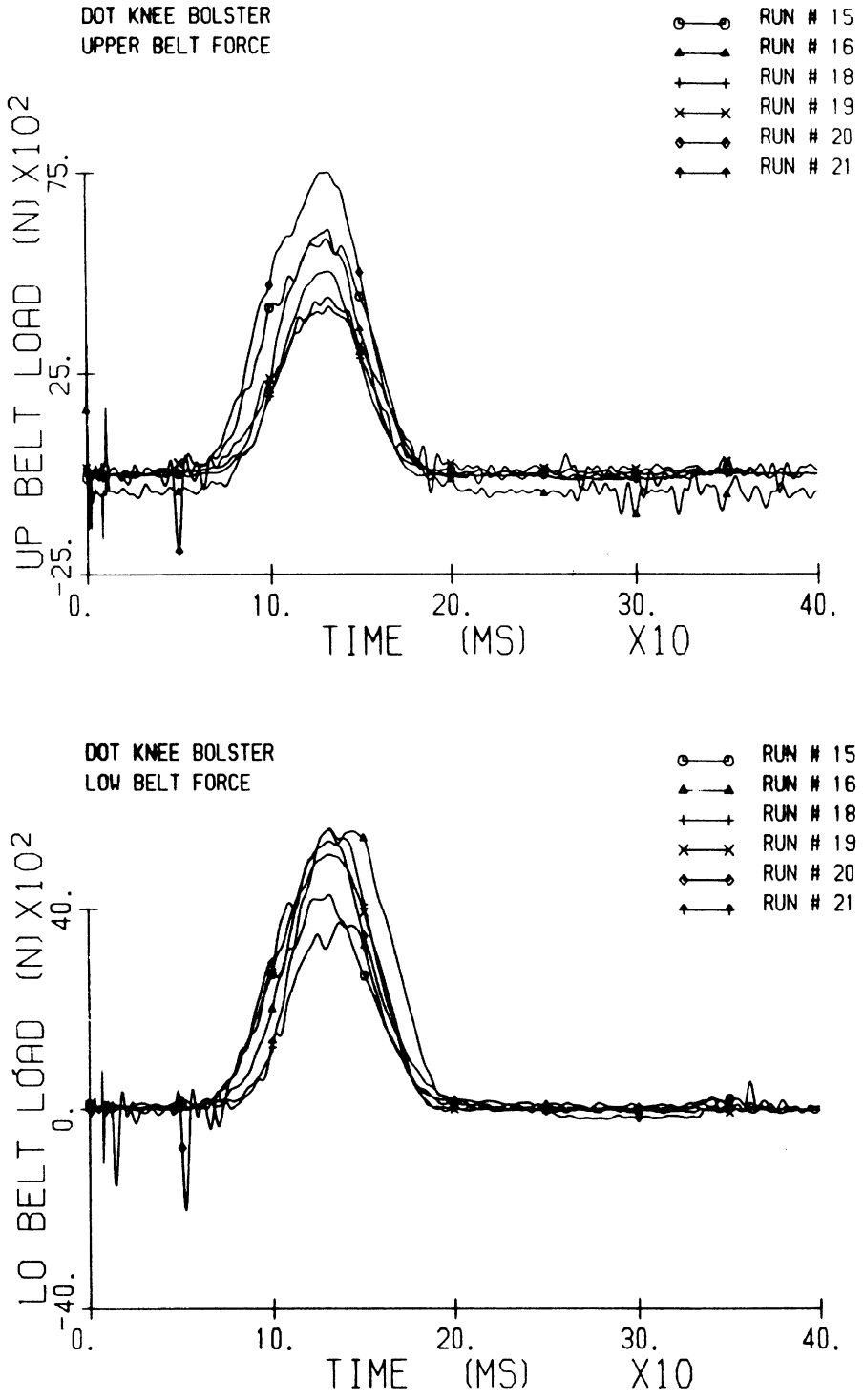

FIGURE 27. Time traces of upper and lower shoulder belt loads for Wayne State University two-point-belt/knee-bolster sled tests (Cheng et al. 1984).

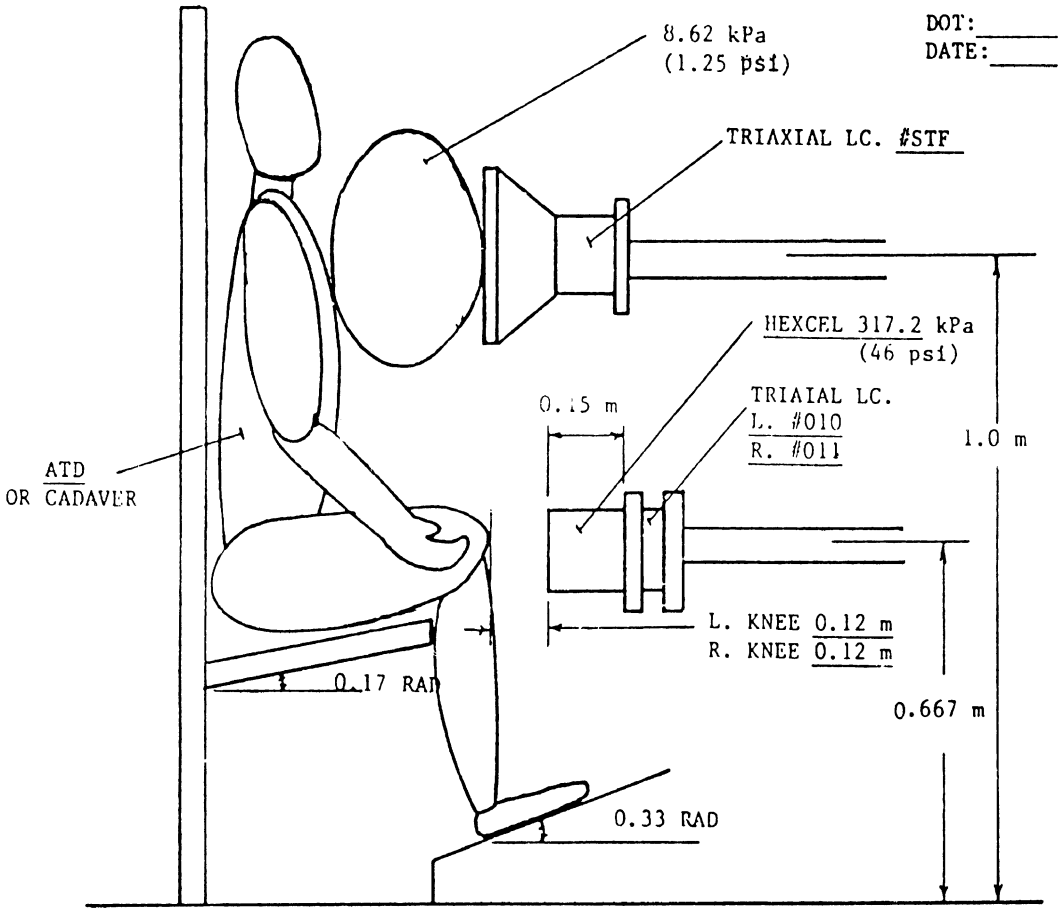

FIGURE 28. Test configuration of WSU airbag sled tests (Cheng et al. 1982).

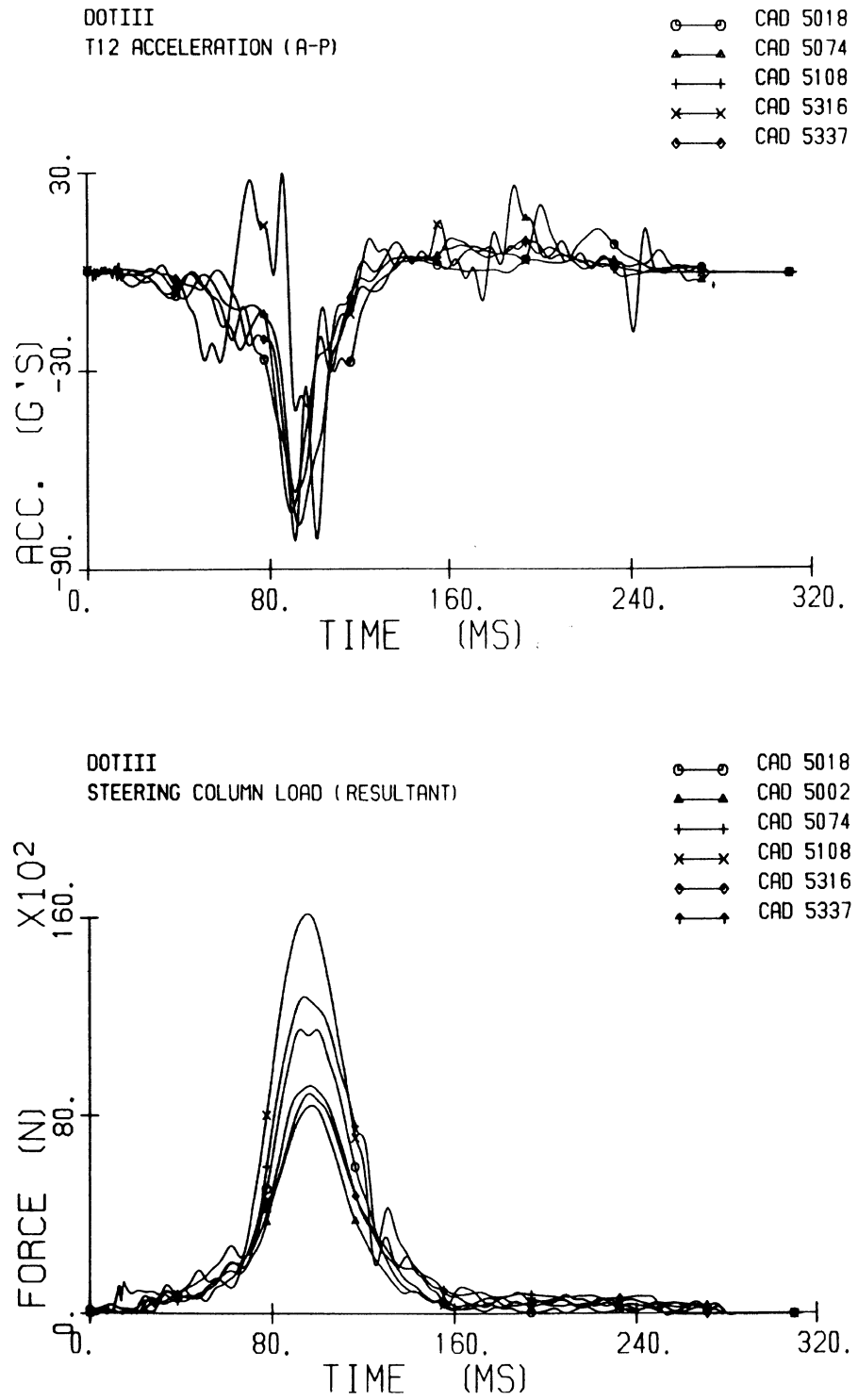

FIGURE 29. Steering column loads and T12 accelerations versus time for WSU cadaver/airbag sled tests (Cheng et al. 1982).

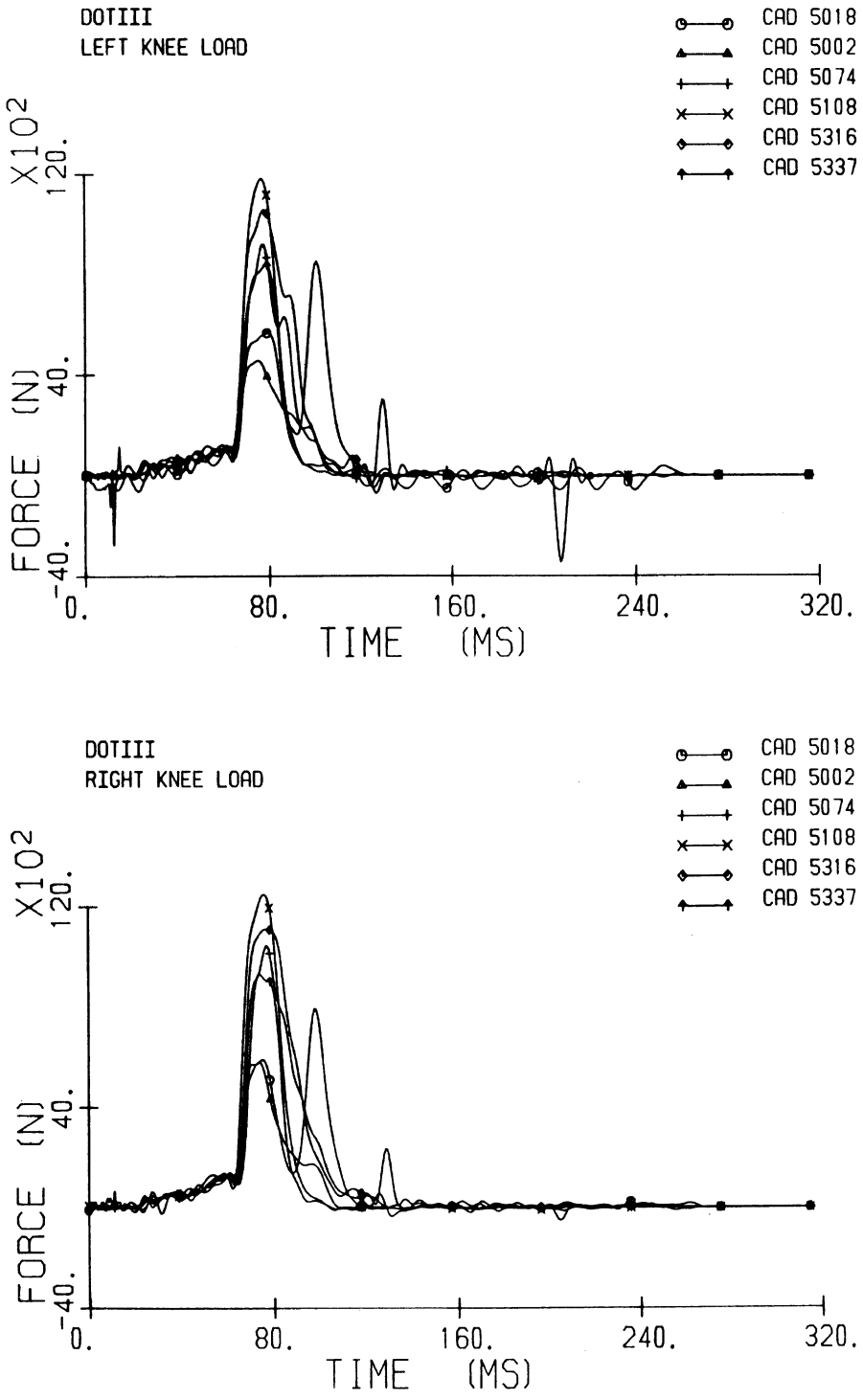

FIGURE 30. Left and right knee bolster load for Wayne State University cadaver/airbag sled tests (Cheng et al. 1982).

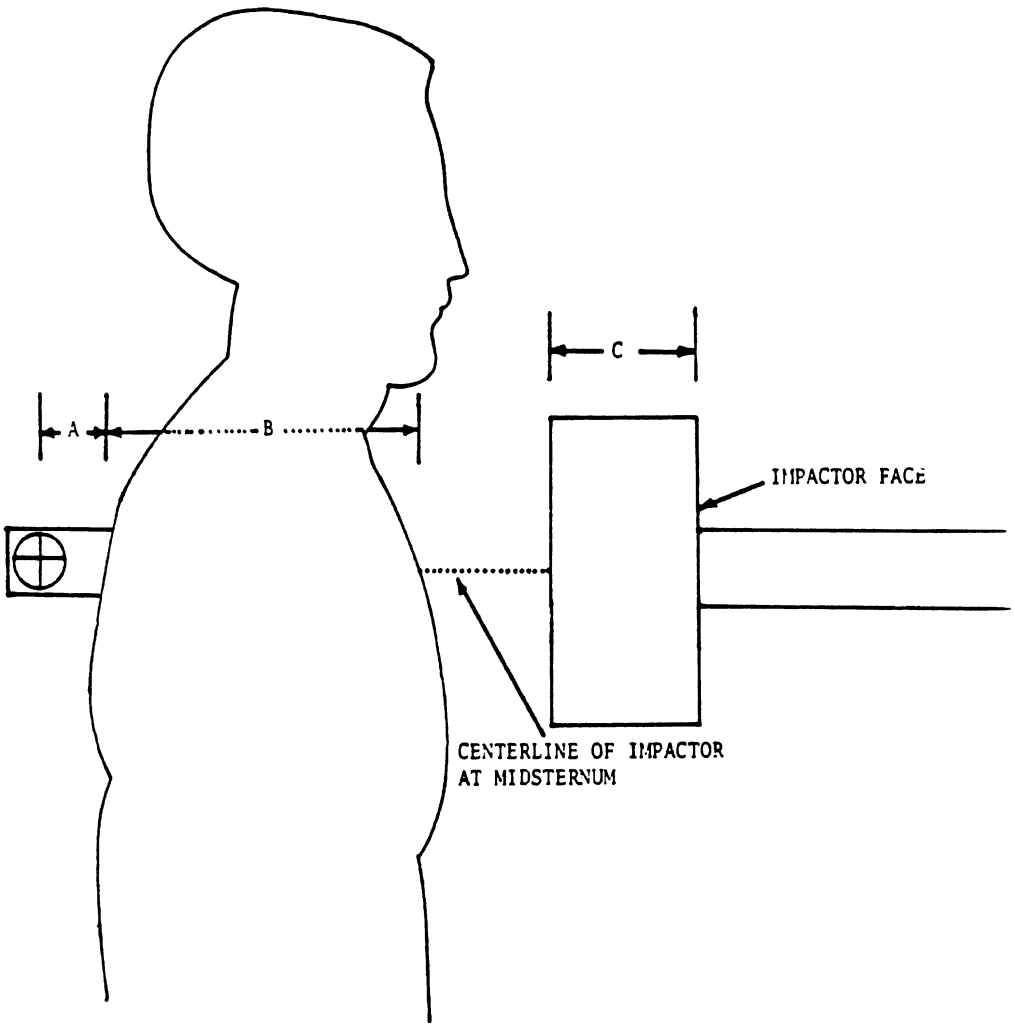

A = Center of target to subject's back
B = Chest Depth
C = Impactor face to reference point

A + B + C = Initial contact point to begin measurement of chest deflection

FIGURE 31. Test setup for Calspan variable-area impact tests.

Force-Deflection Curves

Tests Calman-37, -39, -40: 54 in sq., 21+ ft/sec.

Tests Calman-30, -31: 80 in sq., +/- 30 ft/sec.

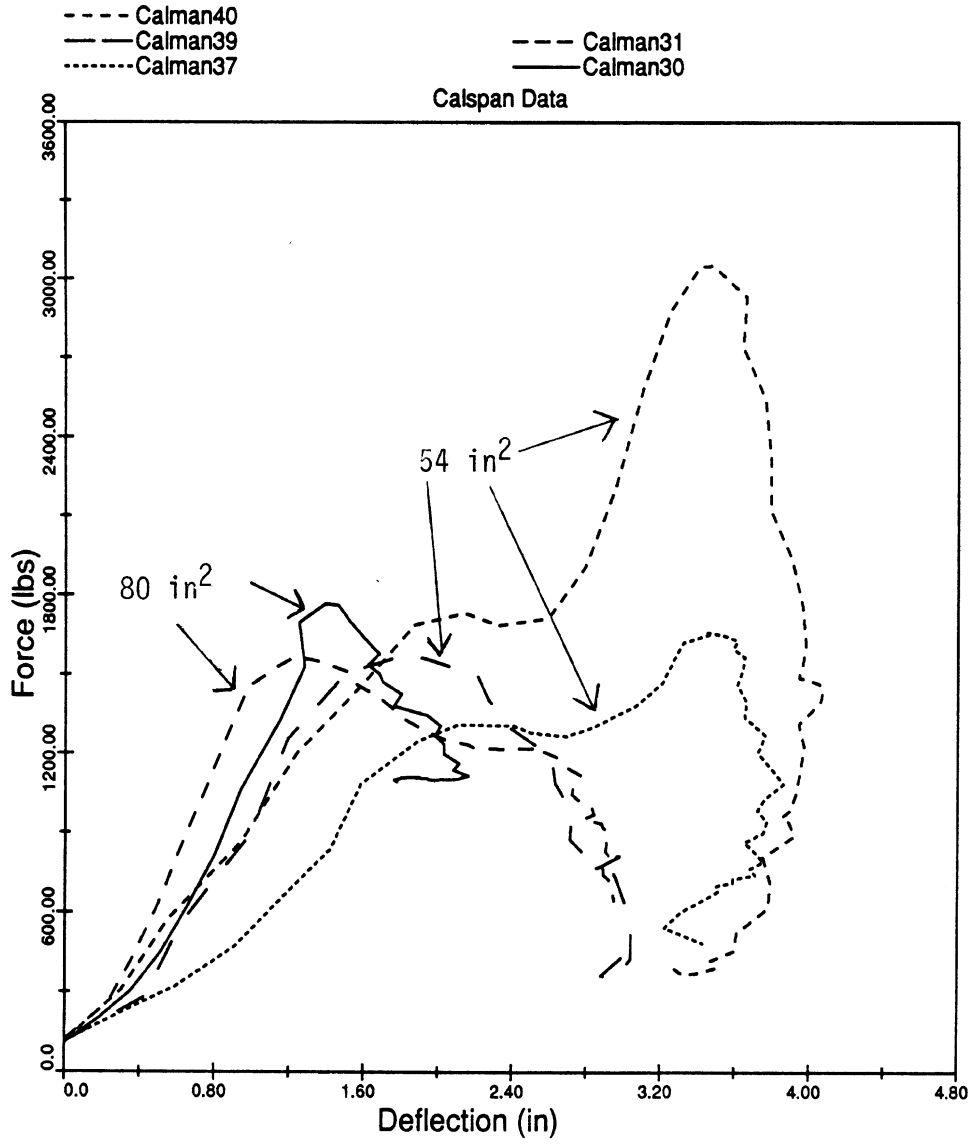

FIGURE 32. Force-deflection curves for Calspan variable-area impact tests to sternal area.

sternal region of volunteers and cadavers using a 15.3-cm- (6-in-) diameter rigid plate. The results obtained with the subject's back against a rigid wall demonstrate the nonlinear nature of the static force-deflection response. The average stiffness ranged from 12.2 N/mm (70 lb/in) for the unembalmed cadaver to 40.2 N/mm (230 lb/in) on relaxed volunteers up to deflections of about 2 cm (0.8 in) and 114 N/mm (650 lb/in) on tensed volunteers up to deflections of only 1.5 cm (0.6 in).

Figure 34 shows static loading corridors reported by Lobdell et al. (1973) for relaxed and tensed volunteers, where again the load was applied to the sternum with a 15.3-cm- (6-in-) diameter rigid plate and the subject's back was fully supported. In contrast to Stalnaker's results, the average stiffness of the relaxed subject was about 7 N/mm (40 lb/in) out to 32 mm (1.25 in) and about 23.6 N/mm (135 lb/in) for the tensed subject.

Additional static or quasi-static loading data have been reported for cardiopulmonary resuscitation types of loading. Tsitlik et al. (1983) have measured the force versus deflection characteristics of the human chest obtained by loading a 6.4-cm x 4.8-cm rubber "thumper" into the sternum of two patients. The curves were fit with a second or third degree polynomial but a best-fit linear regression gave an average stiffness of about 9.1 N/mm (52 lb/in) and a range of 5.25 to 15.9 N/mm (30 to 91 lb/in) for deflections from 30 to 61 mm (1.2 to 2.4 in) and peak forces from 311 to 525 N (70 to 118 lb). Weisfeldt (1979) has reported force-deflection curves for 60 cycle per second sternal loading with a 6.4 cm x 2.2 cm (2–1/2"x1–7/8") pad to maximum forces of 311 to 445 N (70 to 100 lb). As shown in Figure 35, these low-level dynamic loadings showed some hysteresis due to the viscoelastic properties of the thorax. The mean stiffness was about 6.3 N/mm (311 N at 49.3 mm). On one subject, a larger 15.3-cm- (6-in-) diameter pad was used producing a significantly higher stiffness of about 21 N/mm (120 lb/in) as shown in Figure 36.

As reported previously, Melvin et al. (1988a) conclude from a review of the literature that the static load-deflection response of the thorax under loading by a 15.3-cm- (6-in-) diameter flat disc should approximate a linear stiffness of 26.2 N/mm (150 lb/in) up to 41 mm (1.6 in) and 120 N/mm (685 lb/in) for deflections above 76 mm (3 in). Modeling the Kroell data, they demonstrate that the nonlinear force-deflection characteristics can be represented by a quadratic relationship:

$$F = K d^2$$

where $K = 47.6 N/cm^2$.

For static belt loading, Fayon et al. (1975) determined stiffnesses of 17.5 N/mm to 26.3 N/mm (100 to 150 lb/in) for sternal deflections up to 25 mm (1 in) on volunteers laying supine on a flat surface, compared to 8.8 N/mm to 17.5 N/mm (50 to 100 lb/in) for disc loading up to 38 mm (1.5 in). At the second rib, the stiffness was estimated to be in the 17.5 N/mm to 35 N/mm (100 to 200 lb/in) range and at the ninth rib it was estimated at 8.8 N/mm to 17.5 N/mm (50 to 100 lb/in). In addition to the dynamic belt load tests by L'Abbe et al. described above, static belt tests were also conducted. In the Phase 1, Task B report, Melvin and Weber, ed. (1988) report "apparent" static stiffness (i.e., deflection versus maximum total belt force) from the L'Abbe et al. belt loads of 67.5 N/mm (386 lb/in) at the mid-sternum, 40 N/mm (228 lb/in) at the right 7th rib, and 95 N/mm (541 lb/in) at the left clavicle for deflections up to 1 cm (0.4 in) and estimated normal forces up to 667 N (150 lb). Melvin has noted that this static sternal stiffness is significantly higher than that reported by Fayon et al. (1975) and suggests that this may be due to the effect of spinal curvature causing reduced apparent stiffness in the Fayon tests.

Preliminary quasi-static (50 mm/min) load-deflection data for the chest of an average male cadaver (76 kg, 178 cm) are available for one test of an airbag filled with polyurethane foam and one test of a standard shoulder belt (Kallieris 1987). Deflection was measured at six locations on the third, fourth, and fifth ribs indicated in Figure 37 and the belt was placed diagonally across the chest from the right clavicle to the left fifth rib. The peak

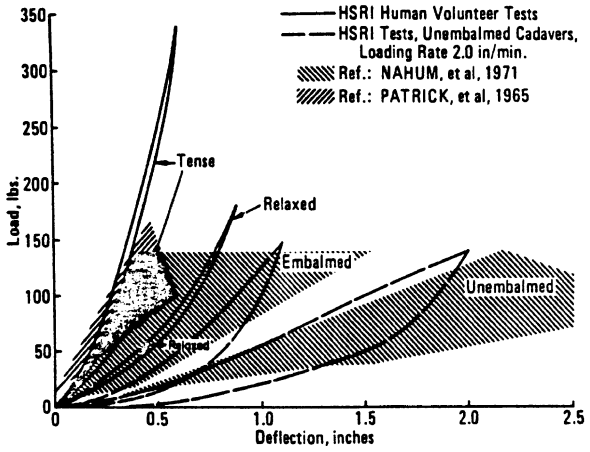

FIGURE 33. Comparison of static chest load-deflection curves, A-P (Stalnaker et al. 1973).

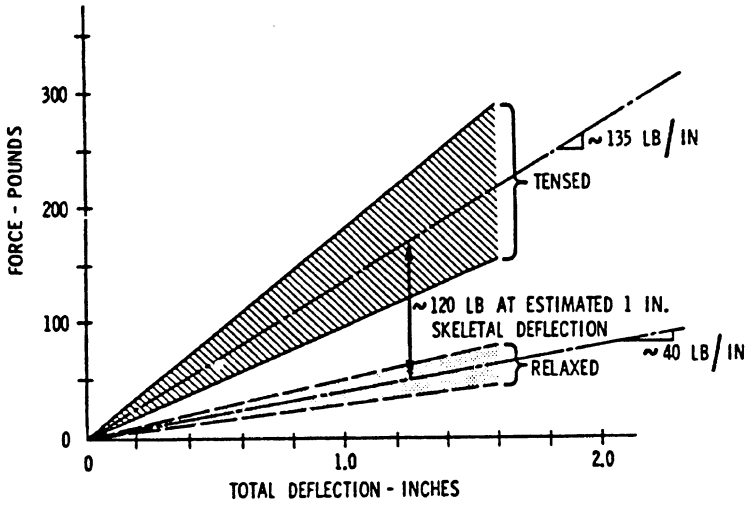

FIGURE 34. Static loading corridors for relaxed and tensed volunteers—back fully supported (Lobdell et al. 1973).

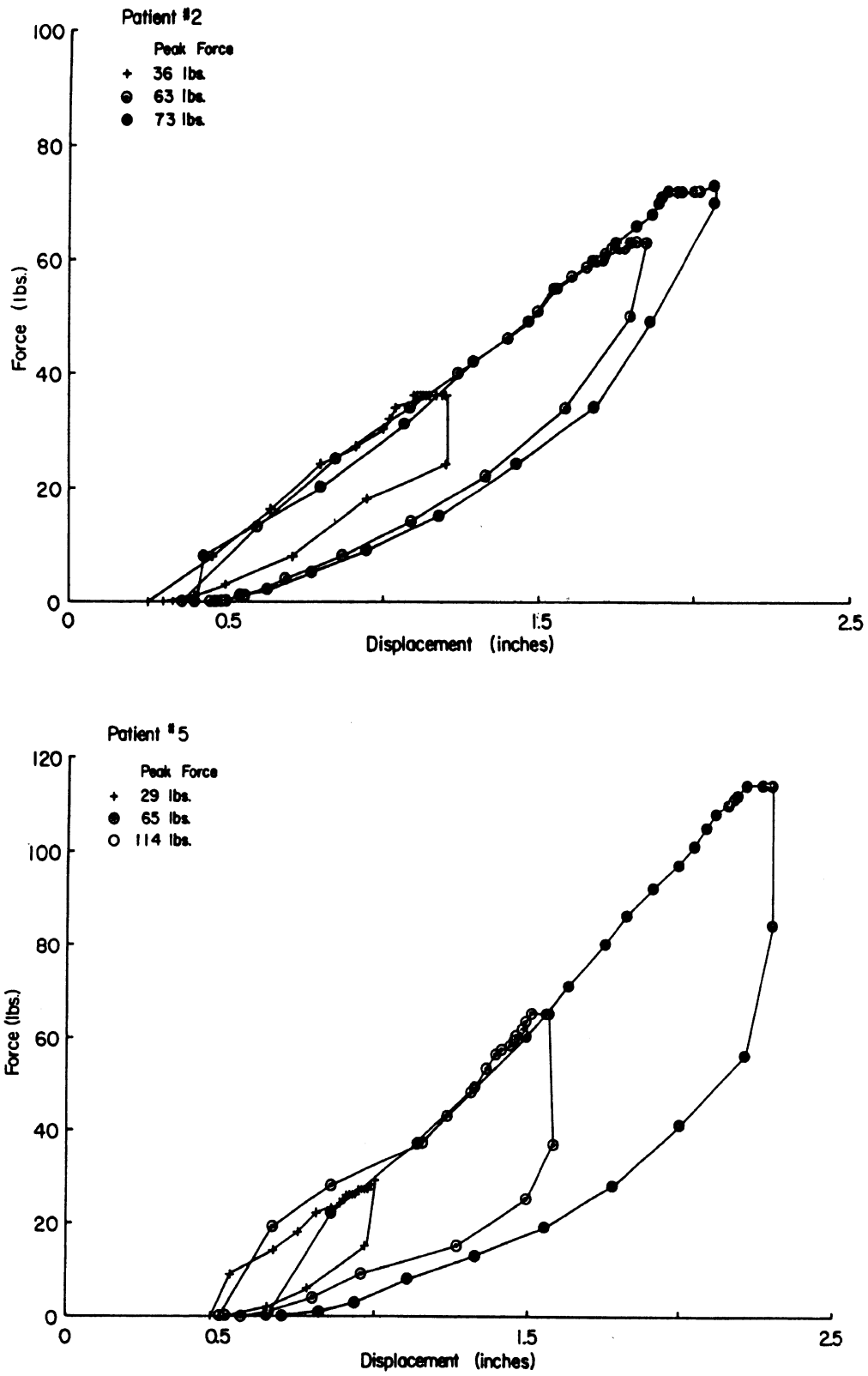

FIGURE 35. Sternal force-displacement diagrams for CPR compression-release cycles in a single subject at three levels of peak force (Weisfeldt 1979).

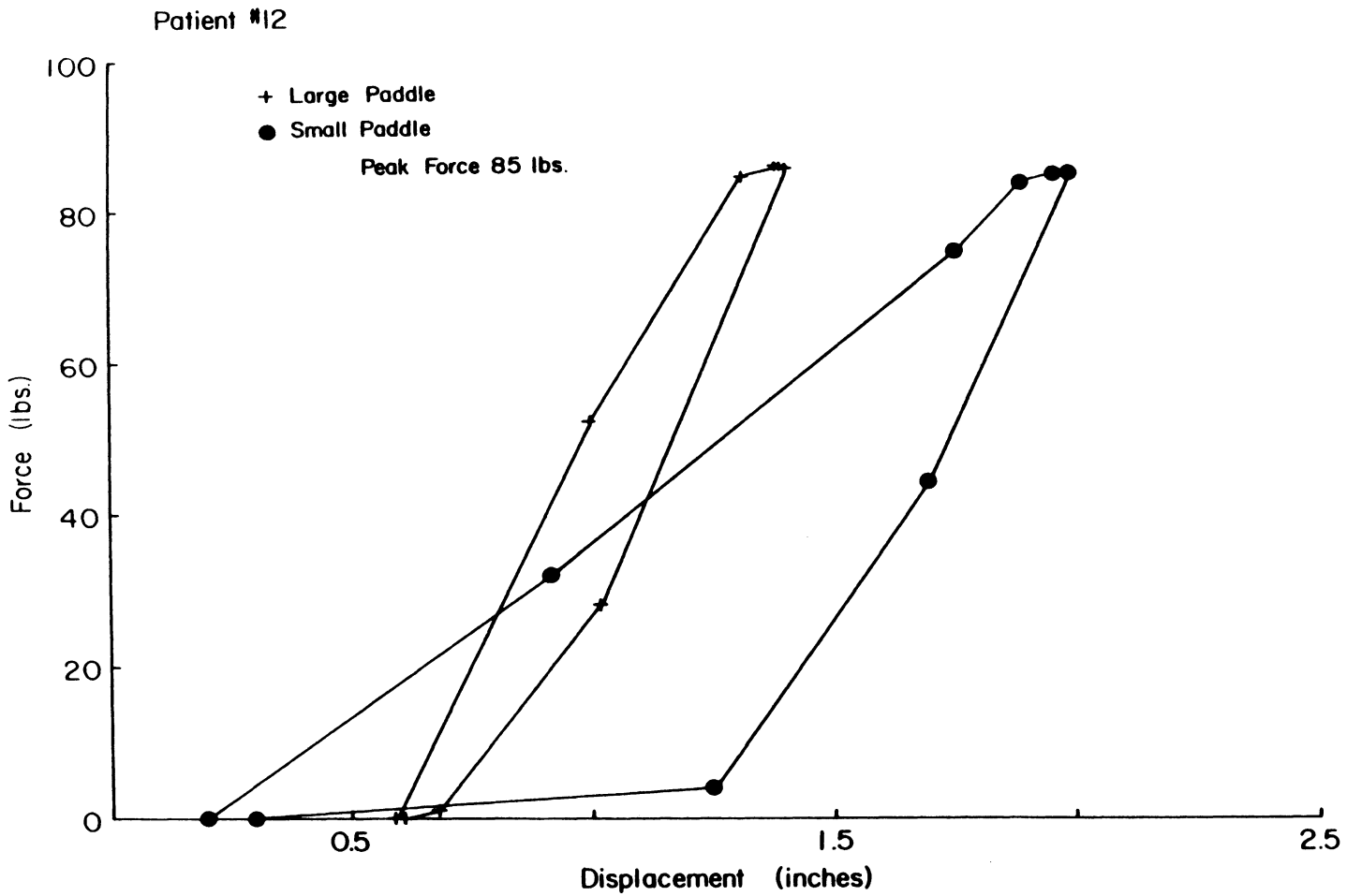

FIGURE 36. Force-deflection diagrams for compression release cycles in a single subject with large and small sternal pad. The large pad with greater surface area and contact with the chest wall outside the sternum resulted in less anterior chest wall deflection (Weisfeldt 1979).

applied load was 1.76 kN for the belt (presumably total belt load) and 1.7 kN for the airbag (applied by a flat plate to the top of the bag). Table 8 summarizes the peak deflections at the six sites for these two tests. As indicated, the peak deflections due to airbag loading are similar at all six locations at about 53 mm or 2 in. In contrast, the shoulder belt produced different deflections at the six locations, with the largest deflection of 85 mm at the fifth rib under the belt and the lowest deflection of 10 mm at the fourth rib away from the belt.

B1.1.11 Other Frontal Impact Response Criteria. In addition to the force-deflection response information described above, additional accelerometer-based response data are available that give a more "global characterization of the structural response of the thorax." For frontal impact response, acceleration response corridors been developed by Melvin et al. (1988a) for the following test conditions:

Pendulum impactor at 4.5 m/sec
Sled three-point belt at 13.4 m/sec
Sled airbag at 13.4 m/sec

Accelerometer locations and directions are illustrated in Figure 38 and include:

Sternum X
Left/right Lower rib X
Left/right lower rib Y
Spine X
Spine Z

Figures 39 through 41 were taken from the Phase I Task E–F report (Melvin et al. 1988a) and show the response corridors for these conditions and accelerometer locations. Signals used to develop the corridors were filtered with a 200-Hz Butterworth filter with a slope of 24-dB/octave. Because these results are primarily useful for evaluating the completed thorax subcomponent installed in the test dummy, Melvin et al. (1988a) have appropriately considered these as "secondary design specifications."

B1.1.12 Ribcage Coupling. In designing a new thorax with regional biofidelity for concentrated loading such as that delivered by a shoulder belt or steering wheel rim, the coupling of one region of the thorax to another is of great importance. There are a limited amount of data, however, that describe this coupling, especially for dynamic loading conditions. Results from static and quasi-dynamic shoulder belt loading of supine volunteers by L'Abbe (1982) have been previously described (Figures 25a and 25b) and demonstrate significant differences between humans and Hybrid III with regard to the pattern of chest deflections at different regions. Similarly, the results of quasi-static airbag and shoulder belt load-deflection tests on an average male cadaver by Kallieris (1987) have been previously described (Figure 37 and Table 8) and demonstrate the importance of compliant coupling between thoracic regions for realistic chest/belt interactions.

Recently, Cavanaugh et al. (1988) has statically loaded the chest of two supine cadavers and a 50th percentile Hybrid III dummy using a 4.5 cm x 10 cm (2"x4") rigid loading plate while measuring chest deflection at eight locations as shown in Figures 42, 43, and 44. The upper, mid, and lower sternum were loaded, as were the ribs at upper, mid, and lower regions. Sternal loading was performed under two support conditions as illustrated in Figure 45a and 45b: (1) support at the spine only, with a rigid aluminum bar supported on unistrut, and (2) support of the spine and ribs posteriorly. Rib support was provided bilaterally approximately 7 cm (2.8 in) lateral to the midline. Rib loading was performed only for the second support condition. Loading rates ranged from 1.3 mm/s to 100 mm/s (0.05 in/s to 4 in/s), and the stroke was usually set at 2.5 cm (1 in). The results are presented in Appendix B.

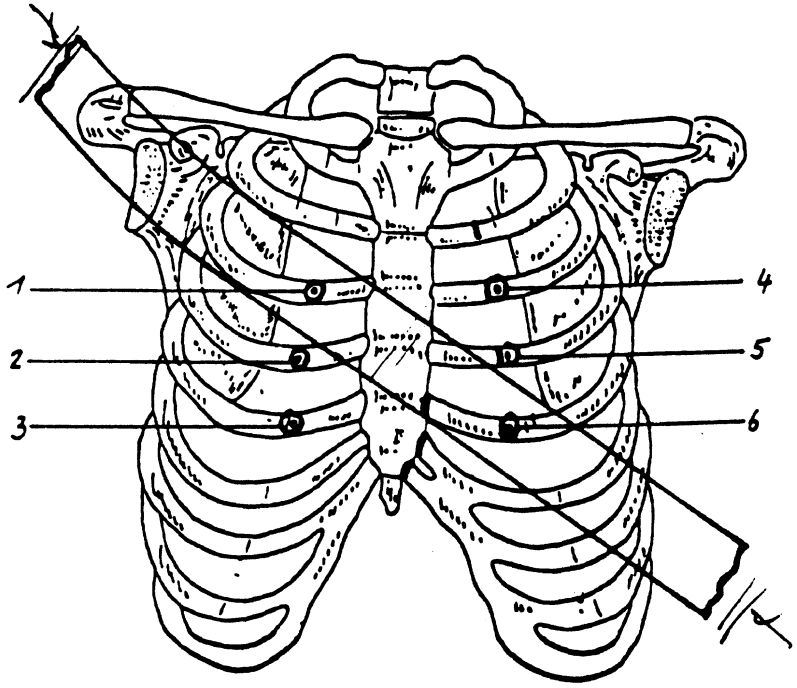

FIGURE 37. Locations of deflection measurement for quasi-static belt and airbag loading tests (Kallieris 1987).

TABLE 8

PEAK DEFLECTION FOR QUASI-STATIC CHEST LOADING WITH AIRBAG AND SHOULDER BELT
(Kallieris 1987)

Measurement Location	Rib Deflection (mm)	
	Airbag	Shoulder Belt
1	56	40
2	55	35
3	56	20
4	52	10
5	53	40
6	51	85

Load for airbag is 1.7 kN. Load for shoulder belt is 1.76 kN.

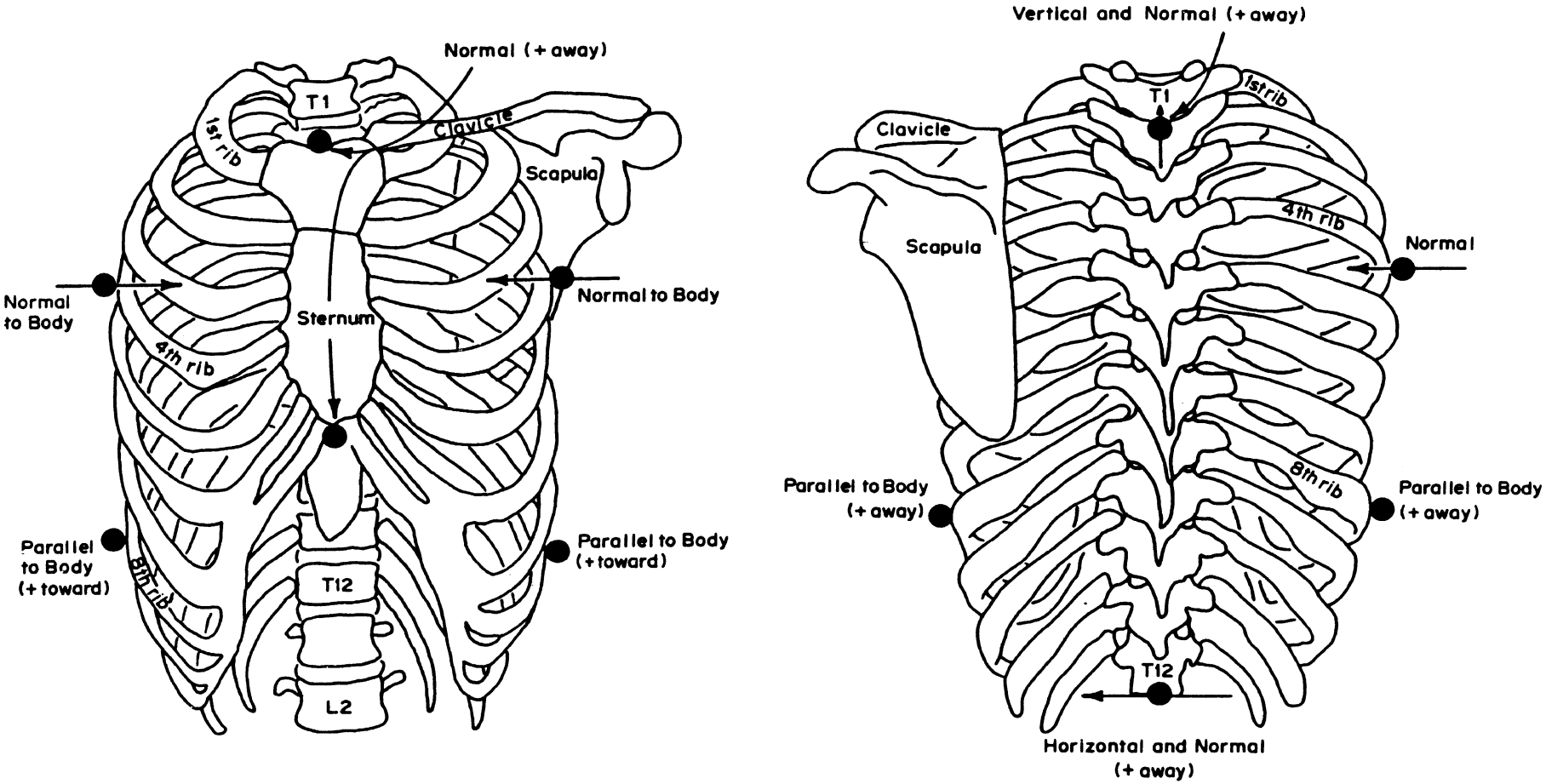

FIGURE 38. Locations of accelerometers for thorax impact tests by Robbins et al. (1976).

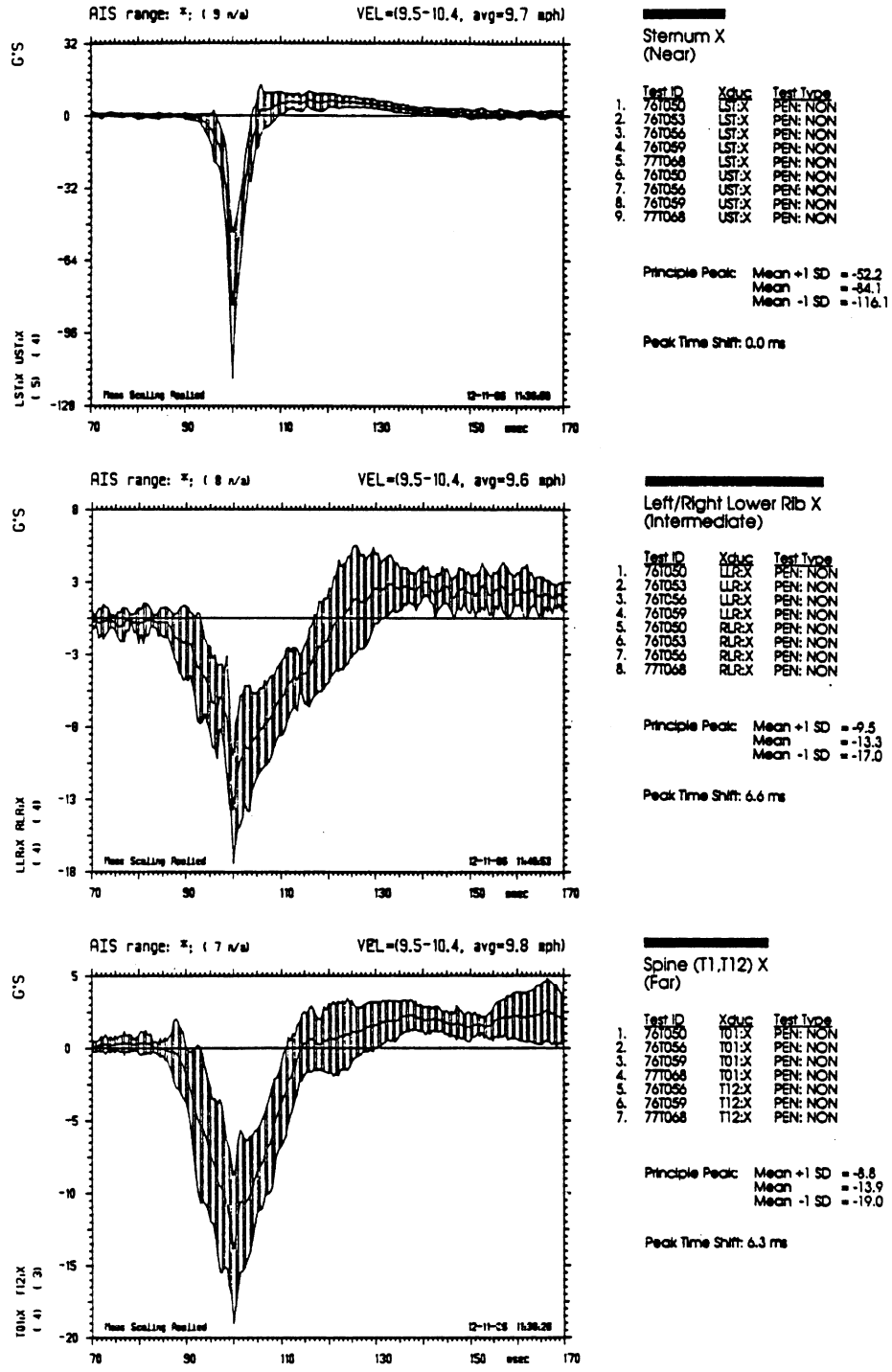

FIGURE 39. Thoracic response in frontal pendulum impactor tests (4.5 m/s) (Melvin et al. 1988a).

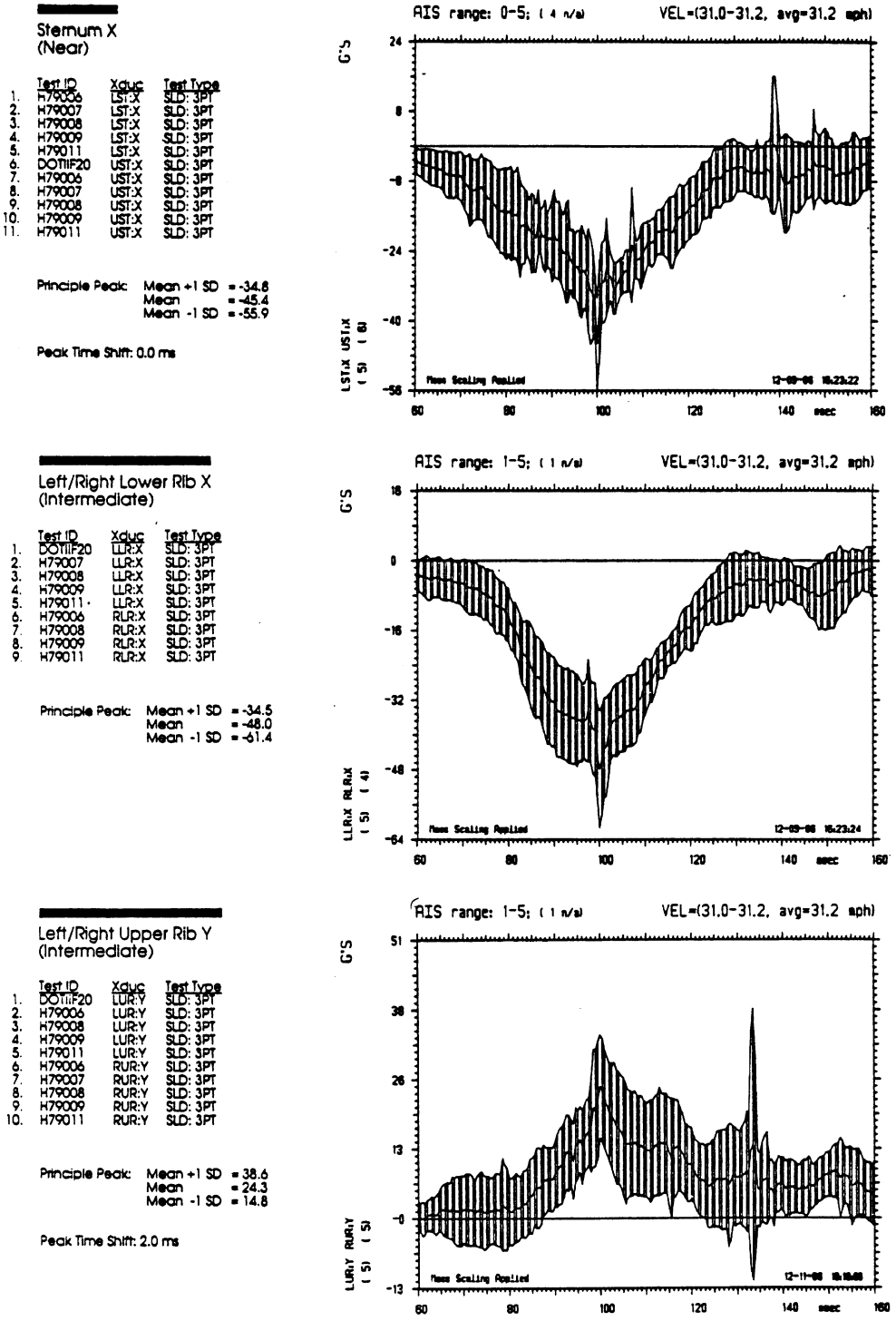

FIGURE 40. Thoracic response in frontal sled three-point-belt tests (13.4 m/s) (Melvin et al. 1988a).

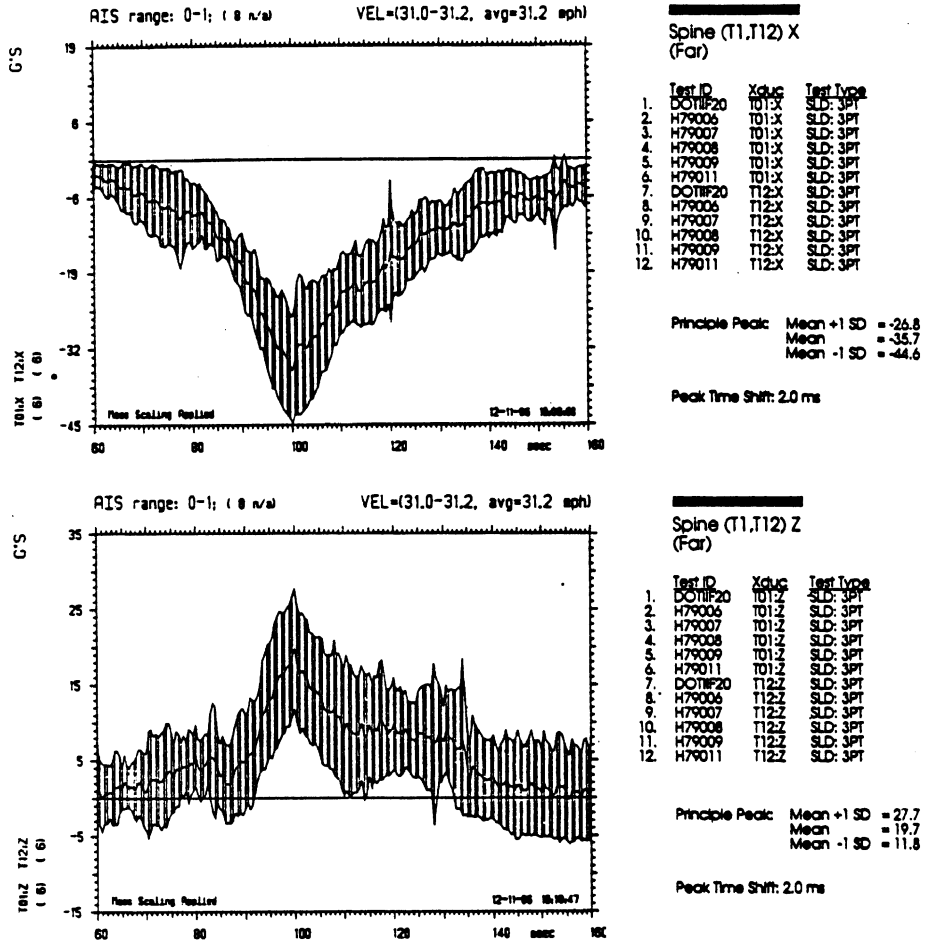

FIGURE 40. Thoracic response in frontal sled three-point-belt tests (continued).

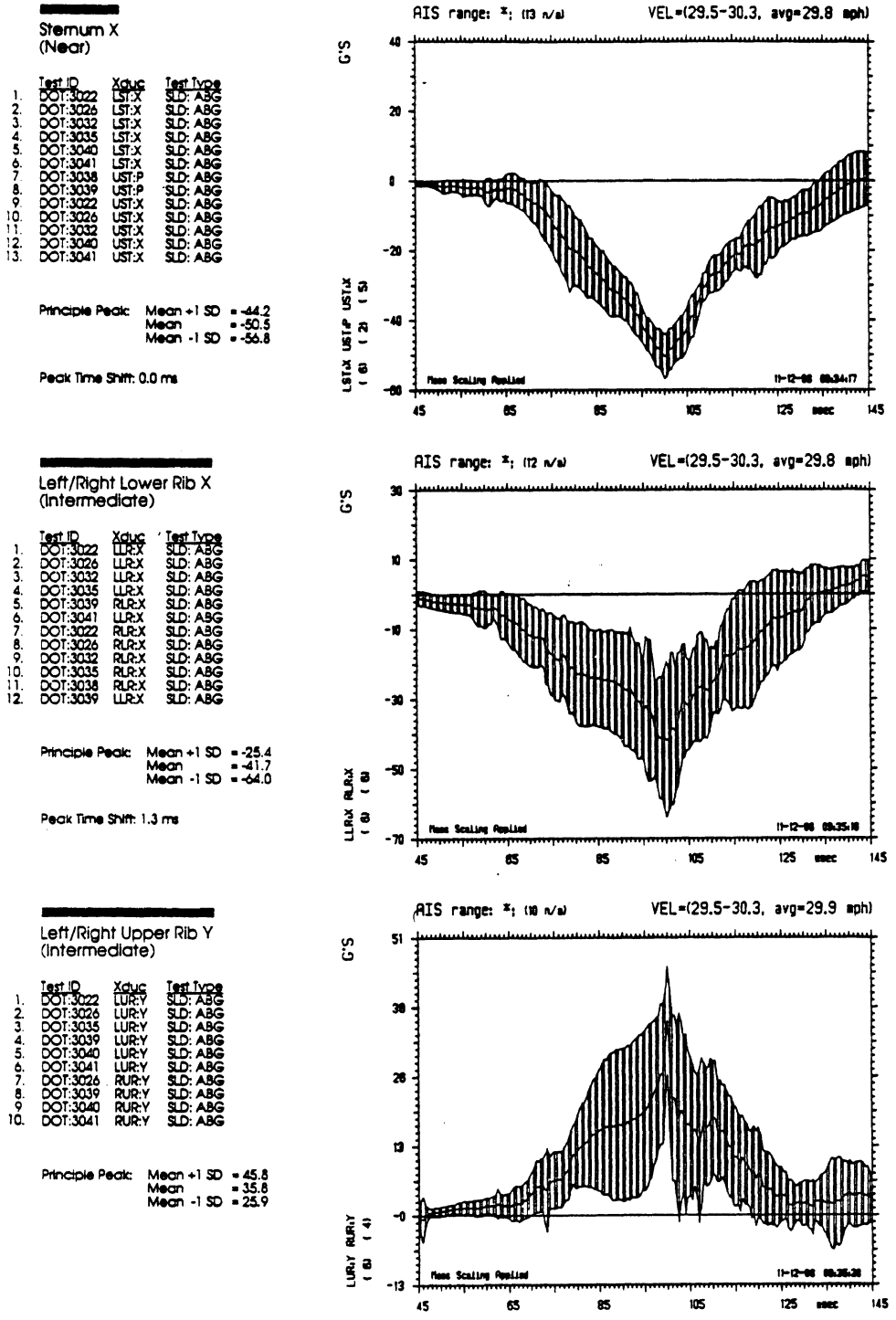

FIGURE 41. Thoracic response in frontal sled airbag tests (13.4 m/s) (Melvin et al. 1988a).

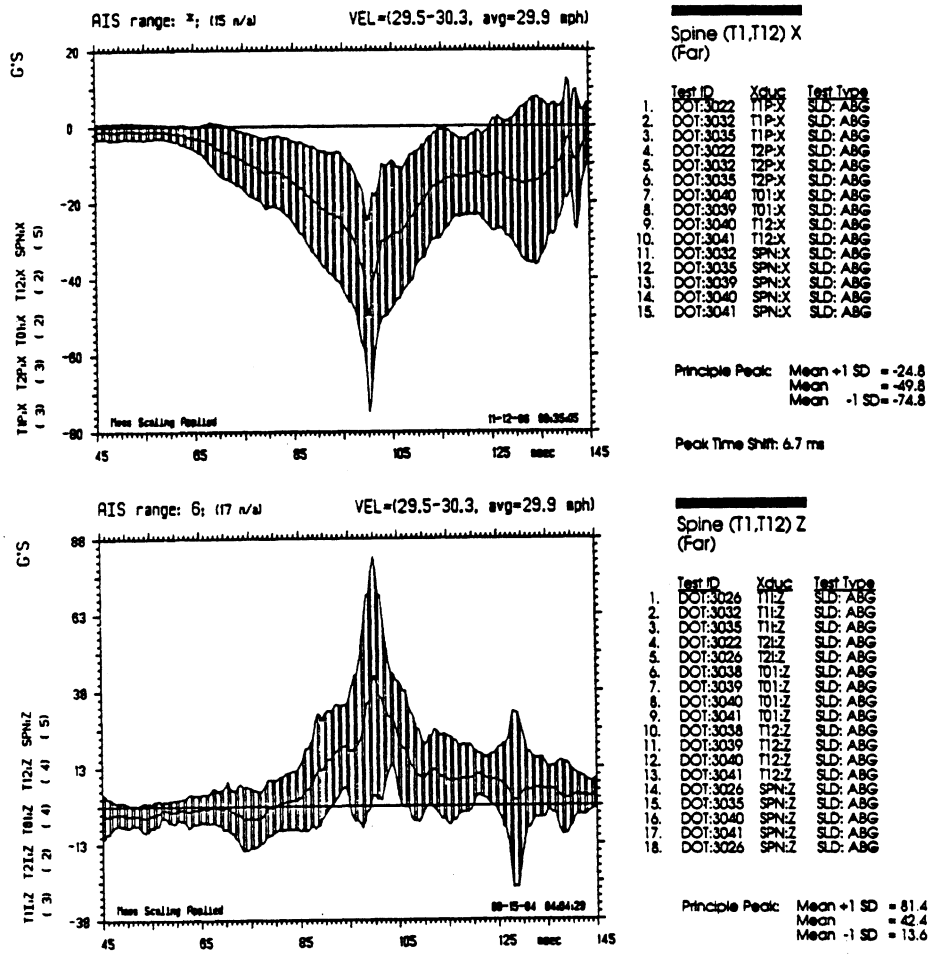

FIGURE 41. Thoracic response in frontal sled airbag tests (continued).

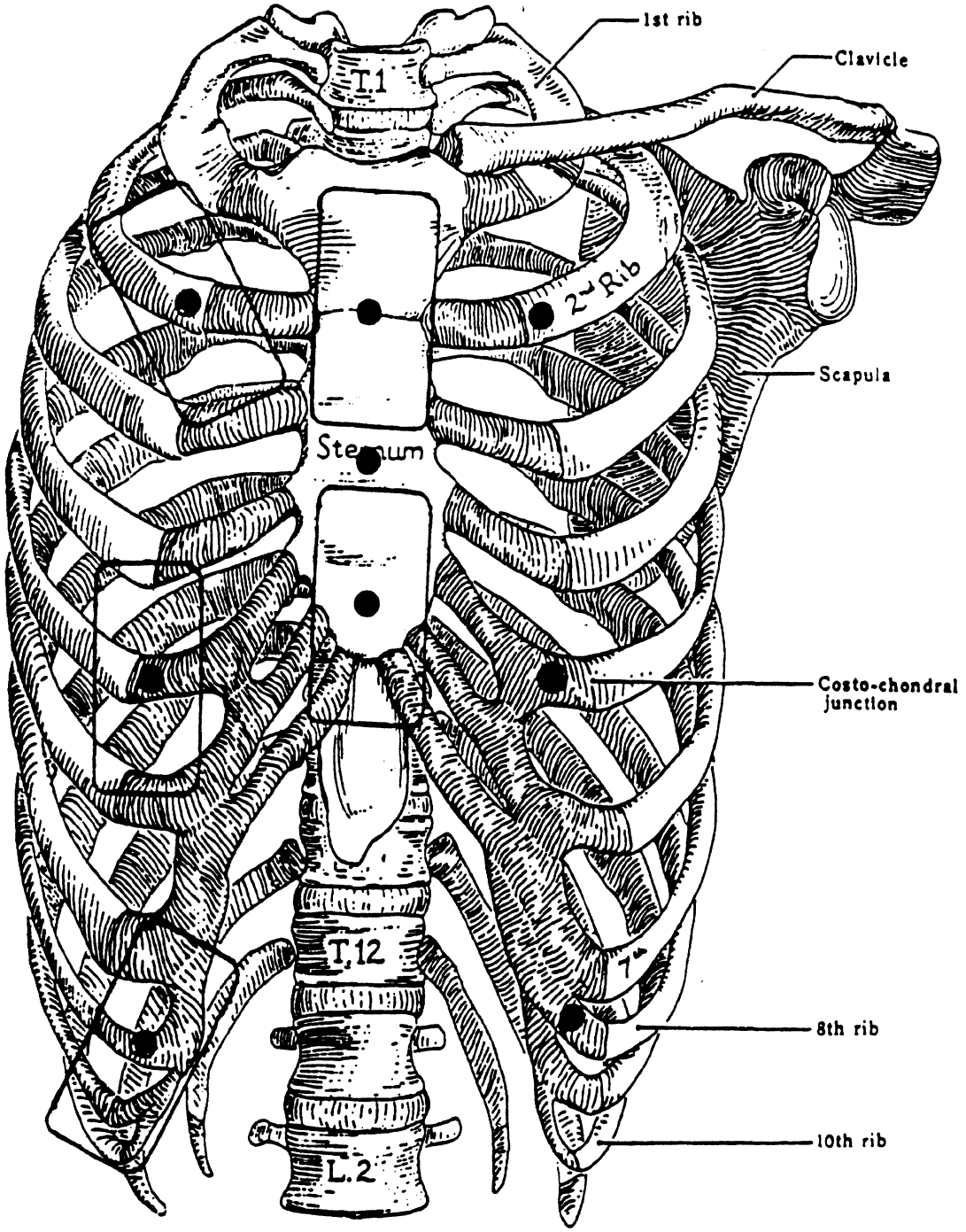

FIGURE 42. Regions of static loading with 5 cm x 10 cm (2"x4") surface and deflection measurement used by Cavanaugh et al. (1988).

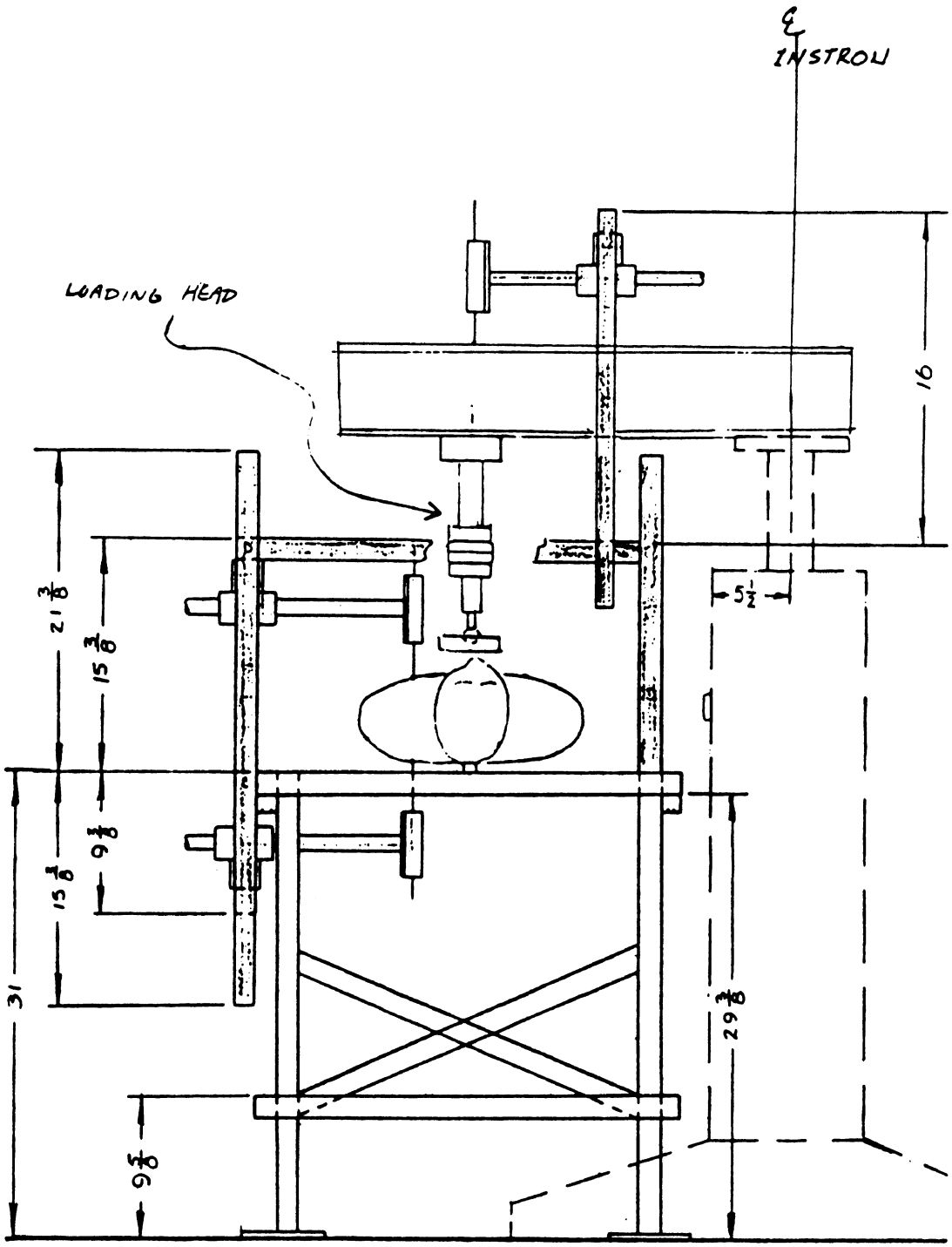

(Dimensions in inches)

FIGURE 43. End view of test setup for static loading tests on a cadaveric thorax (Cavanaugh et al. 1988).

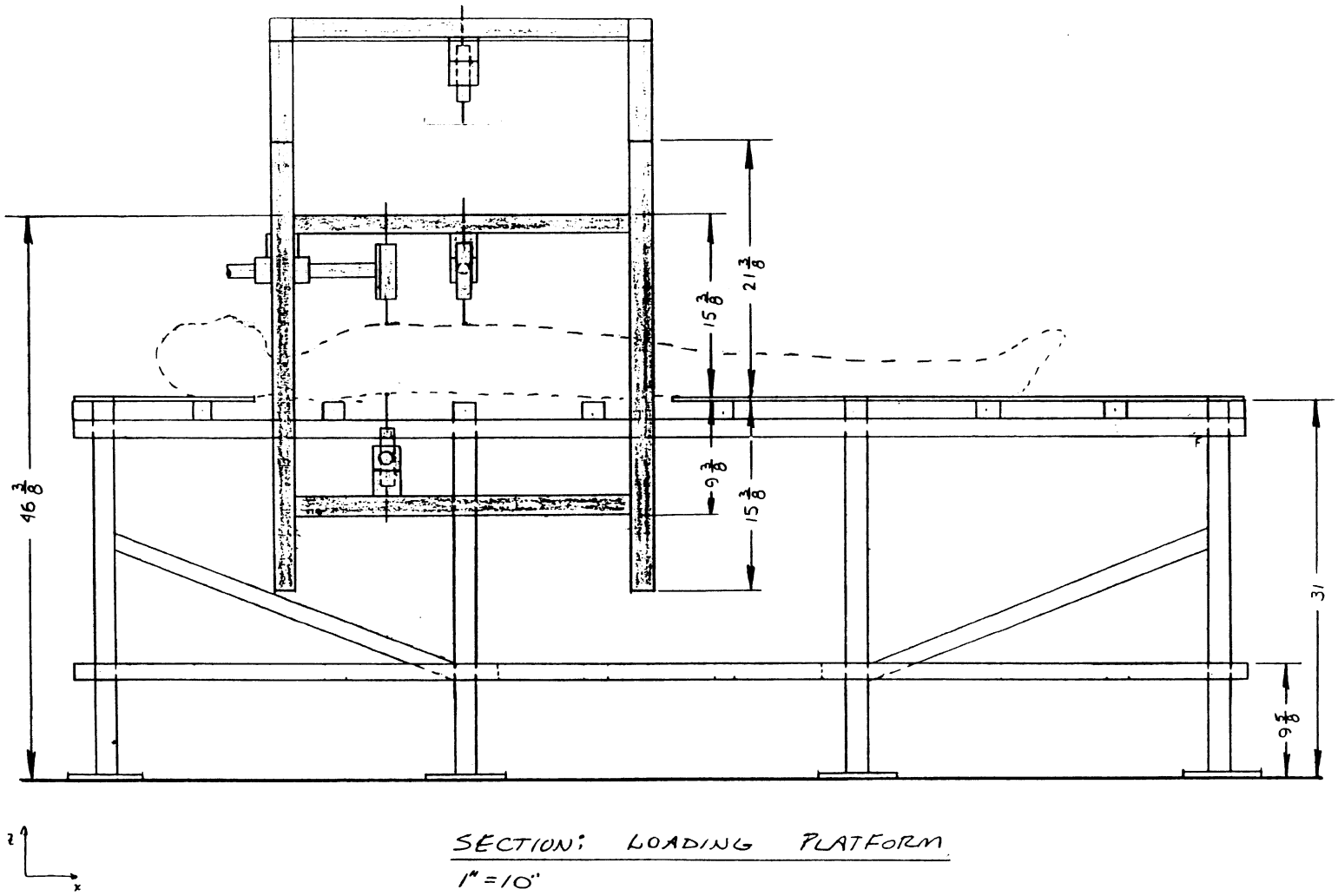

FIGURE 44. Side view of test setup for static loading tests on a cadaveric thorax (Cavanaugh et al. 1988).

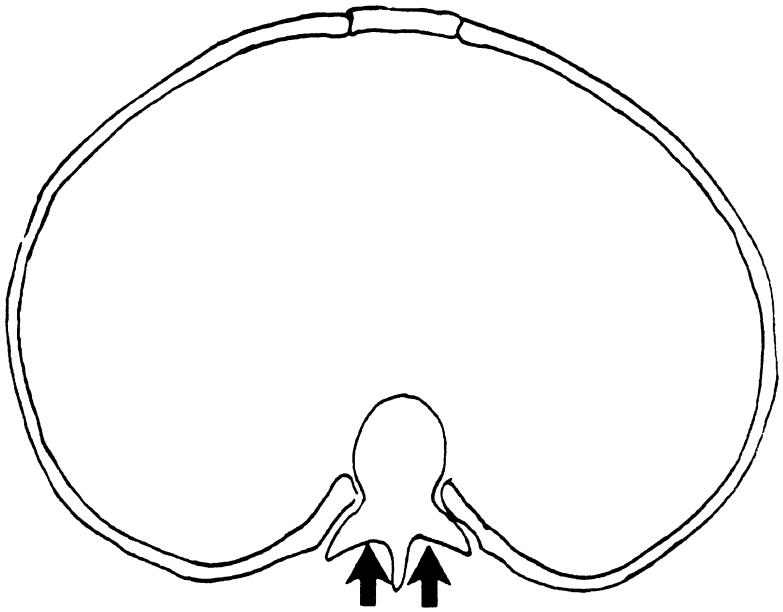

FIGURE 45a. Schematic chest cross-section showing spine support only (Cavanaugh et al. 1988).

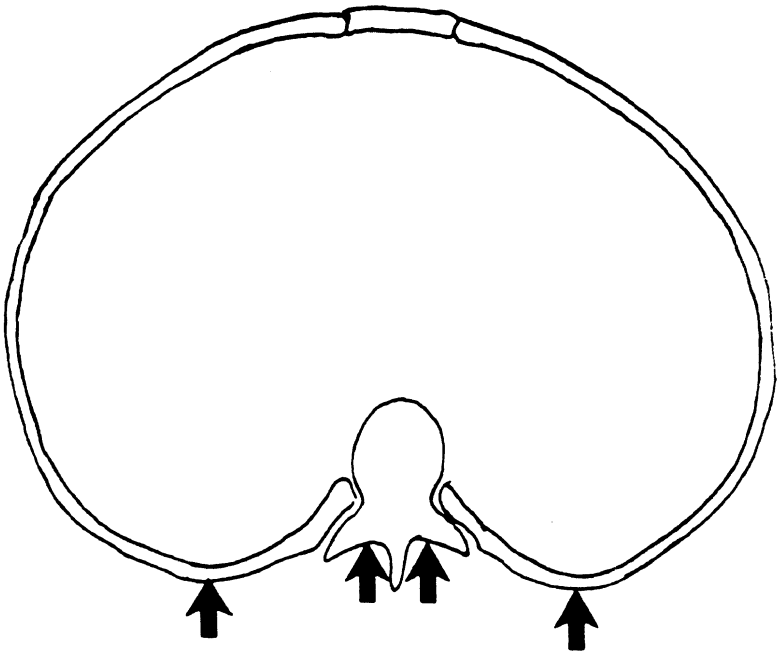

FIGURE 45b. Schematic chest cross-section showing rib plus spine support (Cavanaugh et al. 1988).

While the cadaver data have not been adjusted for muscular contribution, the following observations can be made:

1. Under sternal quasi-static loading, the Hybrid III dummy is three to five times as stiff as the human cadaver.

2. Under rib quasi-static loading, the Hybrid III dummy is at least seven times as stiff as the human cadaver. Representative stiffnesses of Hybrid III and the human cadaver thorax are shown on the figure legends of the force-deflection plots in Appendix B.

3. Under sternal quasi-static loading, the human cadaver is approximately twice as stiff as it is under rib loading.

4. Increasing the loading rate from 1.7 mm/s to 100 mm/s (0.067 in/s to 4 in/s) did not consistently show an increase in thoracic stiffness of the human cadaver.

5. Under sternal quasi-static loading, the rib deflection of the human cadaver was less than 50% of the sternal deflection, while rib deflection of the Hybrid III dummy was greater than 50% of the sternal deflection (Figures B-1 and B-2).

6. Under rib quasi-static loading, the ribs contralateral to the side of loading in the human cadaver deflected much less than the corresponding ribs in the Hybrid III dummy (Figures B-3 and B-4).

7. Under the condition of spine support only, the Hybrid III posterior ribs deflected more than the human cadaver posterior ribs.

8. Under mid-sternal quasi-static loading, the 1st, 3rd, and 6th ribs of the Hybrid III had close to the same magnitude of deflection, while the human cadaver ribs showed a marked difference that was dependent on the level of the rib (Figures B-5, B-6).

With regard to static load-deflection coupling between different regions, Tables 9 and 10 summarize the results for sternal loading and ribcage loading, respectively. The deflection data have been normalized to indicate exactly one unit of deflection at the applied load (nominal maximum stroke was 1 inch). The results provide further definition of the compliance between thoracic regions in the human for static loading and small deflections.

For sternal loading, it is particularly interesting to note the relatively low deflections that occur at one end of the sternum when the load is applied at the other end as well as the low deflection at the lower ribcage when load is applied at mid-sternum.

For ribcage loading, the reduction in chest deflection away from the applied load is again quite striking. In particular, when the load is applied to the 5th rib on one side, the 5th rib on the other side undergoes less than 10% of the deflection. Similarly, when the load is applied to the 2nd rib, the 8th rib on the same side deflects only 5% as much and when the load is applied to the 8th rib, the 2nd rib on the same side does not deflect at all.

Table 11 summarizes the test results with regard to regional static stiffness for approximately 2.5 cm (1 in) of deflection. The upper mid-sternal region demonstrated the highest stiffness at 11 N/mm (63 lbs/in), while the stiffness at the lower sternum was considerably less at 6.1 N/mm (35 lbs/in). It is also interesting to note that the stiffness at the 2nd rib is less than the stiffness at mid-sternum and, as expected, the stiffness at the lower ribcage is the lowest overall.

TABLE 9

STATIC LOAD-DEFLECTION COUPLING BETWEEN REGIONS: RIB LOADING (Cavanaugh et al. 1988)

RIGHT 2ND RIB		
Right Ribs	Sternum	Left Ribs
2: 1.00 5: 0.22 8: 0.05	U: 0.31 L: 0.24	2: 0.13 5: 0.00 8: 0.01
RIGHT 5TH RIB		
2: 0.08 5: 1.00 8: 0.40	U: 0.04 L: 0.49	2: 0.01 5: 0.09 8: 0.12
RIGHT 8TH RIB		
2: 0.00 5: 0.42 8: 1.00	U: 0.00 L: 0.42	2: 0.00 5: 0.11 8: 0.14

Loading Rate: 1.7 mm/s (0.067 in/s)
Max Stroke: 25 mm (1.0 in)
Support Conditions: Spine supported.
Posterior ribs supported bilaterally.
Deflections are shown in *inches* at each location.

TABLE 10

STATIC LOAD-DEFLECTION COUPLING BETWEEN REGIONS: STERNUM LOADING (Cavanaugh et al. 1988)

UPPER STERNUM		
Right Ribs	Sternum	Left Ribs
2: 0.50 5: 0.20 8: 0.07	U: 1.00 L: 0.35	2: 0.50 5: 0.20 8: 0.07
MID-STERNUM		
2: 0.37 5: 0.30 8: 0.16	M: 1.00	2: 0.37 5: 0.30 8: 0.16
LOWER STERNUM		
2: 0.20 5: 0.50 8: 0.55	U: 0.16 L: 1.00	2: 0.20 5: 0.50 8: 0.55

Loading Rate: 1.7 mm/s (0.067 in/s)
Max Stroke: 25 mm (1.0 in)
Support Conditions: Spine supported.
Posterior ribs supported bilaterally.
Deflections are shown in *inches* at each location.

TABLE 11

REGIONAL STATIC STIFFNESS FOR 25 MM (1 IN) DEFLECTION WITH 5 CM x 10 CM (2"x4") LOADING SURFACE (Cavanaugh et al. 1988)

Load Location	Stiffness (N/mm)
Upper Sternum	11.0
Mid-Sternum	11.0
Lower Sternum	6.1
Right Second Rib	4.6
Right Fifth Rib	5.4
Right Eighth Rib	3.5

These results provide further definition of the intra-thoracic (i.e., ribcage) coupling (or decoupling) required which is in sharp contrast to the stiff coupling of Hybrid III. The loading conditions and results can be used to evaluate the new thorax with regard to static coupling biofidelity across the sternum and between the upper and lower ribs. Additional tests in which chest deflection is being measured at different thoracic regions during dynamic shoulder belt loading of unembalmed cadavers are currently being conducted at INRETS. These data will provide additional information to define dynamic thoracic coupling and will be added to these specifications when available.

B1.2 Abdominal Impact Response

B1.2.1 Rigid Bar Impacts. In comparison to the thorax, there are relatively little data that describe the biomechanical response of the abdomen to frontal impacts. Stalnaker and Ulman (1985) conducted and analyzed a series of frontal and lateral abdominal impacts to subhuman primates and found that the force-deflection response characteristics were similar to those of the thorax having an initial rise in force followed by a plateau region. Melvin et al. (1988a) have summarized the results of these tests after scaling to human dimensions and used modeling techniques involving elastic, viscous, and inertial elements (similar to those of Section B1.1.1) to determine the idealized force-deflection response corridors for frontal impacts to the abdomen. The results are shown in Table 12 and Figure 46 for three impact velocities and for a rigid 4-cm by 35-cm bar having a mass of 10 kg. The unloading phase of the abdominal response should produce a hysteresis ratio of more than 75% but less than 85%.

TABLE 12

AATD IDEALIZED ABDOMINAL IMPACT RESPONSE PARAMETERS
(Rigid bar impactor, 4 cm by 35 cm, 10.0 kg)
(Melvin et al. 1988a)

Impactor Vel (m/s)	S_{AI} (kN/cm)	F_P (kN)	d_{PI} (cm)	d_{PF} (cm)
4.3	0.67±0.10	1.33±0.20	2.0	4.32
6.7	1.04±0.16	2.07±0.31	2.0	5.23
12.0	1.86±0.28	3.71±0.56	2.0	7.25

S_{AI}=apparent initial stiffness; F_P=plateau force; d_{PI}=deflection at beginning of plateau region; d_{PF}=deflection at end of plateau region.

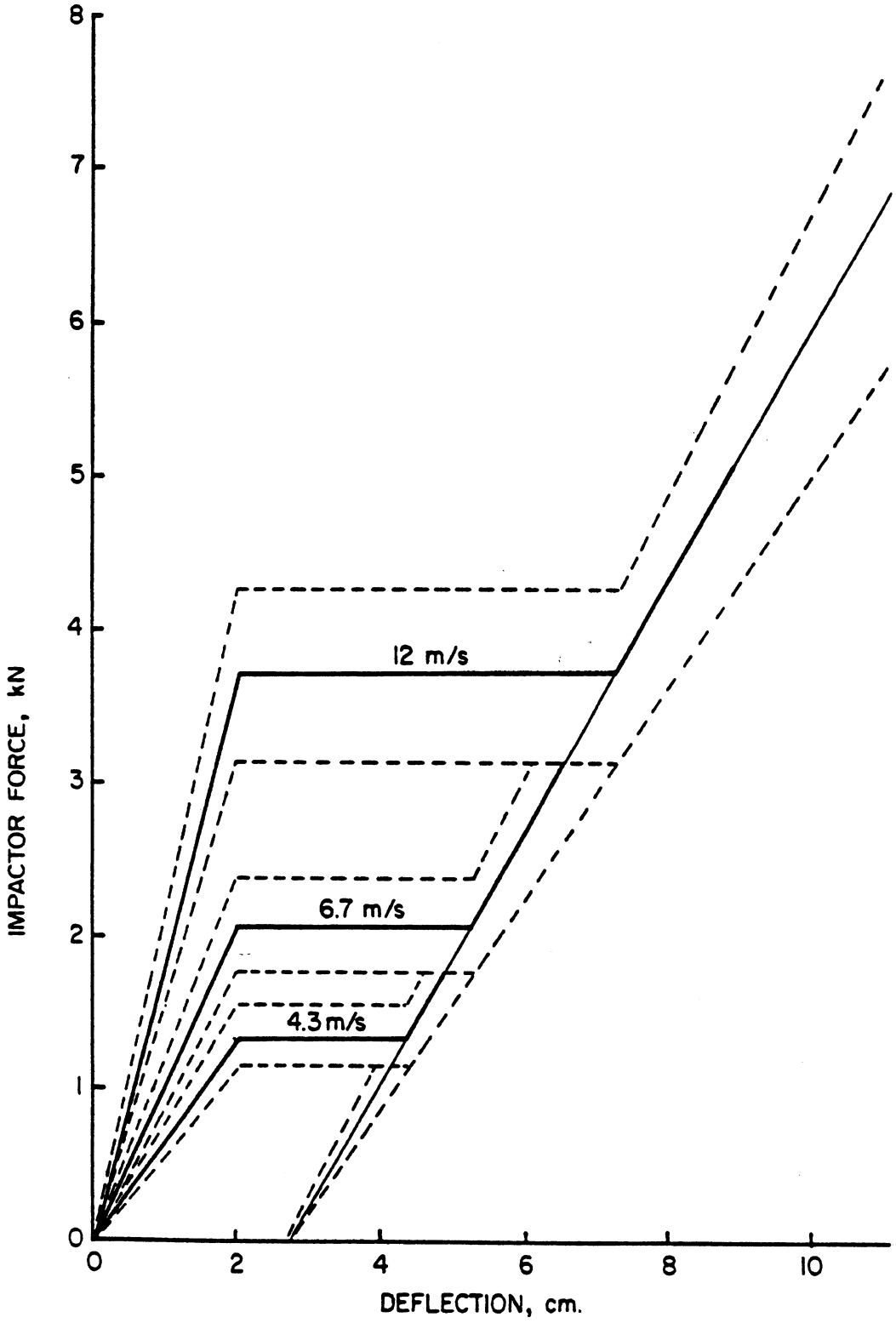

FIGURE 46. AATD abdominal impact response, frontal and lateral (rigid bar impactor 4-cm by 35-cm and 10-kg mass) (Melvin et al. 1988a).

B1.2.2 Steering Wheel Impacts. For the lower abdominal area, at the level of L3, a series of cadaveric impacts simulating steering wheel rim interaction with the abdomen was carried out by Cavanaugh et al. (1986). The impacting surface was a straight cylindrical bar 25 mm (1 in) in diameter and the mass of the impacting pendulum was either 32 or 64 kg (70.5 or 141 lb). Two impact velocities were used. The average low velocity was 6.1 m/s or 22 km/hr (20 ft/s or 13.6 mph) and the average high velocity was 10.4 m/s or 37.4 km/hr (34.1 ft/s or 23.3 mph). Normalized force-deflection corridors for these two impact velocities are shown in Figure 47.

Nusholtz et al. (1988) have reported on results from a series of thoraco-abdominal impacts to unembalmed cadavers using a rigid lower-rim representation of a steering wheel. Figure 48 illustrates the test setup and Table 13 summarizes the test conditions along with peak values of response parameters and calculated injury criteria for impact velocities ranging from 3.9 to 10.8 m/s. Figure 49 shows a composite of the force-deflection plots for these tests. It will be noted that there are no distinct plateaus in force and that peak deflections can be quite large.

B1.2.3 Kroell Impacts to Upper Abdomen. As previously discussed (see Table 7 in Section B1.1.4), four Kroell-type impacts on the midline of the upper abdomen, i.e., impactor centered 7.6 cm (3 in) below xiphoid, have recently been conducted at Wayne State University for General Motors. The force deflection plots for these and future tests will be added to these specifications when they become available.

B2.0 INSTRUMENTATION

The new ATD thorax/abdomen must be instrumented so that it provides the necessary information for computing injury criteria that indicate the probability of injury at different AIS levels sustained in a test. In the Part 572 ATD, the responses measured are the anterior-posterior, lateral, and inferior-superior accelerations at the thoracic spine and the injury criteria parameter is the resultant acceleration computed from these three acceleration components. In the Hybrid III, deflection as a function of time at mid-sternum is also measured and from this it is possible to compute the sternal velocity time-history and the viscous criterion, which is the maximum value of the velocity-times-compression time function.

Whatever the injury criteria used, however, it is clear that injury is produced by the delivery of mechanical energy to the body and current and future injury criteria are measures of the expression of this energy in mechanical response parameters that correlate best with the level and probability of injury. While our understanding of the actual mechanisms by which injuries occur to the different tissues and organs is far from complete, it is useful to review what is known and hypothesized about injury mechanisms in considering the instrumentation needs of a new thorax/abdomen subcomponent.

B2.1 A Review of Thoraco-Abdominal Injury Mechanisms

As indicated above, the aim of this review is to provide a rational basis for design of the thorax/abdomen subcomponent and for installation of new instrumentation in a frontal ATD that will assess the level of injury protection afforded by different restraint systems and other automotive safety features. The types of transducers used, their locations, and the number of each type will depend upon the injury patterns and our understanding of the injury mechanisms based on field investigations. Not all mechanisms of injury are understood or have been shown to be valid through laboratory verification. The following discussion is a compilation of available information with commentary regarding what is still unknown or poorly understood.

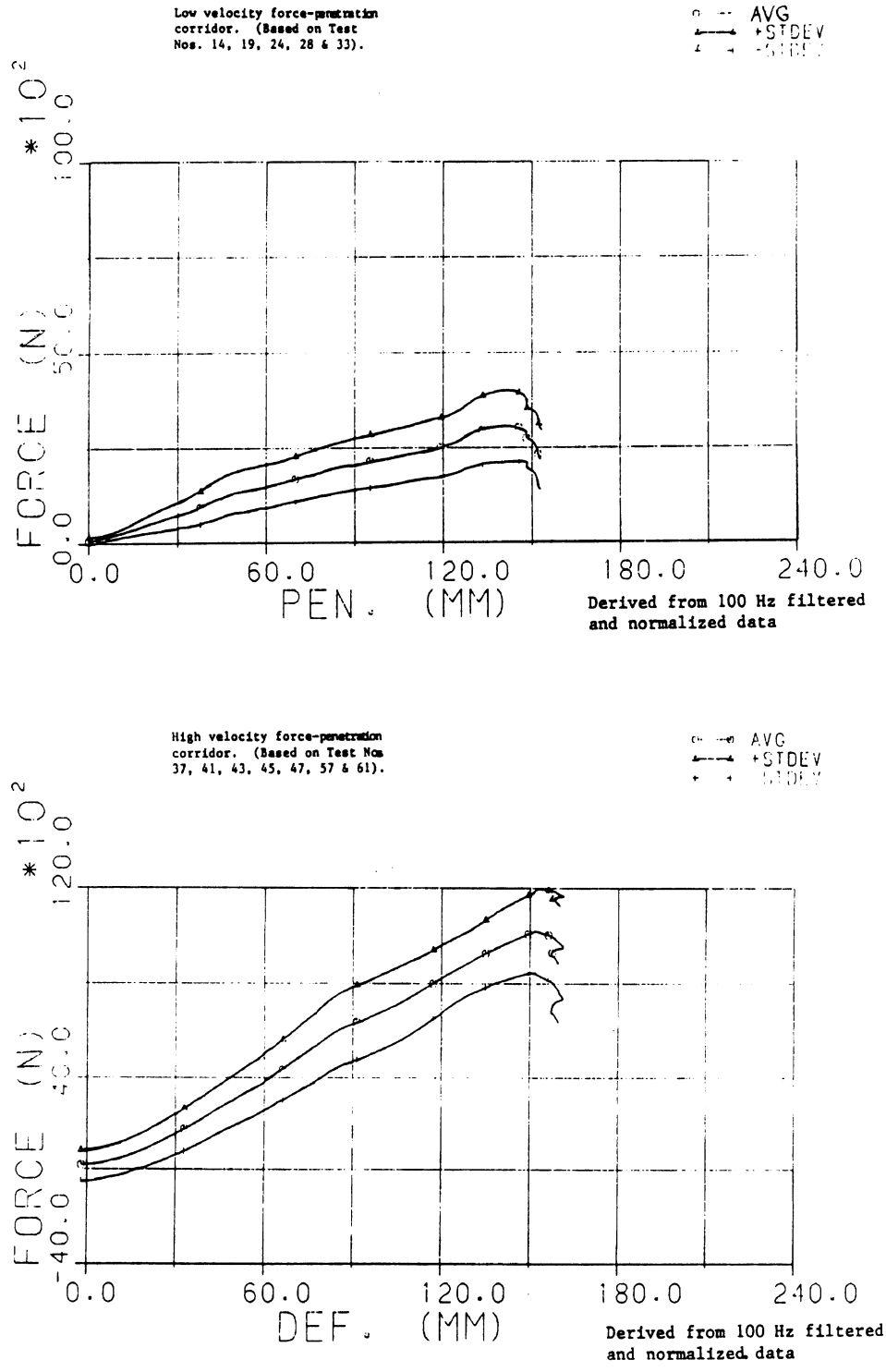

FIGURE 47. Force-penetration corridors for low and high velocity impacts to abdomen with 25-mm- (1-in-) diameter rigid bar (Cavanaugh et al. 1986).

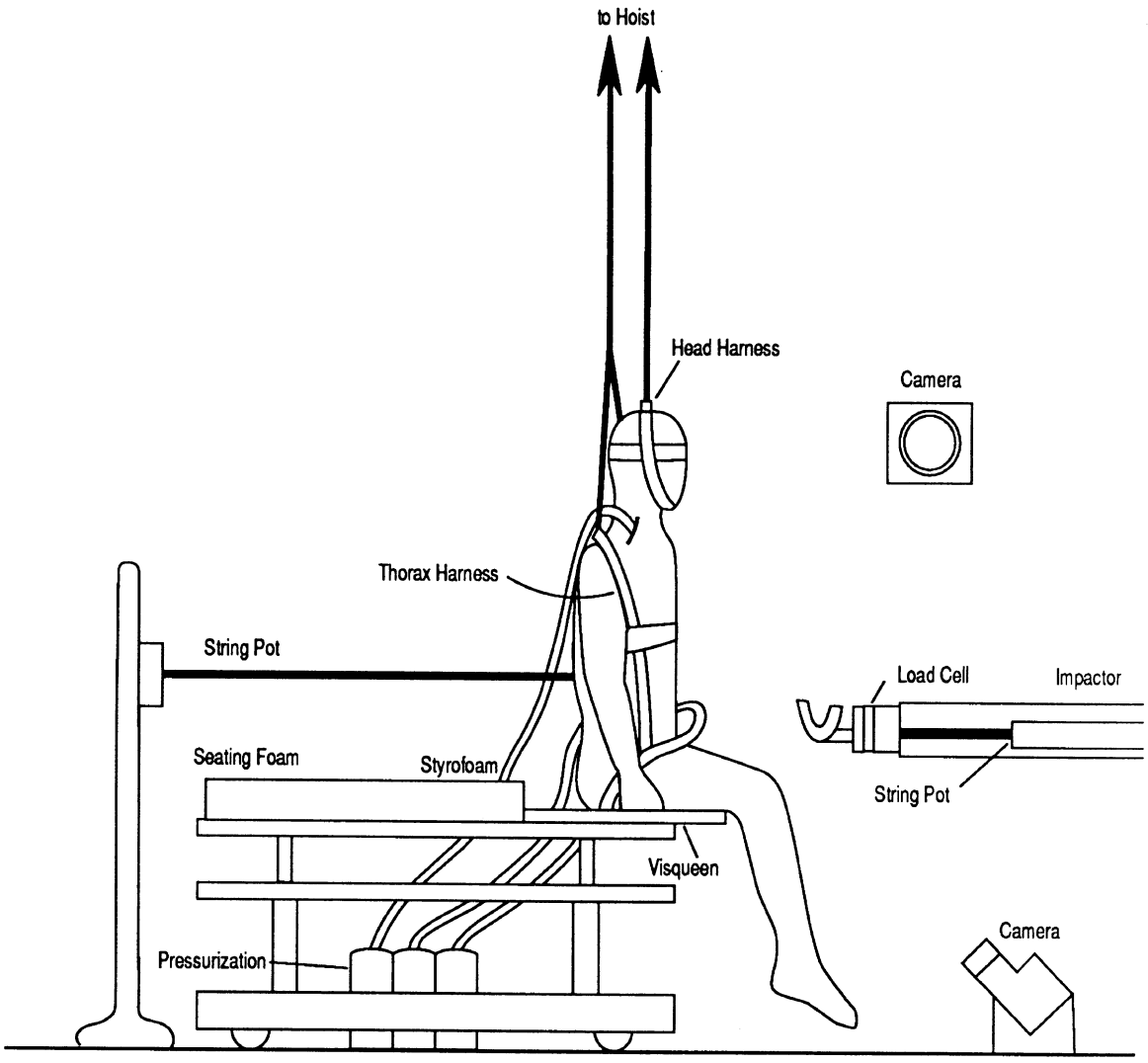

FIGURE 48. Test setup for thoraco-abdominal impacts to unembalmed cadavers using a rigid lower rim representation of a steering wheel (Nusholtz et al. 1988).

TABLE 13

VARIABLES ASSOCIATED WITH INJURY CRITERIA
(Nusholtz et al. 1988)

Test Number	Velocity (m/s)	Peak Force (N)	Energy Loss[2] N-m	Specific[1] Absorbed Energy N-m/kg	Peak Spinal Acc. m/s/s	Peak Viscous V*C m/s	Peak Viscous V*D m^2/s	Peak Normalized Deflection C %	Peak Deflection D	$V_{max}C_{max}$ m/s	$V_{max}D_{max}$ m^2/s
86M006	10.0	8900	520	7.42	620	2.34	0.75	53	0.17	5.31	1.70
86M016	6.5	5300	260	4.13	560	1.04	0.25	38	0.09	2.50	0.60
86M026	7.5	6700	320	4.63	400	1.00	0.28	36	0.10	2.68	0.75
86M042	10.8	8400	570	11.02	420	1.69	0.49	48	0.14	5.17	1.50
86M052	9.3	6700	480	6.40	300	1.42	0.44	48	0.15	4.52	1.40
86M062	3.9	3000	140	1.29	170	0.35	0.12	21	0.07	0.79	0.27

[1]Based on ESV procedure [10].

[2]Based on effective mass from mechanical impedance. Series 000–060: 26, 16, 26, 29, 38, 38, 24 kg.

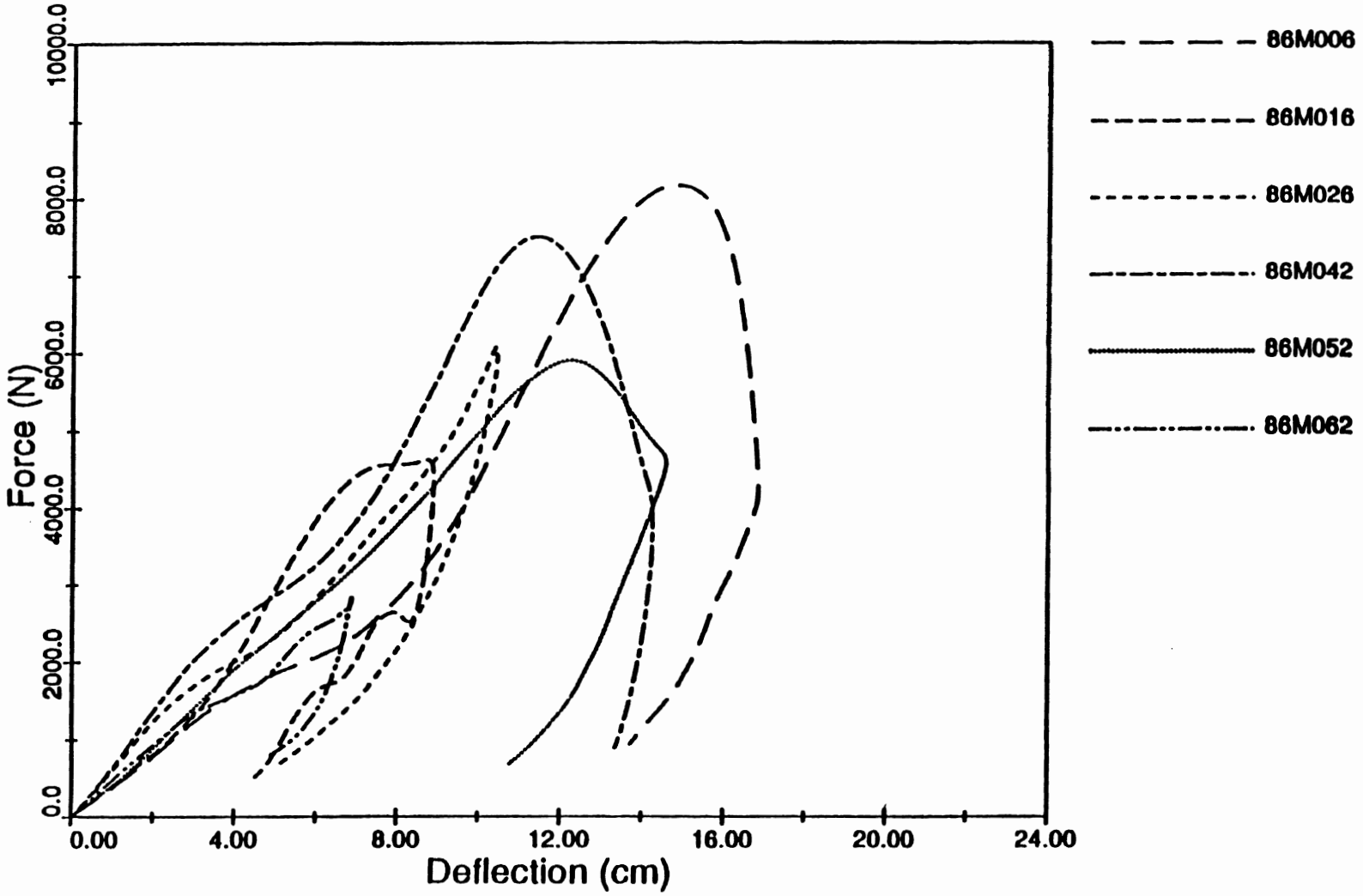

FIGURE 49. Comparison of force-deflection curves for rigid lower-rim impacts to abdomen (Nusholtz et al. 1988). Impact velocities range from 3.9 to 10.8 m/s (see Table 13).

The term "injury mechanisms" can be defined as the mechanical cause of injury to a specific organ. It relates not only to the nature and direction of the applied load but also to the structural and material properties of the organ. An understanding of how an injury occurs is important to the science of biomechanics since it is a crucial element in the determination of human tolerance to injury. It is also important to the design of a new ATD because it dictates the type and placement of transducers in the dummy.

A discussion of injuries sustained by the thoraco-abdominal organs is given by Melvin and Weber, ed. (1988) in the Phase I Task B report. The thoracic injuries are described in Chapter 3 of that report while those of the abdomen can be found in Chapter 4. Figure 50 illustrates the anatomy of the thorax and abdomen and illustrates the positions of the viscera relative to each other. The principal injuries or organs involved are listed below in the order given in the report to facilitate cross-referencing:

1. Flail chest
2. Lung contusion
3. Hemothorax or pneumothorax
4. Heart and great vessels
5. Liver
6. Spleen
7. Kidney
8. Digestive system
9. Urogenital system

B2.1.1 Injury Mechanisms of the Flail Chest (Rib Fractures). Flail chest is the result of multiple rib fractures from blunt impact to the ribcage. Thus, the mechanism of this injury is the same as that of rib fracture. Since bones are weak in tension, it is a commonly accepted notion that ribs fail due to excessive bending, with the failure occurring on the tensile side of the rib. A study by Granik and Stein (1973) proposed the testing of a section of the rib in three-point bending. Although no mention was made of the mechanism of fracture, the method implied that bending stresses were indicative of rib strength. The more important implication was the need to test a short segment of the rib because the loading of an entire rib will result in a very complex strain distribution, including torsional strains.

As pointed out by Stalnaker and Mohan (1974):

> The results of dynamic as well as static tests indicated that maximum deflection and not maximum force is the determining factor for rib fractures . . . rib fractures were more frequent at chest deflections of over 3 in, whereas none occurred at deflections less than 2.3 in.

However, as pointed out by Nahum et al. (1971):

> . . . the force level to the anterior chest wall required to produce a given deflection is also influenced by the contribution to gross chest stiffness offered by the soft tissue elements.

Thus, while the evidence seems to point to the fact that rib fractures and numbers of rib fractures are produced by the amount of chest deflection regardless of the rate of deflection, the amount of deflection produced by a given force is dependent on the rate at which that force is applied due to the viscous nature of the thorax. For seat belt (i.e., shoulder belt) loading rates, Eppinger (1978) has demonstrated that the number of rib fractures can be predicted quite well (for cadavers) by a relationship which considers the total upper torso belt force and age and weight of the subject. The number of fractures (NF) was best determined by the relationship:

$$NF = -18.66 + .00955\ NBF + .327\ AGE \qquad r=0.775$$

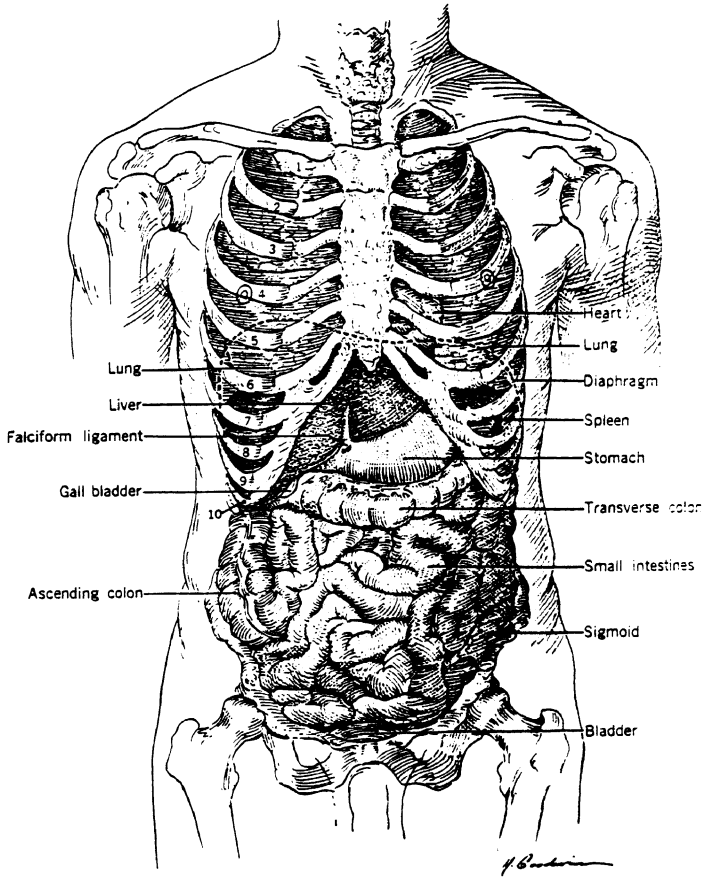

PLATE 21
Abdominal and Thoracic Viscera. Anterior View (After Pernkopf)

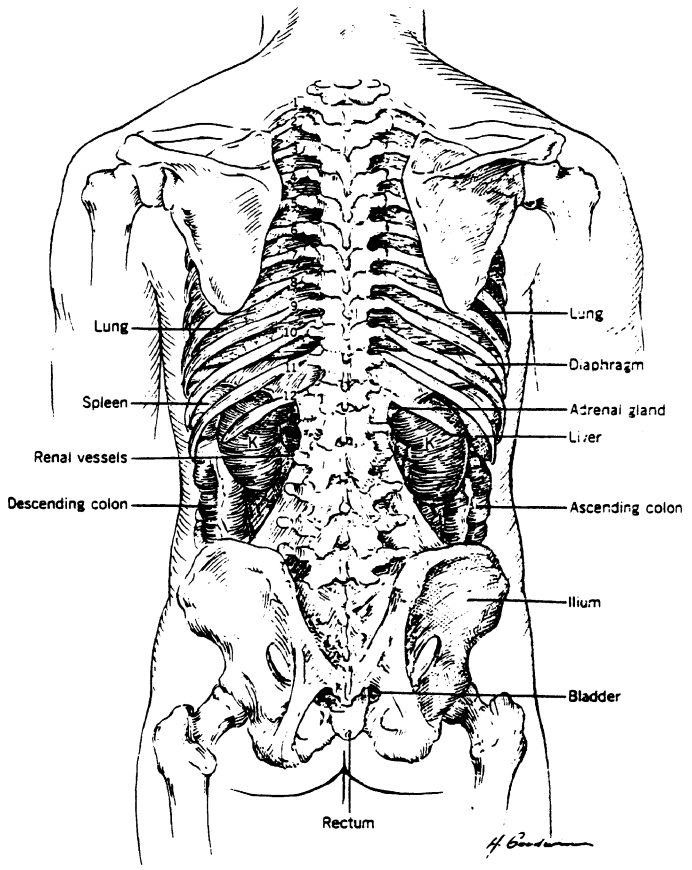

PLATE 22
Abdominal and Thoracic Viscera. Posterior View (After Pernkopf)

FIGURE 50. Illustration of thorax/abdomen anatomy showing primary visceral organs (taken from *Stedman's Medical Dictionary*, 22nd ed. Williams & Wilkins Co., 1973).

where NBF is the *normalized belt force* obtained by scaling the maximum upper torso belt force (TBF) by the mass of the subject (M_S) :

$$NBF = TBF\,[165/M_S]^{2/3}$$

B2.1.2 Mechanisms of Lung Contusion. A common form of injury to the lung is contusion. In recent studies by Fung and Yen (1984), it was found that this injury can be the result of a velocity-dependent phenomenon associated with blunt impact to the lung tissue. That is, at high impact velocities, the compression or pressure wave is transmitted through the chest wall to the lung tissue causing damage to the capillary bed of the alveolar sacs. Another possible mechanism is compression of the lung tissue due to large chest deflections. In some cases, the fractured ends of ribs can cause massive injuries to the lung.

B2.1.3 Mechanisms of Hemothorax and Pneumothorax. Hemothorax is the result of injury to the blood vessels of the lungs. This is usually caused by rib fracture and intrusion of the ribcage by a blunt impactor. If the integrity of the pleura sac around the lungs is compromised, the result is a pneumothorax. The mechanism for pneumothorax or hemothorax is therefore the same as that responsible for rib fractures.

B2.1.4 Mechanisms of Contusion and Rupture of the Heart and Great Vessels. The mechanism of contusion to heart muscle is probably due to both compression and speed of compression. The more serious injury of cardiac laceration and rupture is likely to result from a severe degree of compression of the heart by the sternum. However, no biomechanical studies are available to confirm this mechanism. Damage to heart valves can also be attributed to this compression mechanism. If the speed of impact is very high, the electrical rhythm of the heart is disrupted and ventricular fibrillation or standstill can result. The mechanism of this type of injury is not well understood but it is believed that the heart is an electromechanical transducer which transforms an electrical signal into mechanical energy and its ability to perform as a transducer is lost due to a high-speed, blunt impact. Excessive chest compression is not necessary for this type of velocity-dependent injury. However, the speed of impact needs to be well in excess of 65 km/hr (40 mph).

A more common form of automotive related injury which is frequently fatal is aortic rupture. Again, the precise mechanism of this injury is not known. In a review of the subject by Viano (1983), several mechanisms were proposed to explain the observed injuries at the aortic isthmus, root, and aortic insertion into the diaphragm. The ruptures are generally transverse even though the ultimate strength of the aorta is higher transversely in comparison to that in the longitudinal direction. This suggests that deformation of the aorta (stretching and/or twisting) is a more likely mechanism for rupture than an increase in aortic blood pressure. The contribution of arteriosclerosis and atherosclerosis is suspected. The injury has been duplicated in living animals but is not frequently seen in cadaveric subjects with pressurized arterial systems. In fact, in a series of blunt chest impacts carried out at Wayne State University in 1985–86 on approximately 10 subjects, no aortic ruptures resulted from impacts from various directions. In a study of road traffic accidents involving twelve cases of aortic rupture, Newman and Rastogi (1984) make the observation that in all these cases the impact was not truly head-on and therefore the injured occupants must have been subjected to oblique or transverse forces to the chest that would have imposed shearing stresses at the junction of the fixed and mobile parts of the aorta.

B2.1.5 Mechanisms of Injury to the Liver. Liver injuries range in severity from minor contusions to deep lacerations, tears and ruptures with a star-shaped burst pattern. The mechanism for minor contusions is rib compression or compression against the vertebral column. While minor lacerations can result from fractured ends of ribs, deep and extensive lacerations are due large displacement of the liver, causing it to tear at the ligamentous attachments between the different lobes. Extreme compression due to a high-speed blunt

impact is responsible for the star-shaped bursting injuries. A more detailed discussion of these mechanisms is provided by Chapon (1984). Hepatic injuries can also be attributed to the shoulder belt (Lau and Viano 1984). The mechanisms are presumably the same as those described above.

B2.1.6 Mechanisms of Injury to the Spleen. There are several types of splenic injuries. Minor tears can lead to progressive hemorrhage and hypovolemia. Subcapsular or intraparenchymal hemorrhage can lead to secondary ruptures days or weeks after the initial injury. Deep lacerations and transections result in extensive hemorrhage followed by shock. There are two principal mechanisms of injury. Direct impact to the left upper abdominal area (left hypochondriac region) causes the spleen to contact the rib cage or ends of fractured ribs. Alternately, inertial forces acting on the spleen can cause the same injuries.

B2.1.7 Mechanisms of Injury to the Kidneys. Injury types seen in the kidney due to blunt trauma range from renal contusions to complete tears of the organ, as described by Nash (1969). Minor contusions result in slight disruptions of the renal parenchyma while major tears cause complete disruption of the organ. For frontal impact, the kidney is injured by direct contact with a hard surface, such as the steering wheel (Dejeammes 1984).

B2.1.8 Mechanisms of Injury to the Intestines. Intestinal injuries and their mechanisms are described by Walt and Grifka (1970) and by Williams and Sargent (1963). The injury pattern consists of contusions, perforations, tears and total transection of the large and small intestines. Similar injuries can be sustained by the stomach which is also a hollow abdominal organ. The injury mechanisms are:

- Direct compression with disruption of tissues due to pressure from without.
- Rupture of the hollow viscous due to increased intraluminal pressure which exceeds the bursting strength of the organ.
- Shearing by torsional forces of relatively fixed and inelastic supporting ligaments, mesenteries and blood vessels.
- Perforation by fragments of fractured bones such as ribs and the pelvis.

B2.1.9 Mechanisms of Injury to the Urogenital Organs. The principal organs at risk are the bladder and the gravid uterus. In the case of the bladder, the mechanism of injury is similar to that of the hollow abdominal organs described above. For the gravid uterus, the mechanism of injury to the fetus appears to be pressure build-up within the uterus due to compression of the abdominal cavity. Crosby et al. (1972) showed that the three-point harness has less injury potential than the lap belt alone, as far as the fetus is concerned. There was extreme flexion of the torso in a frontal impact when the lapbelt was used whereas, the degree of flexion was considerably less with the three-point system.

B2.1.10 Spinal Injuries. Although injuries to the thoraco-lumbar spine have an extremely low incidence in motor vehicle crashes, the consequences of an injury to the spinal cord are catastrophic. King (1984) reported that the injury rate for all types of impact was 0.8% for the thoraco-lumbar spine, based on NCSS data files covering 12,050 crashes, 15,973 vehicles and 26,935 occupants. Twenty percent of these injuries were the result of frontal impacts.

Injuries to the thoraco-lumbar spine can be grouped into six different categories:

Anterior wedge fractures
Burst fractures
Dislocations and fracture/dislocations
Chance fractures
Rotational injuries
Hyperextension injuries

Spinal flexion accompanied by axial compression can cause anterior wedge fractures. If the compressive component is large, burst fractures result. The integrity of the spinal cord is threatened by burst fractures which cause some of the fragments of the vertebral body to be propelled posteriorly towards the spinal canal. Dislocations and fracture/ dislocations occur under similar loading conditions when there is rupture of the posterior interspinous ligaments. There is a high probability of cord injury due to intrusion of the vertebral body into the spinal canal. If the lapbelt is used without a shoulder harness and if the belt is worn above the anterior-superior iliac crest, it acts as a fulcrum for the lumbar spine to flex over it, causing a transverse split of the vertebra, beginning with the spinous process or the posterior ligaments. This type of injury was first observed by Chance (1948) and is named after him.

If the spine is twisted about its longitudinal axis, rotational injuries occur. These include lateral wedge fractures, uniform compression of the vertebral body and fractures of the facets and lamina. Hyperextension injuries are seen in military pilots who eject from an F/FB–111 aircraft, as reported by Kazarian (1979). They are due to the rapid rearward pull of the shoulder harness just prior to ejection, causing avulsion of the superior lip of one or more thoracic vertebrae. This injury is not seen among civilians.

B2.2 Thorax/Abdomen Injury Criteria

Injury criteria, as defined by Lau and Viano (1986), are "biomechanical indices of exposure severity which, by their magnitude, indicate the potential for impact-induced injury." They should reflect specific underlying biomechanical responses and mechanisms of injury. In view of the incomplete understanding of such mechanisms for individual visceral organs, the criteria must necessarily reflect injury tolerance of an entire body region to impact as opposed to that of each organ. Both the thorax and abdomen body regions contain soft-tissue organs and large blood vessels. The thorax is surrounded completely by a skeletal structure—the spine and ribcage—both of which partially cover the upper abdominal area.

Since all impact-related injuries are the result of force applied to the human body, it might be expected that injury severity would be best correlated to the level of applied force. However, because the viscous nature of the body tissues and the area over which force is applied dramatically influence the manner in which impact loads affect body kinematics, measurement of force alone is not sufficient to predict injury. Both the rate of loading and the area of loading are essential to assessing the levels of injury that may be result.

Eppinger and Marcus (1985) have suggested that the concept of *absorbed energy* might be a useful predictor of injury and have recommended efforts to "make specific absorbed energy a realizable dummy-based measurement." As with the idea of using force as an injury criteria, however, they have shown that one must know not only the amount of energy absorbed, but also the area over which the impact forces are applied, as well as the length of time needed for the thorax to acquire the non-kinetic energy delivered to it. Using this concept of absorbed energy, contact area, and time, an attempt was made in the Phase I effort (Melvin et al. 1988a) to search for combinations of these parameters that would correlate well with AIS ratings using results from a large number of cadaver impact tests at different facilities. Table 14 shows the sources and symbols for the data used and Figures 51 and 52 show plots of injury criteria based on force, mass, area and absorbed energy with AIS level. As indicated, poor correlations resulted with correlation coefficients for least-square linear regressions of 0.563 or less.

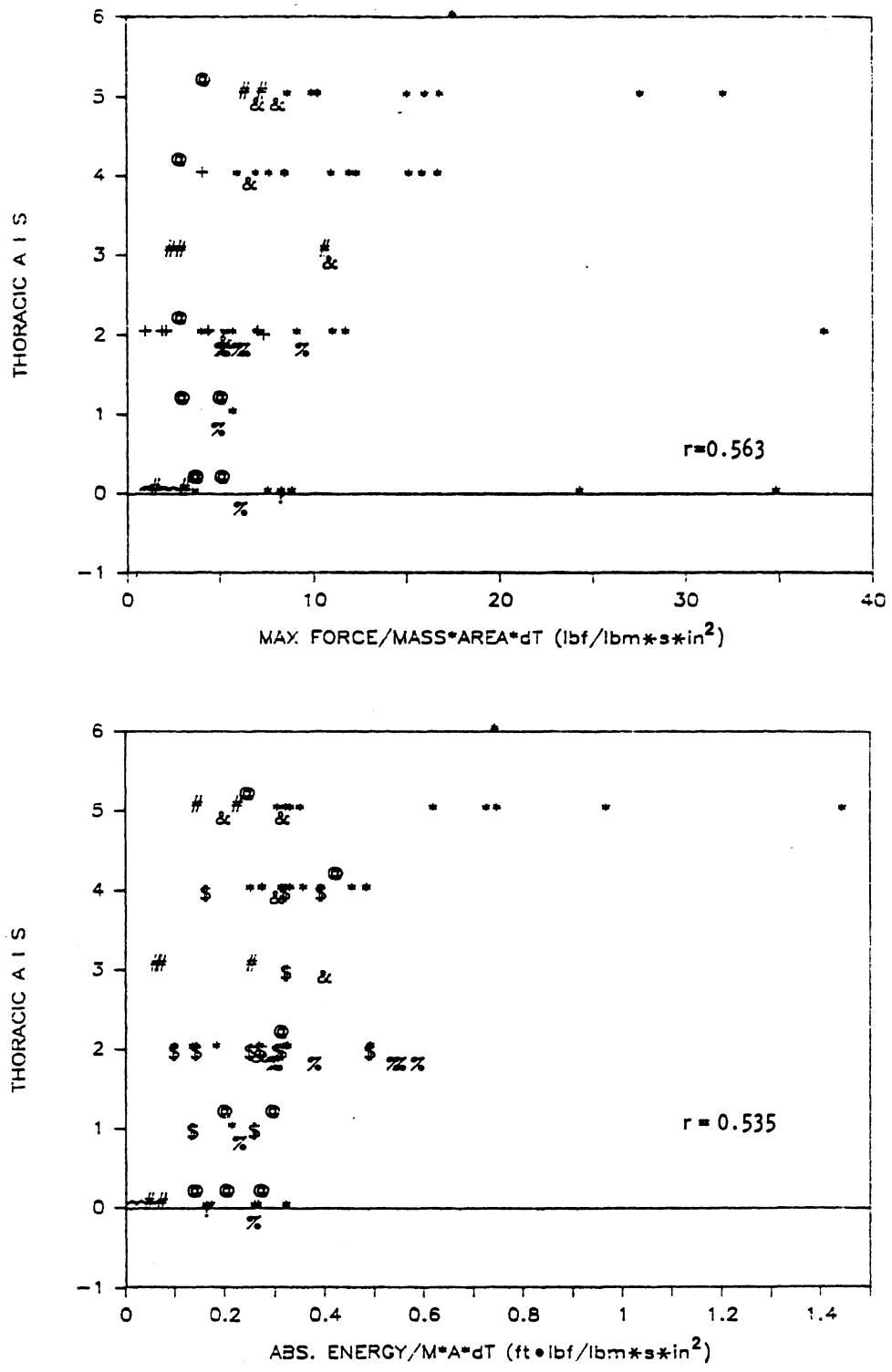

FIGURE 51. Various cadaver and volunteer impacts with revised AIS values using force, mass, area, and absorbed energy as injury predictors (unrestrained steering wheel impacts excluded) (Melvin et al. 1988a).

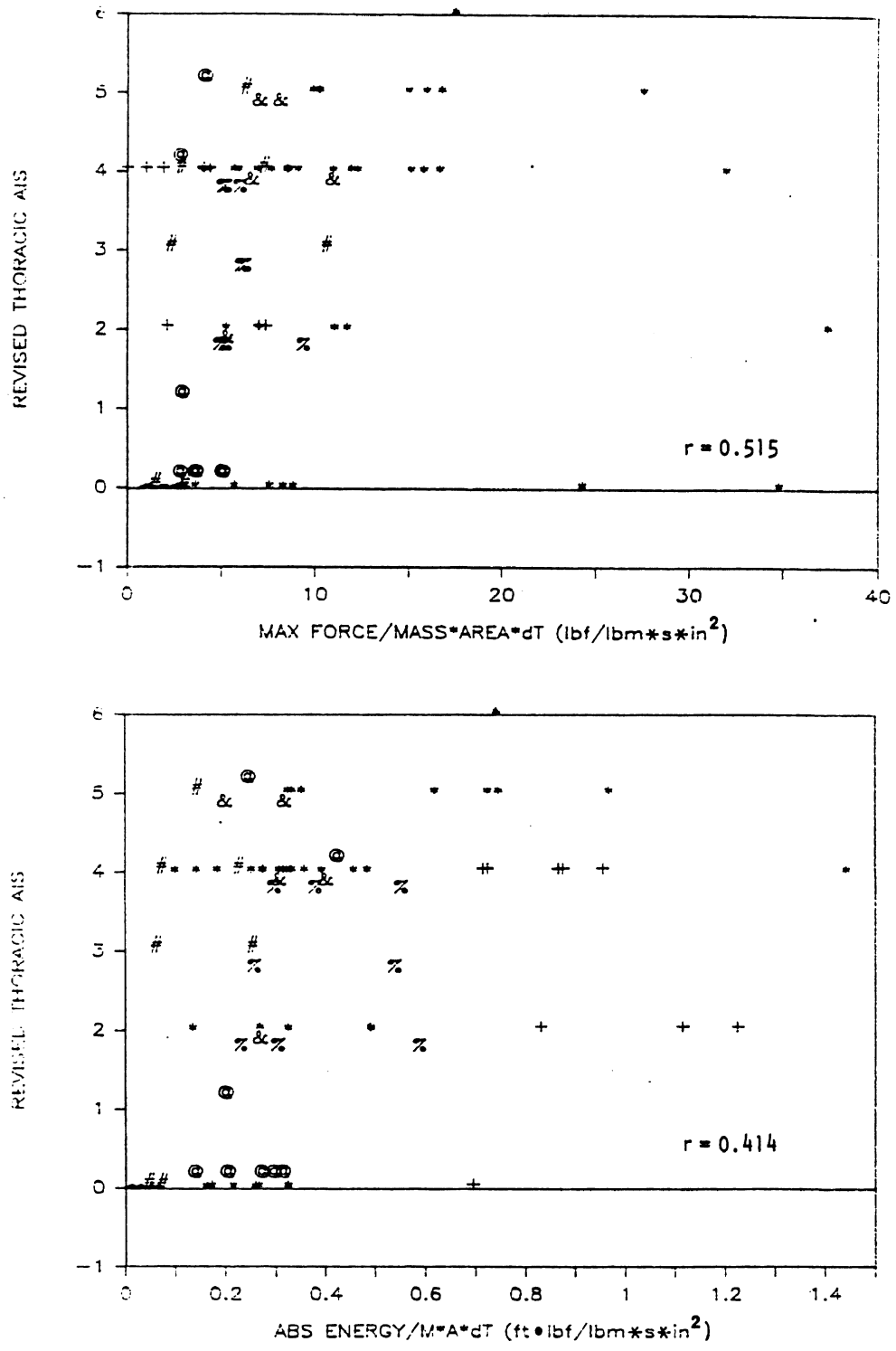

FIGURE 52. Various cadaver and volunteer impacts with revised AIS values using force, mass, area, and absorbed energy as an injury predictor (unrestrained steering wheel impacts excluded) (Melvin et al. 1988a).

TABLE 14

IMPACT MODE AND IDENTIFYING SYMBOLS
FOR VARIOUS THORACIC IMPACT SERIES
(Melvin et al. 1988a)

Symbol	Run Description
*	UCSD pendulum impacts, sponsor GM
#	UM pendulum impacts, sponsor NHTSA
^	WSU low-level pendulum impacts to volunteers
$	Calspan pendulum impacts, sponsor NHTSA
&	UCSD (Schneider) belt impacts
@	WSU airbag sled runs, sponsor NHTSA
?	SRL run 29
%	WSU knee-bolster/belt sled runs, sponsor NHTSA
+	WSU unrestrained driver impacts with steering wheel, sponsor GM
A, etc.	GM pig pendulum impacts

In view of the difficulty in measuring force, absorbed energy, applied area, and time during both cadaver impacts and in ATDs, and the inability to obtain consistently good correlations of injury with these measures, efforts have been directed to using secondary indices of impact to predict injury. The secondary indices that have been proposed are kinematic parameters which are more amenable to biomechanical measurement techniques and include displacements, velocities, and accelerations. Displacement-based criteria assume the system to deform elastically because force is proportional to displacement in an elastic structure. Velocity-based criteria are suitable for viscous systems which respond to the rate of load application rather than to the load itself. Acceleration-based criteria reflect the concept that injury can be caused by inertial forces.

For the thorax, all three parameters have been proposed as viable criteria for injury. In early human tolerance work (Eiband 1959) accelerations were measured at the subject seat or platform of the test subject but in recent surrogate research accelerometers are mounted to bony structures such as ribs, sternum, and/or spinal segments. The current FMVSS thorax tolerance level is based on an acceleration criterion (i.e., Part 572 ATD), requiring that the spinal acceleration at the level of the sternum not exceed 60 G for more than 3 ms.

Subsequent to the collection and analysis of the Kroell data, attempts to correlate AIS ratings with response parameters (Neathery 1974, Neathery et al. 1975, Nahum et al., 1975) suggested that normalized displacement of the sternum is a better predictor of injury than sternal or spinal acceleration. A 40% compression of the chest at the sternal level was determined to be an indication of severe thoracic injury resulting in multiple rib fractures and a high potential for flail chest. As a result of these studies, the Hybrid III thorax was provided with a sternal deflection sensor in addition to the spinal acceleration transducers of Part 572.

Velocity of impact was first considered to be responsible for injury to the lung by Bowen et al. (1968) who studied blast injuries resulting from pressure waves encountered in an explosive environment. Recent studies (Viano and Lau 1985, Lau and Viano 1986) have further demonstrated that impact velocity is important in the prediction of soft tissue injuries. Figure 53 shows a plot from their paper (Lau and Viano 1986) which suggests that, at low velocities of impact (less than 3 m/s), injuries to soft tissues are due primarily to large displacements which cause crushing of the organs against the spine. At high velocities

(greater than 30 m/s), injuries may be produced by the blast phenomenon. Between these two, injuries to the viscera are produced by both compression and velocity of compression. Thus, it is possible to produce serious injuries to the visceral organs with high-velocity, low-deflection loading that does not produce rib fractures which require high deflections (i.e., significant bending stress).

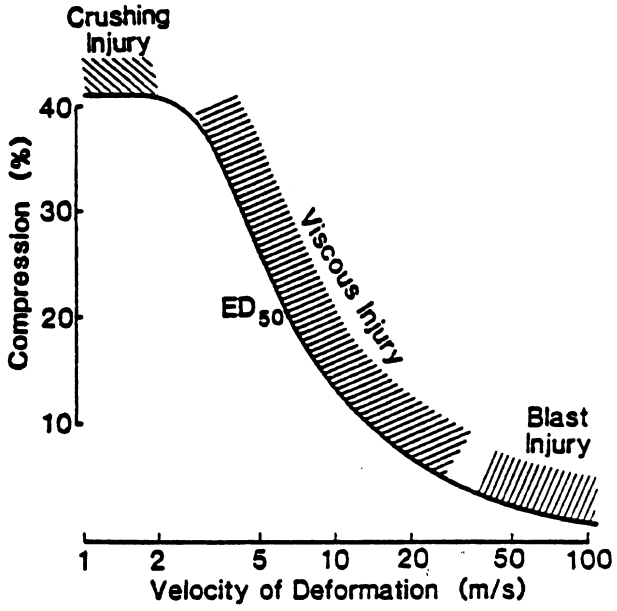

FIGURE 53. Relation of velocity of deformation to injury criteria (Lau and Viano 1986).

A criterion which combines both velocity and deformation of the chest has been proposed by Lau and Viano (1986) in the form of a product—*VC*, where V is the velocity of the impactor and C is the ratio of the chest compression to total chest depth. The maximum value of *VC* is determined from the product of the two time functions, V(t) and C(t). It is based on the premise that the energy dissipated by the viscous system is proportional to *VC*. Fortunately, the Hybrid III ATD measures the time-function of sternal displacement and therefore the sternal velocity and *VC* can be determined by differentiation. Figure 54 shows plots from the Phase I effort of AIS versus two versions of the viscous criterion. As indicated, the correlations are significantly improved over those obtained for criteria involving either force or absorbed energy. Using probability functions based on Logist analysis, Viano (1989) reports that a VC value of 1.5 m/s and a compression (C) value of 38% correspond to 25% probabilities of AIS 4+ for frontal impacts to the sternum at low (less than 3 m/s) and high impact velocities, respectively.

For the abdomen, there has not been an intensive effort to establish an injury criterion. A summary of the work done in the area of abdominal injuries was provided by Stalnaker and Ulman (1985). There were indications that tolerance was proportional to compression at some locations and to velocity at others and to neither of the two at still other locations. It was concluded that the *VC* criterion appeared to provide the best prediction for abdominal injury. Recent Kroell-type impact tests to the abdomens of unembalmed cadavers have confirmed the validity of *VC* as a good injury predictor for abdominal injuries (D. Viano, personal communication, 1988). Viano (1989) reports that a VC value of 2.0 m/s and a compression of 47% correspond to 25% probabilities of AIS 4+ in the abdomen for low- and high-impact velocities, respectively.

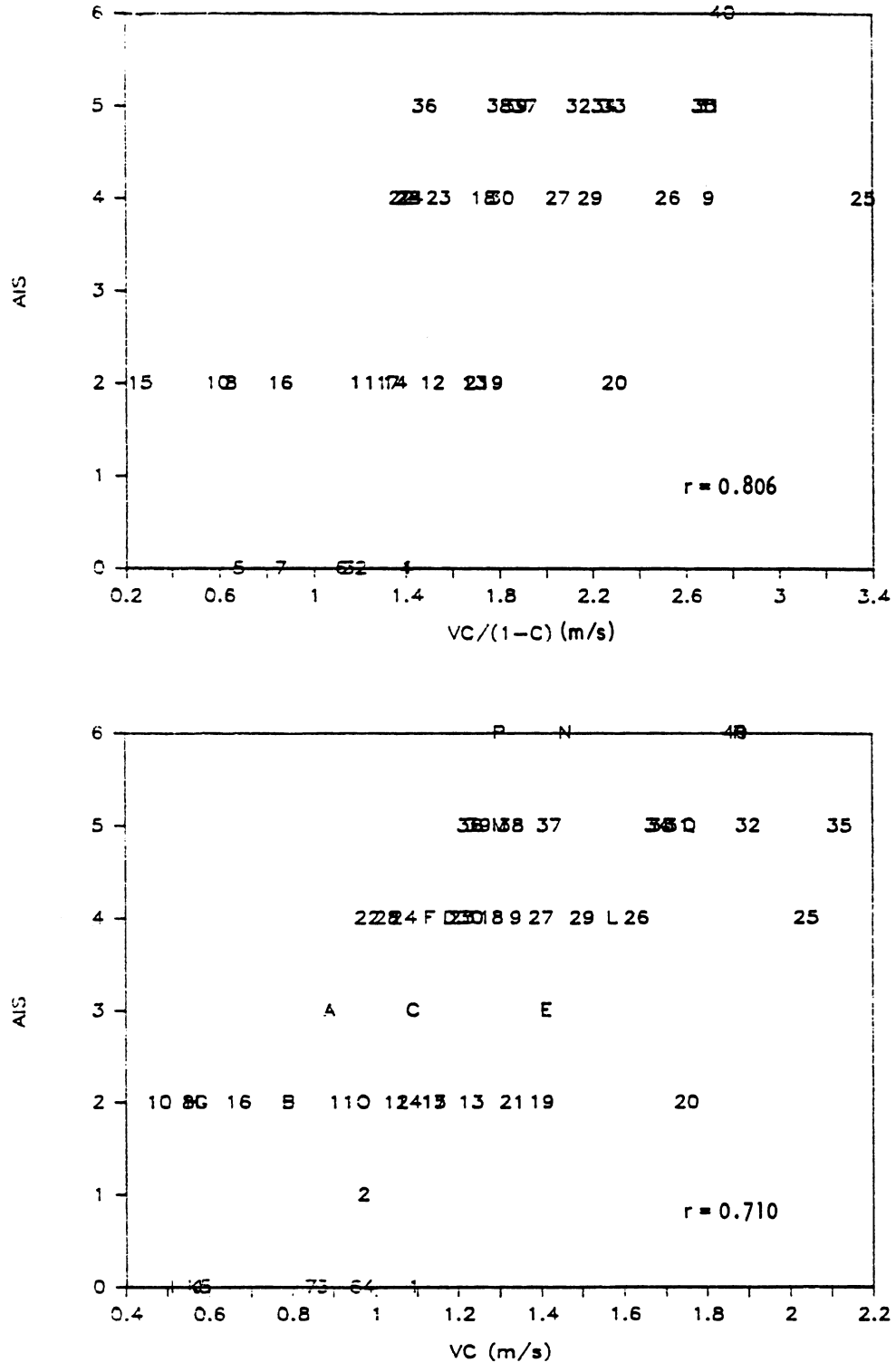

FIGURE 54. UCSD cadaver/pendulum and GM pig/pendulum impacts, with revised AIS values, using two versions of the viscous criteria as injury predictors (Melvin et al. 1988a).

B2.3 Instrumentation for the Thorax and Abdomen

It is evident from the discussion above that the mechanisms of injury to the various visceral organs of the thorax/abdomen are not fully understood or verified. It is also obvious that it is neither feasible nor practical to simulate the response and failure of the individual organs and anatomical structures of the human body.

With this perspective, it seems clear from the state of current knowledge on injury criteria, that an improved ATD thorax must, as a first priority, be able to measure both chest compression (i.e., deflection) and velocity of deflection as functions of time. Furthermore, assuming that the new subcomponent has improved biofidelity in both impact and static loading response at regions other than the sternum, and, assuming that it reproduces humanlike load distributing properties of the rib cage, these measurements of compression and velocity of compression should be made at multiple regions of the chest and abdomen where critical injuries to organs may occur. At a minimum, the thorax should provide these measures near the torso midline at the level of the mid to lower sternum and at the regions of the left and right lower lateral rib cage (i.e., 7th to 10th ribs). The abdomen should also be able to measure penetration and velocity of penetration in the mid-sagittal plane. Additional measurement sites beyond these four would be beneficial to ensuring that injuries due to off-center loading by steering wheels and instrument panels would be properly assessed.

In addition to measuring deflection and velocity-time functions at multiple regions, the new design should incorporate load-sensing clavicles capable of measuring the normal force applied to the clavicle links. This information will be primarily useful to assess relative loading at the shoulder due to different restraint systems (i.e., evaluation of restraint systems) but could also be used to predict the occurrence of clavicle fractures resulting from impact with steering wheels and instrument panels.

Accelerations of the thoracic spine should be measured in the new subcomponent to provide information about whole-body accelerations which can be a factor in spinal injuries and which may also play a role in certain mechanisms of injury to the internal organs. In addition, spinal acceleration may be the best means to quantify injury severity for severe impacts where the thorax or abdomen has bottomed out (i.e., spinal acceleration can be an indicator of how much over AIS 4 the injury severity is). Because, the thoracic spine will probably consist of at least two articulated segments in the new design (i.e., for spinal flexibility), more than one set of accelerometers will be needed.

Load cells are currently available for the spine at levels of T1 (replaces dummy neck bracket), T12 (just above the lumbar spine), and L5 (just below the lumbar spine). The T1 load cell is a six-axis unit, the T12 load cell measures three forces and two moments (Mx and My), while the L5 load cell is usually a three-axis unit measuring Fx, Fz, and My. The new spine should provide for installing these load cells.

For future injury criteria that may be based on absorbed energy or delivered force parameters, measurement of contact area seems essential. In addition, knowledge of the shape and area of the surface to which loads are applied during an impact may prove important in utilizing information from deflection and velocity sensors (i.e., to discriminate a 50-mm-wide belt from a steering wheel hub or a hub from an air bag). For these reasons, it would be ideal if the new thorax/abdomen system (or some later version of it) included instrumentation to measure the contacted area as a function of time during impact.

Viano (personal communication, 1988) has further suggested that measurement of dummy kinematics may be a very good indicator of injury potential. Thus, measurement of flexion/extension angles at femur/pelvis, lumbar, and thoracic spine articulations could be used to assess the potential effectiveness of a restraint system for reducing thoracic injuries. For example, a restraint system (e.g., a three-point belt) that allows the occupant to pitch

forward at the hip so that the shoulder takes more load than the chest will probably result in less thoracic injury than a restraint system (e.g., a two-point shoulder belt) that allows the lower body to slide forward so that the shoulder slides down and stays back (see Figure 58).

B3.0 ANTHROPOMETRIC SPECIFICATIONS

B3.1 Thorax/Abdomen

The anthropometric specifications for the new thorax/abdomen have been determined by Schneider et al. (1985) and Robbins (1985). Included are specifications for exterior dimensions as well as body segment mass, volumes, centers of mass, and mass moments of inertia. The dimensional data have been determined for the vehicle-seated 50th-percentile male and, as such, more closely represent the shape and posture of the average male seated in a car.

Since the current effort requires interfacing the new subcomponent with the Hybrid III ATD at the pelvic, lumbar spine, cervical spine, and arms, it may be necessary to modify the AATD dimensions to attain reasonable hardware interfacing. The full three-dimensional shape of the new thorax/abdomen is represented in the epoxy-fiberglass standard reference form shown in Figure 55 and in the full-size engineering drawings that accompany the NHTSA reports.

Table 15 summarizes the anthropometric specifications for the thorax and abdomen regions. Additional work is necessary to present the anthropometric data provided by Robbins (1985) into formats that are more useful to the designer. For example, the locations of the center of mass of the thorax and abdomen relative to either the whole-body or body-segment coordinate systems are of little value to the designer of an isolated subcomponent when its on the "bench," especially with the sloped angle of the torso relative to the reference system used in the drawings. Providing straight-line distances between more useful reference points such as the front of the chest at sternum level, the back of the thorax, the bottom of the neck, etc. will be more beneficial to the designer. The following distances were measured directly from the full-size drawing of the mid-size male:

Distance of thorax cg from sternum	127 mm
Distance of thorax cg from back	107 mm
Distance of thorax cg from C7/T1	200 mm
Distance of thorax cg below mid-sternum	85 mm
Distance of abdomen cg from front	130 mm
Distance from C7/T1 to T4/T5	76 mm
Distance from T4/T5 to T8/T9	110 mm
Distance from T8/T9 to T12/L1	128 mm
Distance from T12/11 to L2/L1	91 mm

B3.2 Ribcage

As has been documented in Appendix A and elsewhere, one of the limitations of the Hybrid III thorax is with regard to the shape and size of the ribcage which is more barrel-shaped and considerably shorter than that of the human. This presents problems achieving consistent and appropriate interaction with shoulder belts and it is clear that a more humanlike-shaped ribcage is needed for improved performance and injury assessment.

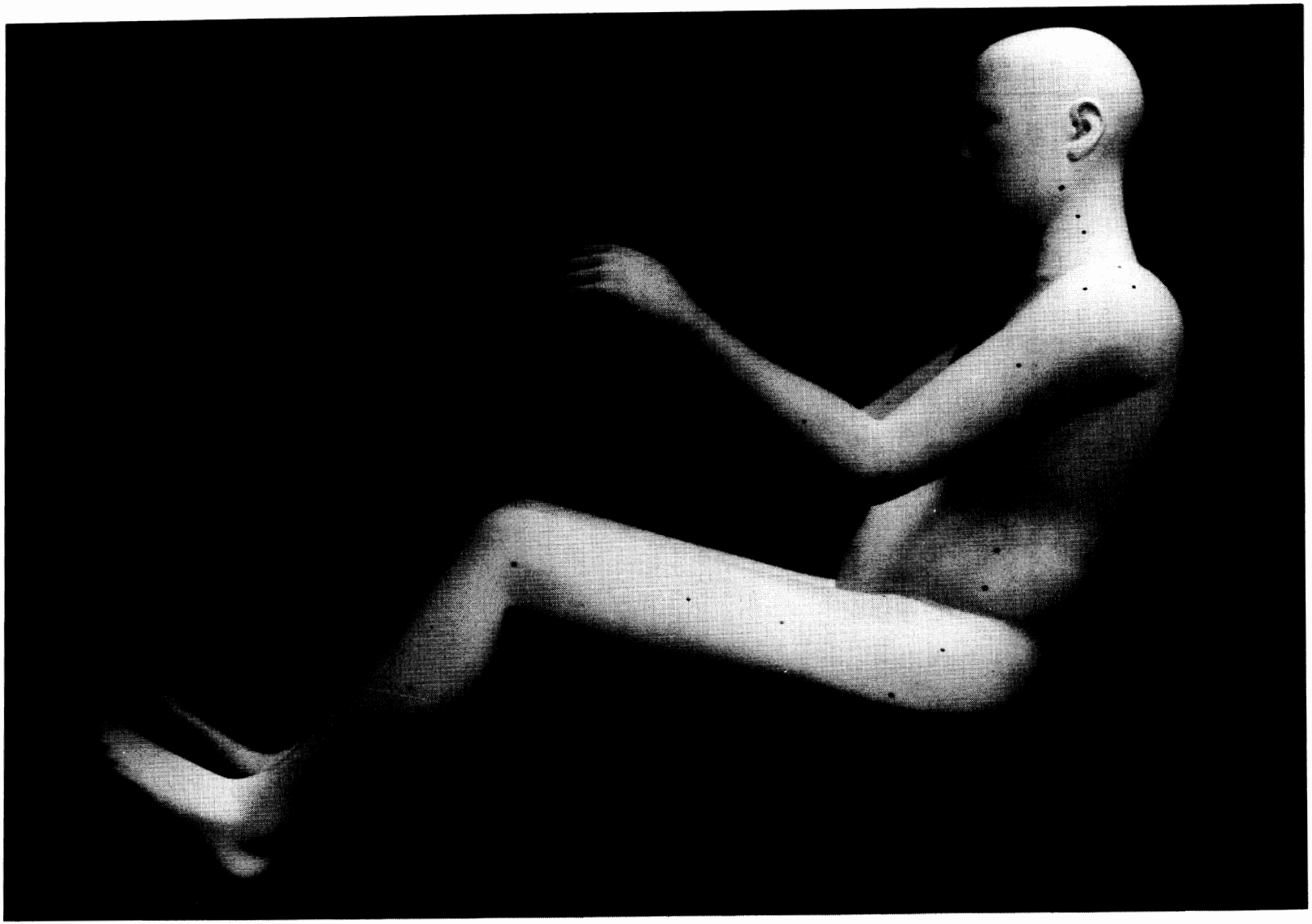

FIGURE 55. Side view of mid-size-male reference form (Schneider et al. 1985).

TABLE 15

ANTHROPOMETRIC SPECIFICATIONS FOR THORAX AND ABDOMEN
(Schneider et al. 1985 and Robbins 1985)

Measurement	Thorax	Abdomen
MASS SPECIFICATIONS		
Volume (cm^3)	23763	2365
Specific Gravity	0.920	1.01
Mass (kg)	21.86	2.39
Ixx ($kg-m^2$)	0.42011	0.01693
Iyy	0.29648	0.01076
Izz	0.27746	0.02574
DIMENSIONS (cm)		
Chest breadth at axilla	30.4	
Chest circumference at axilla	103.9	
Chest breadth at nipple	34.9	
Chest circumference at nipple	100.7	
Chest circumference at 10th rib	90.6	
Chest depth at substernale	23.0	
Chest depth at nipple	23.3	
Waist breadth at umbilicus		31.5
Waist depth at umbilicus		25.2
Waist circumference at umbilicus		91.7
Abdomen breadth (maximum)		32.6
Abdomen depth (maximum)		26.0
Abdomen circumference (maximum)		94.7

Measurements of the three-dimensional shape of the ribcage of ten "normal" subjects have recently been made by Dansereau and Stokes (1988) using stereoradiographic techniques. The results are summarized in Tables 16 and 17 and Figure 56 and while the authors do not provide anthropometric information on the subjects, the information can be used as a guide to the design of a more anatomically-shaped ribcage.

As indicated by these data, there is considerable variability in ribcage geometry between different subjects. In the new thorax, the primary concern is that the structure representing the ribcage (i.e., the structure that distributes loads and couples or decouples the thoracic regions) represents the human ribcage in its most general size and shape. For Hybrid III, this means primarily adding ribs in the lower cage regions (i.e., 7th through 10th ribs) and perhaps adding some upper ribs as well (1st through 3rd ribs). Slanting the ribs is probably not essential except for the purpose of placing the lower ribs in the desired regions below the bottom of the thoracic spine or for improving response biofidelity. As a start, the general ribcage dimensions of the Ogle/MIRA dummy (Searle and Haslegrave 1970; Warner and Ogle 1974) illustrated in Figure 57 can be used as a guide in modifying the Hybrid III design.

TABLE 16

MEANS AND S.D. OF RIB SHAPE AND ORIENTATION MEASUREMENTS
(Dansereau and Stokes 1988)

Level	Rib Length (mm)	Instrinsic Measures		Chord Length (mm)	Extrinsic Measures	
		Enclosed Area (mm^2)	Max Curvature (mm^{-1})		Frontal Angle (degrees)	Lateral Angle (degrees)
T2	203.0 ±28.5	6001 ±1491	0.0331 ±0.0074	113.9 ±16.2	19.5 ±9.2	35.2 ±10.3
T3	254.8 ±25.6	9686 ±1763	0.0286 ±0.0034	142.6 ±16.1	16.9 ±8.4	34.5 ±9.1
T4	289.1 ±24.8	12543 ±2036	0.0253 ±0.0037	168.2 ±19.7	13.6 ±7.0	35.2 ±8.8
T5	304.8 ±28.9	14380 ±2372	0.0242 ±0.0043	190.0 ±19.9	12.1 ±6.5	36.1 ±7.8
T6	313.8 ±31.7	14732 ±3083	0.0239 ±0.0044	202.6 ±17.7	10.4 ±6.0	37.2 ±7.7
T7	307.9 ±37.6	13992 ±3724	0.0236 ±0.0032	212.4 ±21.4	10.9 ±6.2	39.0 ±6.6
T8	297.0 ±32.0	12878 ±3294	0.0225 ±0.0031	212.4 ±17.2	12.7 ±6.4	41.3 ±7.5
T9	279.7 ±29.6	11586 ±2914	0.0207 ±0.0025	200.0 ±15.7	19.7 ±5.8	40.0 ±6.8
T10	250.9 ±22.8	9271 ±2028	0.0184 ±0.0031	186.8 ±13.5	30.0 ±6.1	37.2 ±6.3
T11	195.3 ±27.7	5353 ±1719	0.0170 ±0.0028	154.8 ±18.3	39.5 ±4.9	32.4 ±6.1

TABLE 17

ASYMMETRY OF RIB SHAPE MEASUREMENTS (MEANS AND S.D.)
(Dansereau and Stokes 1988)

Level	Rib Length (%)	Instrinsic Measures		Chord Length (%)	Extrinsic Measures		
		Enclosed Area (%)	Max Curvature (%)		Frontal Angle (degrees)	Lateral Angle (degrees)	Posterior Rotation (degrees)
T2	–0.19 ±9.05	–0.86 ±17.50	2.80 ±22.06	–1.63 ±8.17	0.62 ±5.34	–0.54 ±5.68	0.47 ±4.84
T3	1.41 ±6.44	2.16 ±12.82	4.45 ±13.42	1.55 ±3.97	2.00 ±6.27	–1.23 ±4.23	0.27 ±3.62
T4	–0.39 ±5.76	–0.93 ±11.75	2.17 ±19.61	–2.97 ±3.46	2.88 ±7.87	–0.79 ±2.76	0.55 ±2.89
T5	2.53 ±11.52	–2.88 ±9.35	4.46 ±14.09	0.62 ±4.89	3.05 ±7.11	–0.87 ±2.55	0.35 ±2.49
T6	0.28 ±4.86	–0.36 ±9.89	–0.06 ±14.91	0.17 ±2.60	2.07 ±7.32	–1.57 ±4.89	0.09 ±3.32
T7	1.83 ±7.08	4.00 ±15.12	4.50 ±11.93	0.11 ±6.00	0.89 ±7.98	–1.42 ±2.82	0.71 ±2.98
T8	1.30 ±3.06	3.77 ±6.87	2.74 ±13.63	–0.32 ±4.31	0.99 ±8.63	–1.35 ±2.82	0.55 ±2.09
T9	2.44 ±4.34	4.79 ±8.85	–0.74 ±14.58	0.49 ±3.99	1.64 ±6.77	–1.74 ±6.90	0.48 ±2.55
T10	2.85 ±3.32	6.66 ±7.28	10.55 ±20.79	–0.02 ±5.43	3.53 ±6.33	–3.54 ±5.39	2.36 ±3.27
T11	5.78 ±8.06	12.12 ±19.37	–1.46 ±22.39	2.56 ±8.11	3.66 ±3.65	–3.86 ±7.95	1.36 ±3.15

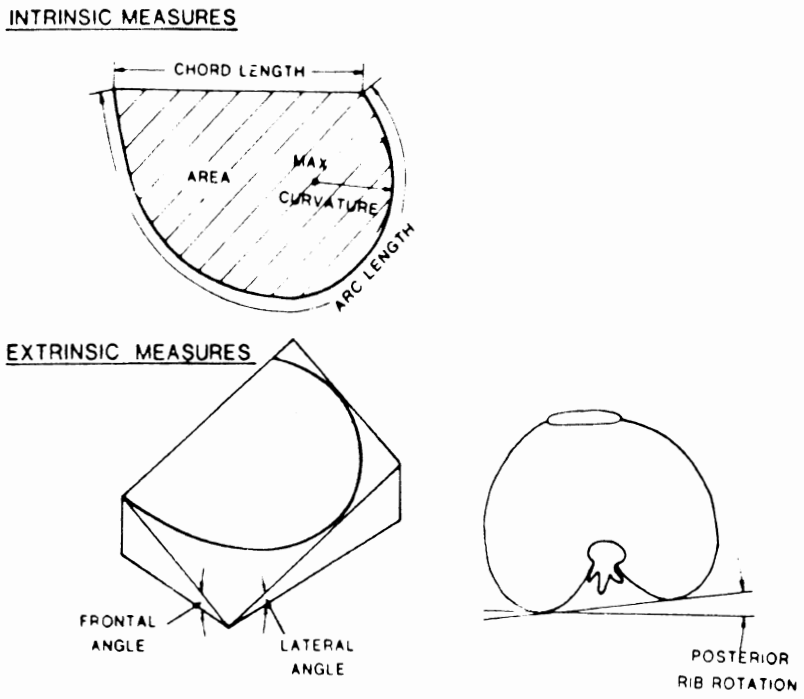

FIGURE 56. Intrinsic and extrinsic rib shape measures. Intrinsic measures were made in the *best-fit plane*. The angulation of this plane to the horizontal was measured by a *frontal angle* and *lateral angle*. Rotation of a pair of ribs in the plan view was measured by the *posterior rib rotation* (from Dansereau and Stokes 1988).

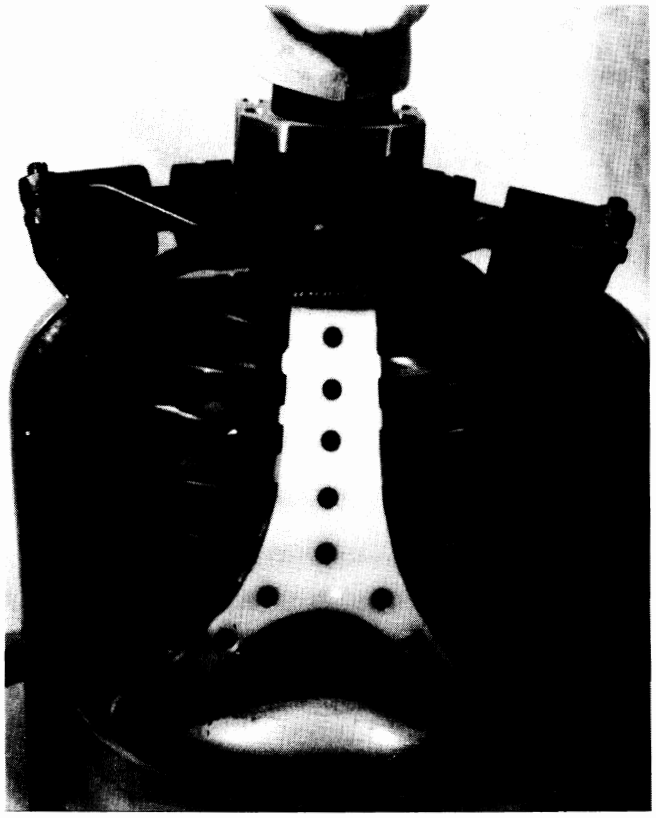

FIGURE 57. OGLE/MIRA dummy ribcage.

B3.3 Thoracic and Lumbar Spines

The thoracic spine of the Hybrid III ATD is rigid and heavy and is considered to be one cause for lack of response biofidelity during steering wheel and shoulder belt loading. The new thorax/abdomen design should include a thoracic spine with some flexibility.

A film analysis of the Kroell impact tests on cadavers was conducted and the results suggest that an average of about 22° of thoracic spinal flexion occurs from pre-test posture to peak spinal flexion. In the AATD anthropometric study, Robbins (1985a) has referenced Mital et al. (1979) as reporting 15° of rotation between T1 and T12 during voluntary flexion. In Phase I of the AATD program, however, Melvin et al. (1988b, Table 4–3) reports that data from studies by Cheng et al. (1979) and Nyquist and Murton (1975) have been used in developing Cal3–D data sets and suggests range-of-motion values of ±10 degrees of motion at both T8/T9 and T4/T5 with linear joint stiffnesses of 14.15 N·m/deg. Based upon these somewhat conflicting data and the need to prevent mechanical interaction of the ribs, it is proposed that the initial goal for thoracic spine range-of-motion be limited to ±10 degrees from the static seated posture.

B3.4 Shoulder Mass and Distribution

As a step toward defining shoulder specifications, Cavanaugh (unpublished) attempted to estimate the mass distribution of the shoulder by dissecting and weighing the shoulder components for three unembalmed cadavers. The results of these dissections are shown in Table 18. The average cadaver weight was 67 kg or 147 lbs and the average total shoulder mass was 3.83 kg or 8.4 lbs, or approximately 6% of body weight. Skin mass was obtained by weighing the skin and subcutaneous tissue (including fat) covering the following regions: (1) the entire humerus, (2) the anterior thorax from clavicle to the 5th rib, and (3) the posterior thorax from clavicle to the bottom of the scapula. In the medial-to-lateral direction, the shoulder skin covering was taken from the body midline to the mid-axillary line.

Estimates were made as to how the average masses of these individual shoulder tissues distribute to the five anatomical regions of: anterior ribcage, posterior ribcage, clavicle, scapula, and humerus. The results are shown in Table 19. These masses were normalized by multiplying by the ratio of the mass of the 50th percentile dummy to the average cadaver mass (78 kg/67 kg) to give the following distribution of shoulder mass.

Clavicle	=	0.29 kg	=	0.64 lbs
Scapula	=	1.06 kg	=	2.34 lbs
Humerus	=	1.37 kg	=	3.02 lbs
Anterior Rib Cage	=	0.20 kg	=	0.44 lbs
Posterior Rib Cage	=	0.24 kg	=	0.53 lbs
Skin Covering	=	1.30 kg	=	2.87 lbs
TOTAL MASS	=	4.46 kg	=	9.83 lbs

TABLE 18

DISTRIBUTION OF SHOULDER MASS
(Cavanaugh, August 1988)

Shoulder Mass	Cadaver UM1 Wt.: 67.6 kg Wt. in Grams		Cadaver UM2 Wt.: 75.8 kg Wt. in Grams		Cadaver 115 Wt.: 57.6 kg Wt. in Grams		Average Weight	Std. Dev.
	Right	Left	Right	Left	Right	Left		
Anterior Group of Muscles								
Anterior Serratus	119	130	81	56	105	70	93.3	23.9
Pectoralis Major	340	312	116	143	98	127	189.2	81.5
Pectoralis Minor	85	71	25	34	28	14	42.5	22.7
Deltoid	468	454	250	292	252	312	338.0	73.7
Subscapularis	170	170	86	99	156	123	133.9	31.3
Posterior Group of Muscles								
Levator Scapulae	62	60	20	37	25	40	40.7	13.4
Greater Rhomboid	91	79	42	15	26	47	50.0	26.1
Smaller Rhomboid	40	31	*	*	*	*	11.8	14.9
Trapezius	340	284	231	181	174	199	234.8	57.9
Infraspinatus	204	198	122	142	163	135	160.6	26.5
Supraspinatus	85	85	42	34	46	41	55.4	17.6
Teres Major & Minor	128	128	209	226	97	81	145.0	61.2
Muscles Along Humerus								
Biceps	184	156	119	133	118	88	132.9	28.8
Triceps	454	454	332	327	297	282	357.6	55.6
Corachobrachialis	57	57	16	13	13	13	28.0	16.3
Bones								
Humerus	340	340	397	408	347	353	364.0	29.1
Clavicle	71	71	79	87	67	69	73.9	8.0
Scapula	241	298	267	245	259	282	265.2	14.7
Skin								
Back	184	198	388	460	347	345	320.3	93.2
Arm	354	354	837	961	478	322	551.0	275.0
Front	180	180	388	460	108	140	242.8	150
TOTALS	4197	4109	4044	4350	3203	3082	3830.9	526.7
Wt. as % Body Mass	6.2	6.1	5.3	5.7	5.6	5.4		

Average body weight of three cadavers=67.0 kg.
Shoulder mass as % of body mass=5.7%.

*Weight included with greater rhomboid.

TABLE 19

AVERAGE MASS DISTRIBUTION OF INDIVIDUAL SHOULDER TISSUES
Shoulder Dissection: Average of Three Subjects*
(Cavanaugh, August 1988)

Shoulder Mass	Avg. Weight (grams)	Std. Dev.	Estimated Distribution of Shoulder Mass to the Following Five Anatomical Regions:				
			Ant. Thorax (grams)	Post. Thorax (grams)	Clavicle (grams)	Scapula (grams)	Humerus (grams)
Anterior Group of Muscles							
Anterior Serratus	93.0	23.9	46.7			46.7	
Pectoralis Major	189.0	81.5	94.6		47.3		47.3
Pectoralis Minor	43.0	22.7	32.0			10.7	
Deltoid	338.0	73.7			126.7	126.7	84.5
Subscapularis	134.0	31.3				100.4	33.5
Posterior Group of Muscles							
Levator Scapulae	41.0	13.4		20.4		20.4	
Greater Rhomboid	50.0	26.1		25.0		25.0	
Smaller Rhomboid	12.0	14.9		5.9		5.9	
Trapezius	235.0	57.9		156.6		78.2	
Infraspinatus	161.0	26.5				120.5	40.2
Supraspinatus	55.0	17.6				41.5	13.8
Teres Major & Minor	145.0	61.2				72.5	72.5
Muscles Along Humerus							
Biceps	133.0	28.8					132.9
Triceps	358.0	55.6					357.6
Corachobrachialis	28.0	16.3					28.0
Bones							
Humerus	364.0	29.1					364.0
Clavicle	74.0	8.0			73.9		
Scapula	265.0	14.7				265.2	
SUBTOTAL: Muscle + Bone Wt.	2718.0		173.3	207.9	248.0	913.6	1174.3
SKIN							
Back	320.0	93.2					
Arm	551.0	275.0					
Front	243.0	150.0					
SUBTOTAL SKIN WEIGHT	1114.0	526.7					

*Average cadaver weight = 67 kg.

B3.5 Shoulder Kinematics

For a belt-restrained occupant involved in a frontal crash, it is intended that the shoulder structure take up a significant portion of the restraint load. What is not clear, however, is how the compliance or mobility of the shoulder complex and its interaction and coupling with the chest influences the proportionate amount of loading and deflection experienced at the chest versus the shoulder. In addition, and as indicated in Figure 58, there is concern that the proportionate sharing of load by the thorax and shoulder may be significantly different for two- and three-point belt systems where the kinematics of the body are different. It would seem, then, that biofidelity in shoulder mobility as well as mass distribution are important to the assessment of thoracic injury from belt-restraint systems. As noted in Appendix A, the Hybrid III dummy shoulder has even less biofidelity than its predecessor, Hybrid II. The design seems to be based on durability considerations rather than biofidelity and this may present serious inaccuracies in evaluation of injury potential to the thorax.

Unfortunately, data that quantitatively describe the kinematics of the different shoulder elements and their effective mass properties during impacts into shoulder belts and steering-wheel rims do not exist. There are also no data that describe the dynamic coupling of the shoulder to the thoracic cage or the effective mass that might be attributed to each component during impact loading. In Phase I of the AATD program, Robbins (in Melvin et al. 1988b) used crash victim simulation modeling to investigate the effect of shoulder mobility and coupling to the thorax on dummy kinematics. It was concluded that both shoulder flexibility and coupling to the thorax have significant effects on dummy motion and it would logically follow that they would also influence chest loading and compression.

In the absence of data that describe shoulder movement and response of the shoulder to impact loading, a first step toward impact biofidelity is to understand the shoulder complex, its structures, and their mobilities under conditions of voluntary motion. The most descriptive information on shoulder mobility and range of motion is provided by Dempster (1965). As shown in Figures 59 and 60, the shoulder consists of three skeletal components or links—the scapula, the clavicle, and the humerus. To understand the movement of the shoulder, it is necessary to understand the manner in which these structures connect and interface with each other and with the thoracic cage and sternum. A detailed treatment of this anatomy is given by Dempster (1965) and will not be reproduced here. The key elements with regard to shoulder motion and mobility, however, are the following:

- The clavicle is a long bone which pivots in three dimensions at its connection with the lateral superior corner of the sternum (sternoclavicular articulation) as illustrated in Figures 61 and 62.

- The scapula slides along the posterior ribcage mediolaterally as well as in the superior-inferior direction. At its lateral region it connects with the lateral end of the clavicle to form the claviscapular articulation and with the humerus where it forms the glenoid fossa on which the head of the humerus rides. In a general sense, the scapula slides on the posterior ribcage with the clavicle acting as a "radius arm" pivoting about the sternoclavicular joint.

- The movement of the scapula has significance in that it allows the lateral end of the clavicle to move and allows reorientation of the glenoid fossa.

- The head of the humerus rotates within the glenoid fossa (i.e., the glenohumeral joint) and pivots about an eccentric pivot at the head-fossa interface (i.e., not at the center of the humeral head) which contributes to additional fore/aft movement of the shoulder.

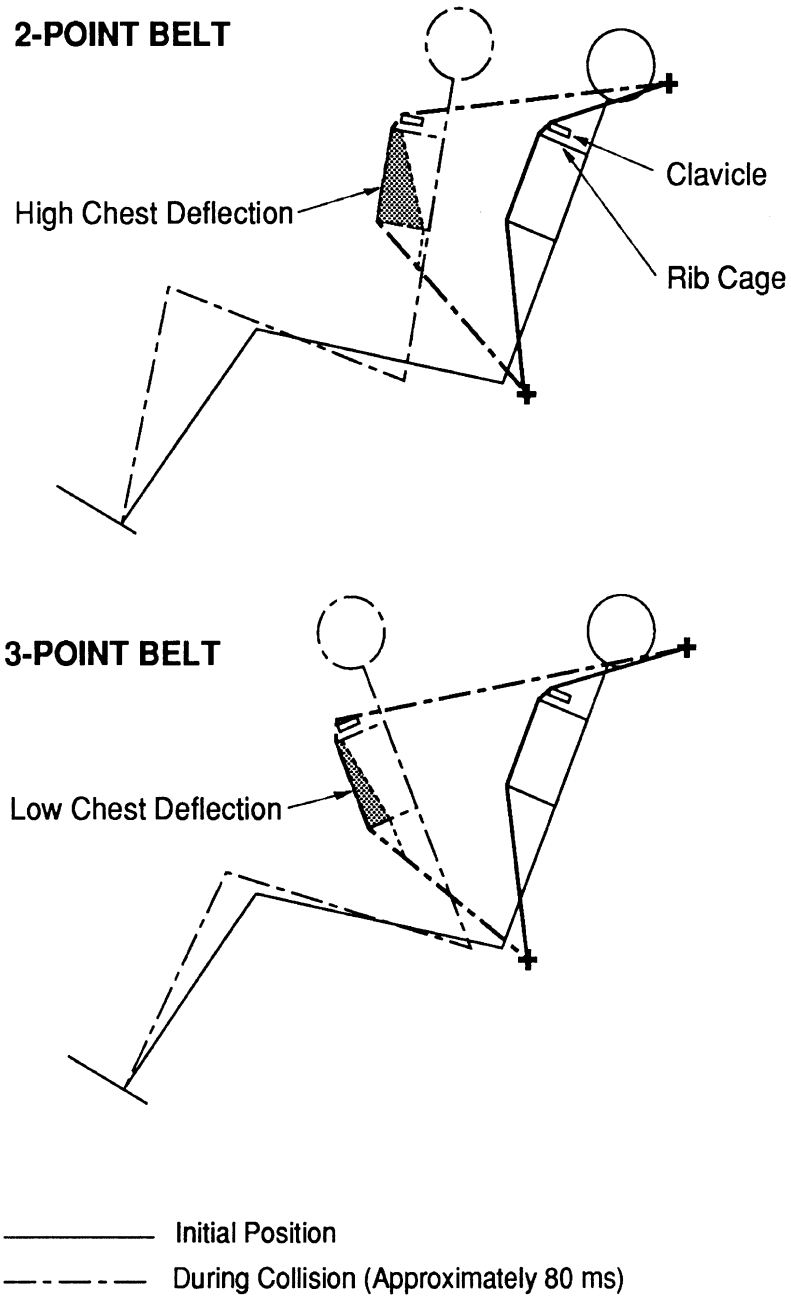

FIGURE 58. Kinematic response to two- and three-point belts (Backaitis 1987).

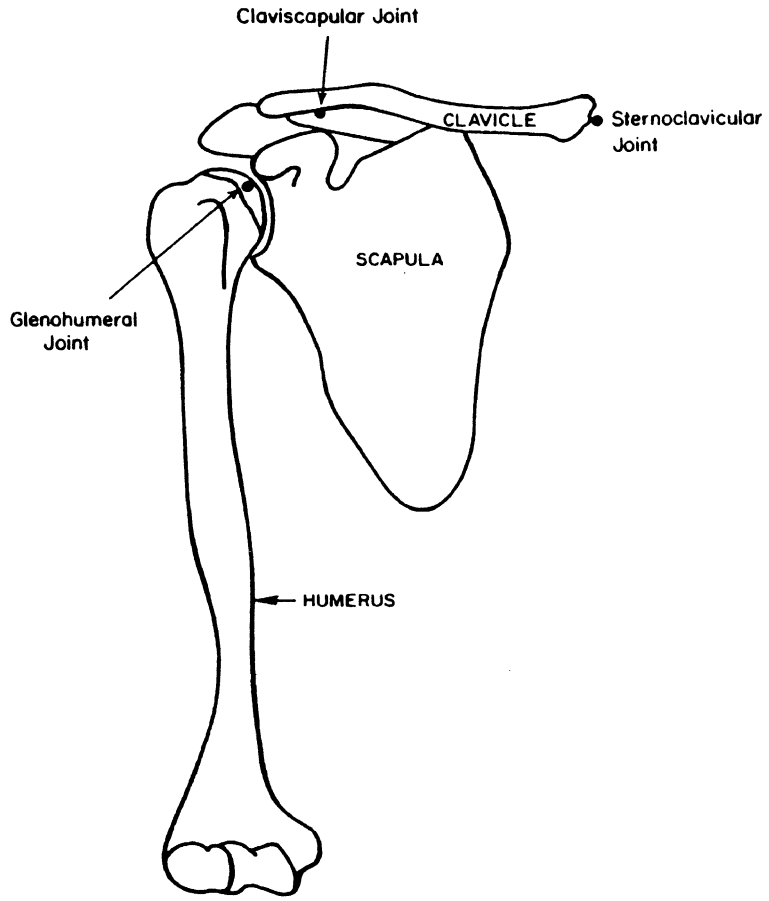

FIGURE 59. The three joints of the shoulder girdle (Dempster 1965).

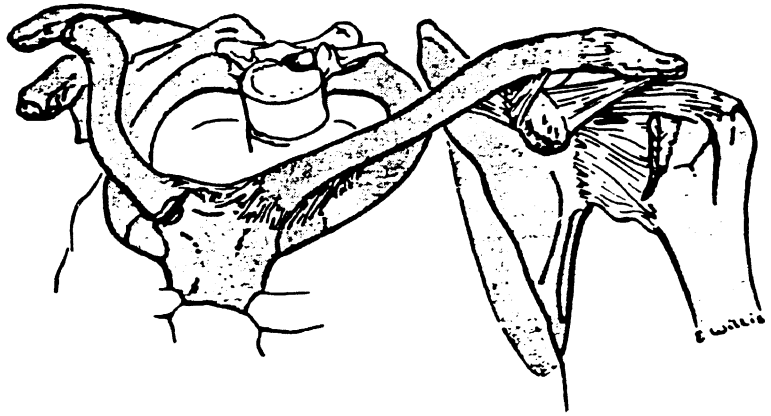

FIGURE 60. Bones and joints of the shoulder complex (Dempster 1965).

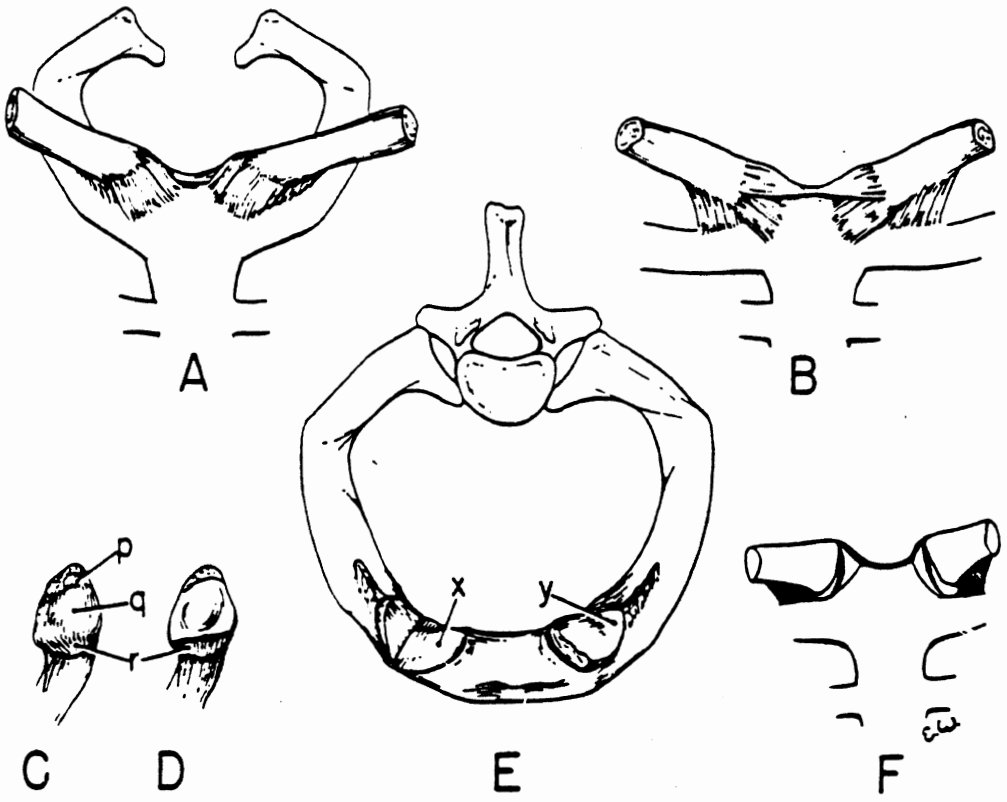

FIGURE 61. (A): Ligaments of anterior aspect of sterno-clavicular joints. (B): Posterior ligaments of sterno-clavicular joints. (C): Sternal surface of left clavicle. (D): Sternal end of clavicle with attached meniscus. (E): Dissection of sternal articulation: meniscus folded back at right joint to show articular surface of the manubrium (x); meniscus in place at left joint to show lateral articular surface over first costal cartilage (y). (F): Diagram showing the upper and lower attachments of the meniscus and the upper and lower ligaments of the sterno-clavicular joint (Dempster 1965).

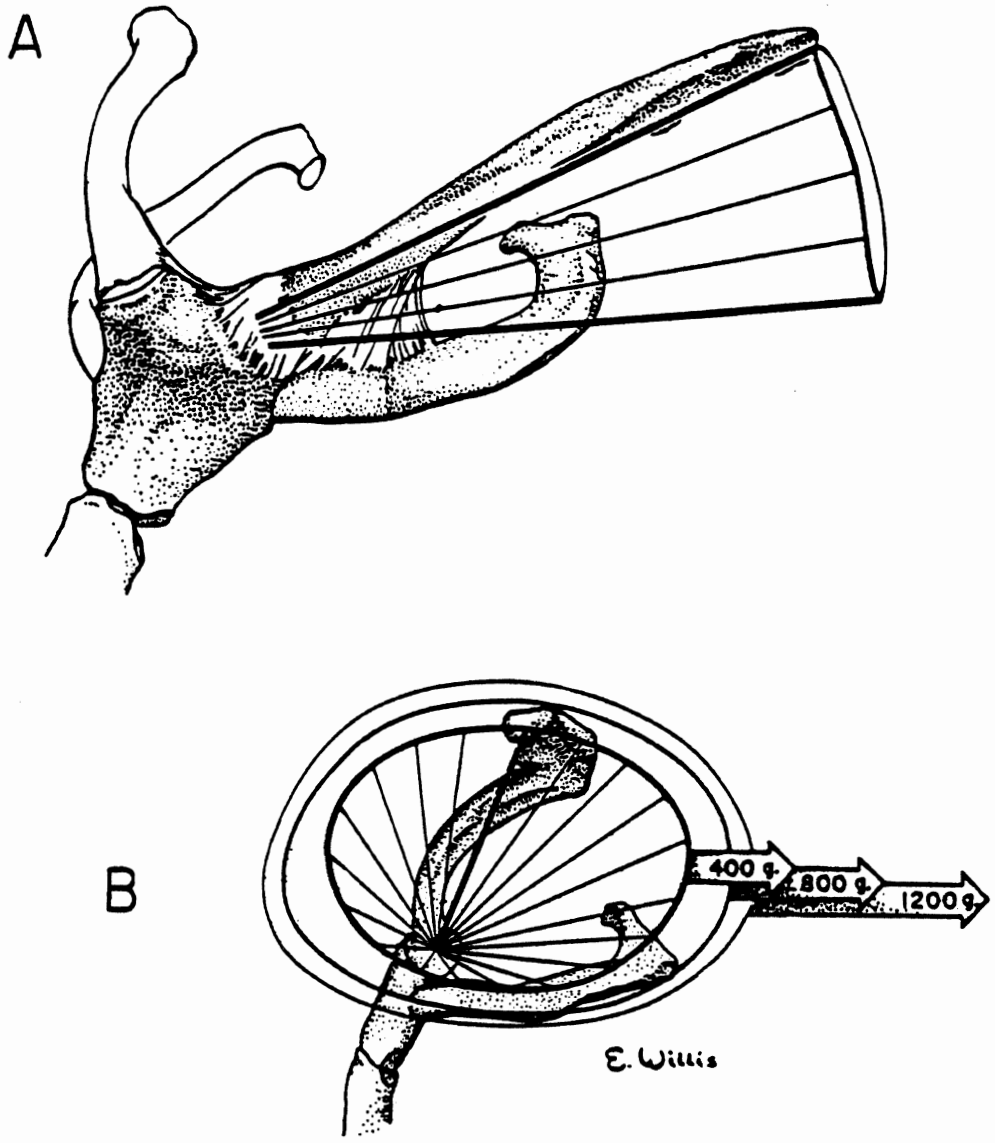

FIGURE 62. (A): Joint sinus of sternoclavicular joint; view is parallel to resting position of the clavicle. (B): Side view, looking into sternoclavicular joint sinus. The three ellipses represent increasing sinus size with increased levels of displacing force (Dempster 1965).

The net result of the shoulder linkage geometry and the allowed range of sliding and rotating movements at the different interfaces and articulations is a wide and complex range of arm movement patterns and ranges of motion illustrated in Figures 63 through 65. It is probably prohibitive to simulate the complete shoulder structure and all its mobility in a crash dummy. Rather, it is important to determine what aspects of the shoulder mobility and movement are most critical to crash dummy performance. Since the current effort is concerned primarily with a frontal impact ATD, this question needs to be focused on the requirements for frontal impact loading.

B3.6 Shoulder Design Criteria

Since a shoulder belt has primary interaction with the clavicle, a critical question is: How does the clavicle move during shoulder-belt loading? As indicated above, there are no data that describe kinematics of the shoulder linkage during restraint-belt loading. A review of belted cadaver runs did not offer much additional insight since it is difficult to separate out movement of the shoulder due to rotation of the humerus in the glenoid fossa and movement of the shoulder due to rotation of the clavicle (and sliding of the scapula) about the sternoclavicular joint. Intuitively, one would expect the clavicle to rotate forward due to the inertial loading of the arm on the scapula and to be pushed rearward by the direct loading of the shoulder belt. It is likely that during any given test, a combination of both forward and rearward movement of the clavicle may occur depending on the timing of these different forces on the shoulder.

It is concluded, therefore, that forward and rearward rotation of the clavicle about the sternoclavicular joint are important aspects of shoulder mobility that should be included in the new design if they can be practically and feasibly achieved while still maintaining durability and biofidelity elsewhere. In order to achieve appropriate coupling and load transfer between the shoulder and spine, it is further considered important for the clavicles to attach to the sternum or ribcage rather than to the spine (as is the case in Hybrid III). In addition, the arms should attach to the shoulder so that their inertial loads produce forward rotation of the clavicles. Finally, it would be ideal if the Hybrid III shoulder/arm joint were modified to simulate the eccentric rotation of the glenohumeral joint which plays an important role in arm kinematics and therefore the inertial loads on the shoulder.

Downward and lateral movements of the clavicle are not currently considered critical to a frontal impact dummy. With regard to the allowed range-of-motion of the clavicle, Robbins (1985a) reports motion limits of 15 degrees protraction (i.e., forward movement) and 20 degrees retraction (rearward movement). For a 14-cm-long (5.5-inch) clavicle link this translates to a forward movement of about 4.5 cm (1.8 in) in an arc, and a rearward movement of about 6 cm (2.4 in). A reasonable initial design goal for an improved shoulder would be to provide for at least 38 mm (1.5 in) of forward, rearward, and upward unrestrained movement of the distal end of the clavicle from its neutral position as it pivots about the proximal end (i.e., the sterno-clavicular articulation). For a 140-mm-long (5.5-in) clavicle link, this corresponds to a rotation angle of about 15 degrees in a hemisphere above the horizontal plane.

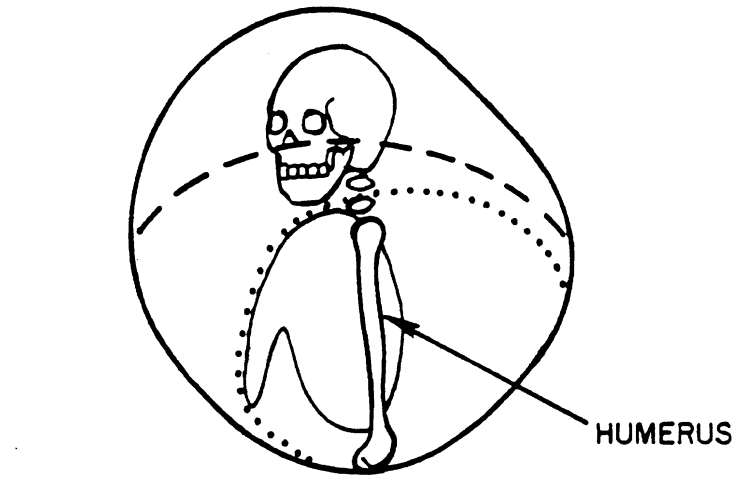

——————— ALL THREE JOINTS FREE

— — — — — GLENOHUMERAL AND CLAVISCAPULAR JOINTS FREE

..... GLENOHUMERAL JOINT FREE

FIGURE 63. Range of motion at shoulder joint as a function of degrees of freedom (Robbins 1985a).

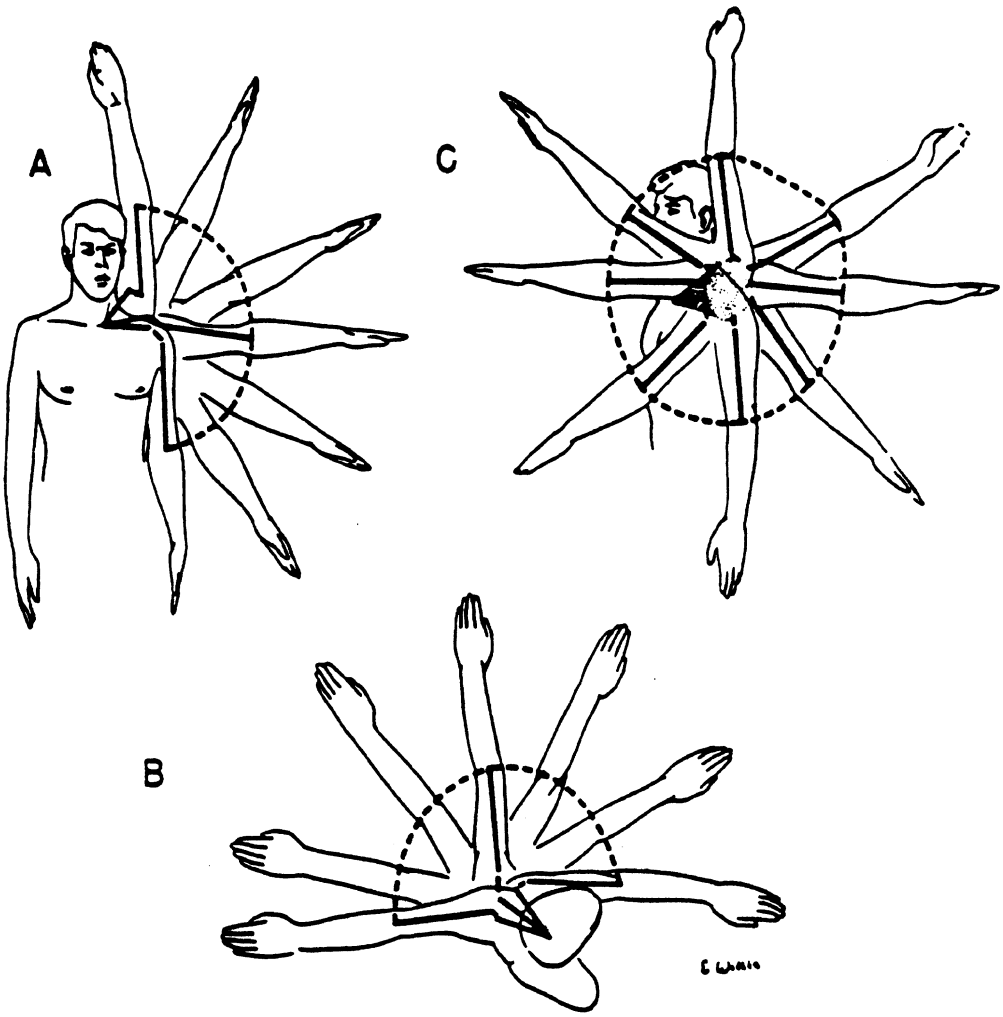

FIGURE 64. (A): Different positions of the upper limb and of the shoulder and arm links, in the plane defined by the scapula at rest. (B): Positions of the limb and links in horizontal movement at shoulder height. (C): Extreme positions of the upper limb; strippled cone represents the range of total clavicular motion. In each sketch, the line of dashes shows the elbow position (Dempster 1965).

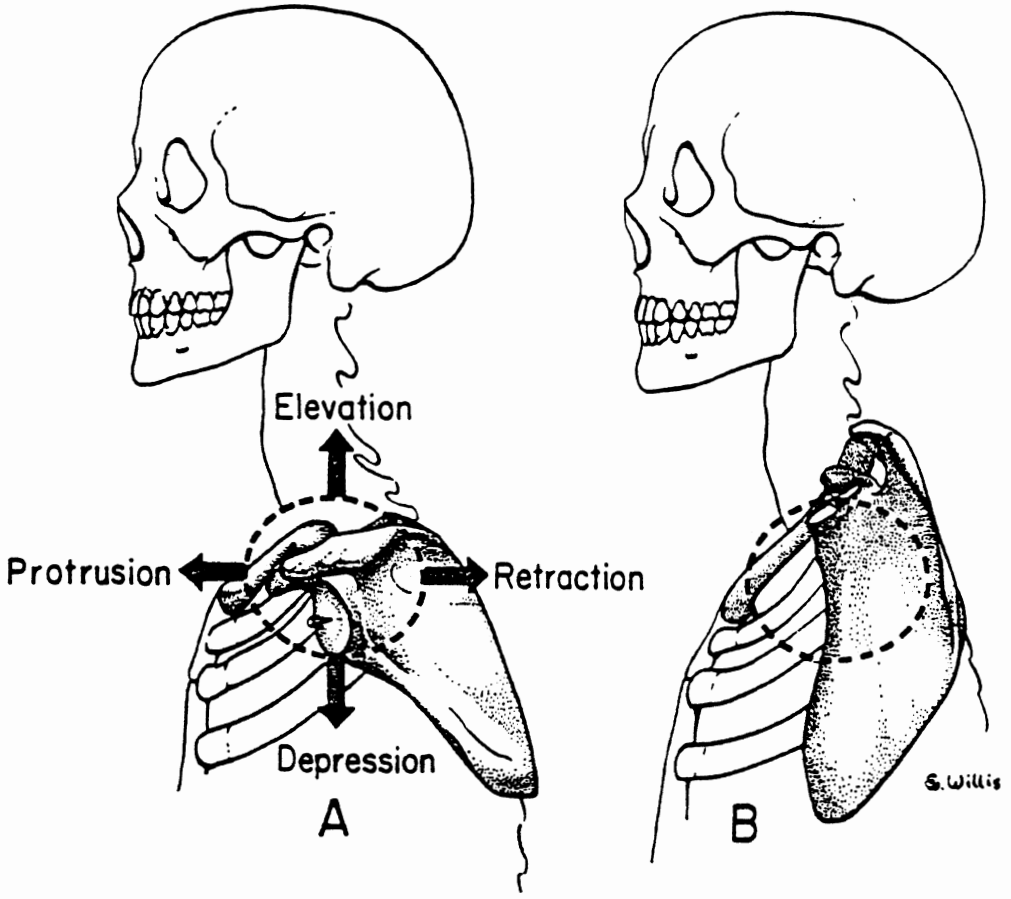

FIGURE 65. (A): Left shoulder girdle of a skeleton-ligament preparation. The end of the pin at the glenoid fossa represents the mean center of the glenohumeral joint. Its maximum range of motion, without rotation of the shoulder girdle, is depicted by the dashed ellipse. (B): The shoulder girdle at its highest position with the glenoid fossa and scapula rotated. Clavicle is rotated upward, elevated, and retracted; the scapula is flexed, medially rotated and adducted (Dempster 1965).

PART C. SUMMARY OF KEY DESIGN REQUIREMENTS AND PERFORMANCE SPECIFICATIONS

Based on the information and discussions of the preceding sections of this document, the following design requirements and performance specifications can be established for the advanced ATD thoracic subcomponent. These requirements and specifications have been prioritized into two categories based on their estimated importance and/or likelihood of implementation in the next generation of a new thorax/spine/shoulder subcomponent.

C.1 PRIMARY PRIORITIES

C1.1 General Requirements

- The new subcomponent should be designed as a retrofit into Hybrid III and should incorporate improvements to the Hybrid III shoulder and thoracic spine.

- The new subcomponent should be designed to perform for frontal vehicle, sled, or component impacts including impacts within 30° of frontal.

C1.2 Thorax/Abdomen Response Biofidelity

- The new subcomponent should be designed to provide biofidelity in impact response to a rigid 150–cm diameter, 23–kg impactor at the mid-lower sternum and left and right lower ribcage over the spleen and liver, in accordance with the force-deflection curves outlined and discussed in Sections B1.1.1 through B1.1.4 of this document. Since the priority in future impact testing is shifting toward the need for a device with humanlike response to restraint systems and from the need for biofidelity of unrestrained ATDs with vehicle components, the priority in meeting dynamic response corridors should be shifted toward achieving the 4.3–m/s corridor rather than the 6.7–m/s corridor.

- The new subcomponent should allow lateral movement of the sternum and ribcage during asymmetric shoulder belt loading similar in magnitude (i.e., about 50 mm either way) to that offered by the Hybrid III chest until new response data suggest otherwise.

- The new subcomponent should have improved biofidelity in response to low-velocity and static loading. This implies a significant reduction in static stiffness for the first two inches of internal deflection than now offered by the Hybrid III thorax.

- Given that all loading-rate response corridors cannot be equally achieved, the priorities in achieving biofidelity should be the following: (1) 4/3 m/s; (2) static F–δ; and (3) 6.7 m/s.

- The new subcomponent should be designed to provide humanlike interaction with different types of restraint systems including two- and three–point shoulder belt systems and airbags, as well as with vehicle components such as the steering wheel and instrument panel. This implies a more humanlike load-distributing ribcage structure as well as more humanlike coupling between different regions of the thorax as described in Sections B1.1.7 and B1.1.12.

- The new subcomponent should provide response biofidelity for impact severities ranging from AIS-2 to AIS-4. For low-velocity loading (i.e., below 3 m/s), this implies response

biofidelity for deflection of about 75 mm (3.0 in) at the sternum and about 90 mm (3.5 in) at the lower ribcage.

- The new subcomponent should incorporate an abdomen with response biofidelity as described in Sections B1.2.1 through B1.2.3.

C1.3 Shoulder/Spine

- The new subcomponent should include a shoulder design that incorporates improved compliance, mobility, mass, and mass distribution in accordance with Sections B3.3 through B3.5. This implies a clavicle-like structure with improved anatomy, compliance, mobility, and more humanlike interaction with the sternum and shoulder/arm complex.

- In order to improve overall kinematics and interaction with restraint systems and steering wheels, the new subcomponent should incorporate a thoracic spine with some flexibility (i.e., at least one articulation) providing at least ±10° of flexion/extension from the initial seated posture.

C1.4 Instrumentation

- The new subcomponent should be designed to provide reliable measurements of injury criteria based on deflection- and velocity–time histories at critical regions of the thorax and abdomen including the sternum, left and right lower ribcage, and the lower abdomen.

- The new subcomponent should be capable of measuring abdominal intrusion from lap belts and vehicle components.

- The new subcomponent should include measurement of tri–axial spinal accelerations at the upper (i.e., sternal level) segment of the articulated thoracic spine.

- The new subcomponent should measure the load applied to the clavicles to assess and compare the shoulder load delivered by different restraint system designs.

- The new subcomponent should include the ability to measure impact loads to the chest that exceed the desired range of injuries (i.e., that exceed AIS–2 to AIS–4 injuries).

- The new subcomponent should have provision for installing a multi–axis load cell near the center of the thoracic spine (i.e., near the articulation) in addition to those at the base (T12/L1) and top (C7/T1) that are currently included in Hybrid III.

- The spine of the new subcomponent should provide for installing the spinal load cells currently available for the Hybrid III at T1 and T12.

C1.5 Anthropometry

- The new subcomponent should incorporate improved anthropometry and geometry of the thorax, abdomen, and ribcage in accordance with Sections B3.1 and B3.2. In particular, the new chest should include improved representation of the lower ribcage than that now offered in Hybrid III.

C1.6 Repeatability and Durability

- The new subcomponent should be durable for crash severities that produce impact forces, accelerations, and deflections beyond the range of desired injury assessment. In terms of vehicle impact velocities, the new subcomponent should be able to survive impact forces generated in unrestrained-occupant tests for 56 km/hr (35 mph) barrier impact tests.

- The new subcomponent should be capable of surviving 50 to 100 rigid-impactor calibration tests without the need for replacement or recalibration of parts.

- The new subcomponent should perform with less than 10% variability in deflection- and velocity-based injury criteria over the temperature range of 65°F to 80°F. It should also withstand shipping and storage temperatures from –20°F to 140°F without deterioration or change in structure and performance.

- The new subcomponent should provide test repeatability (within dummy) and reproducibility (between dummies) in injury criteria values with 5% or less variability.

- The new subcomponent should have provision for overload protection for impacts that produce chest deflections exceeding the range of biofidelic response.

C.2 SECONDARY PRIORITIES

C2.1 General Requirements

- The new subcomponent should have potential application as a subcomponent test device (i.e., to replace Black Tuffy).

- The new subcomponent should have potential for implementation into lateral and omnidirectional test devices.

C2.2 Response Biofidelity

- For improved assessment of injury to out-of-position occupants by airbags, the new subcomponent should offer improved biofidelity (i.e., increased dynamic stiffness) for loading rates of 9 m/s and higher (i.e., 15 to 30 m/s).

- The thorax of the new subcomponent should have a static stiffness that approximates the increasing stiffness with deflection described in Section B1.1.10.

- To the extent possible, the new subcomponent should offer greater chest deflections with biofidelity beyond the 75 mm and 90 mm requirements of C1.2.

C2.3 Instrumentation

- The new subcomponent should be designed to provide reliable measures of injury risk directly without the need for human input as to the structures and/or surfaces contacted. This may imply the need for measurement of the size and shape of the region of the chest being loaded.

- The new subcomponent should have appropriate instrumentation to sense for injury potential for low-deflection, high-velocity impact events due to airbag interaction with out-of-position occupants.

- The new subcomponent should offer the potential for measurement of tri–axial spinal accelerations of other segments (i.e., other than the upper segment) of the articulated thoracic spine.

- The new subcomponent should provide for measurement of lateral displacement of the sternum.

- The new subcomponent should include instrumentation to measure the kinematics of the spine (and pelvis) relative to inertial coordinates and with respect to adjacent ATD segments.

REFERENCES

Arendt R.H.; Segal, D.J.; Cheng, R. (1988) *Review of Anthropomorphic Test Device Instrumentation, Data Processing, and Certification Procedures*. AATD Task C Final Report in DOT-HS-807–224. U.S. Department of Transportation, National Highway Traffic Safety Administration, Washington, D.C.

Backaitis, S.H.; DeLarm, L.; Robbins, D.H. (1982) Occupant kinematics in motor vehicle crashes. *Crash Protection, SP-513*, pp. 107–155. SAE report no. 820247. Society of Automotive Engineers, Warrendale, Pa.

Backaitis, S.H. and St.-Laurent, A. (1986) Chest deflection characteristics of volunteers and Hybrid III dummies. *Proc. 30th Stapp Car Crash Conference*, pp. 157–166. SAE paper no. 861884. Society of Automotive Engineers, Warrendale, Pa.

Backaitis, S.H. (1987) Unpublished SAE handout information.

Balser, J. (1987) Personal communication to L.W. Schneider, UMTRI.

Begeman, P. (1988) Personal communication to L.W. Schneider, UMTRI. Work performed under GM sponsorship, 1983–1985.

Bowen, I.G.; Fletcher, E.R.; and Richmond, D.R. (1968) *Estimate of man's tolerance to the direct effects of air blast*. Summary report. Lovelace Foundation for Medical Education and Research, Albuquerque, New Mexico.

Carsten, O.; and O'Day, J. (1988) *Injury priority analysis*. AATD Task A Final Report in DOT-HS-807–224. U.S. Department of Transportation, National Highway Traffic Safety Administration, Washington, D.C.

Cavanaugh, J.M. (August 1988) Personal communication to L.W. Schneider, UMTRI.

Cavanaugh, J.M.; Nyquist, G.W.; Goldberg, S.J.; King, A.I. (1986) Lower abdominal tolerance and response. *Proc. 30th Stapp Car Crash Conference*, pp. 41–63. Society of Automotive Engineers, Warrendale, Pa.

Cavanaugh, J.M.; Jepsen, K.; and King, A.I. (1988) Quasi-static frontal loading to the thorax of cadavers and Hybrid III dummy. In *Human Subjects for Biomechanical Research, 16th Annual International Workshop*. Atlanta, Georgia.

Chance, G.O. (1948) Note on a type of flexion fracture of the spine. *British Journal of Radiology*, 21:453–453.

Chandler, R.F. (May 1988) Personal communication to L.W. Schneider, UMTRI.

Chapon, A. (1984) Thorax and upper abdomen: Anatomy, injuries, and possible mechanisms of injury. *The Biomechanics of Impact Trauma*, pp. 227–250. Edited by B. Aldman and A. Chapon. Elsevier Science Publishers, Amsterdam.

Cheng, R.; Mital, N.K.; Levine, R.S.; and King, A.I. (1979) Biodynamics of the living human spine during $-G_x$ impact acceleration. *Proc. 23rd Stapp Car Crash Conference*, pp. 721–763. Society of Automotive Engineers, Warrendale, Pa.

Cheng, R.; Yang, K.H.; Levine, R.S.; King, A.I.; and Morgan, R. (1982) Injuries to the cervical spine caused by a distributed frontal load to the chest. *Proc. 26th Stapp Car Crash Conference*, pp. 1–40. Society of Automotive Engineers, Warrendale, Pa.

Cheng, R.; Yang, K.H.; Levine, R.S. and King, A.I. (1984) Dynamic impact loading of the femur under passive restrained condition. *Proc. 28th Stapp Car Crash Conference*, pp. 101–118. Society of Automotive Engineers, Warrendale, Pa.

Cohen, D.S. (1987) *The safety problem for passengers in frontal impacts: Analysis of accidents, laboratory and model simulation data.* Presented at the 11th International Technical Conference on Experimental Safety Vehicles, 12–15 May 1987, Washington, D.C.

Crosby, W.M.; King, A.I.; and Stout, L.C. (1972) Survival following impact: Improvement with shoulder harness restraint. *American Journal of Obstetrics and Gynecology*, 112:1101–1106.

Dalmotas, D.J. (1980) Mechanism of injury to vehicle occupants restrained by three-point seat belts. *Proc. 24th Stapp Car Crash Conference*, pp. 439–476. Society of Automotive Engineers, Warrendale, Pa.

Daniel, R.; and Prasad, P. (April 1988) Personal communication to L.W. Schneider, UMTRI.

Dansereau, J.; and Stokes, I.A.F. (1988) Measurements of the three-dimensional shape of the rib cage. *Journal of Biomechanics*, 21:11, 893–901.

Dejeammes, M. (1984) Lower abdomen and pelvis: Kinematics, tolerance levels and injury criteria. *The Biomechanics of Impact Trauma*, pp. 289–307. Edited by B. Aldman and A. Chapon. Elsevier Science Publishers, Amsterdam.

Dempster, W.T. (1965) Mechanisms of shoulder movement. *Archives of Physical Medicine and Rehabilitation*, 46:49–70.

Eiband, A.M. (1959) *Human tolerance to rapidly applied accelerations: A summary of the literature*. NASA Memorandum 5–19–59E. NASA Lewis Research Center, Cleveland.

Eppinger, R. H. (1978) Prediction of Thoracic Injury Using Measurable Experimental Parameters. *Proc. 6th International Technical Conference on Experimental Safety Vehicles*, pp. 770–780. National Highway Traffic Safety Administration, Washington, D.C.

Eppinger, R.H.; and Marcus, J. (1985) Production of Injury in Blunt Frontal Impact. *Proc. 10th International Technical Conference on Experimental Safety Vehicles*, pp. 90–104. National Highway Traffic Safety Administration, Washington, D.C.

Fayon, A.; Tarriere, C.; Walfisch, G.; Got, C.; and Patel, A. (1975) Thorax of three-point-belt wearers during a crash (experiments with cadavers). *Proc. 19th Stapp Car Crash Conference*, pp. 195–223. Society of Automotive Engineers, Warrendale, Pa.

Fung, Y.C.; and Yen, M.R. (1984) *Experimental investigation of lung injury mechanisms*. Topical Report, U.S. Army Medical Research and Development Command. Contract No. DAMD17–82-C-2062.

Gloyns, P.F.; Rattenbury, S.J.; and Hayes, H.R.M. (1982) Accident and laboratory studies of driver interaction with the steering system in European cars, pp. 31–44. SAE report no. 820479. Society of Automotive Engineers, Warrendale, Pa. *Occupant Crash Interaction with the Steering System*.

Granik, G.; and Stein, I. (1973) Human ribs: Static testing as a promising medical application. *Journal of Biomechanics*, 6:237–240.

Haffner, M. (1987) Trauma assessment device development program: Thorax-abdomen development task. Preliminary goals and design requirements statement. Contract communication. National Highway Traffic Safety Administration, U.S. Department of Transportation, Washington, D.C.

Horsch, J.D. (1987) Evaluation of occupant protection from responses measured in laboratory tests. *Restraint Technologies: Front Seat Occupant Protection*, pp. 13–42. SAE paper no. 870222. Society of Automotive Engineers, Warrendale, Pa.

Kallieris, D. (1987) Correspondence to Rolf Eppinger, U.S. Department of Transportation, National Highway Traffic Safety Administration, Biomechanics Branch, Washington, D.C.

Kazarian, L.E. (1979) *F/FB-111 escape injury mechanism assessment*. Wright-Patterson Air Force Base, Ohio. AMRL Technical Report AMRL-TR-77–60

King, A.I. (1984) The spine: Its anatomy, kinematics, injury mechanisms and tolerance to impact. In *The Biomechanics of Impact Trauma*, pp. 191–226. Edited by B. Aldman and A. Chapon. Elsevier Science Publishers, Amsterdam.

Kroell, C.K.; Schneider, D.C.; and Nahum, A.M. (1971) Impact tolerance and response to the human thorax. *Proc. 15th Stapp Car Crash Conference*, pp. 84–134. Society of Automotive Engineers, Warrendale, Pa.

Kroell, C.K.; Schneider, D.C.; and Nahum, A.M. (1974) Impact tolerance and response to the human thorax II. *Proc. 18th Stapp Car Crash Conference*, pp. 383–457. SAE paper no. 741187. Society of Automotive Engineers, Warrendale, Pa.

Lau, V.K.; and Viano, D.C. (1981) An experimental study of hepatic injury from belt-restraint loading. *Aviation, Space and Environmental Medicine*, 52:611–617.

Lau, I.V.; and Viano, D.C. (1986) The viscous criterion: Bases and applications of an injury severity index for soft tissues. *Proc. 30th Stapp Car Crash Conference*, pp. 123–142. Society of Automotive Engineers, Warrendale, Pa.

Lobdell, T.E.; Kroell, C.K.; Schneider, D.C.; Hering, W.E.; and Nahum, A.M. (1973) Impact response of the human thorax. In *Human Impact Response Measurement and Simulation*, pp. 201–245. Edited by W.F. King and H.J. Mertz. Plenum Press, New York.

L'Abbe, R.J.; Dainty, D.A.; and Newman, J.A. (1982) An experimental analysis of thoracic deflection response to belt loading. *Seventh International IRCOBI Conference on the Biomechanics of Impacts*, pp. 184–194. BRON, France.

Malliaris, A.C.; Hitchcock, R.; and Hedlund, J. (1982) A search for priorities in crash protection. *Crash Protection, SP–513*, pp. 1–33. Society of Automotive Engineers, Warrendale, Pa.

Matsuoka, F.; Kumagai, K.; and Takahashi, H. (1989) *Problem and improvement of Hybrid III dummy rib cage features*. Report no. 89–4A-0–009. Toyota Motor Corporation.

Melvin, J.W. (1988) *The engineering design, development, testing, and evaluation of an advanced anthropometric test device. Phase 1: Concept definition.* In report no. DOT-HS-807–224. U.S. Department of Transportation, National Highway Traffic Safety Administration, Washington, D.C.

Melvin, J.W.; and Weber, K., eds. (1988) *Review of biomechanical impact response and injury in the automotive environment.* Phase 1 Task B Final Report in DOT-HS-807–224. U.S. Department of Transportation, National Highway Traffic Safety Administration, Washington, D.C.

Melvin, J.W.; King, A.I.; and Alem, N.M. (1988a) *AATD system technical characteristics, design concepts, and trauma assessment criteria.* AATD Task E-F Final Report in DOT-HS-807–224 U.S. Department of Transportation, National Highway Traffic Safety Administration, Washington, D.C.

Melvin, J.W.; Robbins, D.H.; Weber, K.; Campbell, K.L.; and Smrcka, J. (1988b) *Review of dummy design and use.* AATD Task D Final Report in DOT-HS-807–224. U.S. Department of Transportation, National Highway Traffic Safety Administration, Washington, D.C.

Mital, N.K.; Cheng, R.; King, A.I.; and Eppinger, R.H. (1979) A new design for a surrogate spine. *Proc. 7th International Technical Conference on Experimental Safety Vehicles*, pp. 427–428. U.S. Government Printing Office, Washington, D.C.

Morgan, R. (1987) Personal communication to M. Haffner, NHTSA. CIRA data.

Morgan, R.M.; Schneider, D.C.; Eppinger, R.H.; Nahum, A.M.; Marcus, J.H.; Awad, J.; Dainty, D.; and Forrest, S. (1987) Interaction of human cadaver and Hybrid III subjects with a steering assembly. *Proc. 31st Stapp Car Crash Conference*, pp. 79–93. Society of Automotive Engineers, Warrendale, Pa.

Nash, T. (1969) *The medical and surgical management of road injuries.* St. Vincent's Hospital, Sydney, Australia.

Nahum, A.M.; Schneider, D.C.; and Kroell, C.K. (1975) Cadaver skeletal response to blunt thoracic impact. *Proc. 19th Stapp Car Crash Conference*, pp. 259–293. SAE paper no. 751150. Society of Automotive Engineers, Warrendale, Pa.

Neathery, R.F.; and Lobdell, T.E. (1973) Mechanical simulation of human thorax under impact. *Proc. 17th Stapp Car Crash Conference*, pp. 451–466. Society of Automotive Engineers, Warrendale, Pa.

Neathery, R.F. (1974) Analysis of chest impact response data and scaled performance recommendations. *Proc. 18th Stapp Car Crash Conference*, pp. 459–493. Society of Automotive Engineers, Warrendale, Pa.

Neathery, R.F.; Kroell, C.K.; and Mertz, H.J. (1975) Prediction of thoracic injury from dummy responses. *Proc. 19th Stapp Car Crash Conference*, pp. 295–316. Society of Automotive Engineers, Warrendale, Pa.

Newman, R.J.; and Rastogi, S. (1984) Rupture of the thoracic aorta and its relationship to road traffic accident characteristics. *Injury*, 296:296–299.

Nusholtz, G.S.; Kaiker, P.S.; and Lehman, R.J. (1988) *Steering system abdominal impact trauma.* The University of Michigan Transportation Research Institute, final report to MVMA. Report no. UMTRI–88–19.

Nyquist, G.W.; and Murton, C.J. (1975) Static bending response of the human lower torso. *Proc. 19th Stapp Car Crash Conference*, pp. 513–542. Society of Automotive Engineers, Warrendale, Pa.

Patrick, L.M. (1981) Impact force-deflection of the human thorax. *Proc. 25th Stapp Car Crash Conference*, pp. 471–496. Society of Automotive Engineers, Warrendale, Pa.

Robbins, D.H.; Melvin, J.W.; Stalnaker, R.L. (1976) The prediction of thoracic impact injuries. *Proc. 20th Stapp Car Crash Conference*, pp. 697–729. SAE paper no. 760822. Society of Automotive Engineers, Warrendale, Pa.

Robbins, D.H. (1985a) *Anthropometric specifications for mid-sized male dummy, Volume 2.* Final report no. DOT-HS-806–716. U.S. Department of Transportation, National Highway Traffic Safety Administration, Washington, D.C.

Robbins, D.H. (1985b) *Anthropometric specifications for small female and large male dummies, Volume 3.* Final report no. DOT-HS-806–717. U.S. Department of Transportation, National Highway Traffic Safety Administration, Washington, D.C.

Rouhana, S.W.; Lau, I.V.; and Ridella, S.A. (1985) Influence of velocity and forced compression on the severity of abdominal injury in blunt, non-penetrating lateral impact. *Journal of Trauma*, 25:6, pp. 490–500.

Rutherford, W.H.; Greenfield, T.; Hayes, H.R.M.; and Nelson, J.K. (1985) *The medical effects of seat belt legislation in the United Kingdom.* HMSO Research Report 13. Department of Health and Society Security, Office of the Chief Scientist, London.

Saul, R. (1984) *State-of-the-art dummy selection.* Vol. 1 and II. Final Report. National Highway Traffic Safety Administration, Vehicle Research and Test Center, East Liberty, Ohio.

Searle, J.A.; and Haslegrave, C.M. (1970) Improvements in the design of anthropometric/ anthropomorphic dummies. *MIRA Bulletin*, 5:10–23.

Schneider, D.; Nahum, A.; Dainty, D.; Awad, J.; Forrest, S.; Morgan, R.; Eppinger, R. (1987) Interaction of cadavers and the Hybrid III dummy with a steering assembly. *Proc. 31st Stapp Car Crash Conference*, pp. 79–93. SAE paper no. 872202. Society of Automotive Engineers, Warrendale, Pa.

Schneider, L.W.; Robbins, D.H.; Pflug, M.A.; and Snyder, R.G. (1985) *Development of anthropometrically based design specifications for an advanced adult anthropomorphic dummy family, Volume 1.* Final report no. DOT-HS-806–715. U.S. Department of Transportation, National Highway Traffic Safety Administration, Washington, D.C.

Seiffert, U.W.; and Leyer, H.E. (1976) *Dynamic dummy behavior under different temperature influence.* R&D Volksvagenwerk AG, Germany. SAE 760804.

Simione, L. (1987) Personal communication to M. Haffner, NHTSA. MVMA-2D simulations conducted at DOT Transportation Systems Center.

Stalnaker, R.L.; McElhaney, J.H.; and Roberts, V.L. (1973) Human torso response to blunt trauma. In *Human Impact Response Measurement and Simulation*, pp. 181–199. Edited by W.F. King and H.J. Mertz. Plenum Press, New York.

Stalnaker, R.L.; and Ulman, M.S. (1985) Abdominal trauma: Review, response and criteria. *Proc. 29th Stapp Car Crash Conference*, pp. 1–16. SAE paper no. 851720. Society of Automotive Engineers, Warrendale, Pa.

Stucki, S. (1987) Personal communication to M. Haffner, NHTSA. PADS simulations conducted at DOT/NHTSA.

Stedman's Medical Dictionary, 22nd ed. (1973) Williams and Wilkins Co., Baltimore, Md.

Tsitlik, J.E.; Weisfeldt, M.L.; Chandra, N.; Effron, M.B.; Halperin, H.R.; and Levin, H.R. (1983) Elastic properties of the human chest during cardiopulmonary resuscitation. *Critical Care Medicine*, 11:9, pp.685–692.

Verriest, J.P.; and Chapon, A. (1985) Validity of thoracic injury criteria based on the number of rib fractures. *The 10th International Technical Conference on Experimental Safety Vehicles*, pp. 124–132. National Highway Traffic Safety Administration, Washington, D.C.

Viano, D.C. (1983) Biomechanics of non-penetrating aortic trauma: A review. *Proc. 27th Stapp Car Crash Conference*, pp. 109–114. SAE paper no. 831608. Society of Automotive Engineers, Warrendale, Pa.

Viano, D.C. (1988) Personal communication to L.W. Schneider, UMTRI.

Viano, D.C. (1989a) *Live fire testing: Assessing blunt impact and acceleration injury vulnerabilities*. Report no. GMR-6690. General Motors Research Laboratories, Warren, Michigan.

Viano, D.C. (1989b) Biomechanical responses and injuries in blunt lateral impact. *Proc. 33rd Stapp Car Crash Conference*, pp. 113–142. Society of Automotive Engineers, Warrendale, Pa.

Viano, D.C. (May 1989) Personal communication to L.W. Schneider, UMTRI.

Viano, D.C.; and Lau, I.V. (1985) Thoracic impact: A viscous tolerance criterion. *The 10th International Technical Conference on Experimental Safety Vehicles*, pp. 104–152. National Highway Traffic Safety Administration, Washington, D.C.

Viano, D.C.; and Lau, I.V. (1988) Personal communication to L.W. Schneider, UMTRI.

Walfisch, G.; Chamouard, F.; Lestrelin, D.; Fayon, A.; Tarriere, C.; Got, C.; Guillon, F.; Patel, A.; and Hureau, J. (1982) Tolerance limits and mechanical characteristics of the human thorax in frontal and side impact and transposition of these characteristics into protection criteria. *Proc. 7th International Conference on the Biomechanics of Impacts*, pp. 122–139. IRCOBI, Bron, France.

Walt, A.J.; and Grifka, T.J. (1970) Blunt abdominal injury: A review of 307 cases. In *Impact Injury and Crash Protection*, pp. 101–124. Edited by E.S. Gurdjian et al. Charles C. Thomas, Springfield, Ill.

Warner, P.; and Ogle, D. (1974) *The development of U.K. standard occupant protection assessment test dummy*. SAE paper no. 740115. Society of Automotive Engineers, Warrendale, Pa.

Weichel, J.F.; Bell, S.; Pritz, H.; and Guenther, D. (1985) Enhancement of the Hybrid III dummy thorax. *Proc. 29th Stapp Car Crash Conference*, pp. 147–158. SAE paper no. 851732. Society of Automotive Engineers, Warrendale, Pa.

Williams, R.D.; and Sargent, F.T. (1963) The mechanism of intestinal trauma. *Journal of Trauma*, 3:288–294.

Weisfeldt, Myron L. (1979) *Compliance characteristics of the human chest during cardiopulmonary resuscitation*. Final Report no. DOT-HS-805–800. The Johns Hopkins Hospital, Baltimore, Maryland.

APPENDIX A

REVIEW OF HYBRID III ENHANCEMENT NEEDS

APPENDIX A

REVIEW OF HYBRID III ENHANCEMENT NEEDS

While the design of the Hybrid III thorax is generally recognized as an improvement of the Hybrid II or Part 572 thorax, especially with regard to its dynamic response at the sternum and deflection measurement capability, there is increasing recognition of the need for additional improvement in the design and performance of the thorax, shoulder, spine, and abdomen components. The problems with Hybrid III are now being addressed by members of the Human Biomechanics Simulation Subcommittee (HBSS) of the SAE. Among the needs that have been noted are the following.

Durability. Compared to its predecessor, Part 572, the Hybrid III thorax is much less durable. The primary problem lies in the damping material that is bonded to the steel ribs. Although improvements have been made in the past year or so, separation of the damping material from the steel and breakdown of the damping material still occur after approximately thirty calibration-level tests. Costs of rib replacement and the need for frequent calibration and inspections to detect material failure continue to present serious problems to users.

Temperature Sensitivity. Because the damping and rate sensitivity of the Hybrid III response is derived from material properties, the Hybrid III thorax exhibits undesirable sensitivity to ambient temperature. While equations for adjusting measured *peak* chest deflection for temperature are available, the application of these equations to adjustment of the deflection and velocity-time histories required for calculations of viscous criterion is not so straightforward and the need to make such adjustments for peak deflection values is an additional burden on the user. A design solution with reduced temperature sensitivity would be extremely desirable.

Lack of Biofidelity in Lower Cage. The Hybrid III thorax was designed to provide dynamic F-δ response curves within the Kroell corridors only at the sternum. It is becoming more and more evident that an ATD must also have biofidelity and measurement capability at the lower ribcage over the liver and spleen, since serious and fatal injuries can occur in these regions both from shoulder belts and steering-rim intrusion. Cavanaugh (see Appendix B) has demonstrated that the Hybrid III ribcage is statically stiffer at the lower cage about three inches lateral to the midline than it is at the sternum, whereas the human ribcage is less stiff in this region, both statically (Cavanaugh, Appendix B) and dynamically (see Table 7 in Section B1.1.4). It is important that this problem with Hybrid III be corrected for proper assessment of injury potential in frontal crashes.

Lack of Humanlike Ribcage Geometry. The Hybrid III ribcage consists of six pairs of composite ribs that comprise an essentially barrel-shaped thorax. As shown in Figure A-1 from Toyota's Comments to Docket No. 74–14 (Matsuoka et al. 1989), the Hybrid III ribs do not adequately represent the shape of the human ribcage. Of particular note is the lack of ribcage representation at the levels of rib 7 through rib 10 and the abrupt discontinuity that results as the ribcage is suddenly terminated after the lower or 6th rib. As noted in the Toyota comments, this lack of human geometry at the lower cage results in a sensitivity problem when testing with two-point shoulder belts:

> Chest deflection in the H-III dummy varies easily. In the H-III, there are two "shortest" seat belt paths possible (over the side of the ribs and under the bottom edge of the ribs). Which path is taken is determined by probability. Therefore, a slight difference in the test conditions causes a difference in the final belt path (Matsuoka et al. 1989).

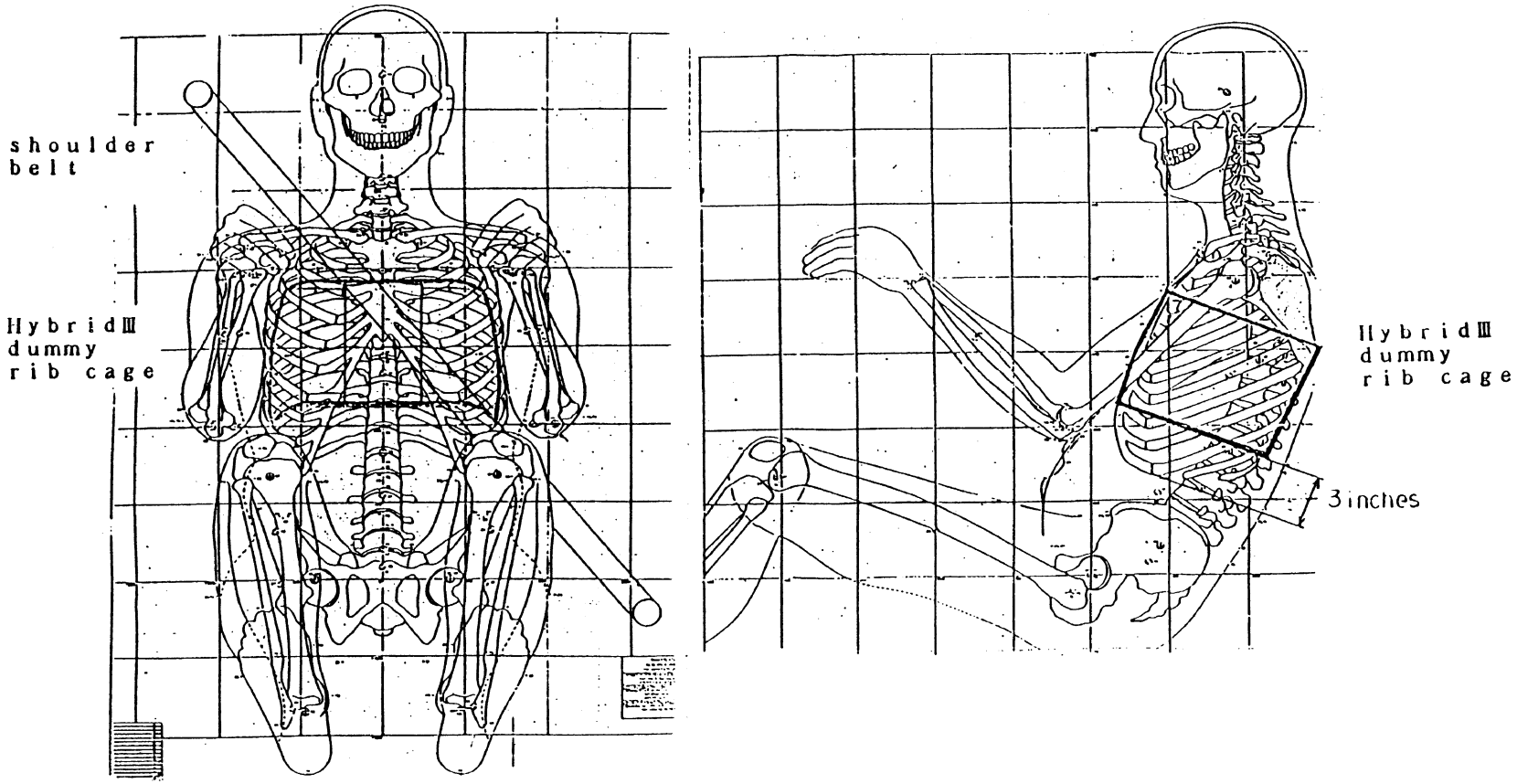

Source: "Development of Anthropometrically Based Design Specifications for an Advanced Adult Anthropomorphic Dummy Family, Vol. 1" L. W. Schneider, et.al., UMTRI, Dec. 1983

FIGURE A-1. Difference in ribcage between human and Hybrid III dummy (Matsuoka et al. 1989).

As illustrated in Figure A-2, a difference in belt positioning of about an inch as it crosses this bottom rib can result in significant differences in chest compression from identical tests. If the belt is positioned slightly high it will ride up the side of the ribcage and result in relatively little chest compression. If it is positioned slightly lower, the belt will catch under the ribcage and thereby cause significant compression of the chest. It should be noted that while the geometry of the Hybrid III ribcage lends itself to this problem, the static stiffness of the cage in this region (i.e., the lower cage) and the stiff coupling between ribs (discussed below) probably also contribute to the problem.

Inappropriately Stiff Coupling Between Thoracic Regions. The Hybrid III ribcage has been "tuned" to provide humanlike dynamic response characteristics to Kroell impacts at the sternum (i.e., for human impacts centered at the xiphoid process). This is accomplished by the contributions of six pairs of damped steel ribs which are fairly rigidly coupled by a delrin sternum and a narrow span of urethane between the delrin and the ribs on each side. The consequence of this design is that the coupling, both up and down the ribcage and between the left and right sides, is much too stiff. This has been demonstrated in static tests by L'Abbe et al. (1982) and Kallieris (1987), and more recently by Cavanaugh (Appendix B and Section B1.1.12). Clearly, this aspect of biofidelity is important to achieving repeatable and realistic injury assessment for shoulder-belt- and steering-rim-type loadings and must be an important consideration in an improved ATD thorax.

High-Static Stiffness. A consequence of achieving the dynamic response characteristics through the damped steel-rib design of Hybrid III is a thorax which is too stiff statically, both to the lower sternum where it has dynamic biofidelity, but perhaps more importantly, at the lower ribs lateral to the midline. This elevated stiffness has been noted by L'Abbe et al. (1982), and more recently confirmed by Cavanaugh (Appendix B), who found that the human ribcage demonstrates a static stiffness for the first 25 mm (1 in) of deflection on the order of 10 N/mm, which is in good agreement with the relationship of $69 \cdot D^2$ (where D is in inches and force is in lbs) established by Melvin et al. (1988a). In contrast, Hybrid III demonstrates a static stiffness three to five times greater. Even more significant is that the lower cage of the human demonstrates a lower static stiffness than at the sternum, while the Hybrid III dummy demonstrates a higher stiffness. While static biofidelity is not of great importance for crash testing of an unbelted dummy, this is not the case for tests of restrained dummies where the velocities of loading can be quite low.

Lack of Shoulder Mobility. The Hybrid III shoulder has limited mobility compared to that of the Part 572 ATD. While the Hybrid III shoulder design offers greater durability, there is concern that the shoulder will not interact appropriately with restraint belts and steering rims, particularly with regard to the percentage of load on the shoulder compared to the load on the chest. For this reason, as well as the influence of shoulder mobility and coupling on dummy kinematics (Melvin et al. 1988b), the shoulder design should be modified to provide greater mobility if it can be done without significant sacrifices in durability and repeatability.

Lack of Clavicle and Clavicle Loading-Sensing. Associated with the lack of shoulder mobility in Hybrid III is the lack of a clavicle structure by which loads can be transmitted to both the ribs (i.e., in the human, to the first rib at the sternum) and the spine. Instead, loads to the Hybrid III shoulder are transmitted solely to the rigid spine. A clavicle-like structure is needed in the Hybrid III. Such a structure, with representative mass, mobility, and coupling to the spine will play an important role in load distribution across the chest from shoulder belts. In addition, the ability to measure the load applied to the clavicle will provide useful information to the restraint system and automotive designer.

Unrealistically Rigid Thoracic Spine. As in its predecessors, the Hybrid III ATD uses a rigid steel box to represent the thoracic spine. While, in the human, most spinal mobility is in the cervical and lumbar regions, the thoracic spine is not absolutely rigid, especially during dynamic loading of the chest. The importance of this flexibility is not

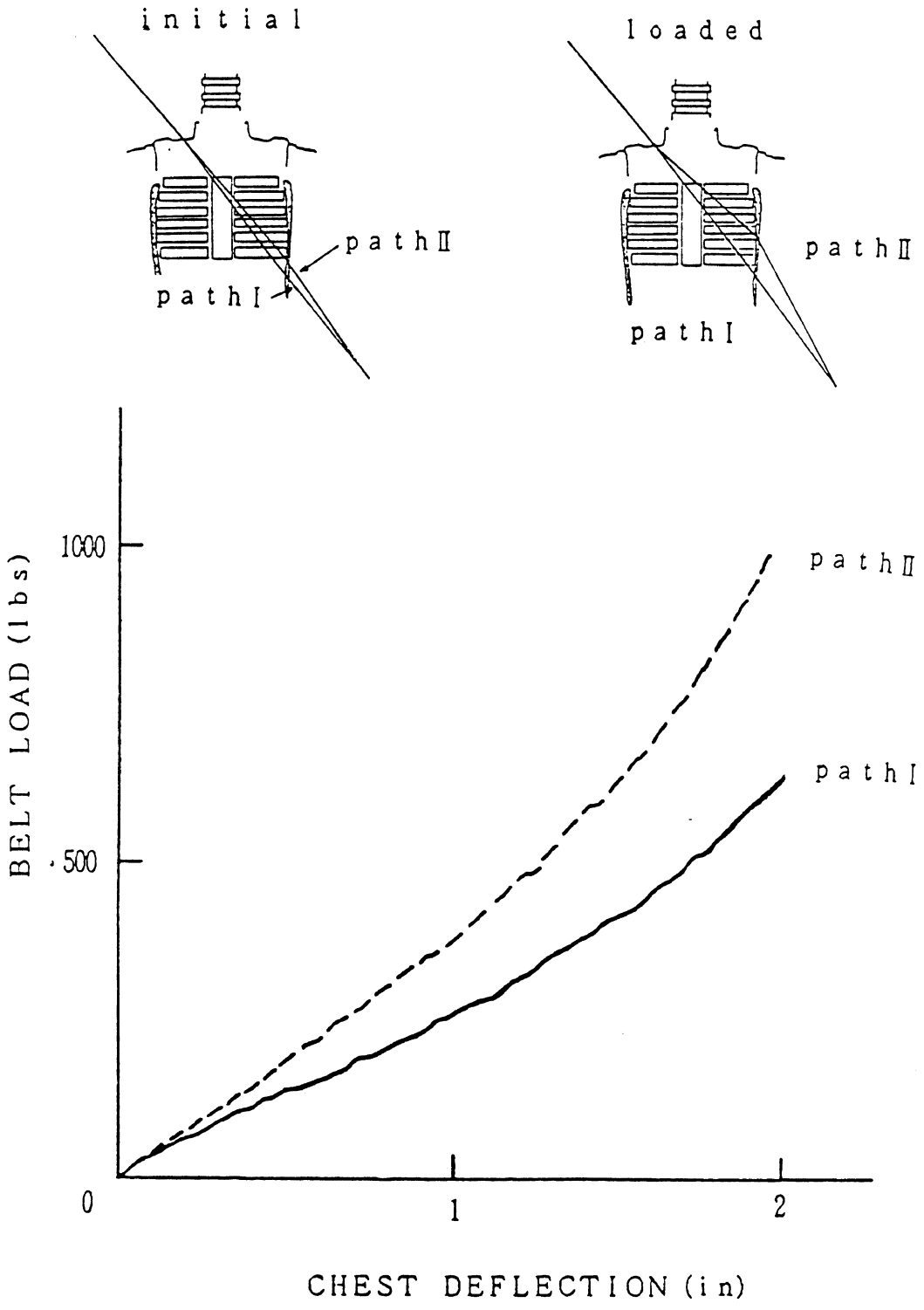

FIGURE A-2. Chest deflection as a result of different belt positioning (Matsuoka et al. 1989).

totally understood, but there is little doubt that it contributes to the manner in which the chest interacts with steering wheels and shoulder belts, and therefore to the resulting chest loads and deflections. It is therefore considered important that the new thorax include a thoracic spine with some degree of flexibility.

Lack of Biofidelic, Injury-Sensing Abdomen. As with its predecessors, the Hybrid III dummy has only a simple leaky-air/foam-filled bag for an abdomen which has neither biofidelity nor injury-sensing capability. A pressure-sensing abdomen for the Hybrid III was recently developed at VRTC and consists of a closed airbag with a pressure transducer and backing plate. While this is an improvement over the stock Hybrid III abdomen, it lacks biofidelity in that it is essentially an air spring and has little energy absorption capability. Furthermore, it must be inserted in one of two ways depending on whether upper or lower abdomen intrusion is expected. An improved abdomen is clearly needed that will sense both upper and lower abdominal loading from lap belts, shoulder belts, steering rims, and other vehicle components.

APPENDIX B

QUASI-STATIC FRONTAL LOADING OF THE THORAX OF HUMAN CADAVERS AND THE HYBRID III DUMMY

APPENDIX B

QUASI-STATIC FRONTAL LOADING OF THE THORAX OF HUMAN CADAVERS AND THE HYBRID III DUMMY

Dr. John Cavanaugh
Wayne State University
September 1988

Two unembalmed human cadavers and the 50th percentile male Hybrid III dummy were loaded quasi-statically at various anterior locations of the thorax using an Instron load testing machine. The upper, mid, and lower sternum were loaded. The ribs were also loaded anteriorly at upper, mid, and lower rib locations. Sternal loading was performed under two support conditions: (1) support of the spine only, with a rigid aluminum bar supported on unistrut, and (2) support of the spine and ribs posteriorly. Rib support was provided bilaterally approximately 7 cm (3 in) lateral to midline. Rib loading was performed with the posterior ribs and spine supported, but not under the spine-only support condition. Loading rates ranged from 1.27 mm/s (0.05 in/s) to 100 mm/s (4 in/s), and the stroke was usually set at 25 mm (1 in).

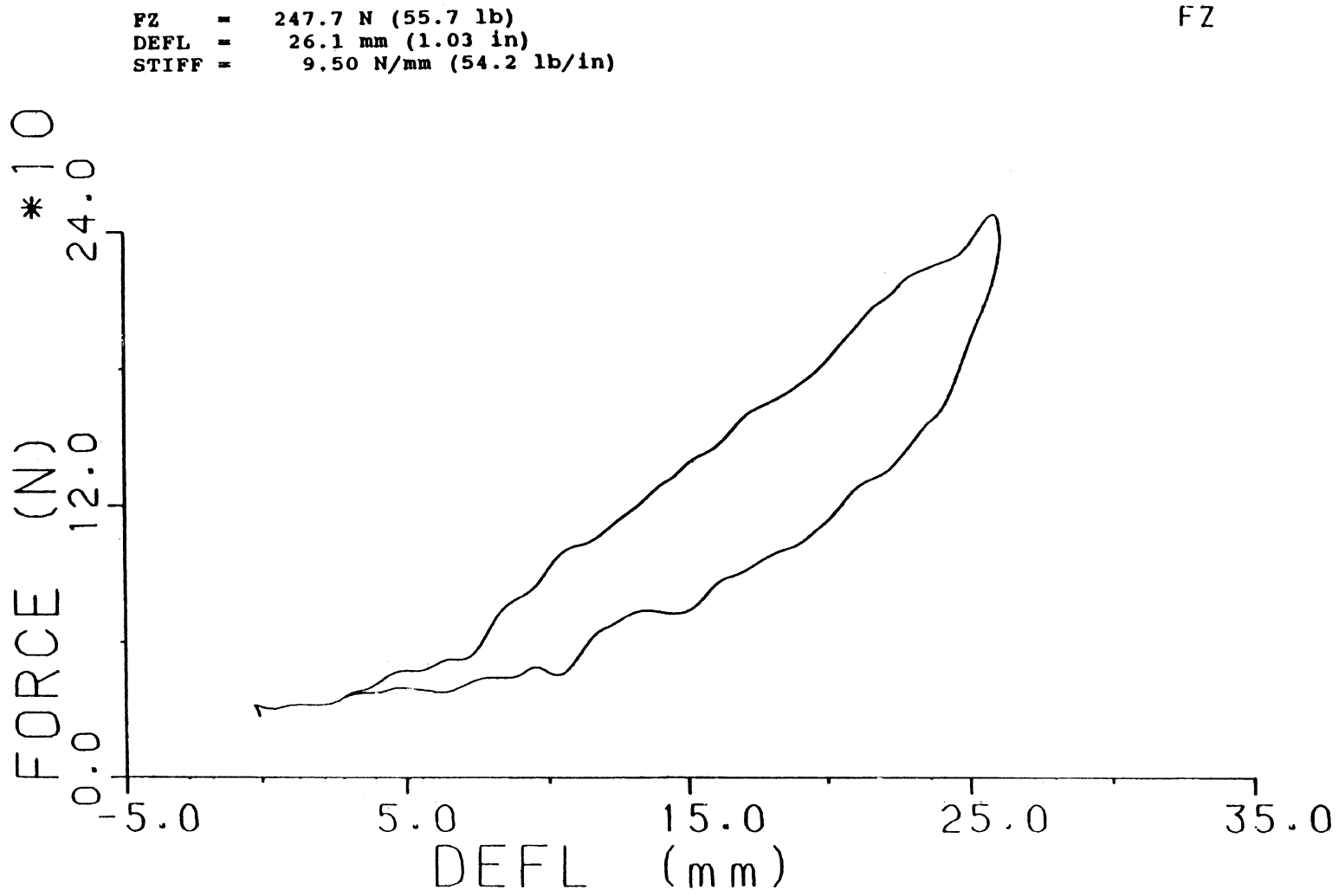

FIGURE B-1A. Force-deflection curve of AATD5, Run 1A, Cadaver #115, loaded at mid-sternum with a 25 mm (1 in) stroke at 1.7 mm/s (0.067 in/s).

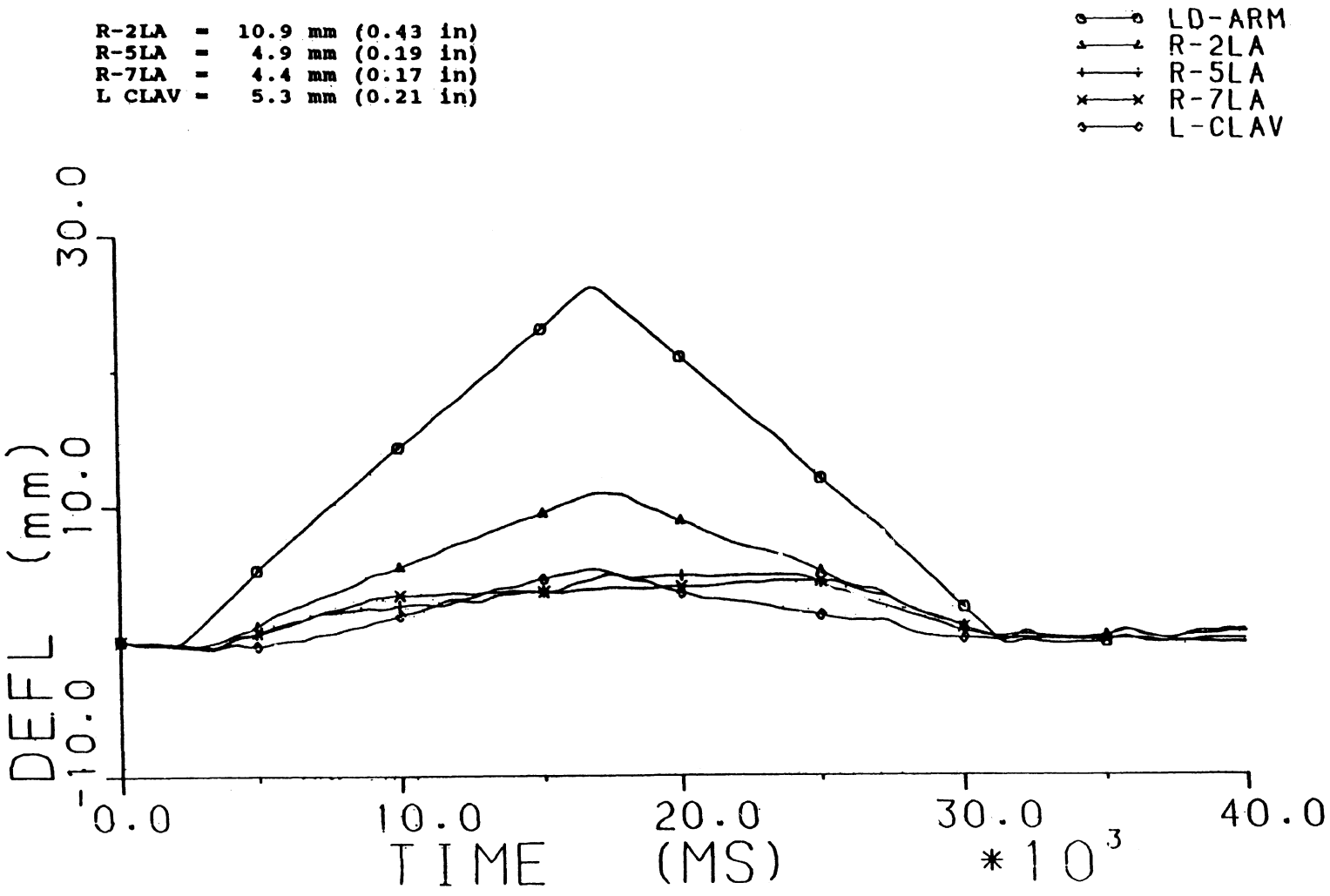

FIGURE B-1B. Deflection-time history at mid-sternal load arm, second, fifth, and seventh ribs and left clavicle.

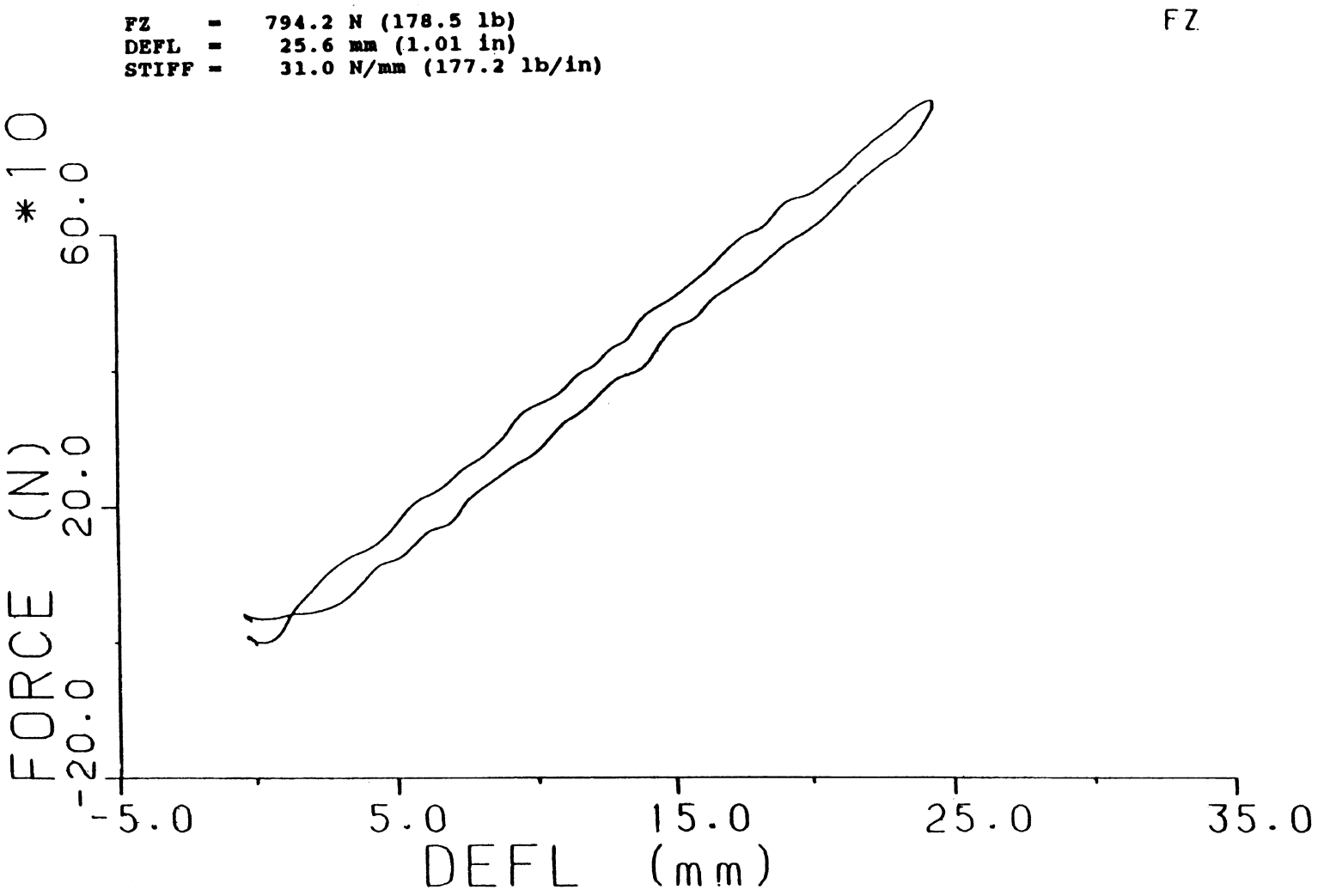

FIGURE B-2A. Force-deflection curve of AATD3, Run 2, Hybrid III, loaded at mid-sternum with 25 mm (1 in) stroke at 1.7 mm/s (0.067 in/s).

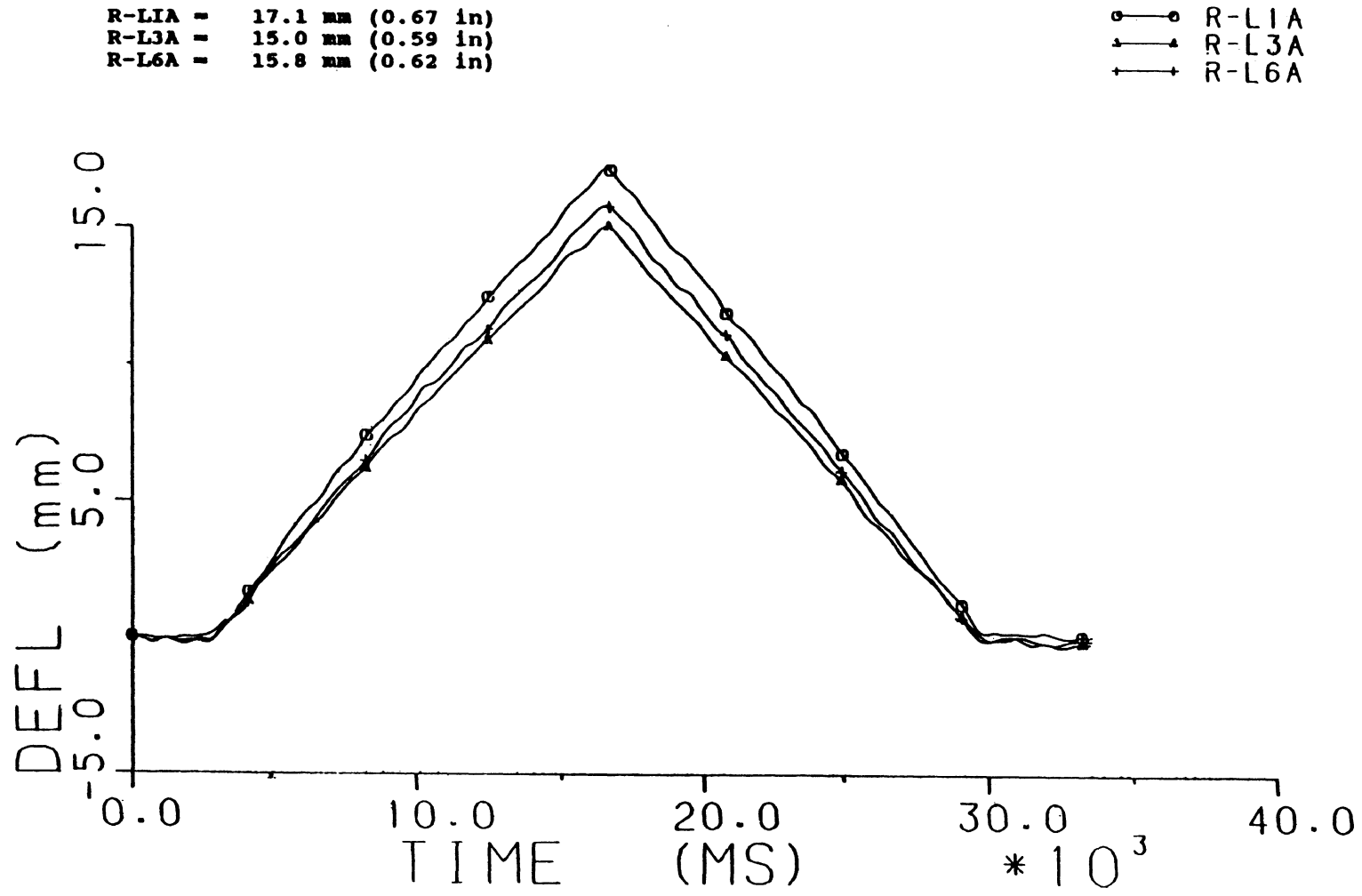

FIGURE B-2B. Deflection-time history at first, third, and sixth right ribs, anteriorly.

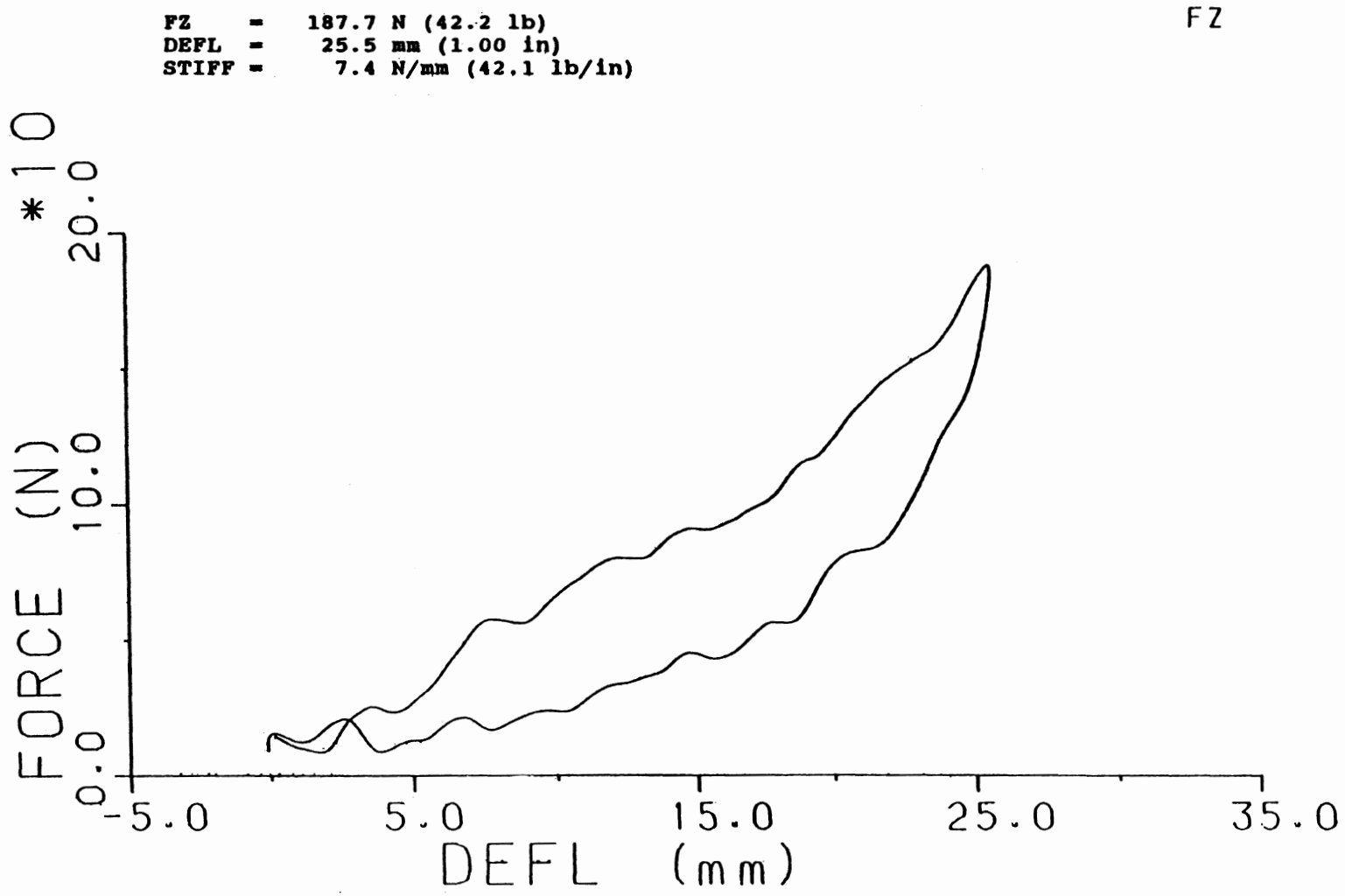

FIGURE B-3A. Force-deflection curve of AATD5, Run 5, cadaver #114, loaded at upper sternum with 25 mm (1 in) stroke at 1.7 mm/s (0.067 in/s).

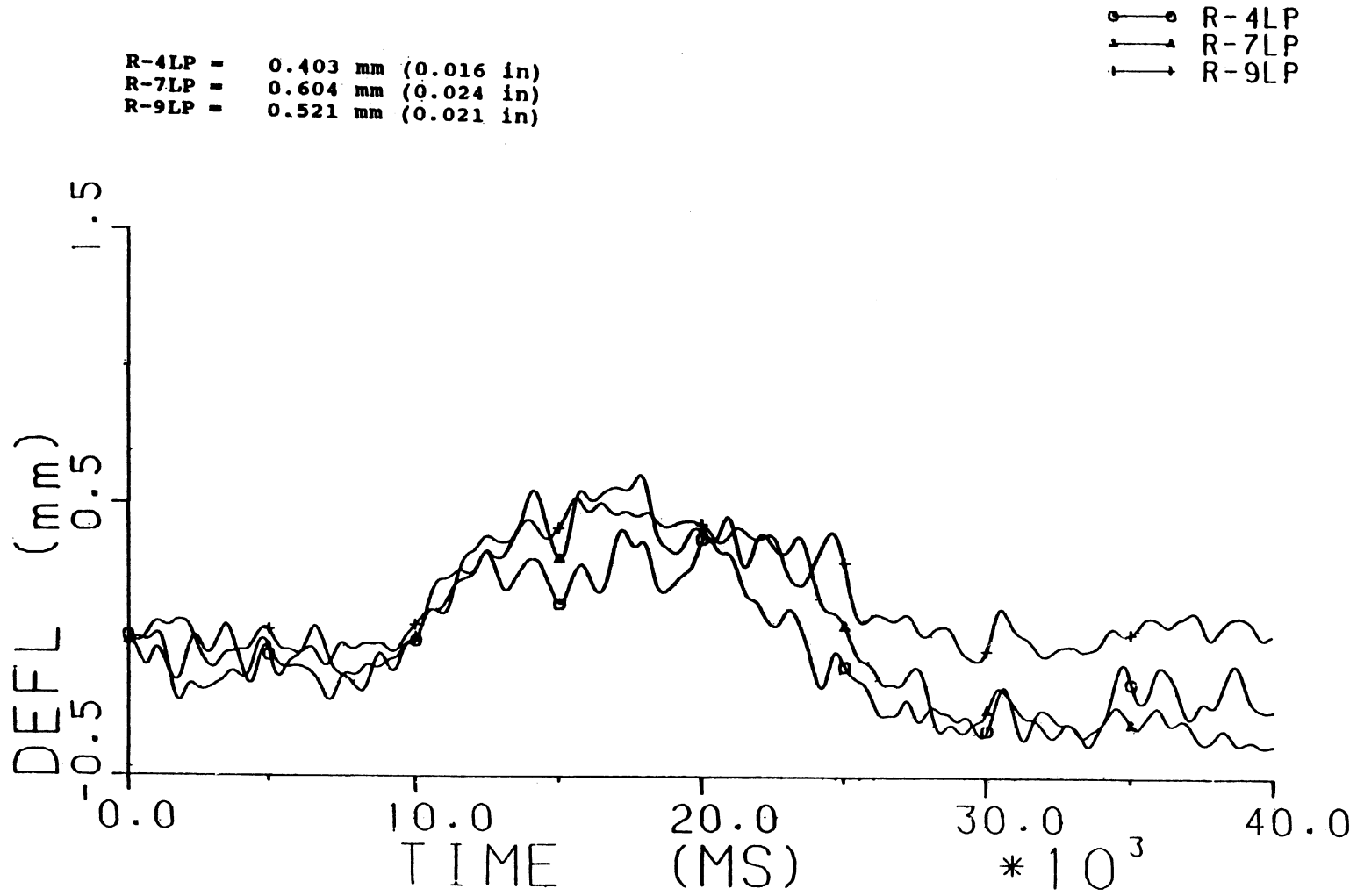

FIGURE B-3B. Deflection-time history at fourth, seventh, and ninth left ribs, posteriorly.

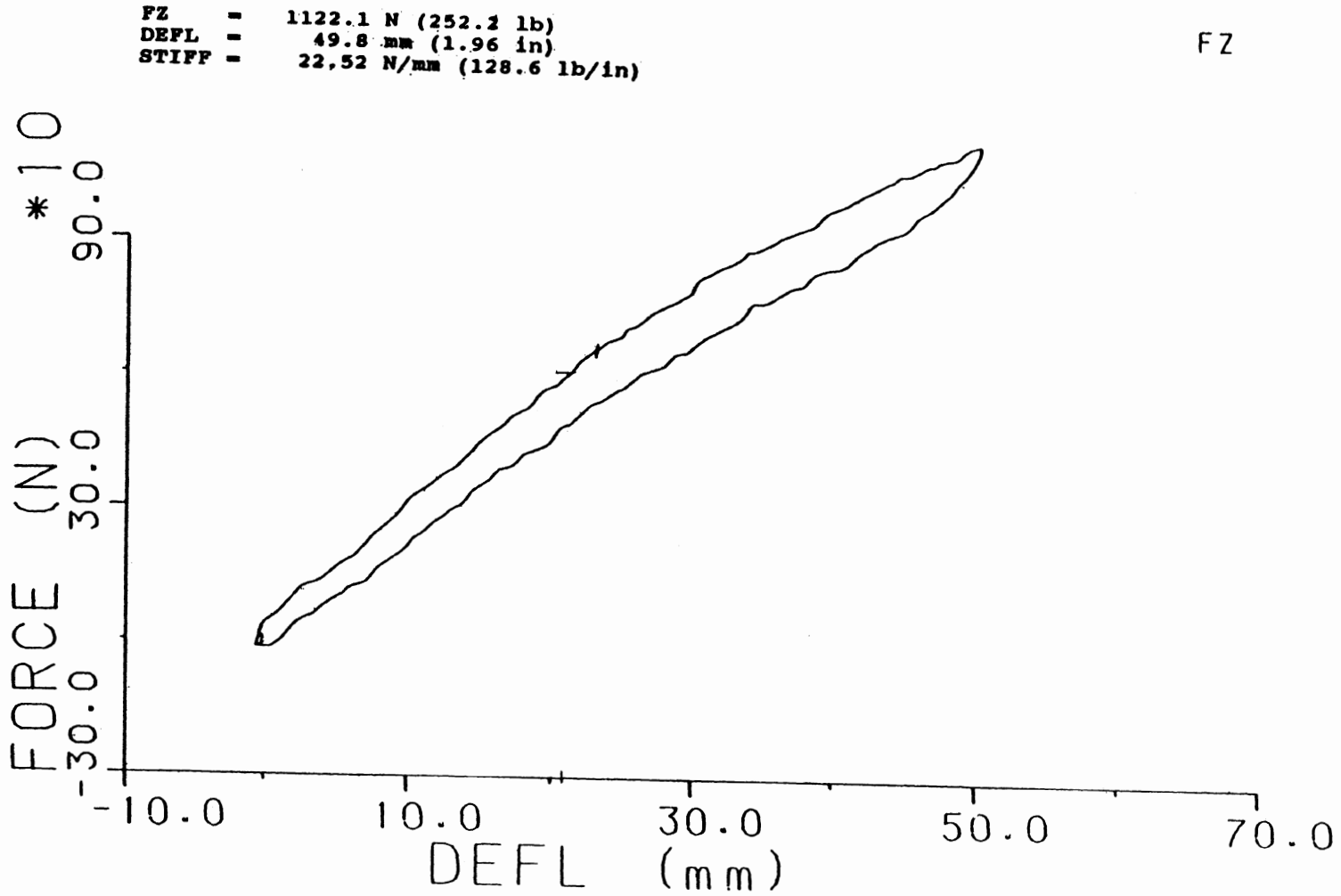

FIGURE B-4A. Force-deflection curve of AATD3, Run 7, Hybrid III, loaded at upper sternum with 50 mm (2 in) stroke at 1.7 mm/s (0.067 in/s).

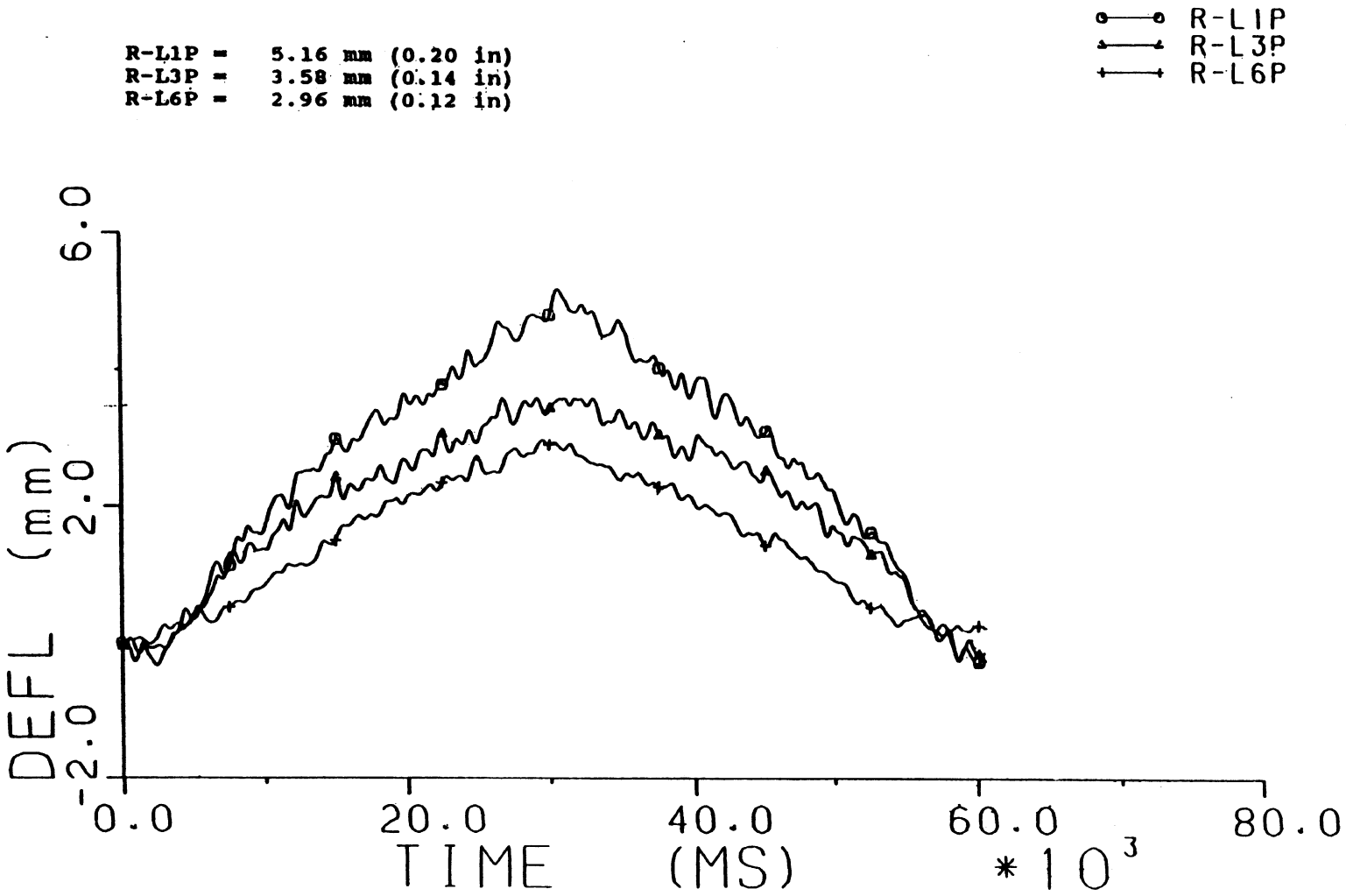

FIGURE B-4B. Deflection-time history at first, third, and sixth left ribs, posteriorly.

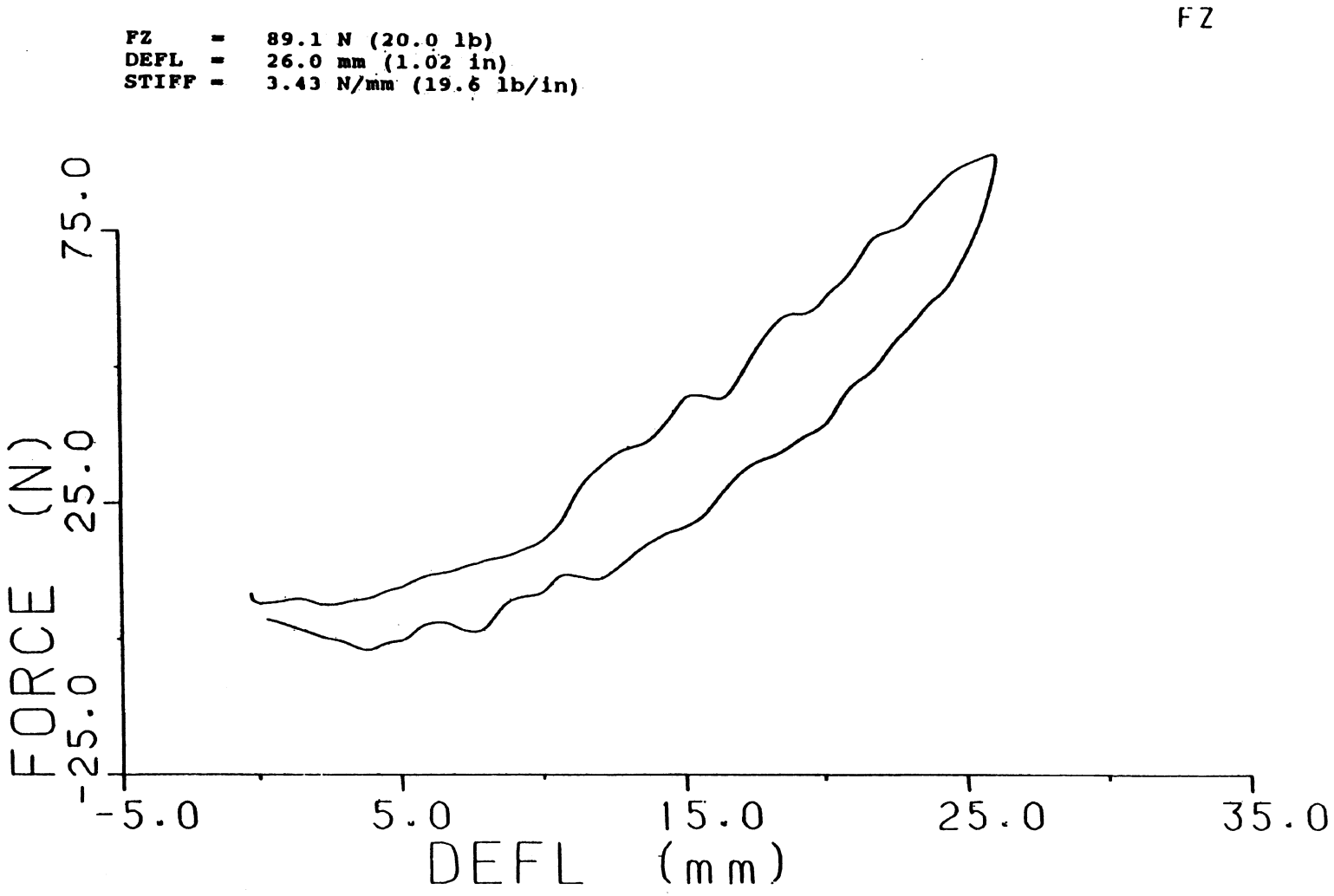

FIGURE B-5A. Force-deflection curve of AATD5, Run 17, Cadaver #115, loaded at right seventh rib with 25 mm (1 in) stroke at 1.7 mm/s (0.067 in/s).

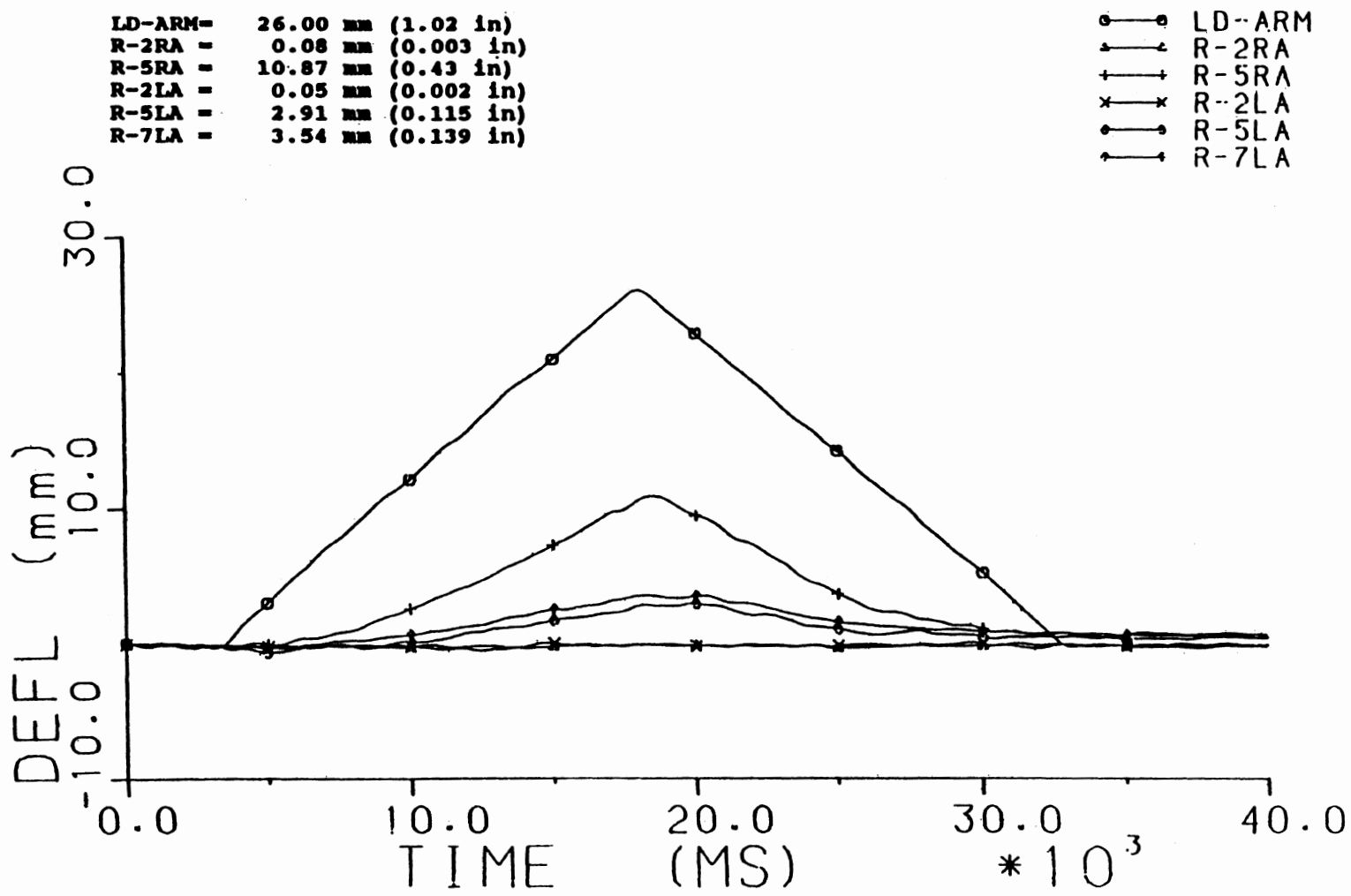

FIGURE B-5B. Deflection-time history at load arm (right seventh rib), right second rib, right fifth rib, and left second, fifth and seventh ribs, anteriorly.

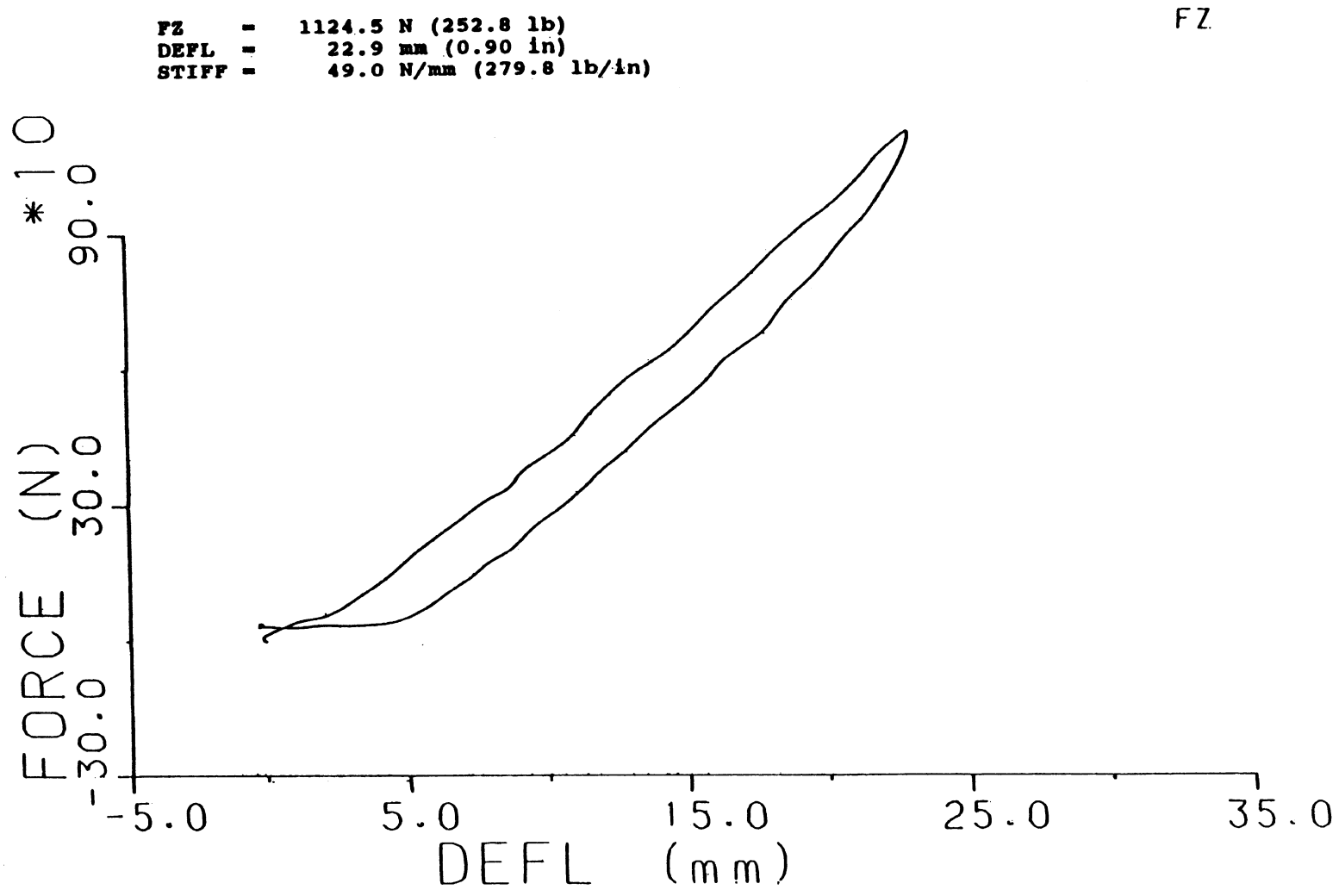

FIGURE B-6A. Force-deflection curve of AATD4, Run 5, Hybrid III, loaded at right sixth rib with 25 mm (1 in) stroke at 1.7 mm/s (0.067 in/s).

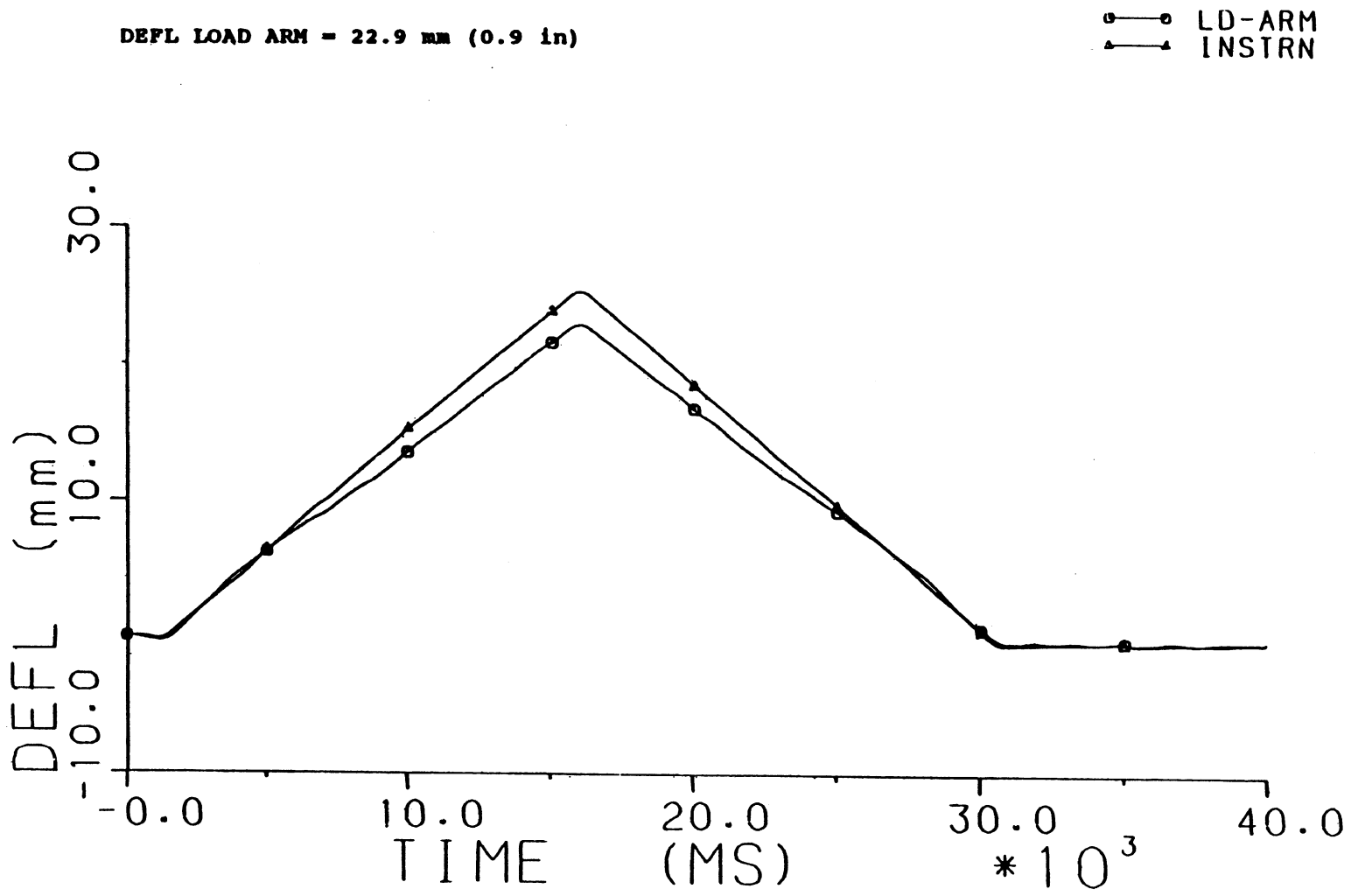

FIGURE B-6B. Deflection-time history of load arm and Instron actuator.

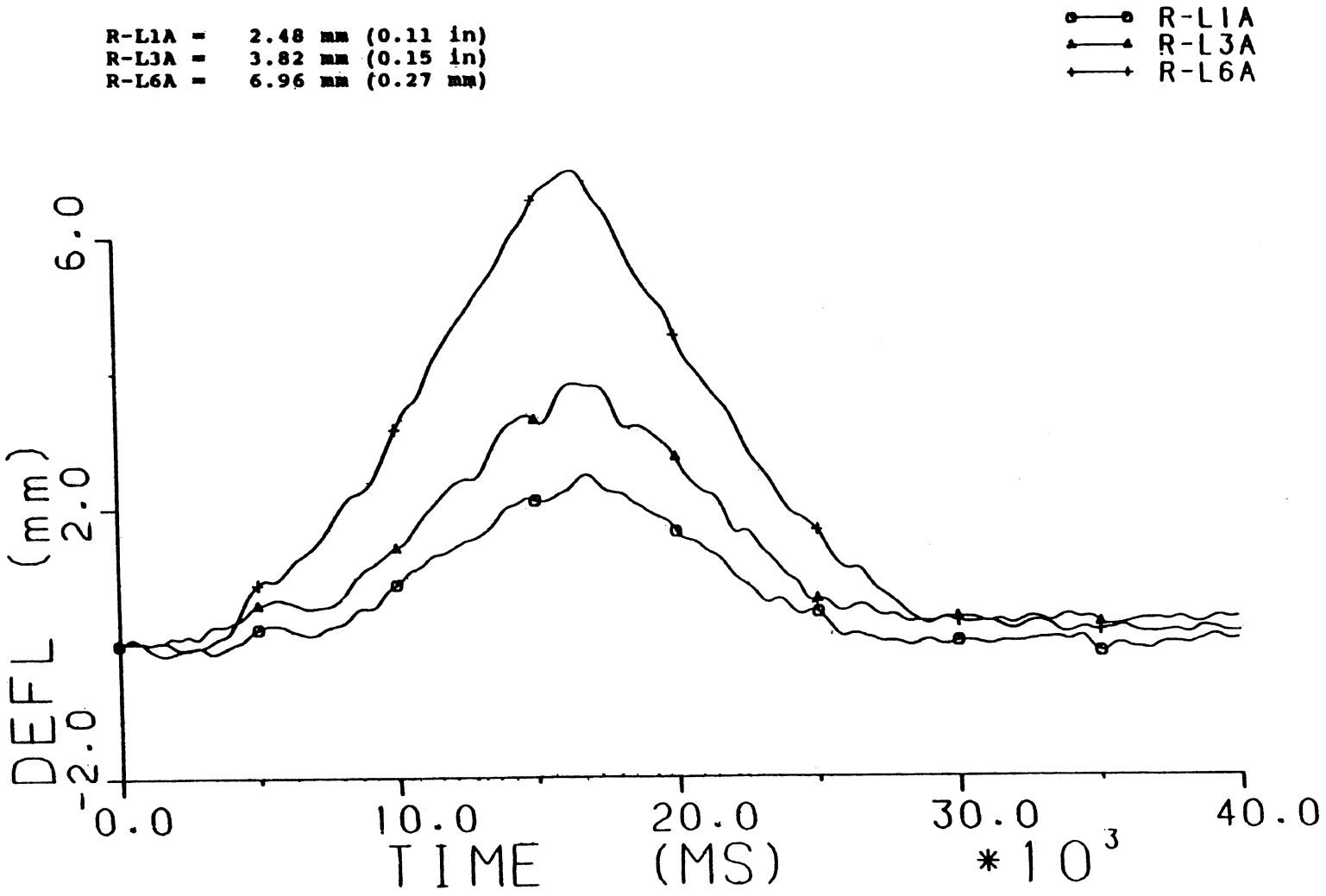

FIGURE B-6C. Deflection-time history of first, third, and sixth left ribs, anteriorly.

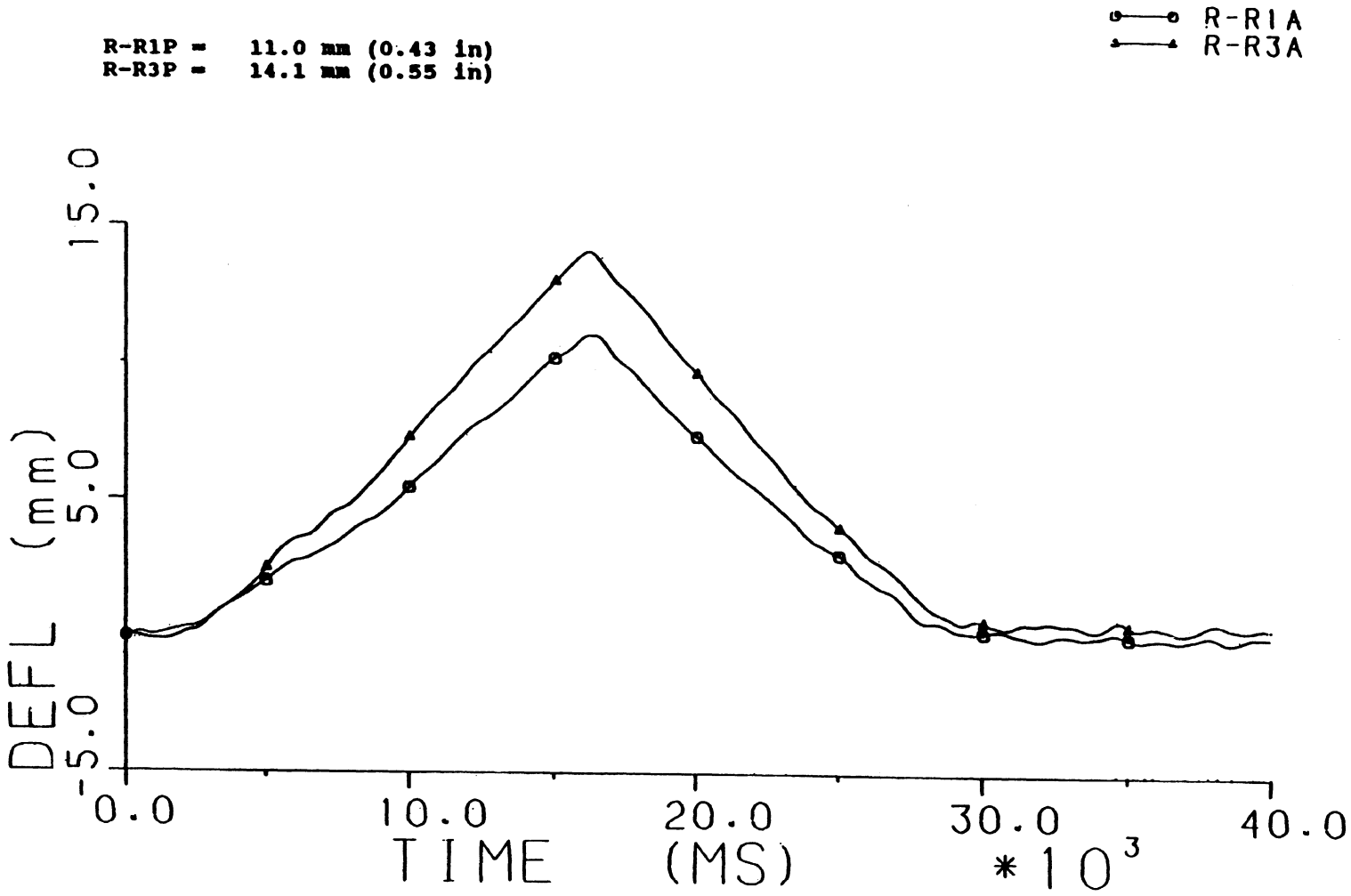

FIGURE B-6D. Deflection-time history of first and third right ribs, posteriorly.

APPENDIX C

FORCE-TIME AND FORCE-DEFLECTION CURVES
Kroell et al. 1971, 1974

EXPT. 61 SPEC. 12 FF

67 YRS. 5'4" 138 LB.
7-3/8" A-P 33" GIRTH
COD - HEART DISEASE
DOD 2/28/70 DOT 3/10/70 DOA 3/12/70

STRIKER MASS 50.4 LB. KINETIC ENERGY = 442 FT.-LB.
VEL. 16.2 MPH MOMENTUM = 37.2 LB.-SEC.

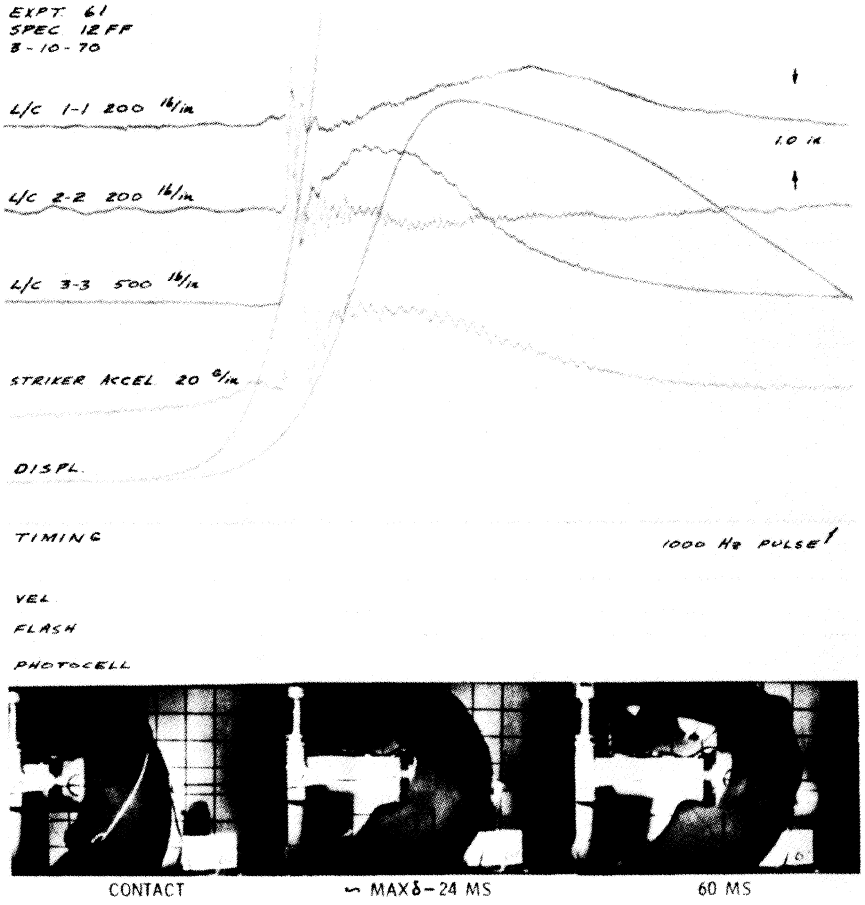

CONTACT ~ MAXδ - 24 MS 60 MS

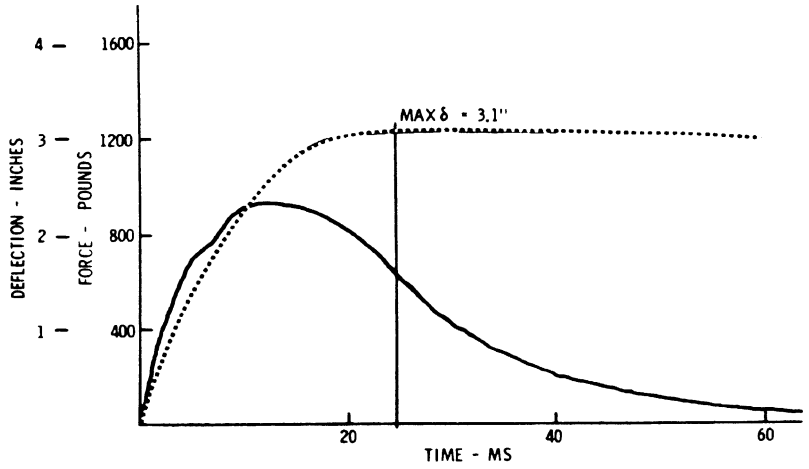

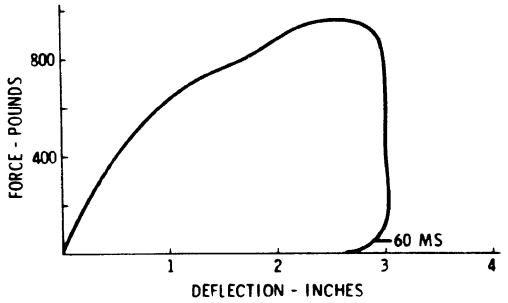

THORACIC AUTOPSY

FRACTURES:
R1, R2(2), R3(2), R4(2), R5(2), R6, R7, L1, L2(2), L3(2), L4(2), L5, L6(2), L7 (22 TOTAL)
STERNAL AT 1ST AND 3RD INTERSPACES

(1) POSSIBLE "FLAIL CHEST" IN VIVO
(2) SLIGHT LACERATION OF RIGHT LUNG BELOW INNERMOST FRACTURE OF RIB 4

EXPT. 65 SPEC. 13 FM

81 YRS. 5'6" 168 LB.
9-1 1/16" A-P 38" GIRTH
COD - RENAL FAILURE
DOD 3/9/70 DOT 3/13/70 DOA 3/16/70

STRIKER MASS 50.4 LB. KINETIC ENERGY = 464 FT.-LB.
VEL 16.6 MPH MOMENTUM = 38.1 LB.-SEC.

VASCULAR BASELINE 130 mm Hg

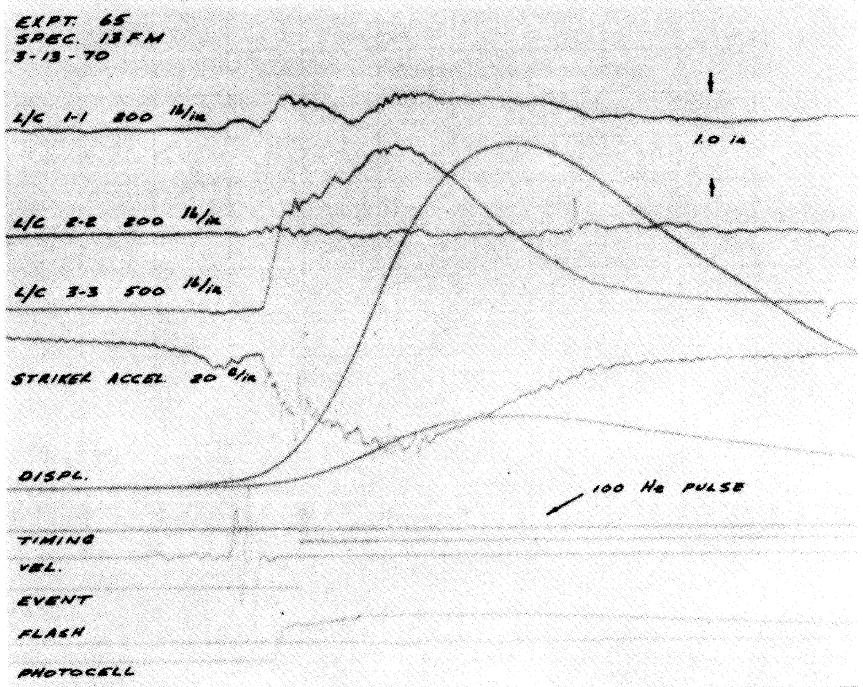

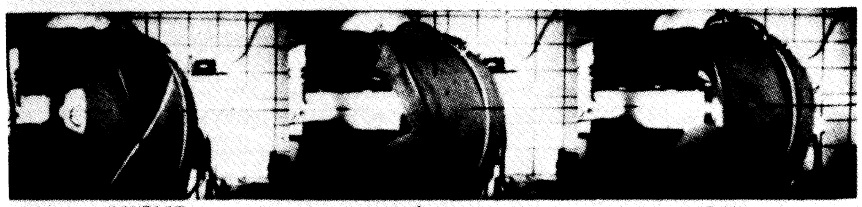

CONTACT MAXδ-32 MS 60 MS

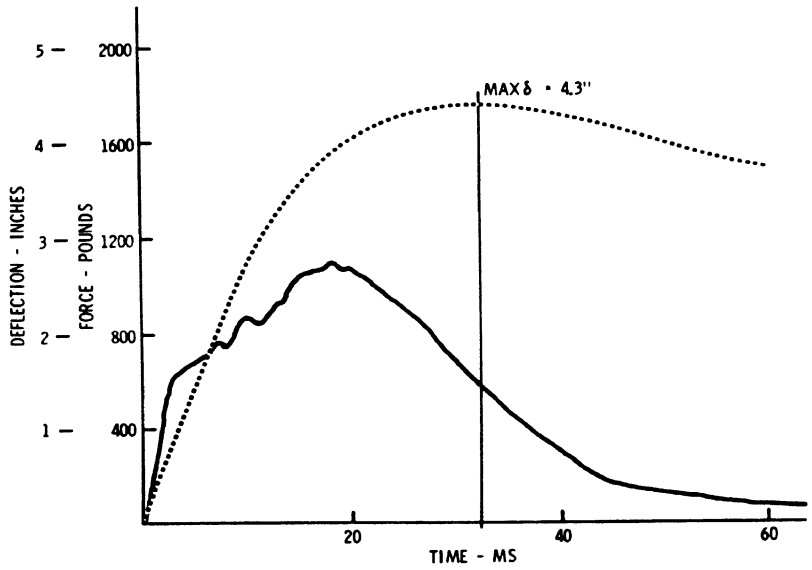

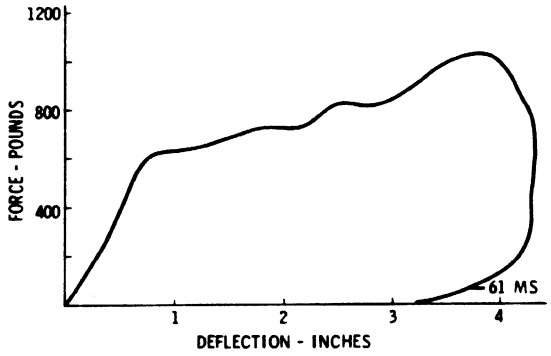

THORACIC AUTOPSY

FRACTURES:
R2(2), R3(2), R4(2), R5(2), R6, L1, L2(2) L3(3), L4(2), L5(2), L6, L7, (21 TOTAL)

(1) POSSIBLE "FLAIL CHEST" IN VIVO
(2) 1/2 IN. VERTICAL LACERATION IN HEART WALL COMMUNICATING WITH LEFT VENTRICLE; PERICARDIUM INTACT

EXPT. 66 SPEC. 14 FF

76 YRS. 5'1½" 127 LB.
8½" A-P 35" GIRTH
COD - MYOCARDIAL INFARCTION
DOD 4/6/70 DOT 4/10/70 DOA 4/13/70

STRIKER MASS 50.4 LB. KINETIC ENERGY = 453 FT.-LB.
VEL 16.4 MPH MOMENTUM = 37.6 LB.-SEC.

VASCULAR BASELINE 150 mm Hg

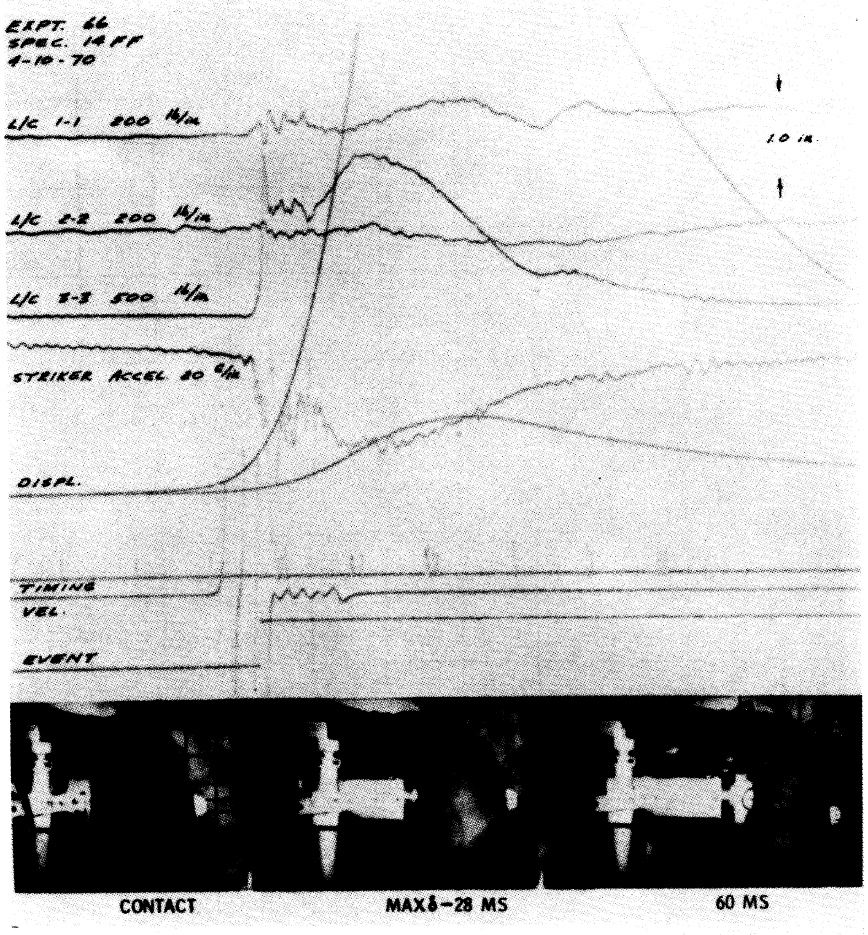

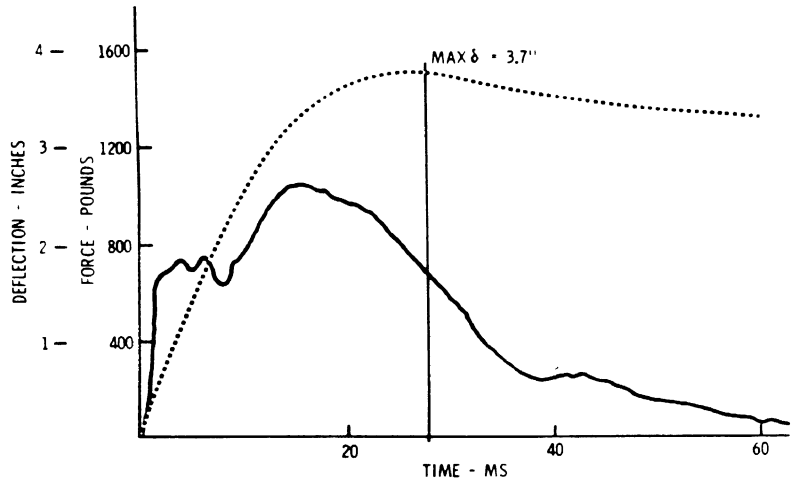

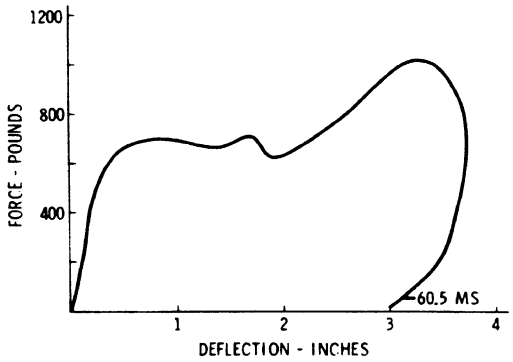

THORACIC AUTOPSY

FRACTURES:
R2, R3, R5, R6, L2, L3(2), (7 TOTAL)
STERNAL AT 2ND AND 6TH INTERSPACES

(1) BENEATH STERNAL FRACTURES: PARIETAL PLEURA PUNCTURES; CONTUSIONS OF ANTERIOR WALLS OF HEART AND PERICARDIUM, AND OVERLYING FATTY TISSUE
(2) HEMORRHAGE ON POSTERIOR WALL OF PERICARDIUM
(3) LARGE LACERATION AT JUNCTION OF INFERIOR VENA CAVA AND RIGHT ATRIUM
(4) MULTIPLE HEMORRHAGES IN ADVENTITIAL LAYER OF DECENDING AORTA

EXPT. 76 SPEC 18 FM

78 YRS. 5'9½" 145 LB.
8-5/8" A-P 36" GIRTH
COD - STRANGULATION
DOD 6/16/70 DOT 6/18/70 DOA 6/18/70

STRIKER MASS 52.0 LB. KINETIC ENERGY = 391 FT.-LB
VEL 15.0 MPH MOMENTUM = 35.5 LB.-SEC.

VASCULAR BASELINE 50 mm Hg

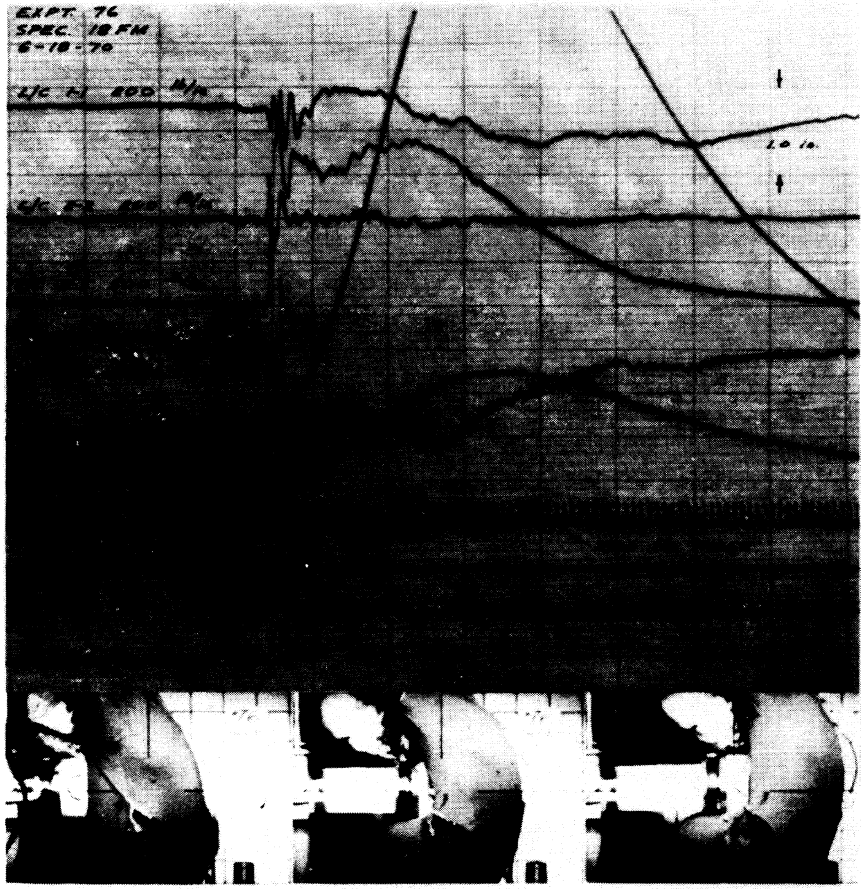

CONTACT MAX δ - 31 MS 60 MS

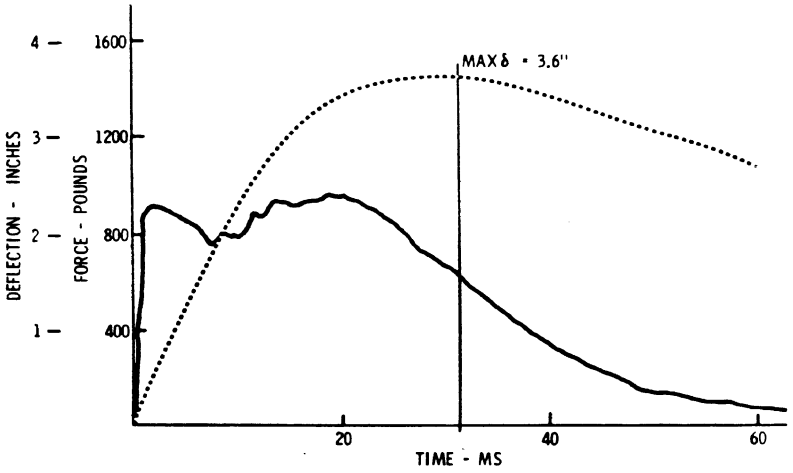

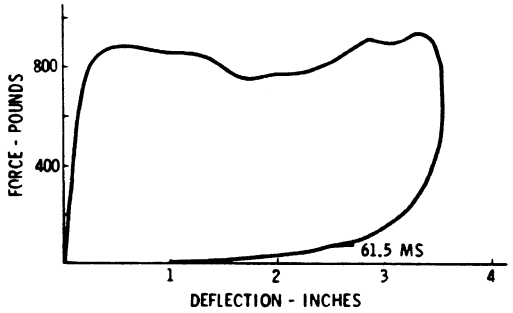

THORACIC AUTOPSY

FRACTURES:
R1, R2, R3, R4, R6(2), L2, L3, L4, L5, L6(2), L7(2), (14 TOTAL)
STERNAL AT XYPHOID PROCESS AND 2ND INTERSPACE

PARIETAL PLEURA PENETRATED BY STERNAL FRACTURE AT THE XYPHOID PROCESS

EXPT. 79 SPEC. 20 FM

29 YRS. 5'11" 125 LB.
8" A-P 32" GIRTH
COD - METASTATIC PULMONARY CARCINOMA
DOD 7/26/70 DOT 7/28/70 DOA 7/28/70

STRIKER MASS 52.0 LB KINETIC ENERGY = 391 FT.-LB.
VEL 15.0 MPH MOMENTUM = 35.5 LB.-SEC.

VASCULAR BASELINE 25 mm Hg
PRESSURES MONITORED - AORTIC ARCH

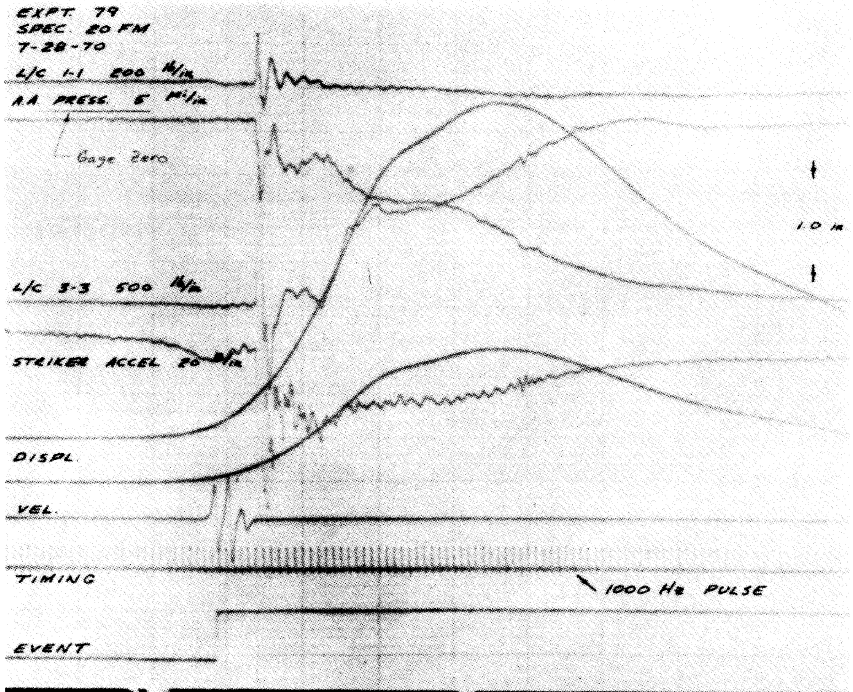

CONTACT MAX δ - 30 MS 60 MS

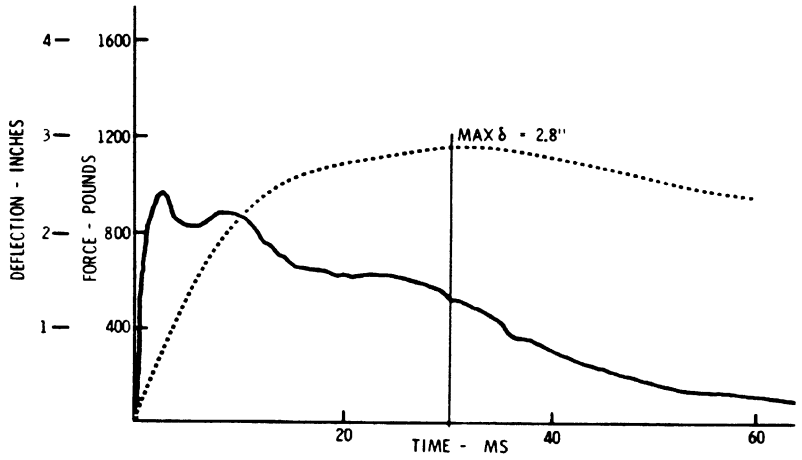

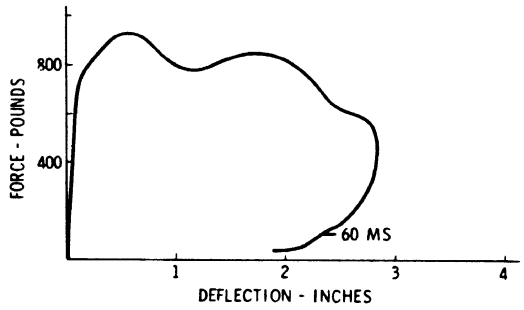

THORACO-ABDOMINAL AUTOPSY

FRACTURES:
NONE

NO VISCERAL DAMAGE

EXPT. 83 SPEC. 22 FM

72 YRS. 6'0" 165 LB.
8-7/8" A-P 40½" GIRTH
COD - MYOCARDIAL INFARCTION
DOD 9/2/70 DOT 9/4/70 DOA 9/4/70

STRIKER MASS 52.0 LB. KINETIC ENERGY = 391 FT.-LB.
VEL 15.0 MPH MOMENTUM = 35.5 LB.-SEC.

VASCULAR BASELINE ~ 95 mm Hg
PRESSURES MONITORED - AORTIC ARCH, LEFT VENTRICLE

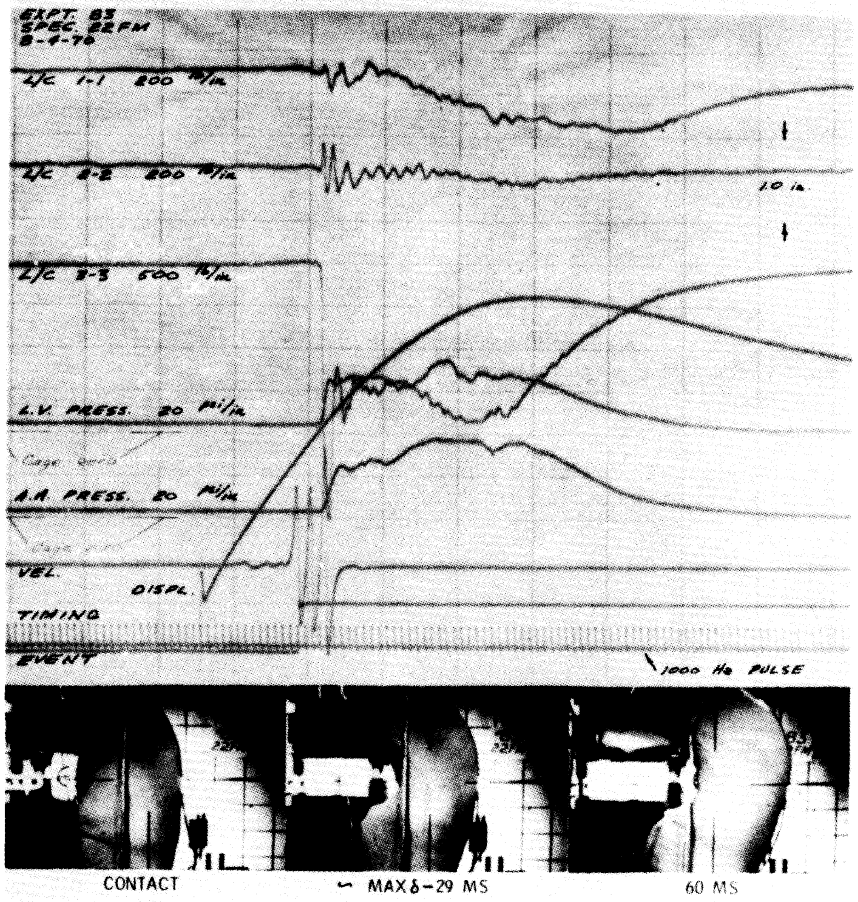

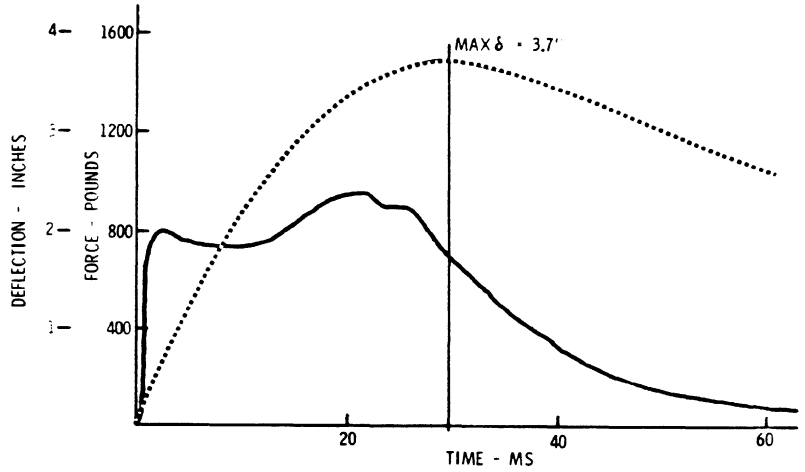

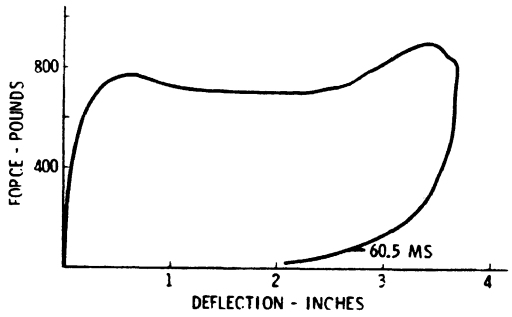

THORACO-ABDOMINAL AUTOPSY

FRACTURES:
R2, R3(3), R4(2), R5, R6, L2, L3(2), L4(3), L5(2), L6, (17 TOTAL)

(1) CONTUSION WITHIN LEFT ANTERIOR CHEST WALL WITH HEMORRHAGE IN ANTERIOR AXILLARY LINE AT RIB 5; HEMORRHAGE OF POSTERIOR CHEST WALL WITH BLEEDING INTO PRE-PERICARDIAL FAT
(2) SMALL CONTUSION AND 3/8 IN. SUPERFICIAL LACERATION OF UNDERSURFACE OF RIGHT LOBE OF LIVER

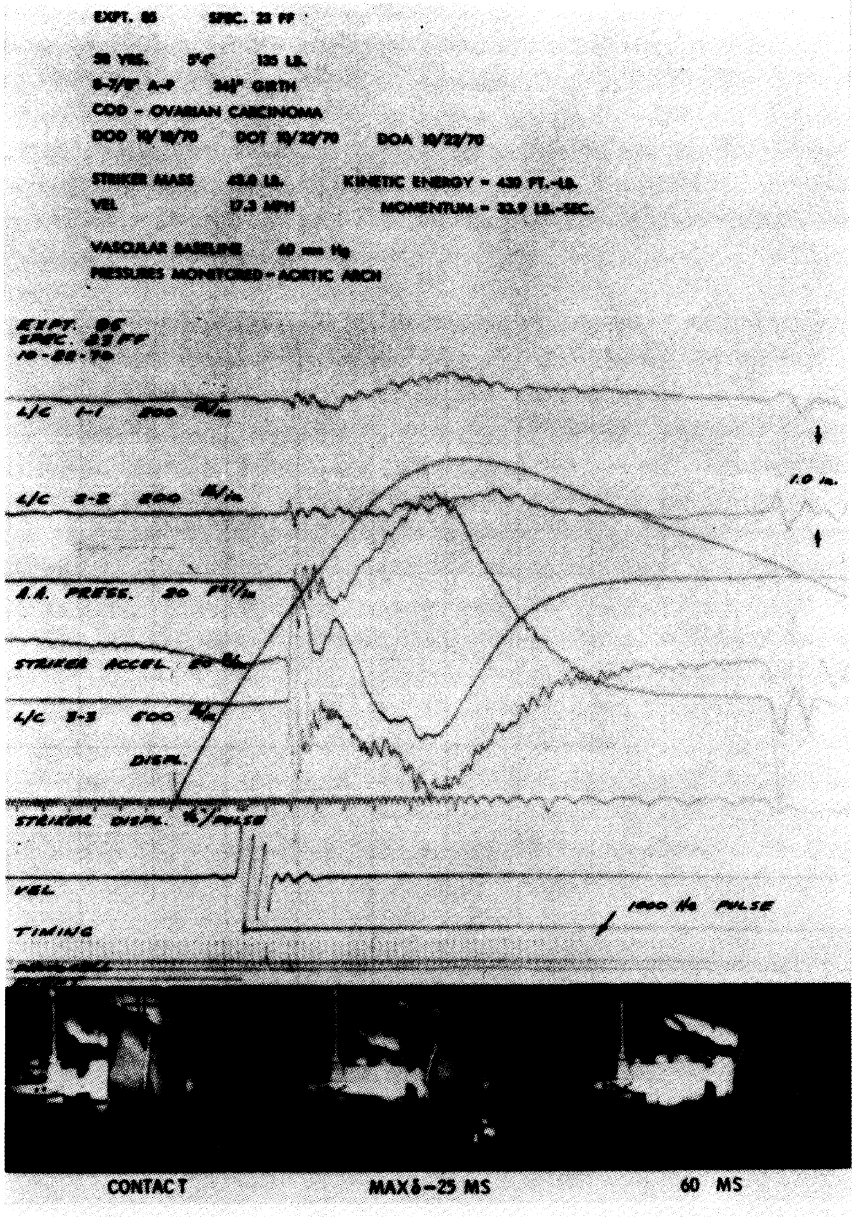

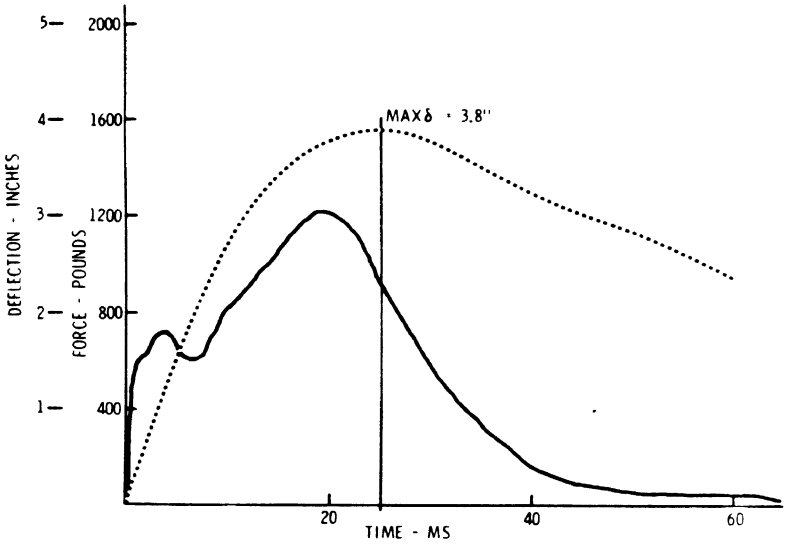

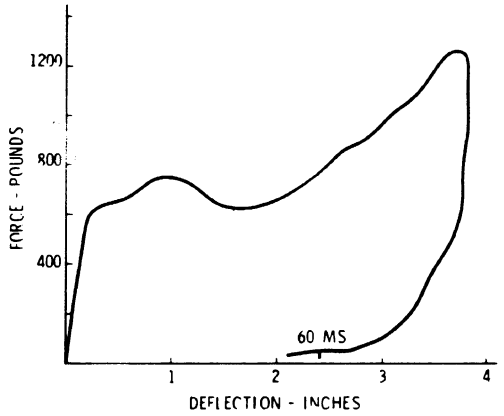

THORACO-ABDOMINAL AUTOPSY

FRACTURES:
R2, R3(2), R4(3), R5(3), R6(3), R7, L2(2), L3(3), L4(2), L5, L6(2), (23 TOTAL)

PARIETAL PLEURA PUNCTURES BELOW FRACTURES OF RIBS R5 and L4; POSSIBLE FLAIL CHEST AND BI-LATERAL PNEUMOTHORACES IN VIVO

EXPT. 86 SPEC 24 FM

65 YRS. 6'0" 180 LB.
9-7/8" A-P 40" GIRTH
COD - STRANGULATION
DOD 10/28/70 DOT 11/2/70 DOA 11/3/70

STRIKER MASS 50.4 LB. KINETIC ENERGY = 785 FT.-LB.
VEL 21.6 MPH MOMENTUM = 49.6 LB.-SEC.

VASCULAR BASELINE 70 mm Hg
PRESSURES MONITORED - AORTIC ARCH

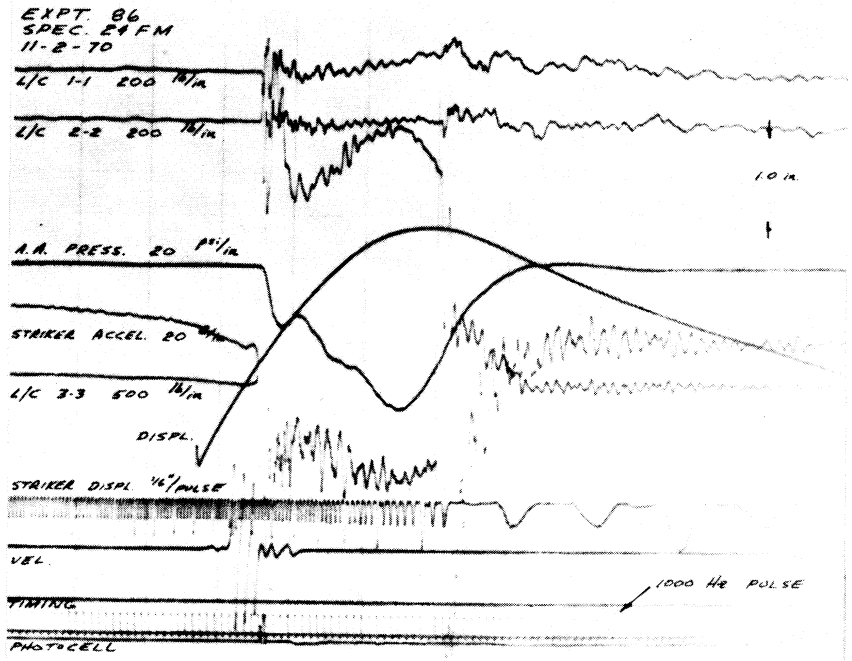

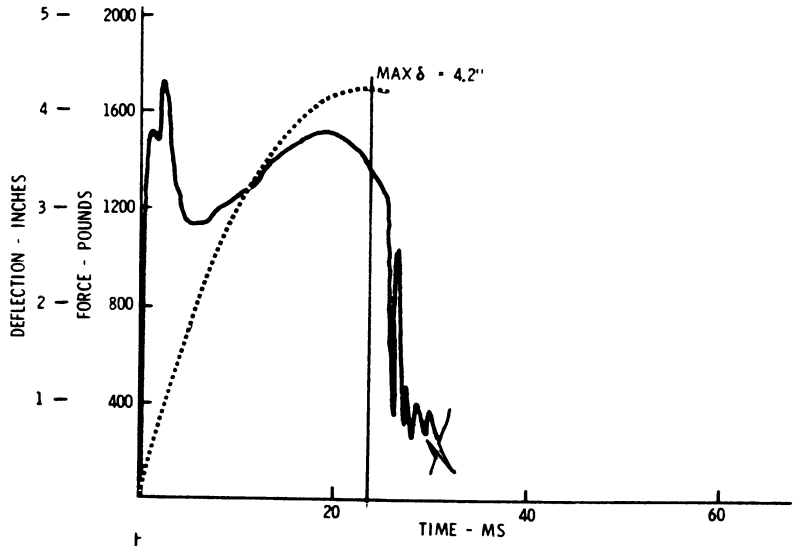

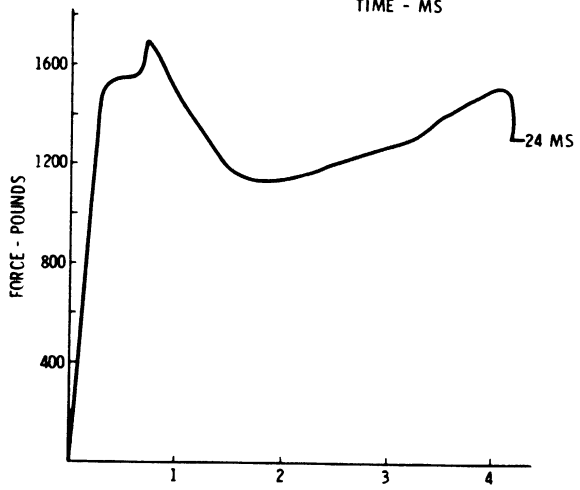

THORACO-ABDOMINAL AUTOPSY

MULTIPLE RIB FRACTURES RESULTING IN ABNORMAL MOBILITY OF CHEST WALL; STERNAL FRACTURES AT 1ST AND 2ND INTERSPACES

(1) POSSIBLE FLAIL CHEST AND PNEUMOTHORAX IN VIVO
(2) 2½ IN. LINEAR FRACTURE OF ANTERIOR SURFACE OF LIVER EXPOSING UNDERLYING PARENCHYMA; "Y" SHAPED FRACTURE OF INFERIOR SURFACE OF LEFT LOBE OF LIVER HAVING SEGMENT LENGTHS OF 2 IN. AND 3-5/8 IN.; A NODULAR APEX ON THE XYPHOID PROCESS IS ASSOCIATED WITH THE LEFT LOBE FRACTURE

EXPT. 87 SPEC. 25 FM

65 YRS. 5'6" 120 LB.
8-1/8" A-P 34" GIRTH
COD - CORONARY THROMBOSIS
DOD 1/27/71 DOT 1/29/71 DOA 1/29/71

STRIKER MASS 12.1 LB. KINETIC ENERGY = 386 FT.-LB.
VEL 30.9 MPH MOMENTUM = 17.0 LB.-SEC.

VASCULAR BASELINE 50 mm Hg
PRESSURES MONITORED - AORTIC ARCH, LEFT VENTRICLE

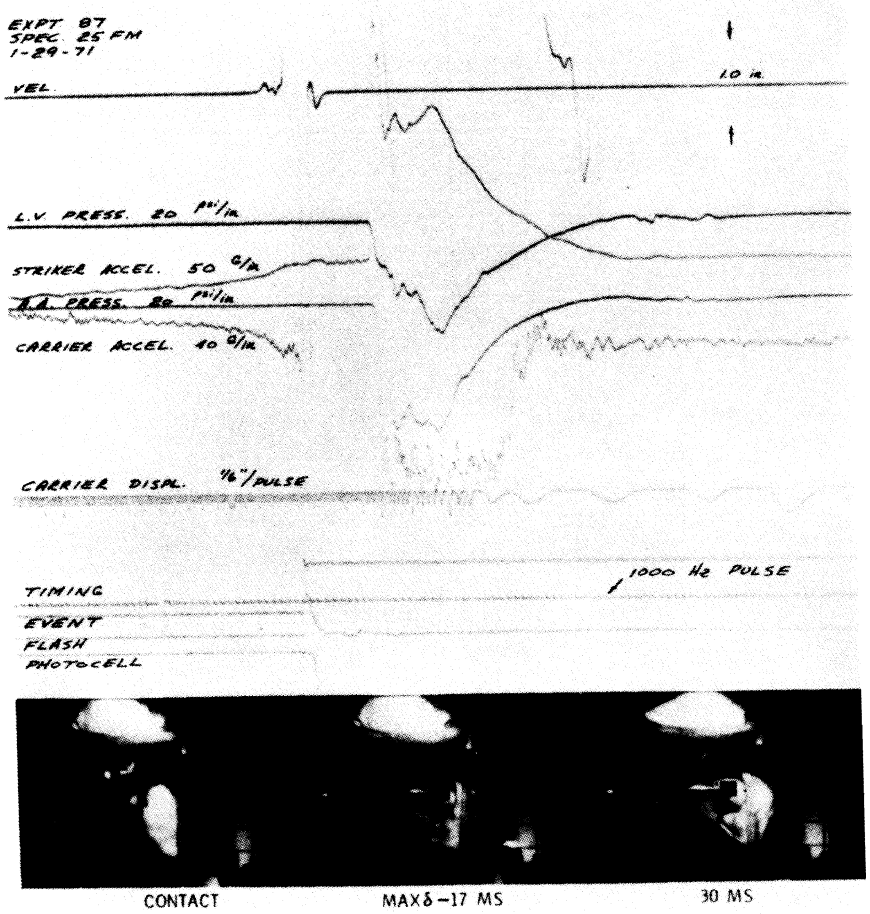

CONTACT MAXδ -17 MS 30 MS

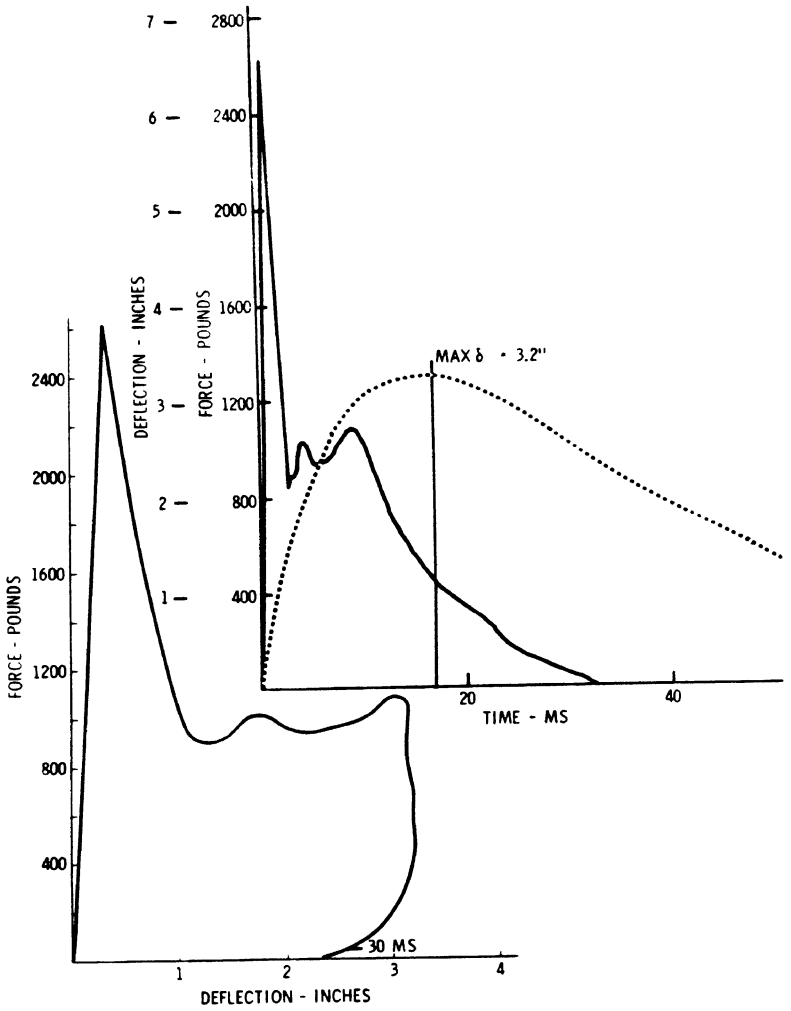

THORACO-ABDOMINAL AUTOPSY

FRACTURES:
R2(3), R3(2), R4(2), R5(2), R6, R8, L2, L3(2), L4(2), L5, L6, (18 TOTAL)

(1) PARIETAL PLEURA PUNCTURES BELOW FRACTURES OF RIBS L3 AND L4 COULD HAVE RESULTED IN A PNEUMOTHORAX IN VIVO
(2) BLOOD BLISTER OF THE SUPERIOR POSTERIOR ASPECT OF THE LEFT LOBE OF THE LIVER; 1-3/8 IN. LACERATION OF THE INFERIOR SURFACE OF THE LEFT LOBE OF THE LIVER

EXPT. 88 SPEC 26 FM

75 YRS. 5'8" 140 LB.
9-3/4" A-P 37" GIRTH
COD - CEREBRAL OCCLUSION
DOD 2/28/71 DOT 3/3/71 DOA 3/3/71

STRIKER MASS 4.1 LB. KINETIC ENERGY = 85.4 FT.-LB.
VEL 25.0 MPH MOMENTUM = 4.7 LB.-SEC.

VASCULAR BASELINE 65 mm Hg
PRESSURES MONITORED - AORTIC ARCH, LEFT VENTRICLE

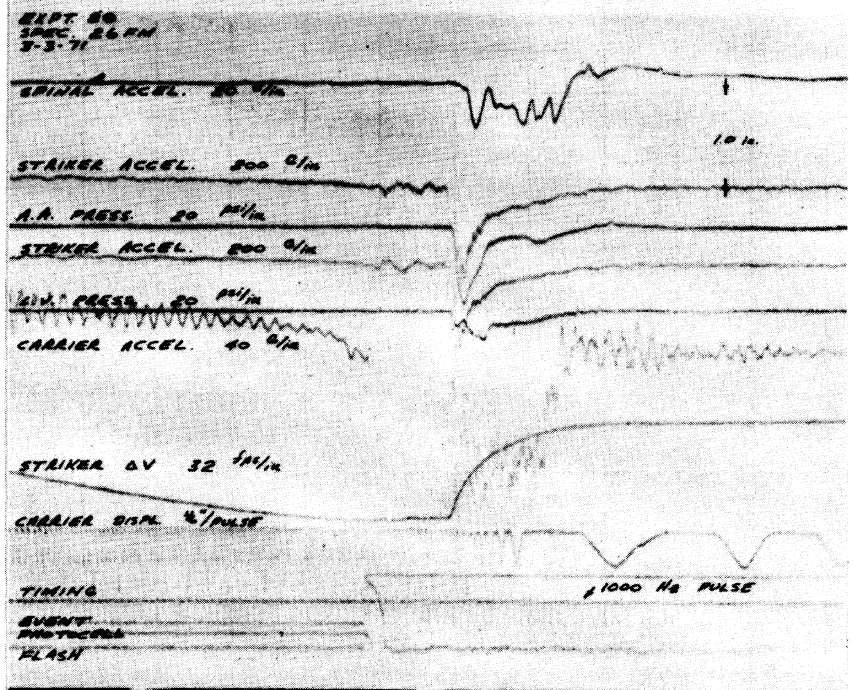

CONTACT MAX δ - 12 MS 30 MS

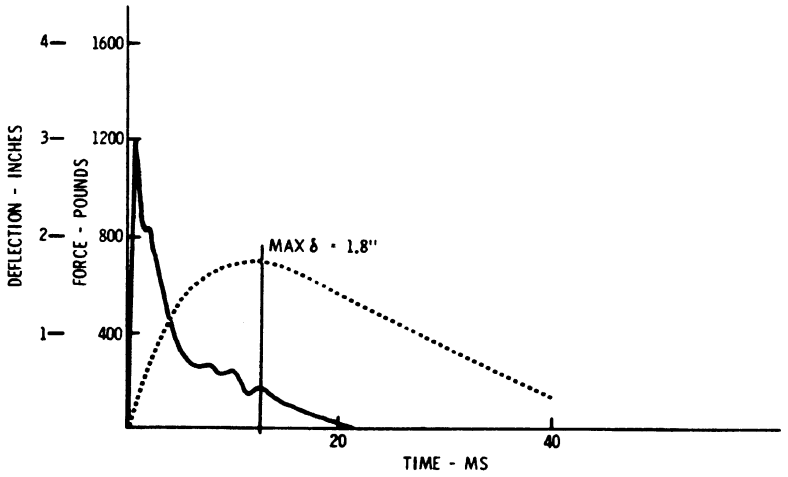

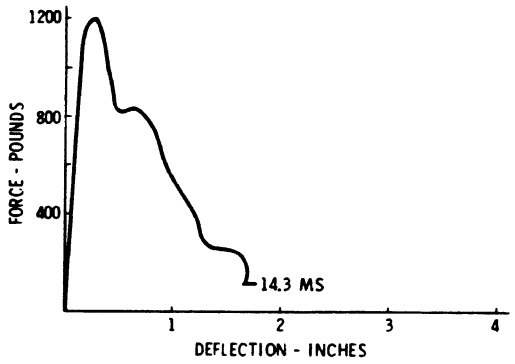

THORACO-ABDOMINAL AUTOPSY

NO SKELETAL OR VISCERAL DAMAGE

EXPT. 90 SPEC. 28 FM

54 YRS. 6'0" 150 LB.
9-3/8" A-P 34½" GIRTH
COD - LARGE BOWEL CARCINOMA
DOD 5/5/71 DOT 5/7/71 DOA 5/7/71

STRIKER MASS 3.6 LB. KINETIC ENERGY = 126 FT.-LB.
VEL 32.4 MPH MOMENTUM = 5.3 LB.-SEC.

VASCULAR BASELINE ~ 70 mm Hg
PRESSURES MONITORED - AORTIC ARCH, LEFT VENTRICLE
RIGHT VENTRICLE, INTRATHORACIC

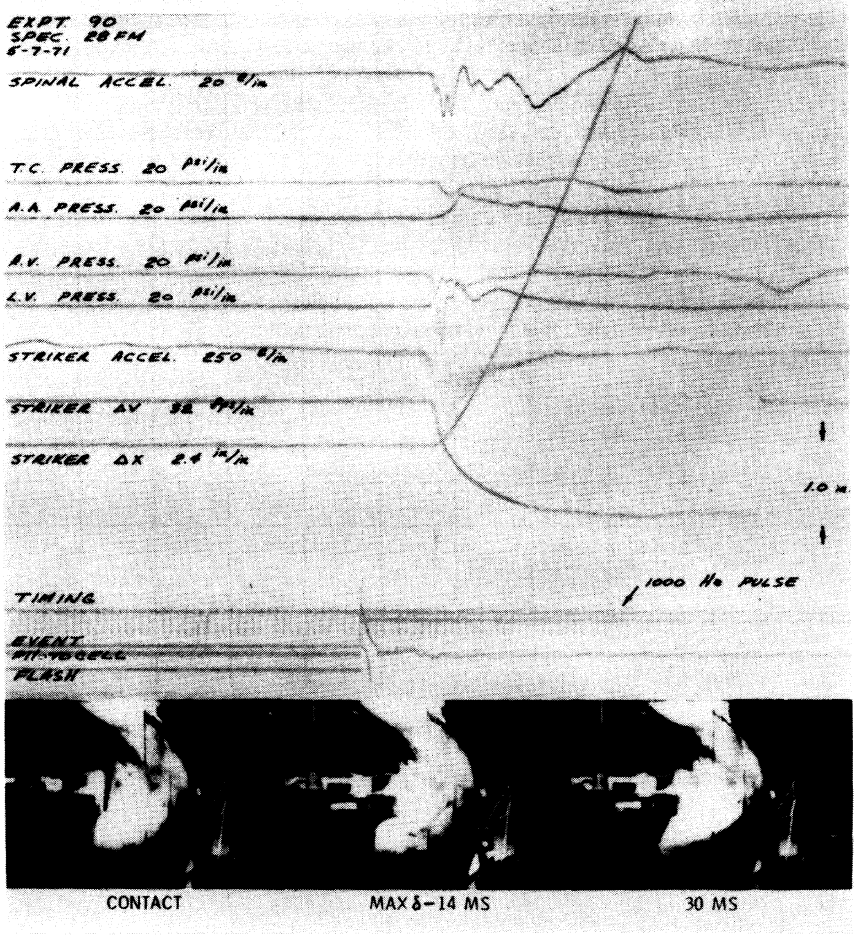

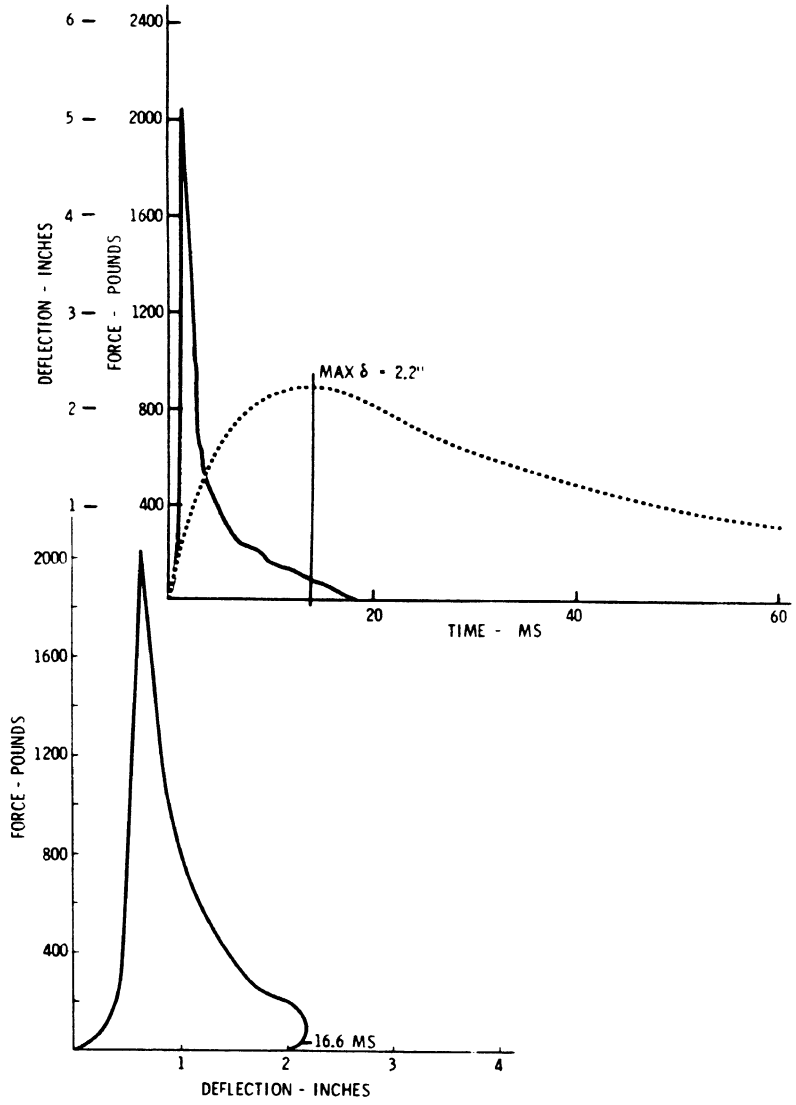

THORACO-ABDOMINAL AUTOPSY

NO SKELETAL OR VISCERAL DAMAGE

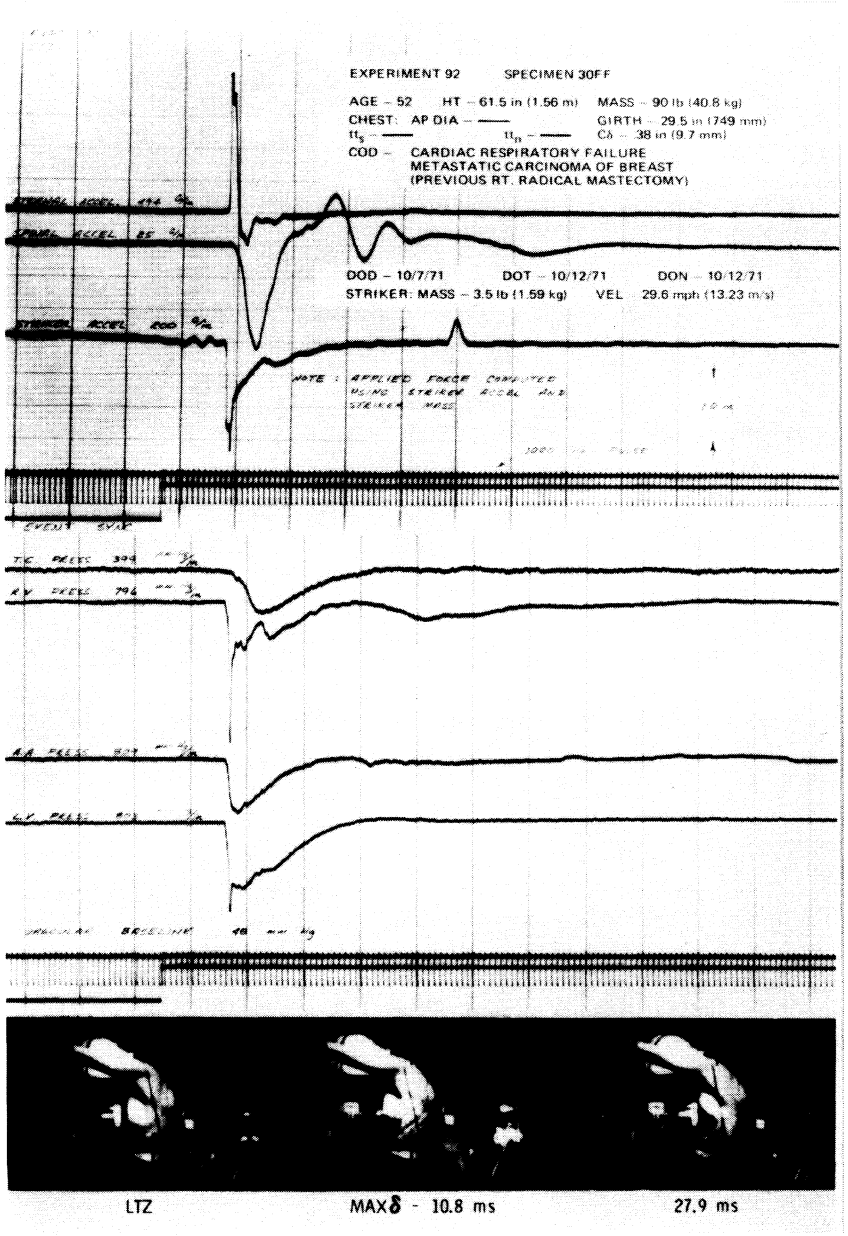

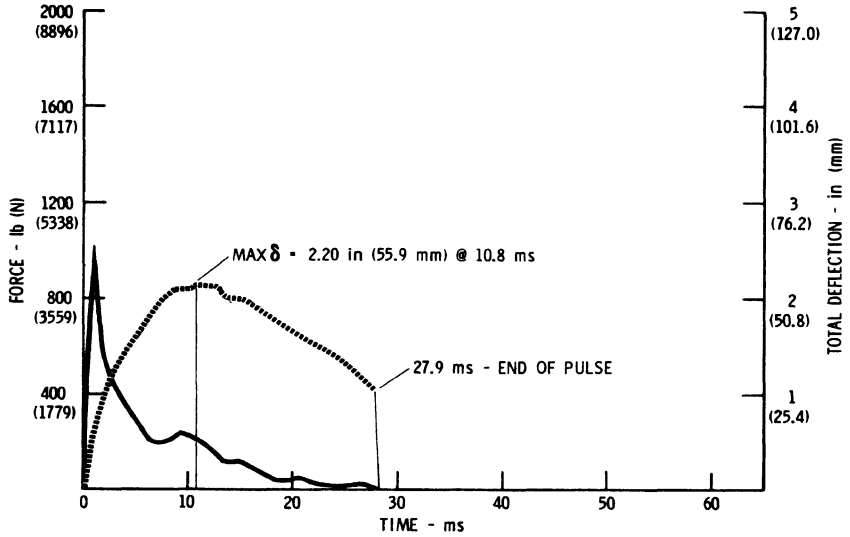

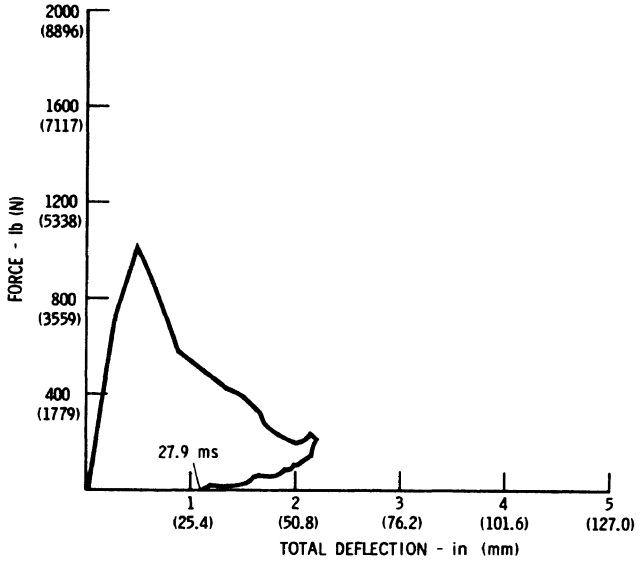

THORACO-ABDOMINAL NECROPSY

FRACTURES:
R3, L2, L3, (3 TOTAL)

NO VISCERAL DAMAGE

AIS = 2

EXPERIMENT 93 SPECIMEN 31FM

AGE – 51 HT – 72 in (1.83 m) MASS – 165 lb (74.8 kg)
CHEST: AP DIA – 9.38 in (238 mm) GIRTH – 36.5 in (927 mm)
tt_s – —— tt_n – —— Cδ – .5 in (12.7 mm)
COD – GASTROINTESTINAL BLEEDING AND HEPATIC COMA DUE TO HEPATIC CIRRHOSIS
DOD – 11/12/71 DOT – 11/16/71 DON – 11/16/71
STRIKER: MASS – 50.8 lb (23.04 kg) VEL – 22.8 mph (10.19 m/s)

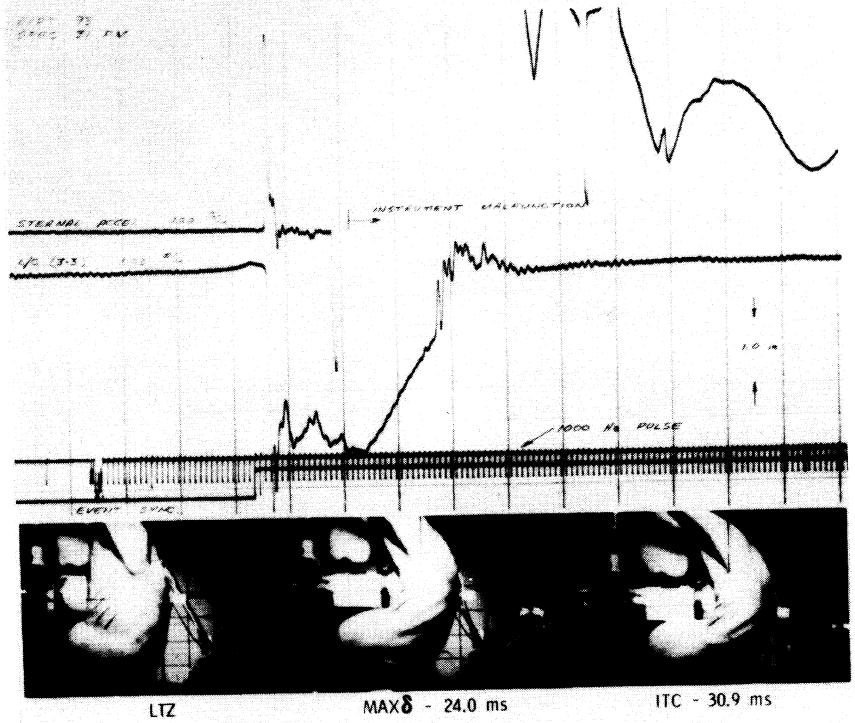

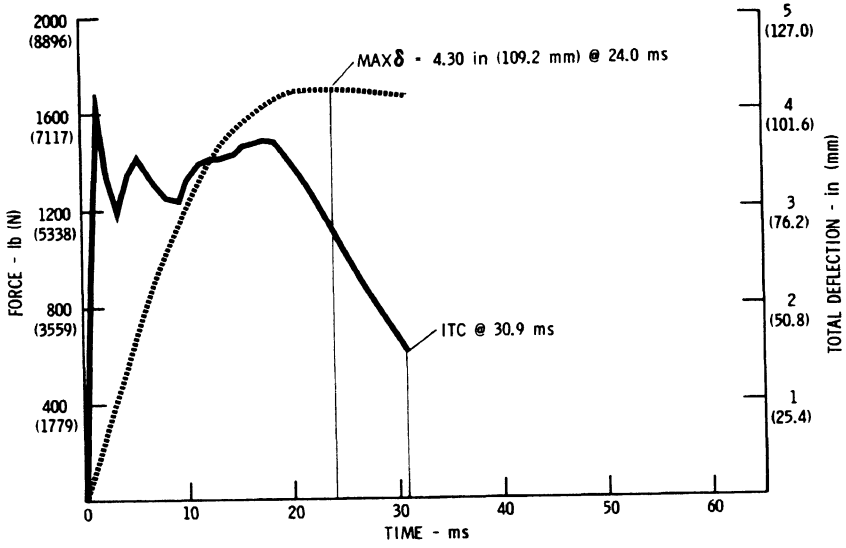

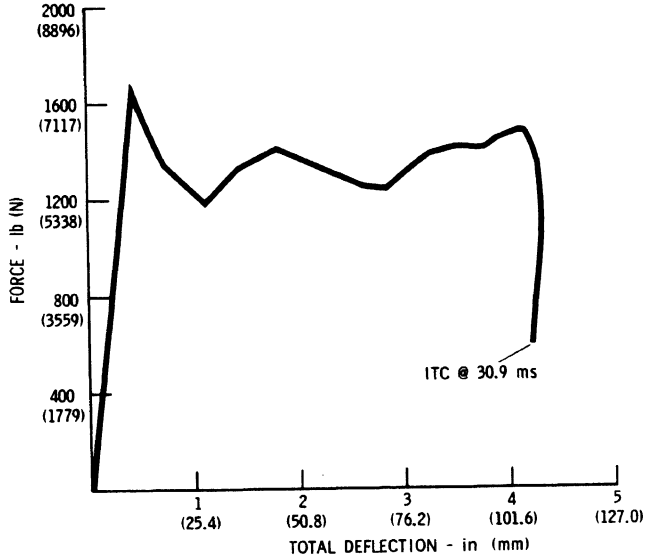

THORACO-ABDOMINAL NECROPSY

FRACTURES:
R2, R3, R4(2), R5, R6, R7, L2, L3, L4(2), L6(2), L7, (14 TOTAL)
STERNAL AT 3RD INTERCOSTAL SPACE

(1) LACERATION OF LEFT VENTRICLE
(2) LACERATION OF INTERVENTRICULAR SEPTUM
(3) SEVERED MITRAL VALVE PAPILLARY MUSCLES
(4) PARIETAL PLEURA PUNCTURED BELOW R5 RIB FRACTURE

AIS = 6

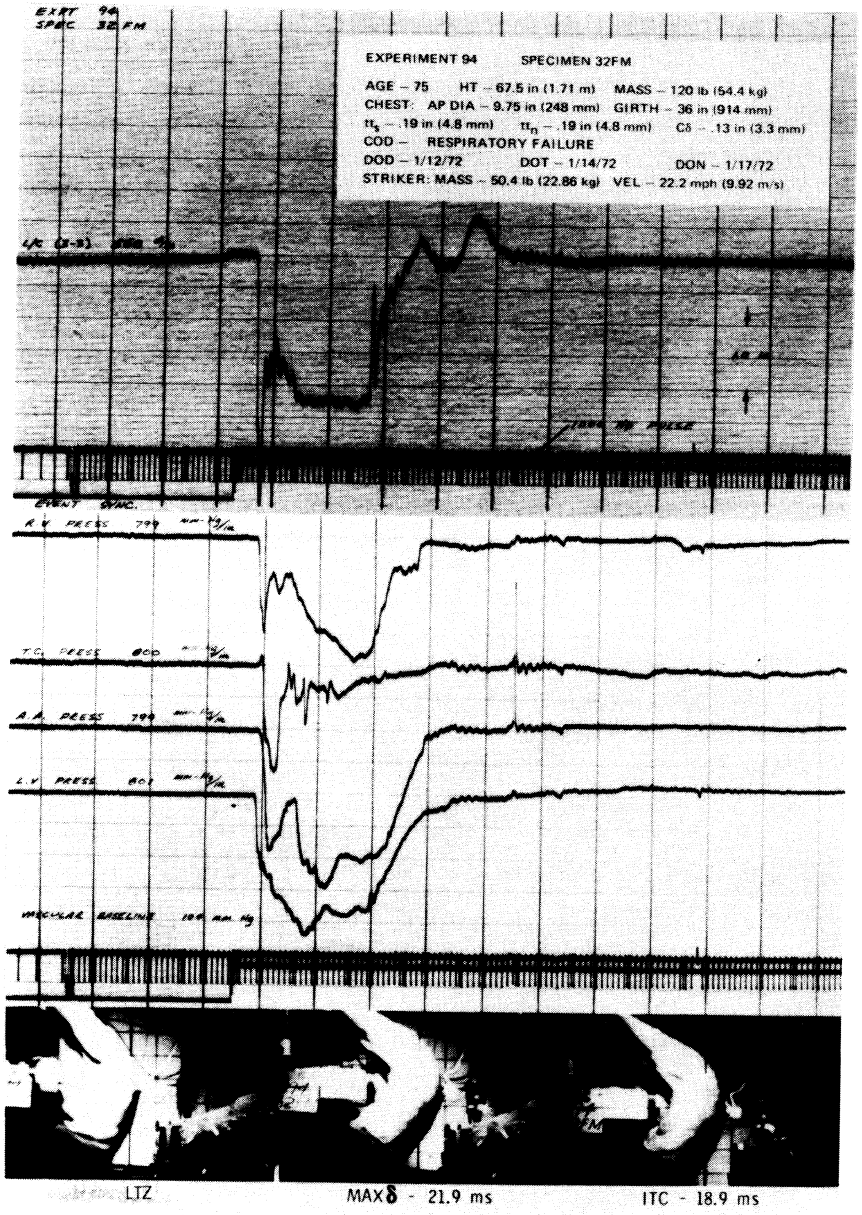

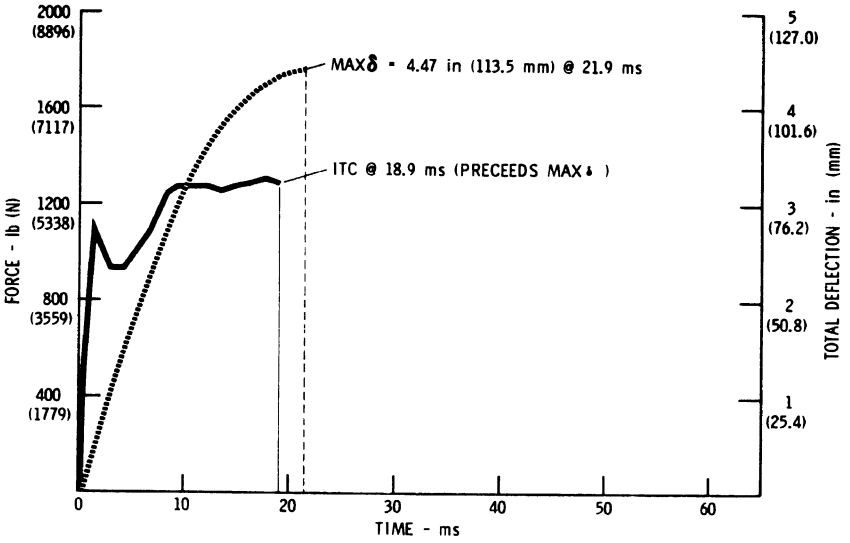

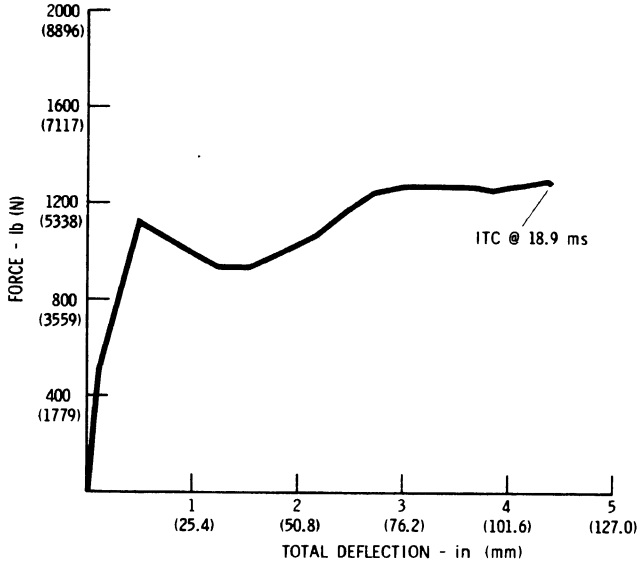

THORACO-ABDOMINAL NECROPSY

FRACTURES:
R2, R3, R4, R5, R6(2), R7(2), R8(2), L2(2), L3(2), L4(2), L5(2), L6, L7, (20 TOTAL)
STERNAL AT 3RD INTERSPACE

(1) PERICARDIAL LACERATION
(2) LACERATION OF LEFT AND RIGHT ATRIA, ATRIAL APPENDAGE, AND INTERVENTRICULAR SEPTUM
(3) TRANSECTION OF LEFT MAINSTEM BRONCHUS

AIS = 6

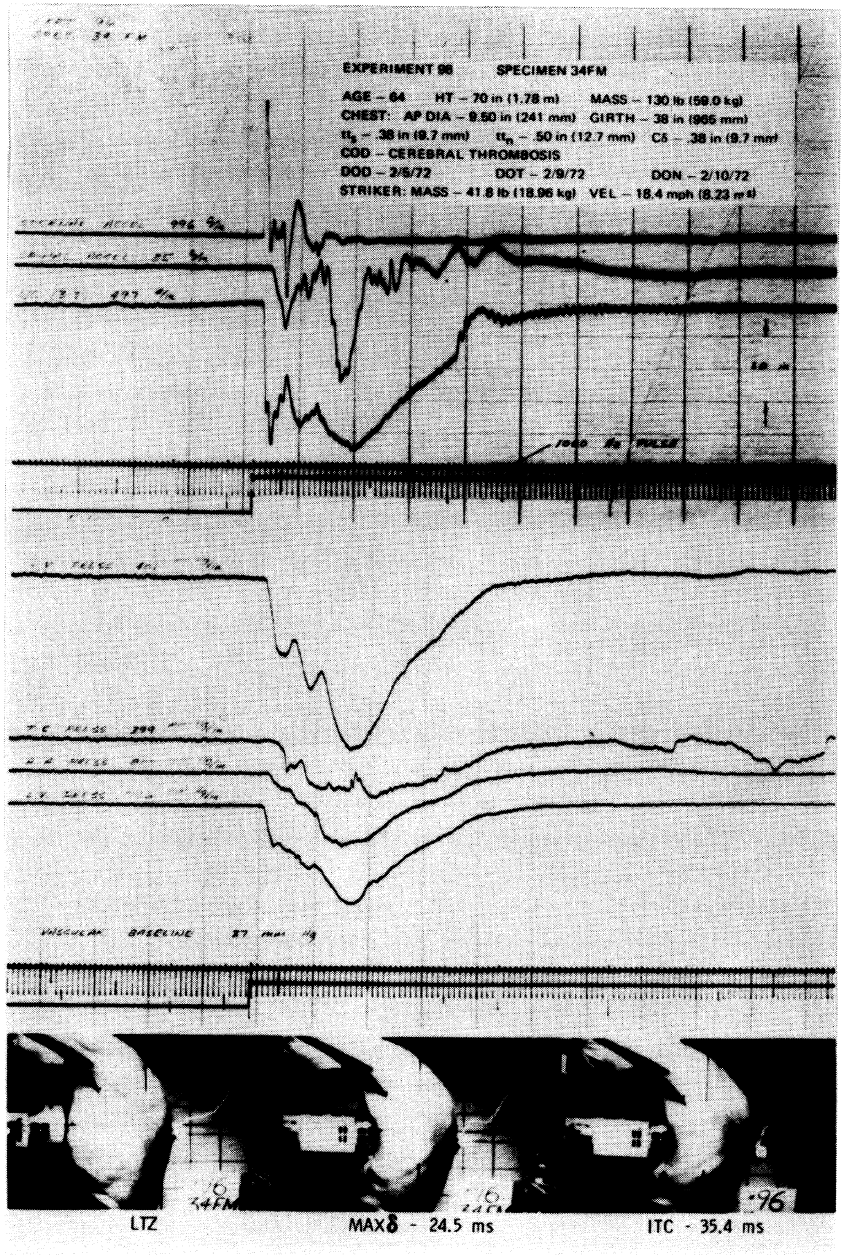

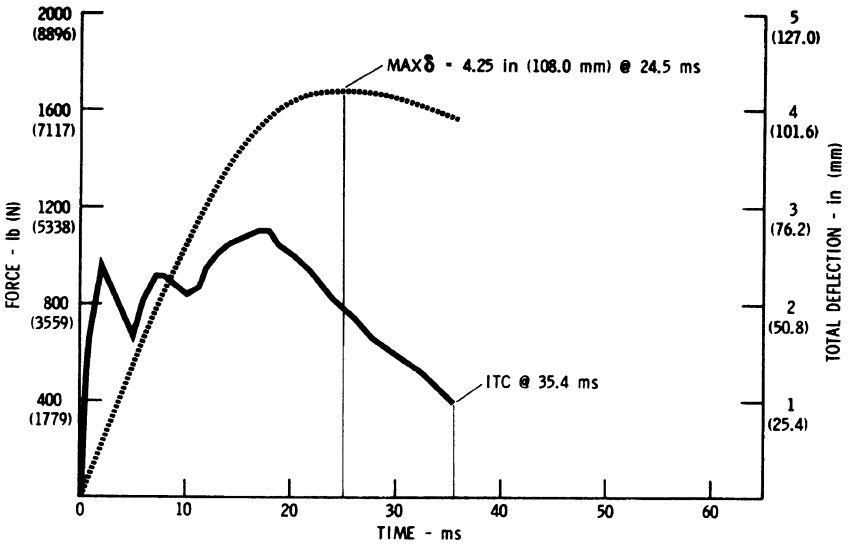

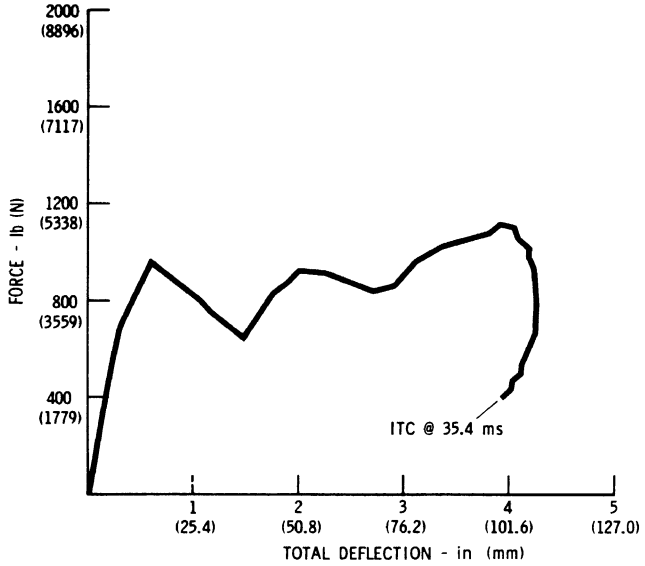

THORACO-ABDOMINAL NECROPSY

FRACTURES:
R2, R3, R4, R5, R6, L2, L3(2), L4, L5, L6(2), L7, (13 TOTAL)

LACERATION OF PARIETAL PLEURA AT 6TH INTERCOSTAL SPACE

AIS = 4

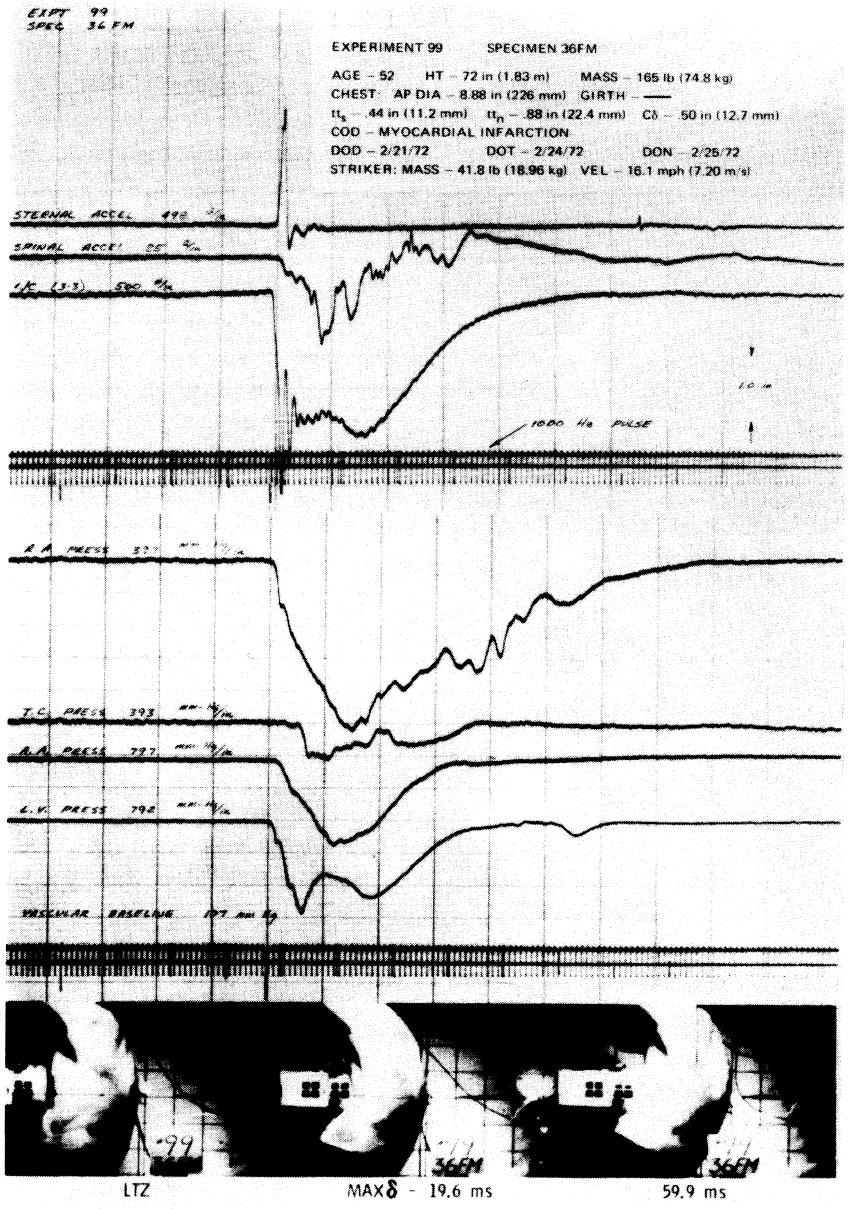

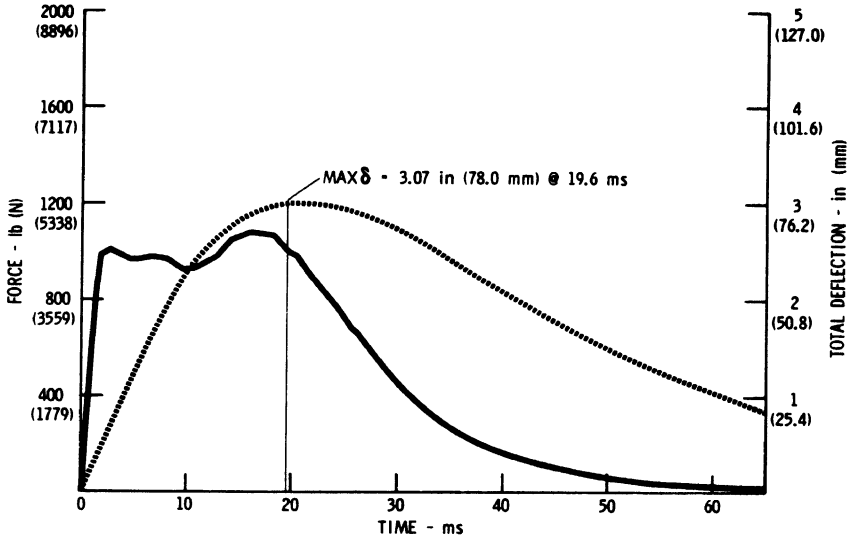

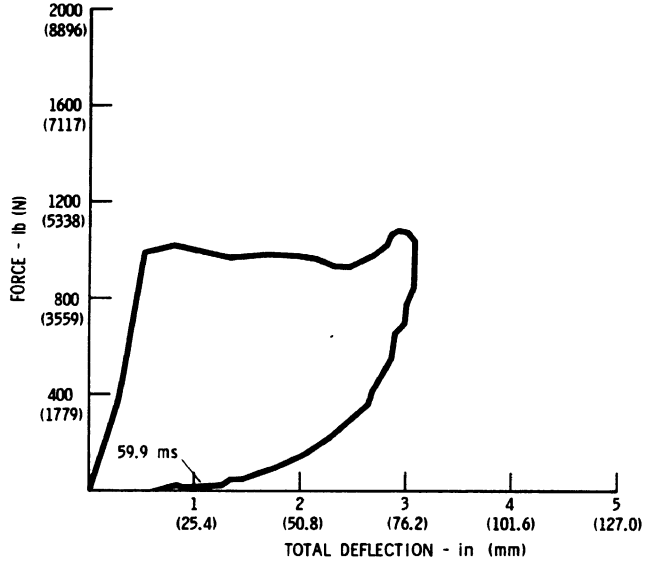

THORACO-ABDOMINAL NECROPSY

FRACTURES:
R2, R4, R5, L4, L5, L6, L7, (7 TOTAL)

2-5/8 in (67 mm) LACERATION OF DOME OF RIGHT LOBE OF LIVER

AIS = 4

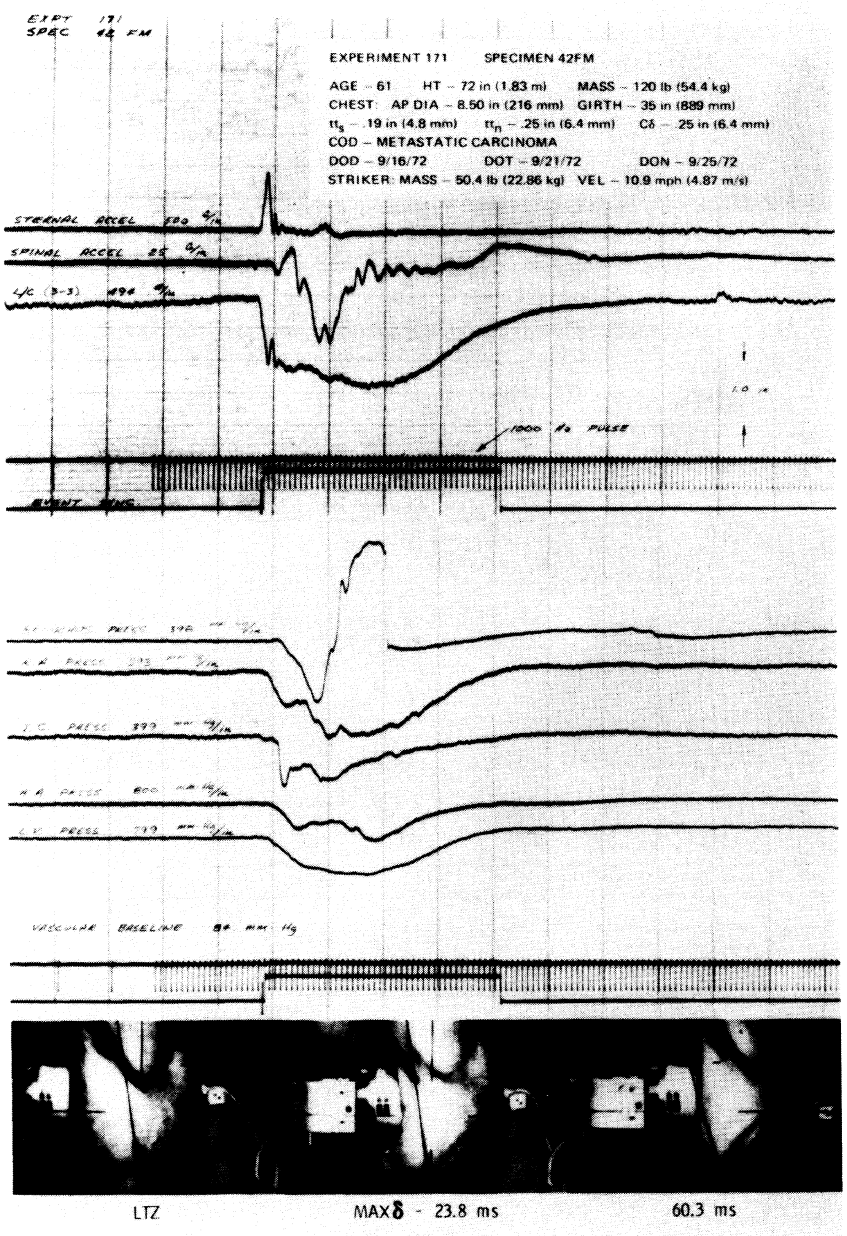

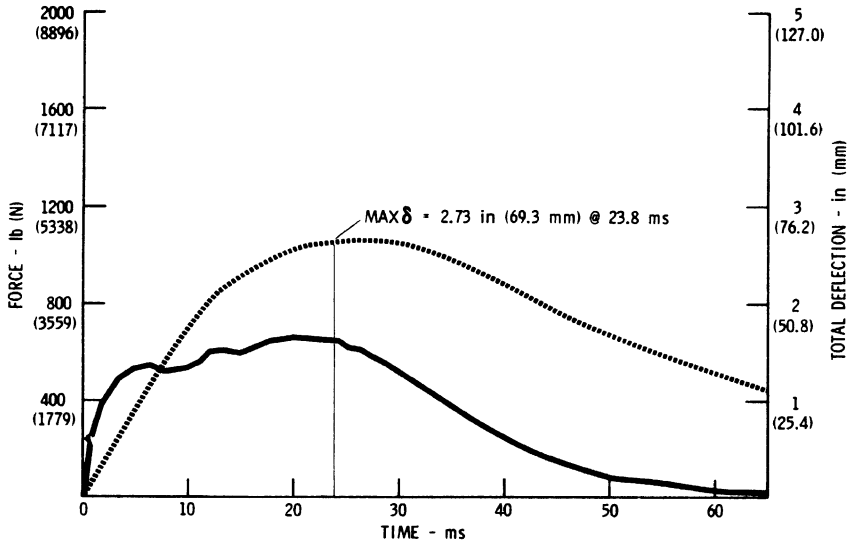

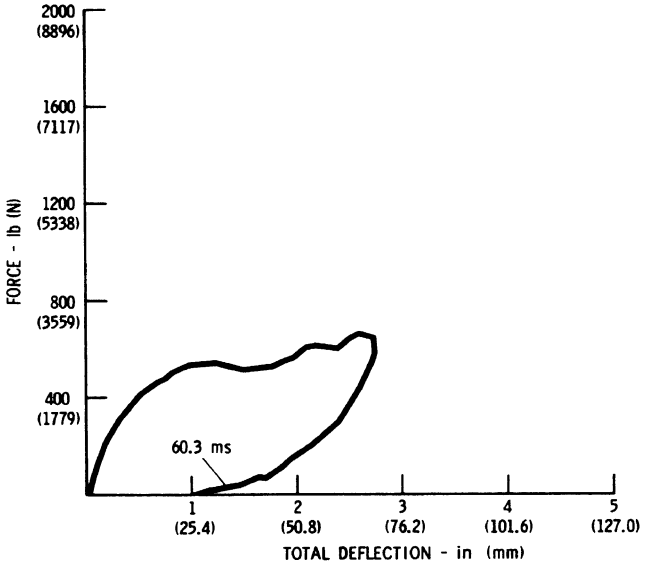

THORACO-ABDOMINAL NECROPSY

NO SKELETAL OR VISCERAL DAMAGE

AIS = 0

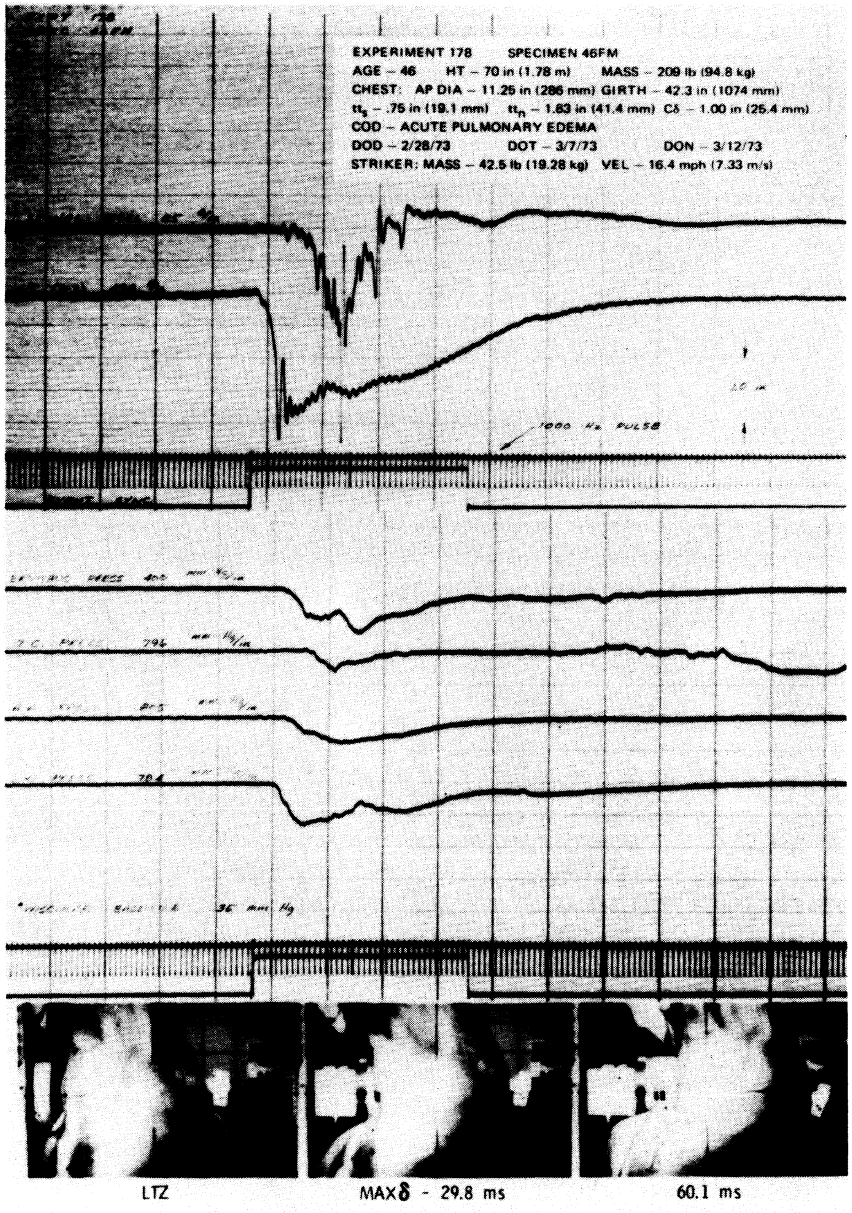

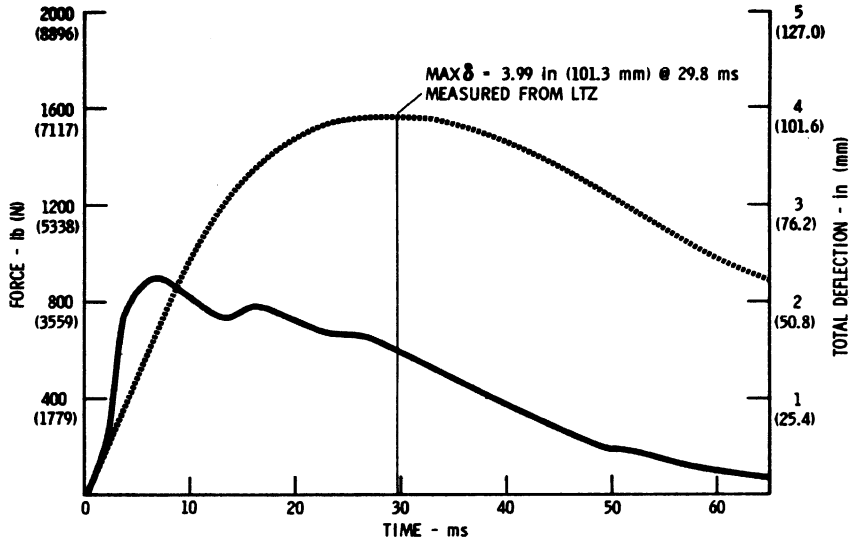

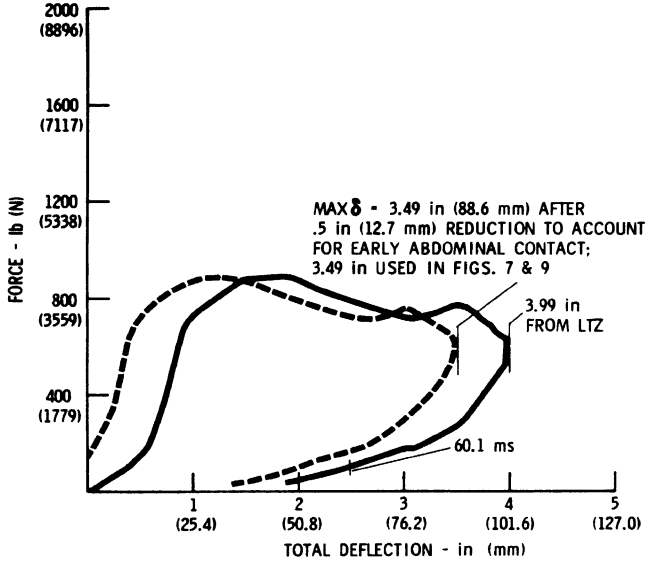

THORACO-ABDOMINAL NECROPSY

NO SKELETAL OR VISCERAL DAMAGE

AIS = 0

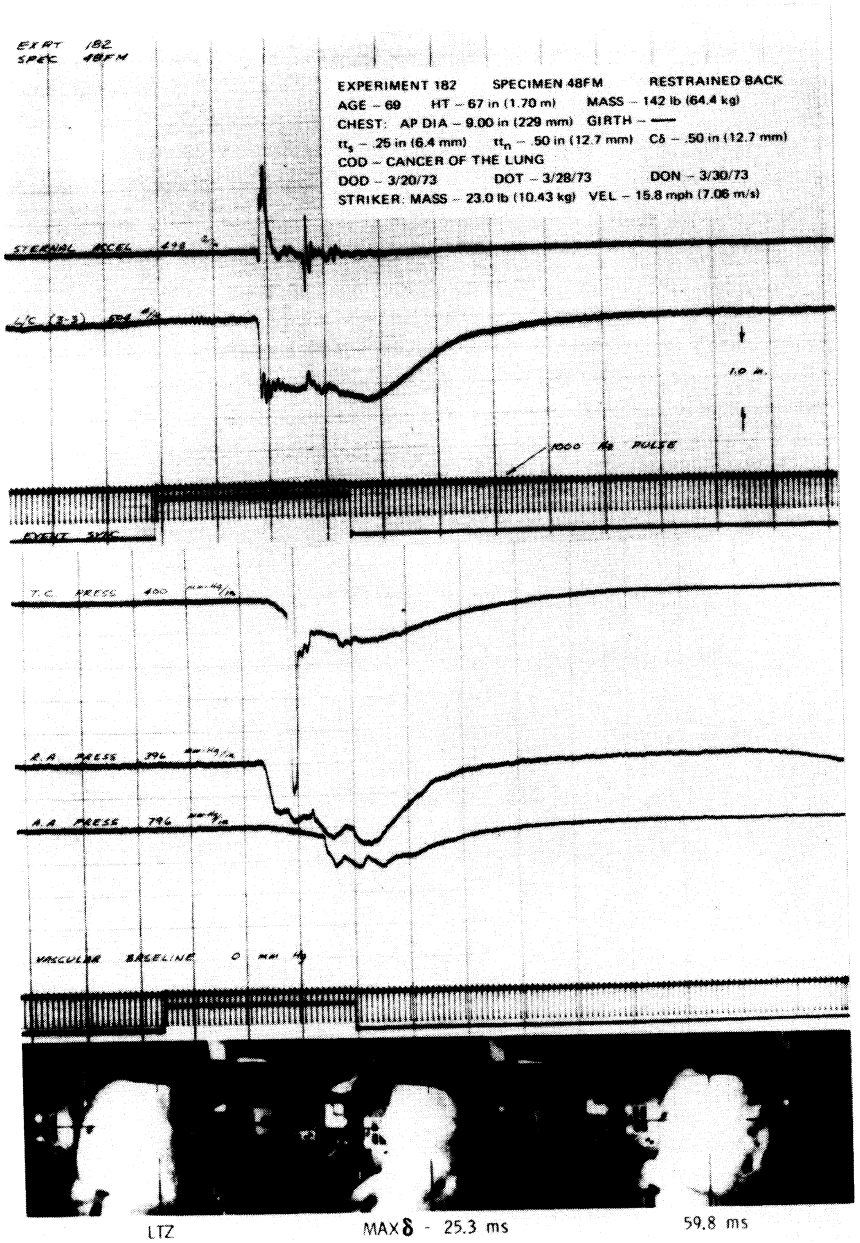

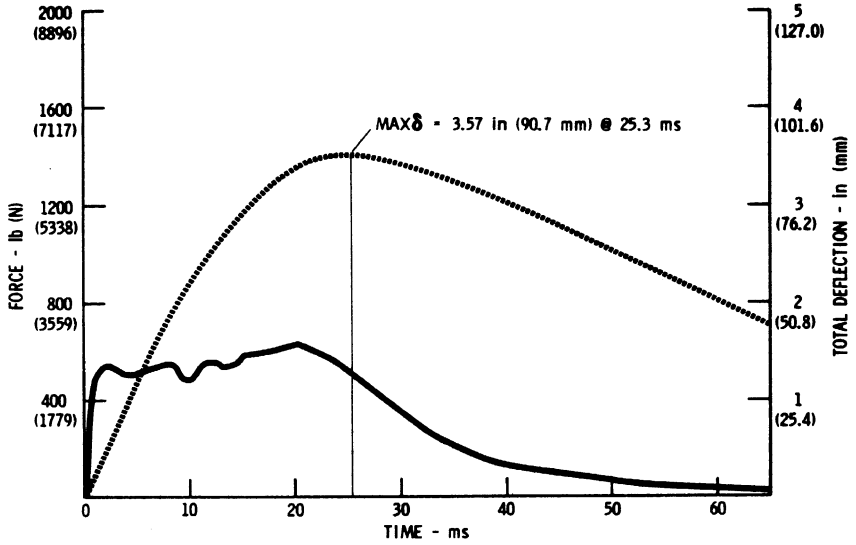

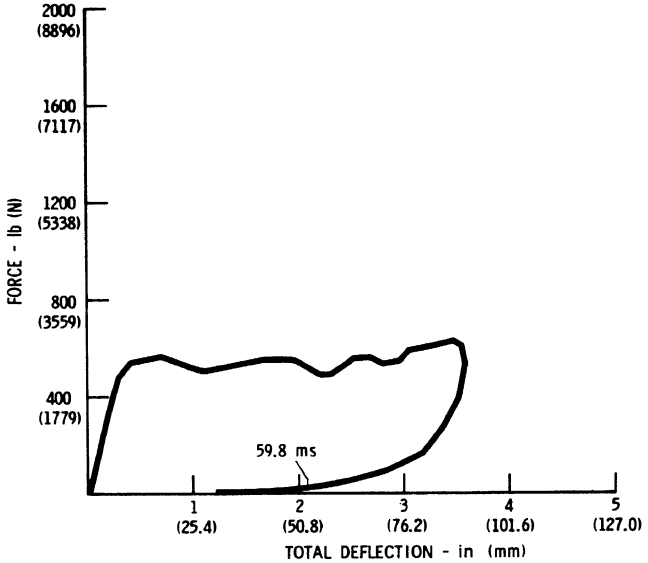

THORACO-ABDOMINAL NECROPSY

NO SKELETAL OR VISCERAL DAMAGE

AIS = 0

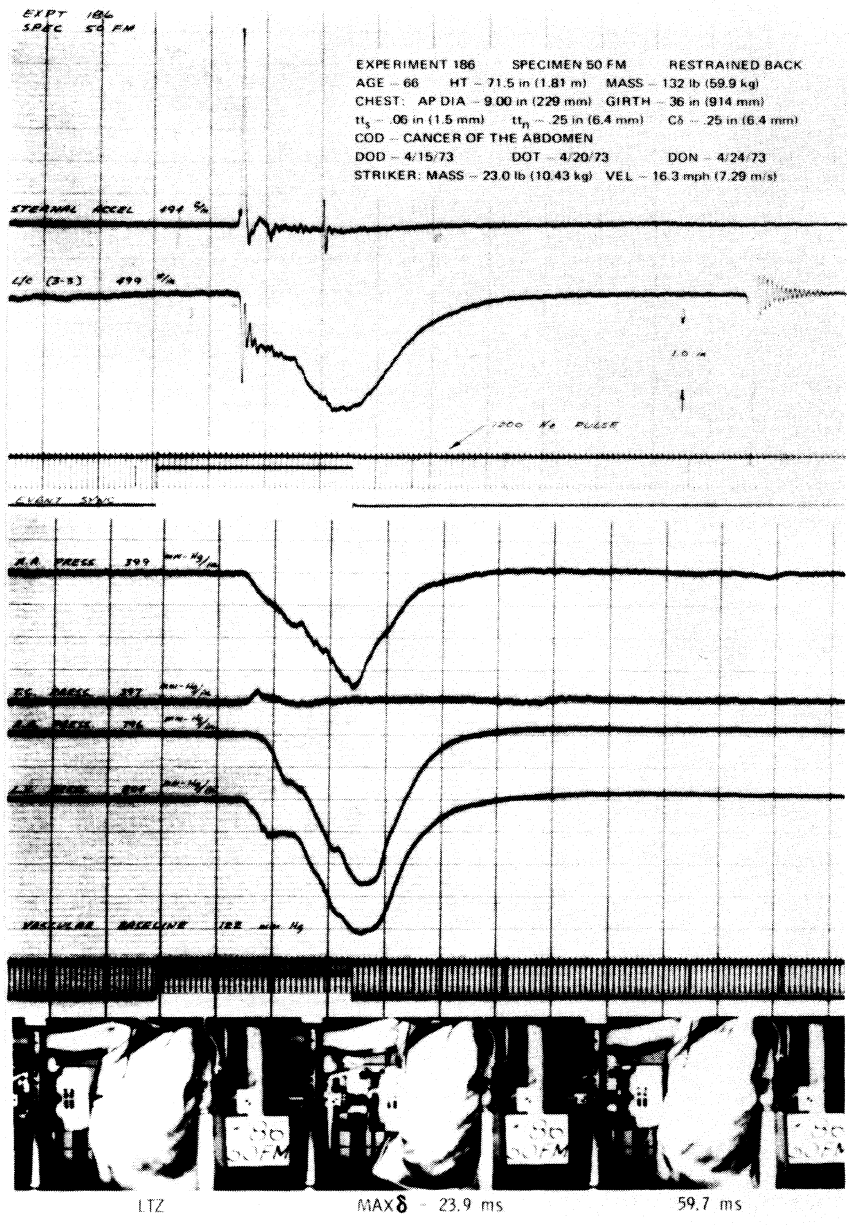

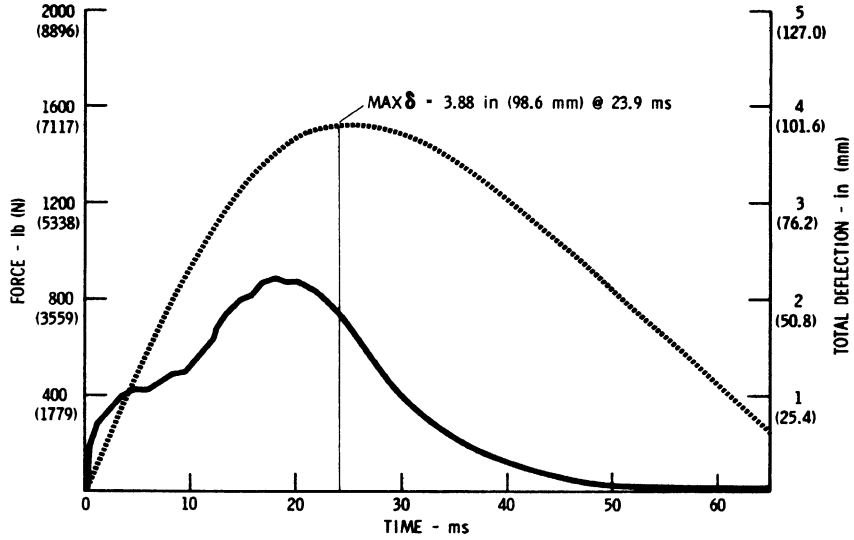

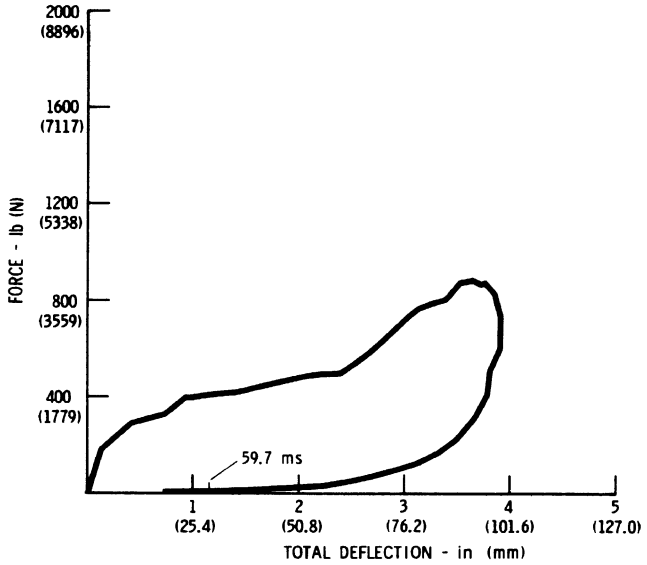

THORACO-ABDOMINAL NECROPSY

FRACTURES:
R2, R3, R4(2), R5(2), R6, R7, L2, L4, L5, L6, (12 TOTAL)
STERNAL AT 2nd INTERCOSTAL SPACE

PARTIAL TRANSECTIONS OF THORACIC AORTA 1/2 in (13 mm) AND 2-3/8 in (60 mm) BELOW JUNCTURE OF LEFT SUBCLAVIAN ARTERY (INVOLVED 85% AND 20% OF VESSEL CIRCUMFERENCE, RESPECTIVELY)

AIS = 6

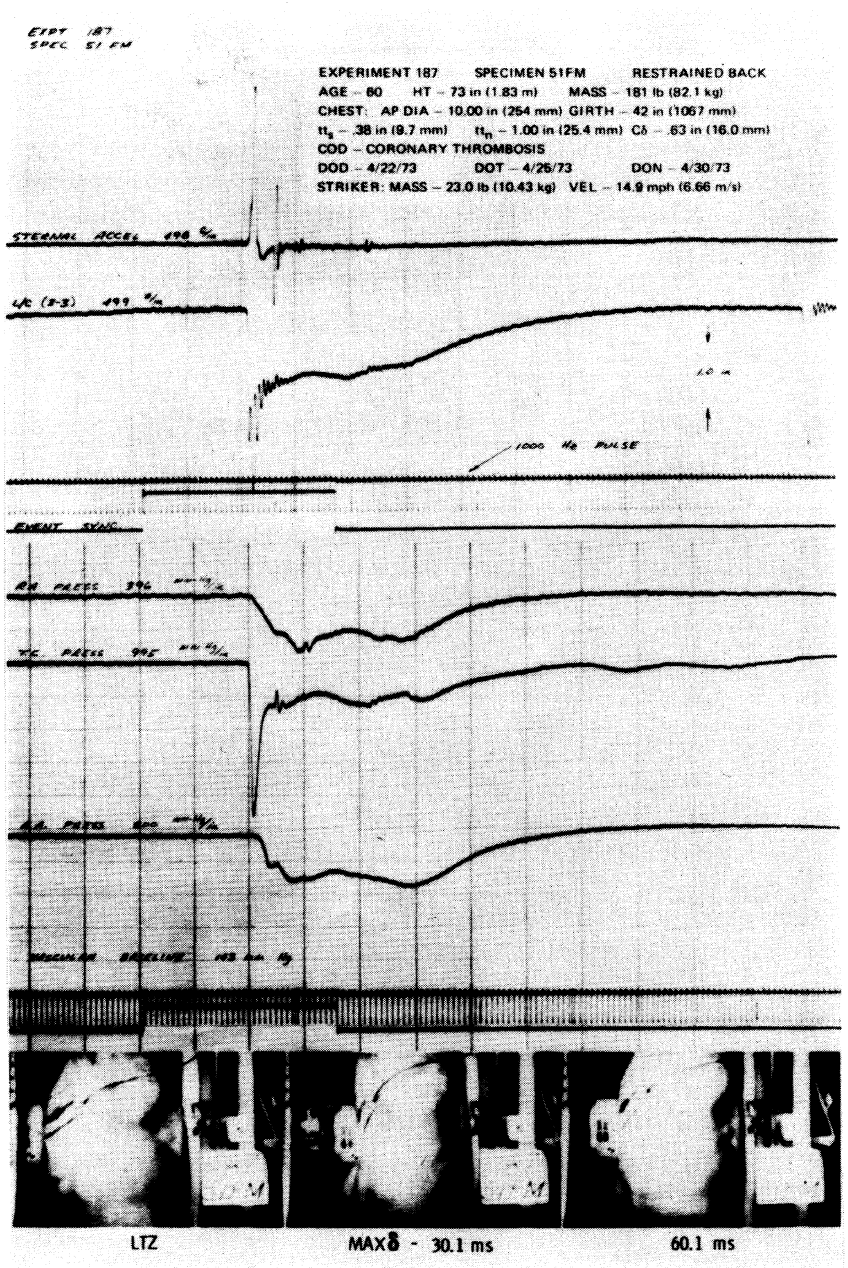

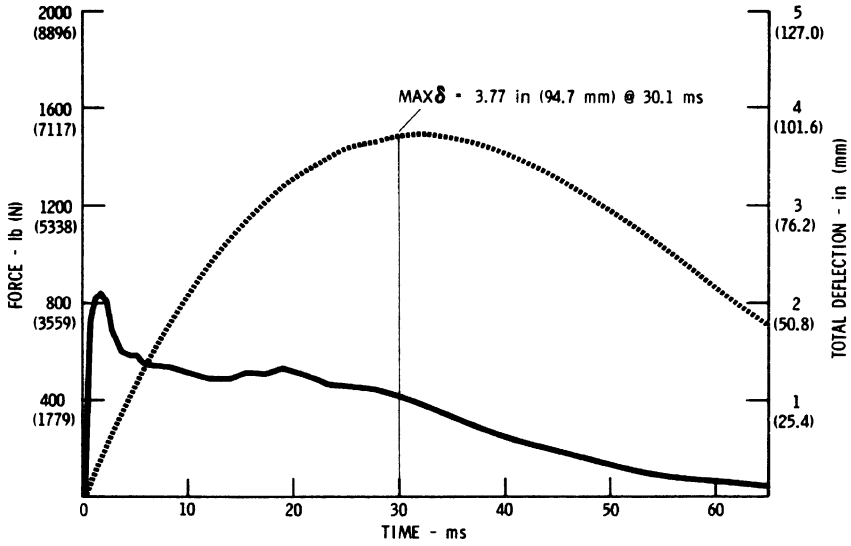

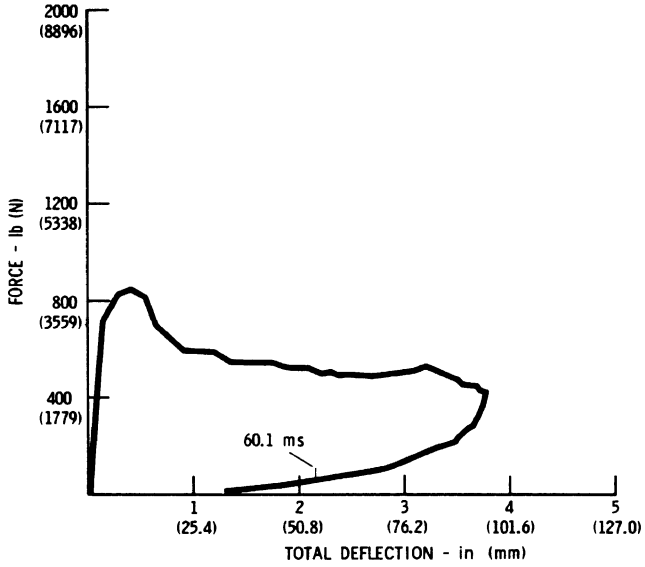

THORACO-ABDOMINAL NECROPSY

NO SKELETAL OR VISCERAL DAMAGE

AIS = 0

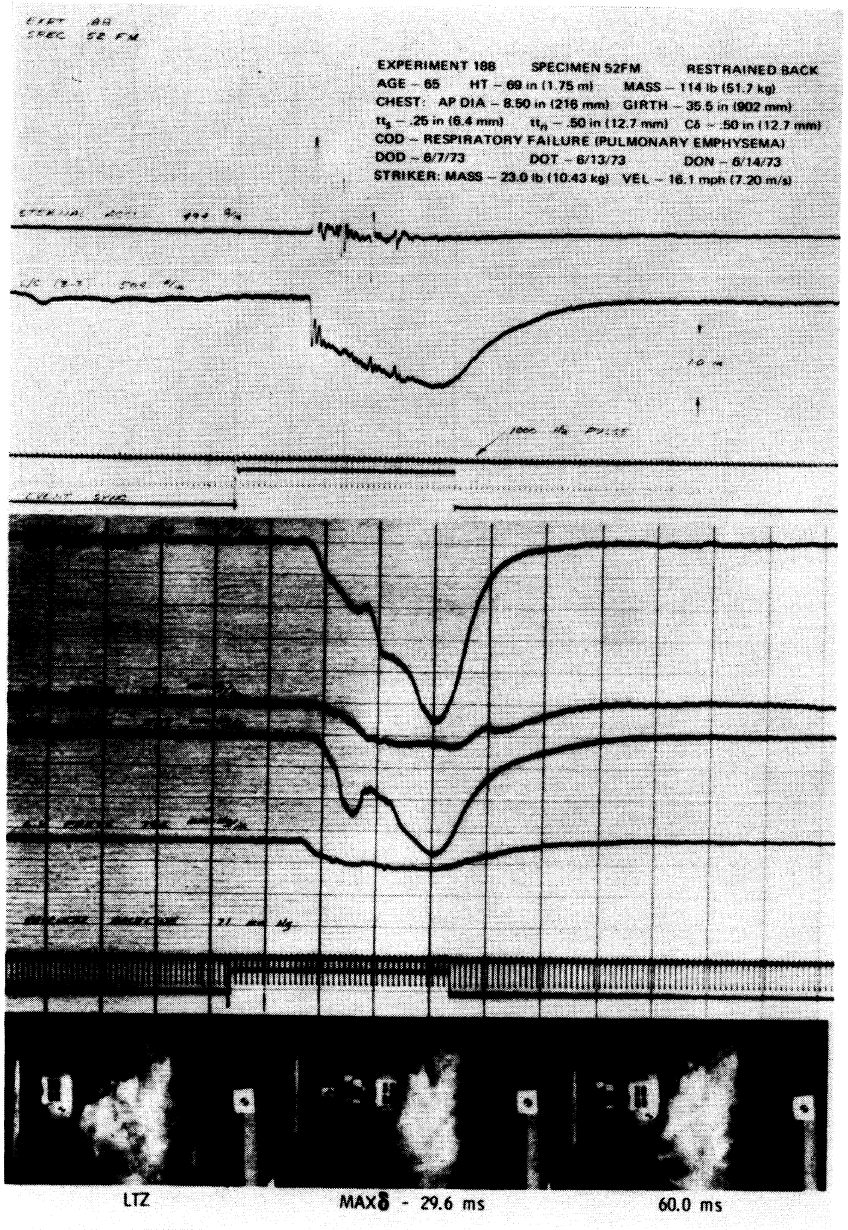

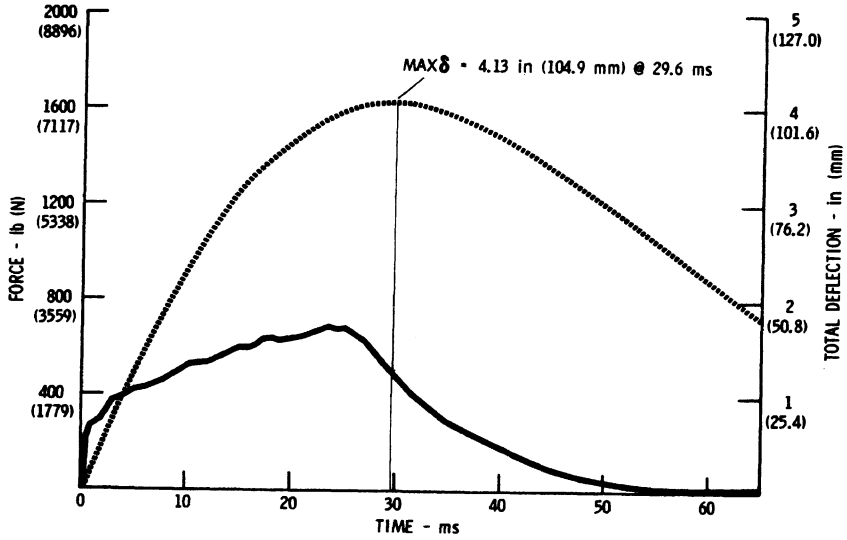

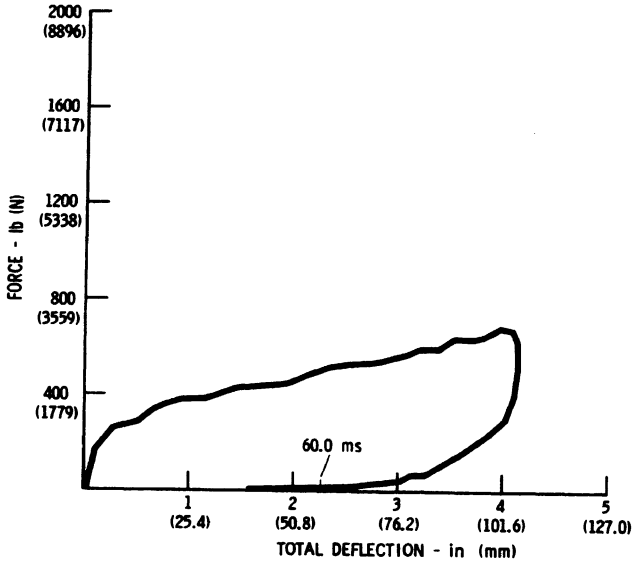

THORACO-ABDOMINAL NECROPSY

FRACTURES:
R2, R3, R4, R5, L3, L4, L5(2), L6(2), L7, (11 TOTAL)
STERNAL AT 2nd INTERCOSTAL SPACE

NO VISCERAL DAMAGE

AIS = 4

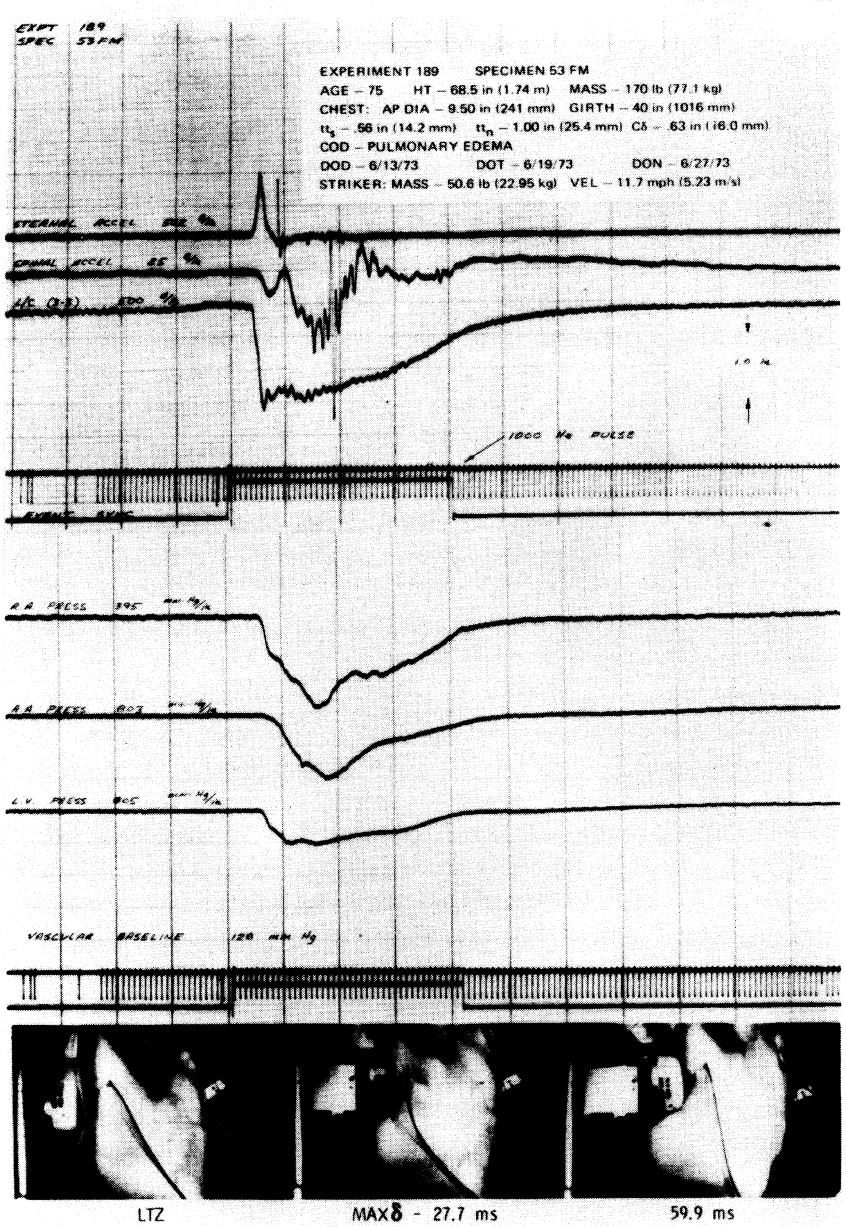

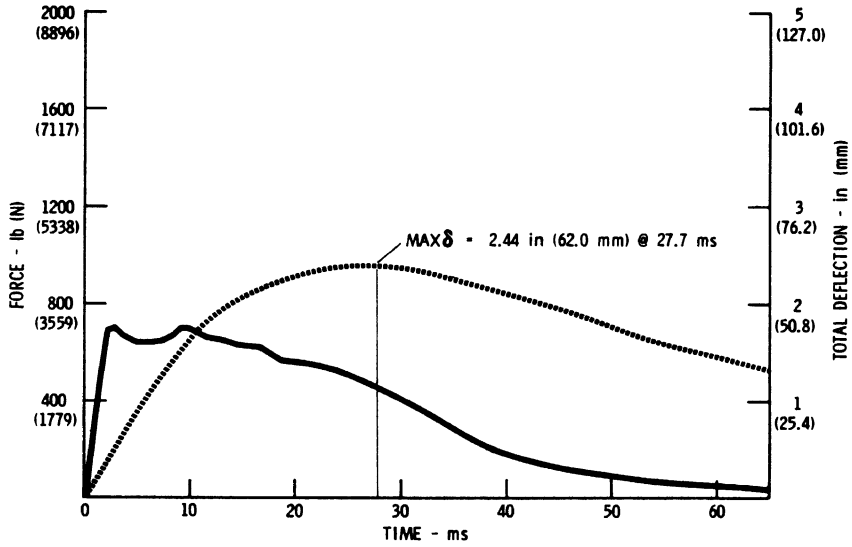

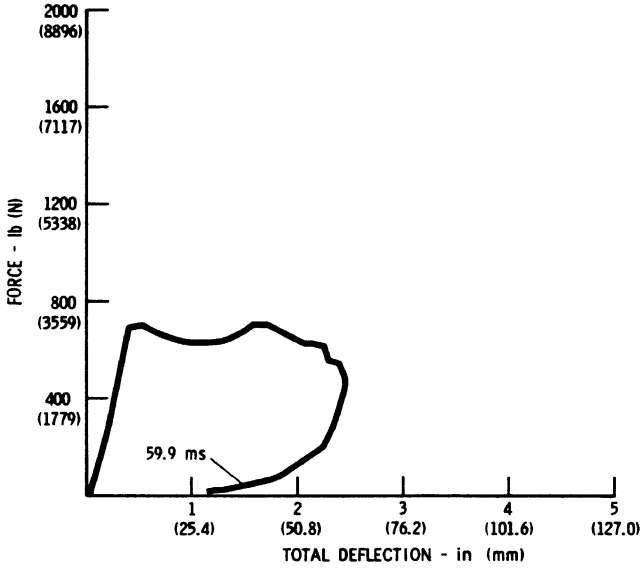

THORACO-ABDOMINAL NECROPSY

FRACTURES:
L3, L4, L5, (3 TOTAL)

NO VISCERAL DAMAGE

AIS = 2

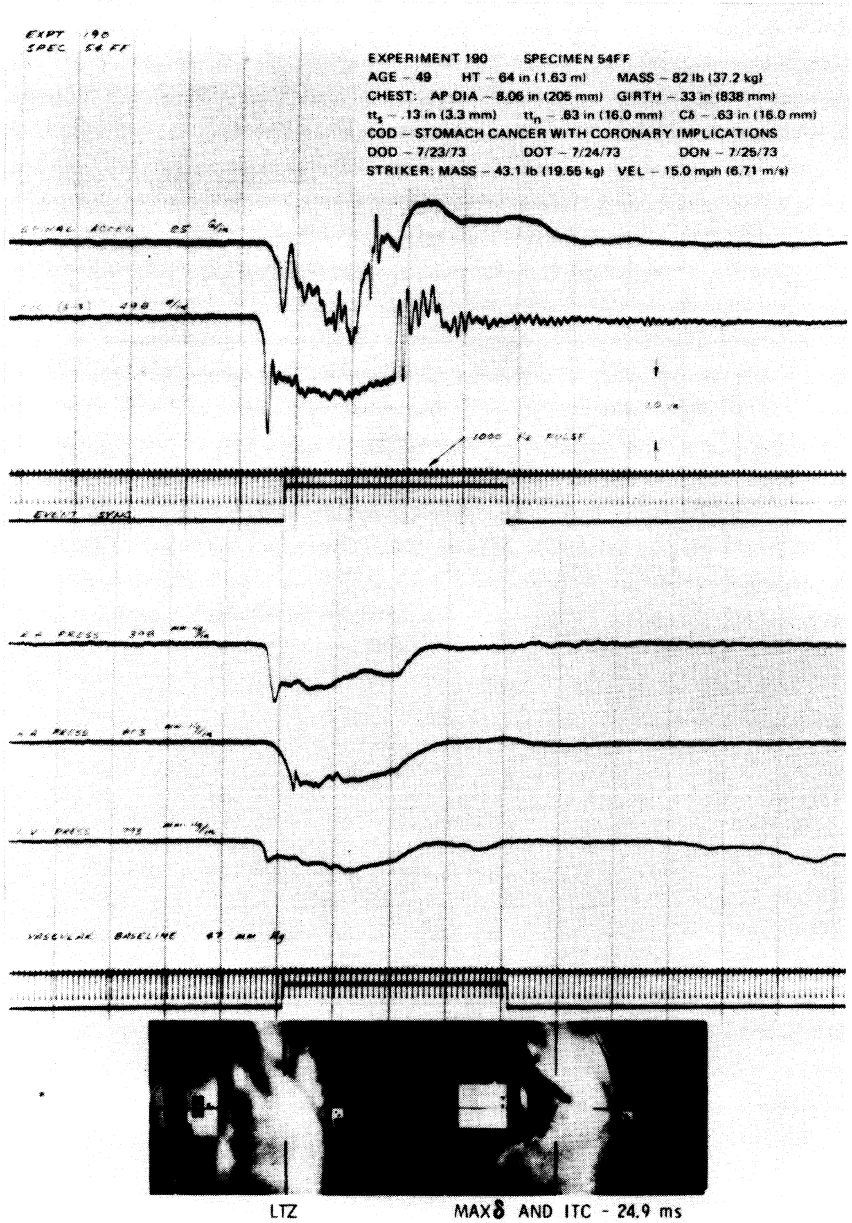

LTZ MAXδ AND ITC - 24.9 ms

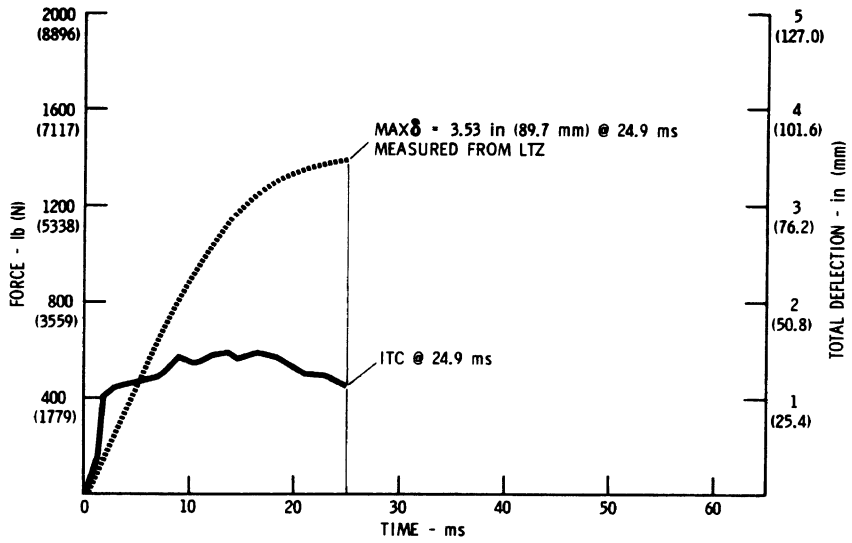

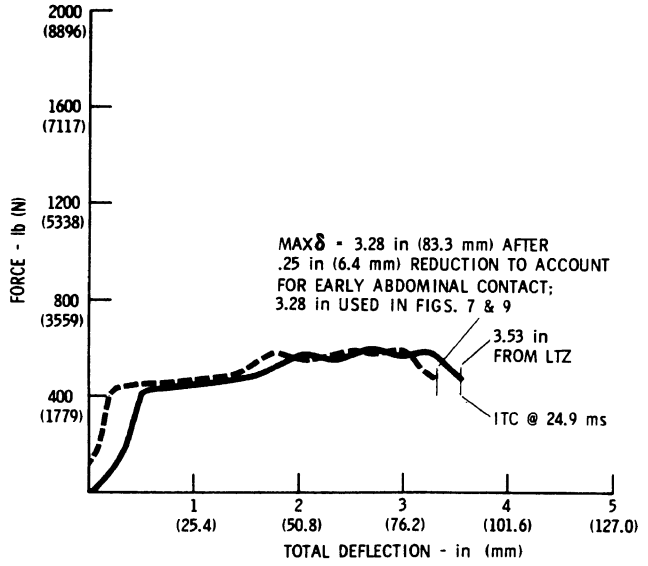

THORACO-ABDOMINAL NECROPSY

FRACTURES:
R3, R4, R5, L3, L4, L5, L6, (7 TOTAL)

(1) 1/8 in (3 mm) TEAR OF AORTIC INTIMA, 5/8 in (16 mm) BELOW JUNCTURE OF LEFT SUBCLAVIAN ARTERY
(2) "Y" SHAPED FRACTURE OF POSTERIOR SURFACE OF LEFT LOBE OF LIVER HAVING SEGMENT LENGTHS OF 1-5/8 in (41 mm) AND 3/4 in (19 mm); 1-3/4 in (44 mm) LINEAR FRACTURE ON POSTERIOR SURFACE OF LEFT LOBE OF LIVER

AIS = 5

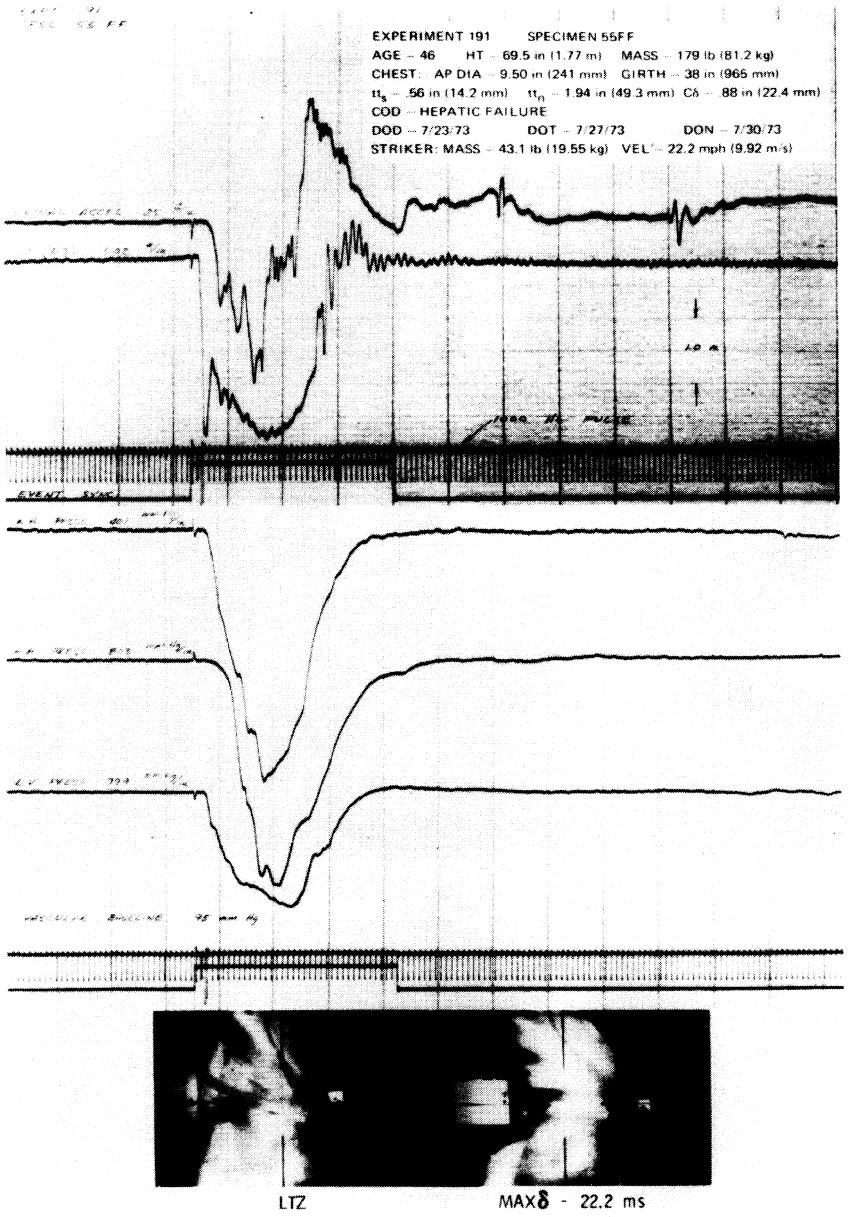

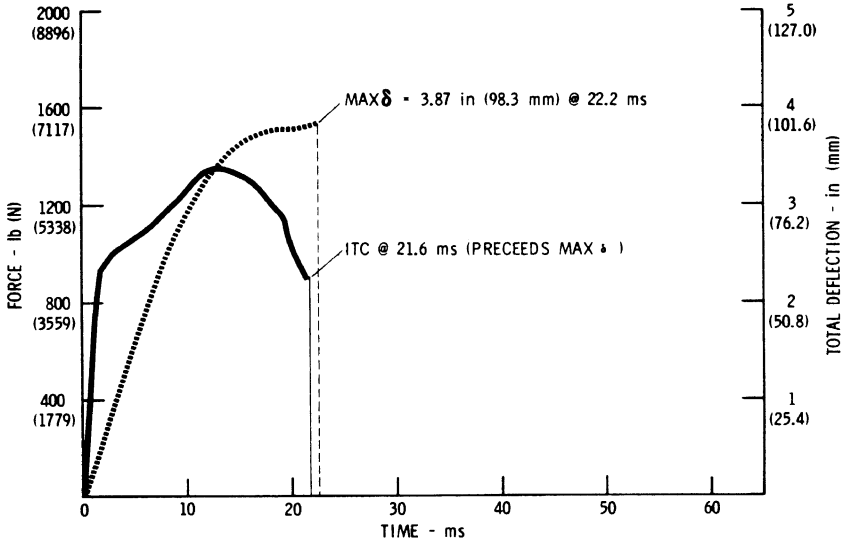

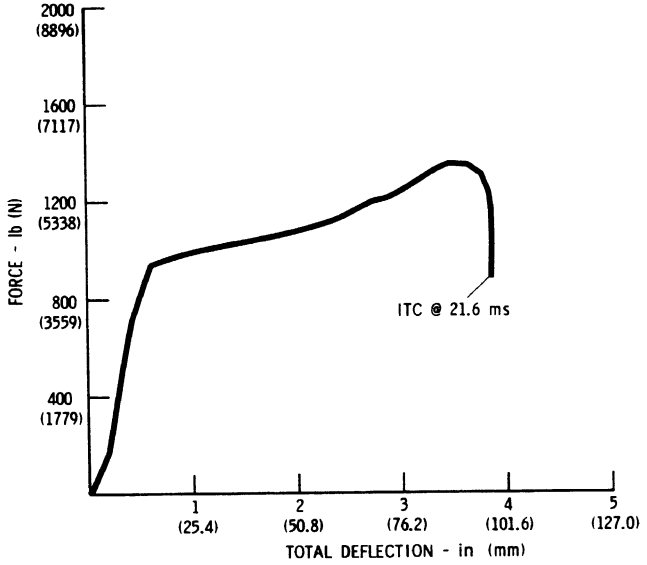

THORACO-ABDOMINAL NECROPSY

FRACTURES:
R1, R2, R3, R4, R5, R7, L2, L3, (8 TOTAL)

(1) PERICARDIAL LACERATION
(2) LACERATIONS OF LEFT VENTRICLE
(3) SEVERED AORTIC VALVE PAPILLARY MUSCLES

AIS = 6

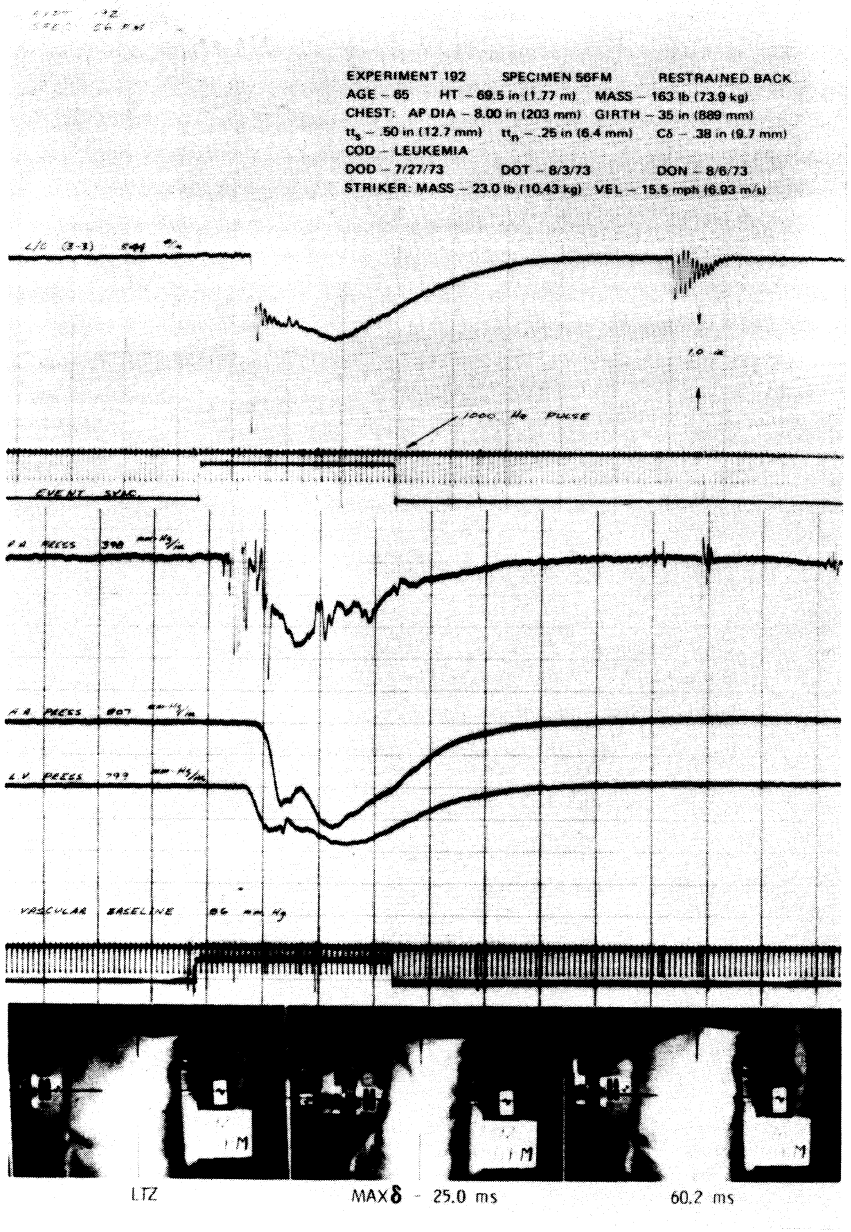

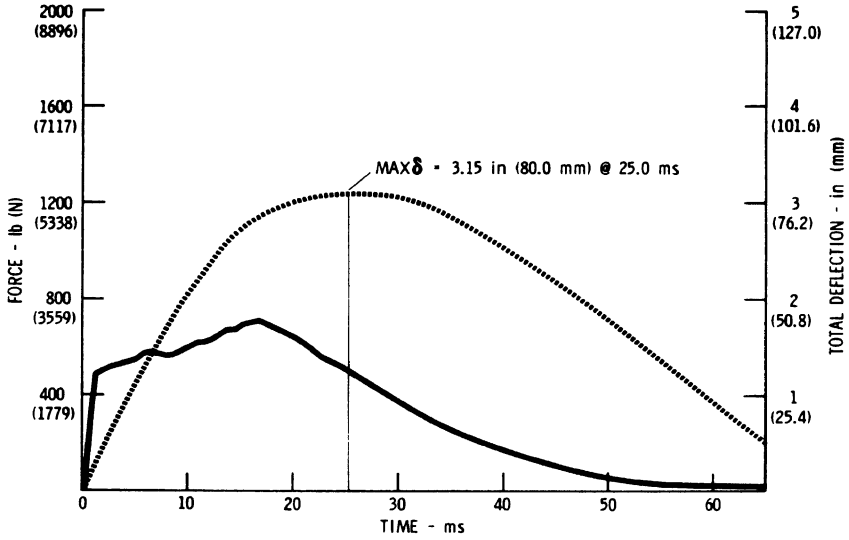

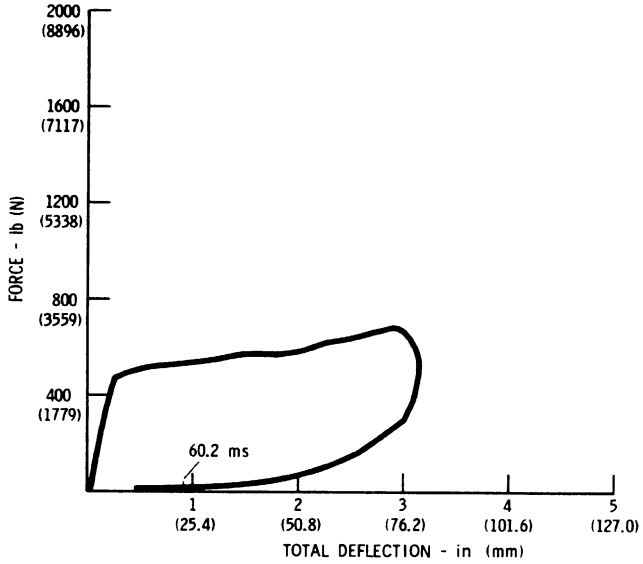

THORACO-ABDOMINAL NECROPSY

FRACTURES:
L3, L4, L5, (3 TOTAL)

NO VISCERAL DAMAGE

AIS = 2

EXPERIMENT 196 SPECIMEN 58FM RESTRAINED BACK
AGE – 68 HT – 70.5 in (1.79 m) MASS – 152 lb (68.9 kg)
CHEST: AP DIA – 9.00 in (229 mm) GIRTH – 37 in (940 mm)
tt_s – .63 in (16.0 mm) tt_n – .25 in (6.4 mm) Cδ – .50 in (12.7 mm)
COD – PNEUMONIA
DOD – 9/1/73 DOT – 9/6/73 DON – 9/10/73
STRIKER: MASS – 23.0 lb (10.43 kg) VEL – 15.1 mph (6.75 m/s)

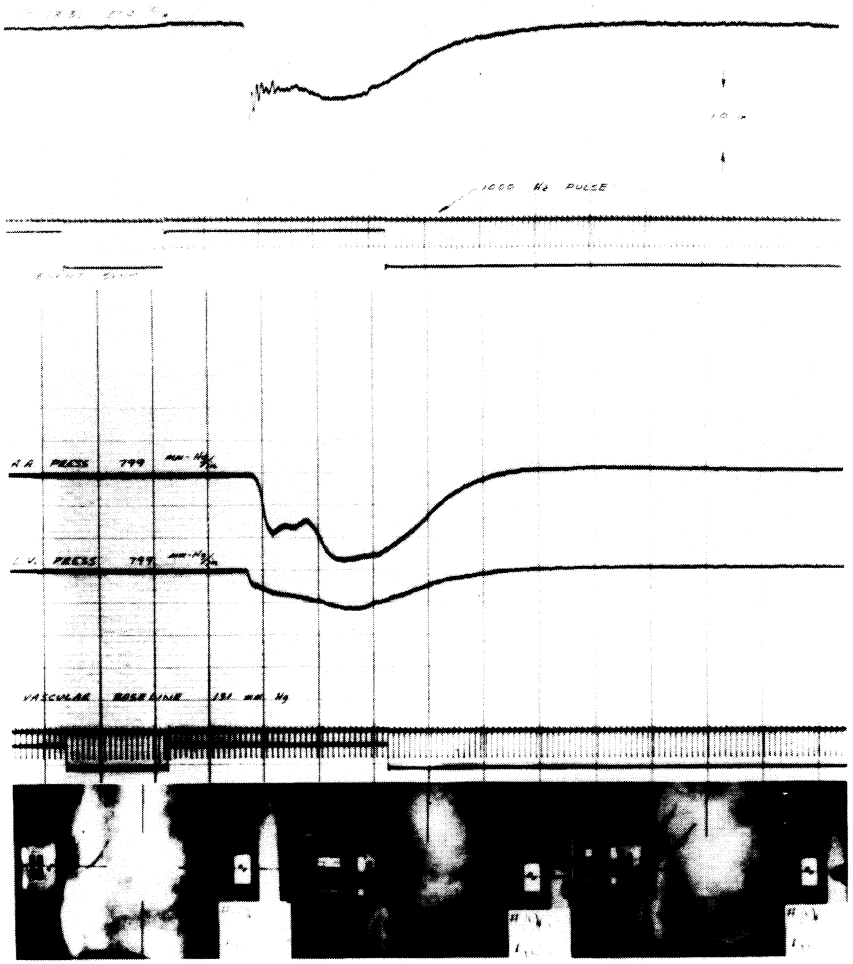

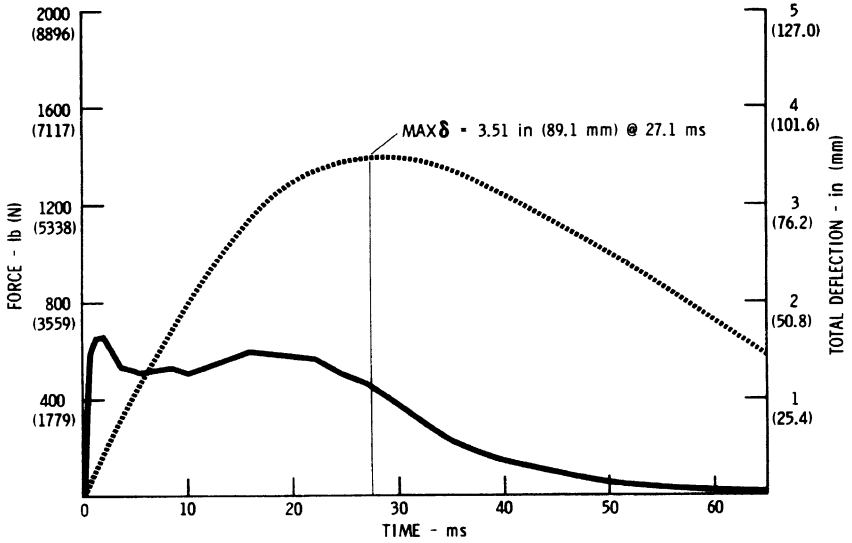

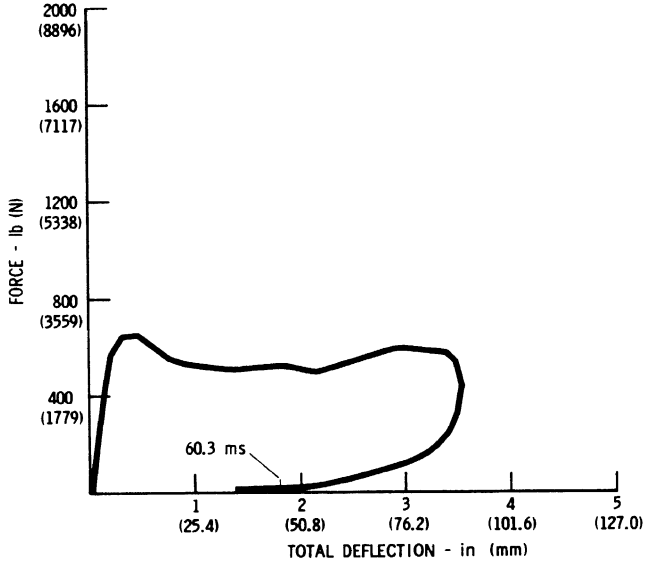

THORACO-ABDOMINAL NECROPSY

FRACTURES:
R5, L2, L3, L6, (4 TOTAL)

LACERATION ON ANTERIOR SURFACE OF LEFT LOBE OF LIVER

AIS = 3

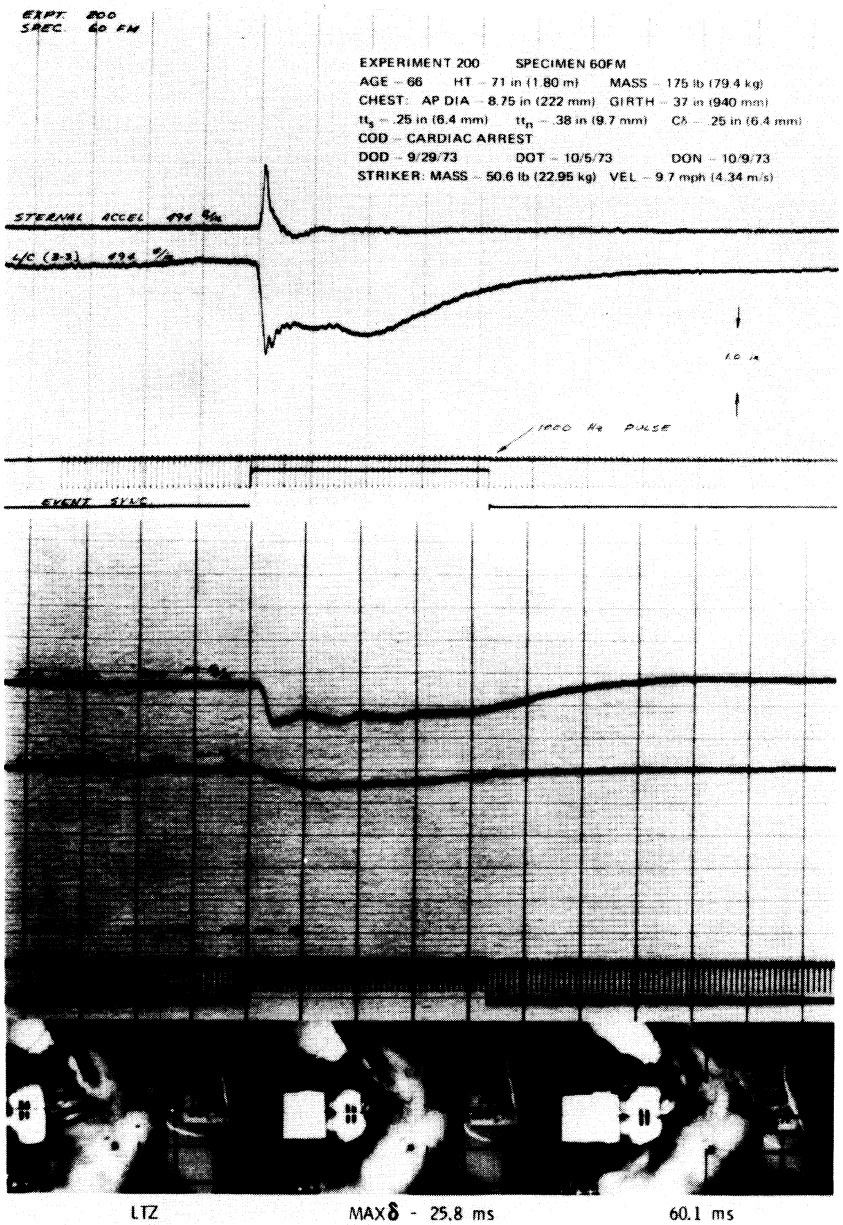

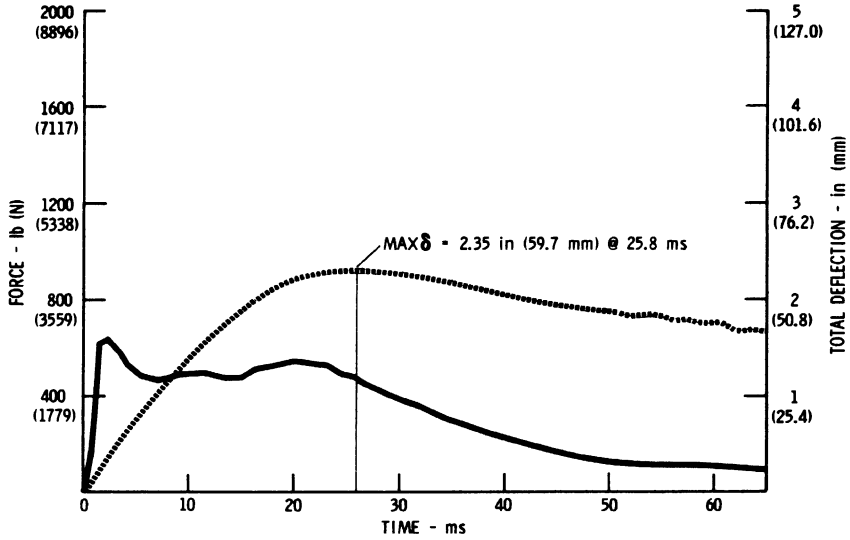

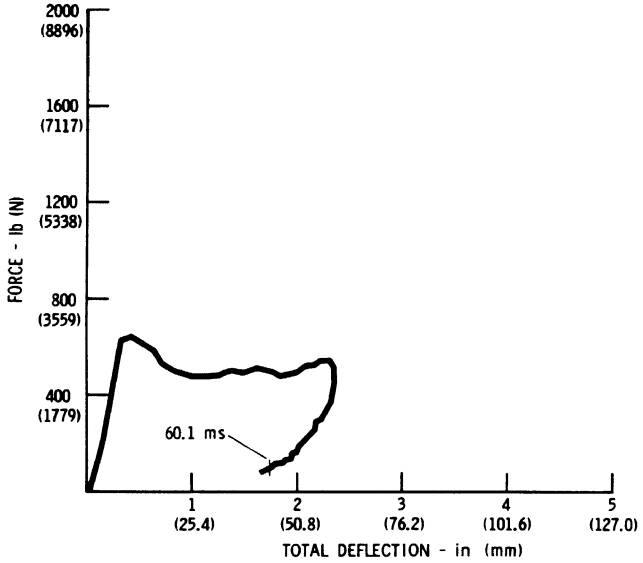

THORACO-ABDOMINAL NECROPSY

FRACTURES:
R4, R5, R6, R7, L3, L4, L5, L6, L7, (9 TOTAL)

NO VISCERAL DAMAGE

AIS = 3

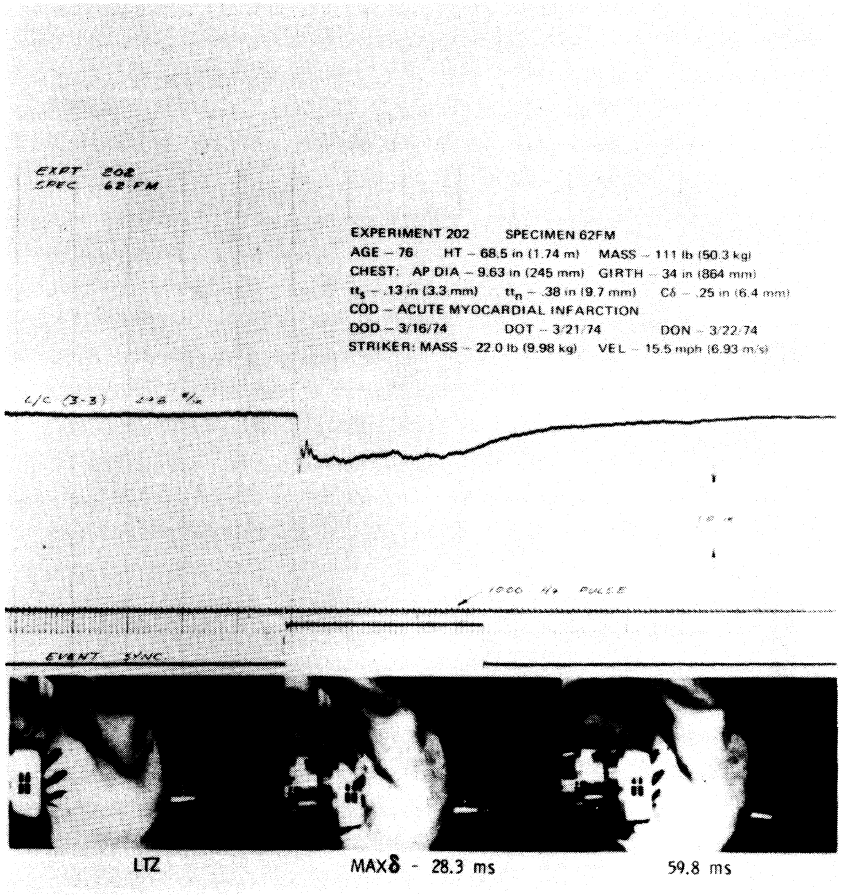

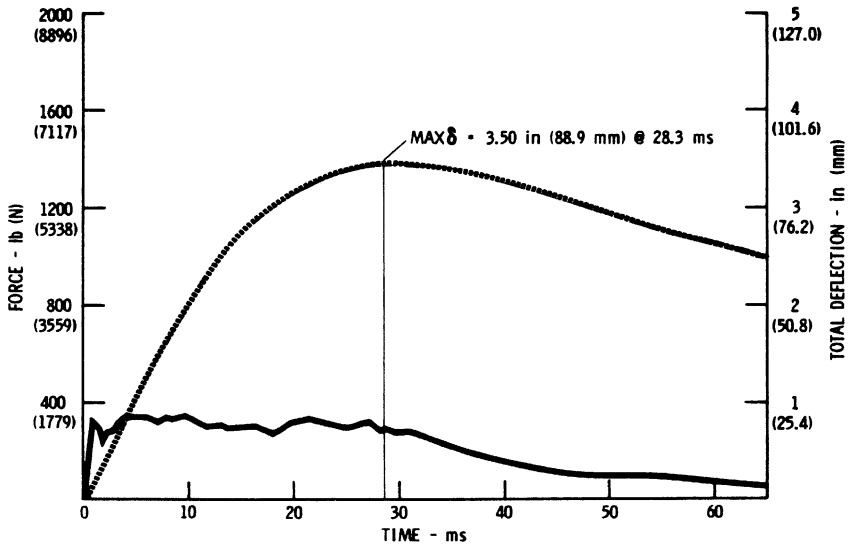

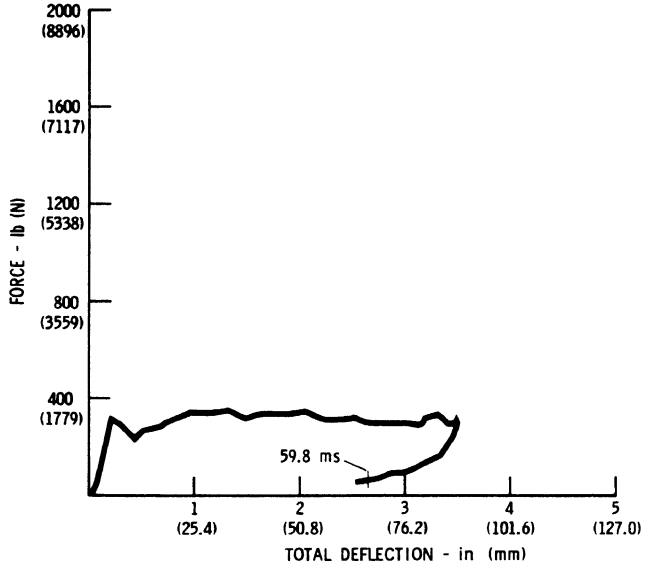

THORACO-ABDOMINAL NECROPSY

FRACTURES:
R1, R2, R3, R4, R5, L2, L3, L4, L5, (9 TOTAL)
STERNAL AT 2nd INTERCOSTAL SPACE

NO VISCERAL DAMAGE

AIS = 4

EXPERIMENT 203 SPECIMEN 63FM RIGOR
AGE – 53 HT – 72 in (1.83 m) MASS – 194 lb (88.0 kg)
CHEST: AP DIA – 8.88 in (226 mm) GIRTH – 37 in (940 mm)
tt_s – .50 in (12.7 mm) tt_n – .75 in (19.1 mm) Cδ – .50 in (12.7 mm)
COD – CARCINOMA
DOD – 4/15/74 DOT – 4/15/74 DON – 4/17/74
STRIKER: MASS – 50.7 lb (23.00 kg) VEL – 15.5 mph (6.93 m/s)

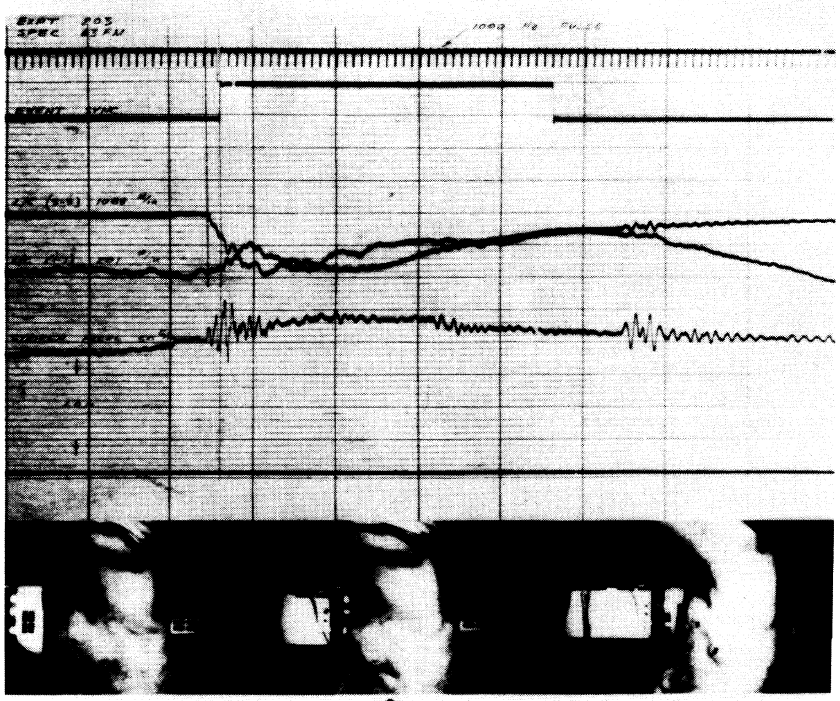

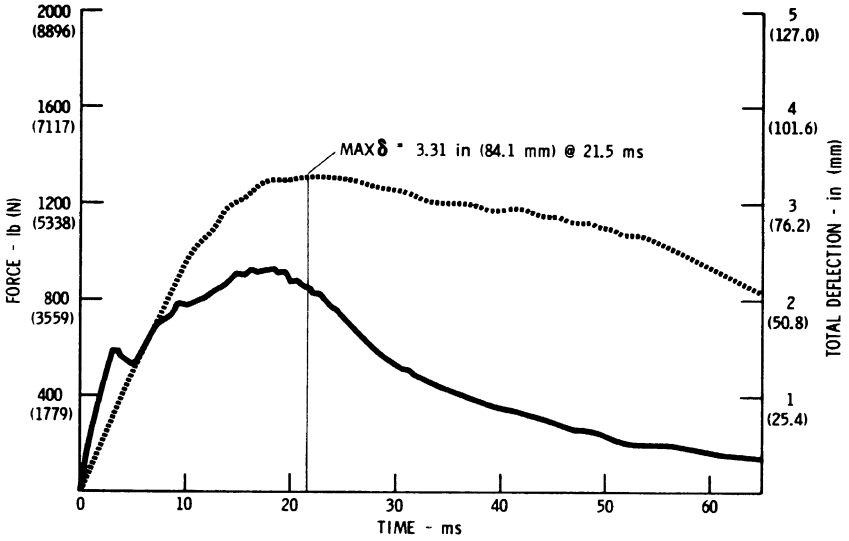

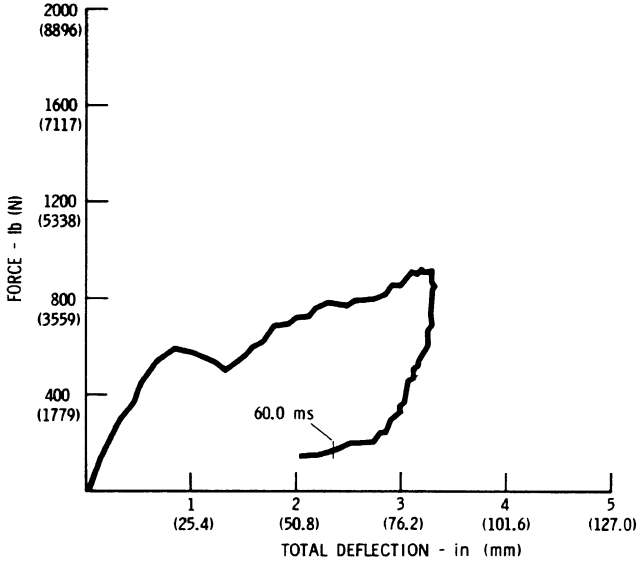

THORACO-ABDOMINAL NECROPSY

FRACTURES:
R3, R5, L2, L3, (4 TOTAL)
STERNAL AT 4th INTERCOSTAL SPACE

TRANSVERSE LACERATION OF SPLEEN, 1.18 in (30 mm) LONG AND .39 in (10 mm) FROM TIP; FIBROUS ADHESION FROM SPLENIC TIP TO ABDOMINAL WALL CONSIDERED CONTRIBUTORY TO LACERATION

AIS = 4

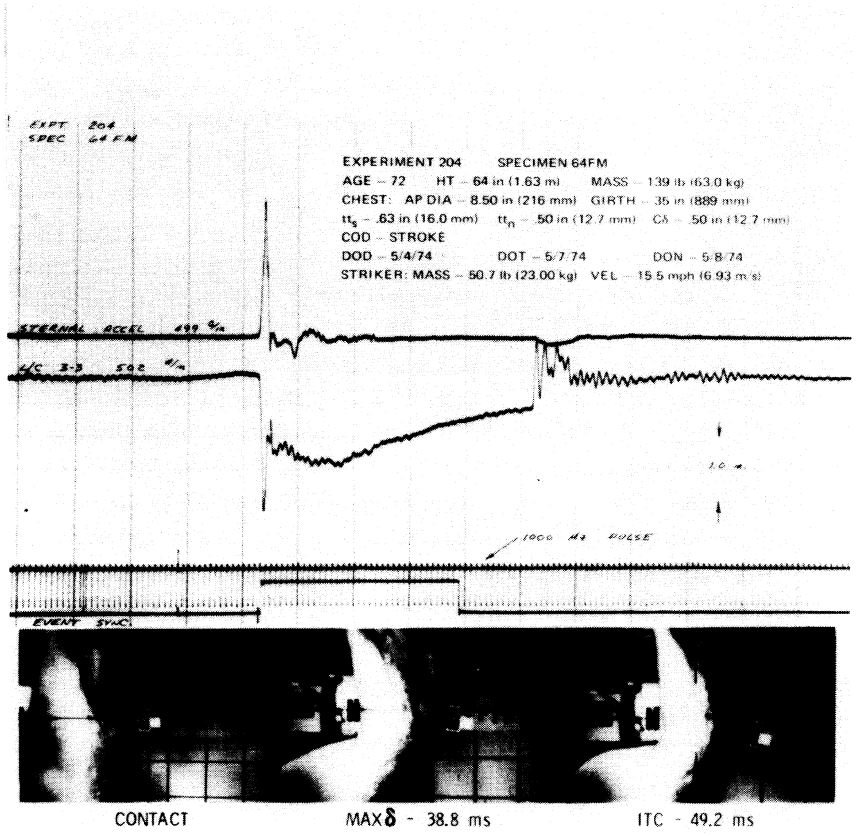

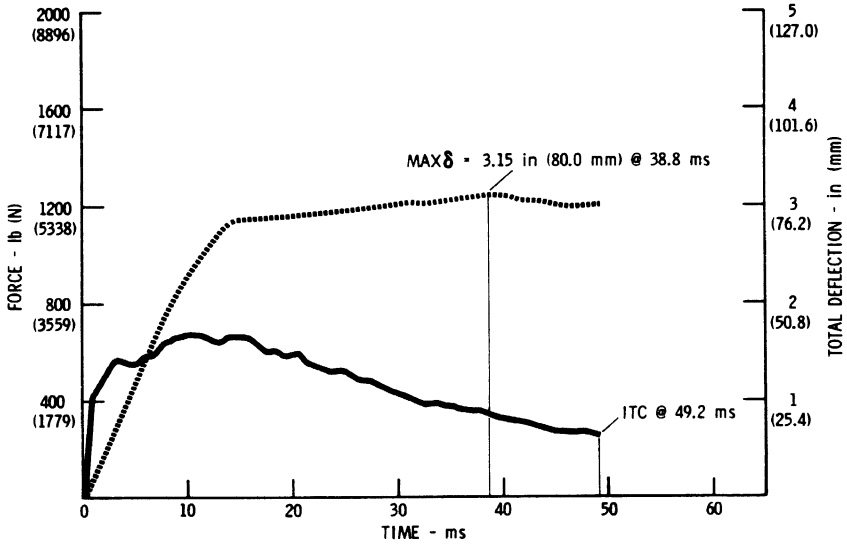

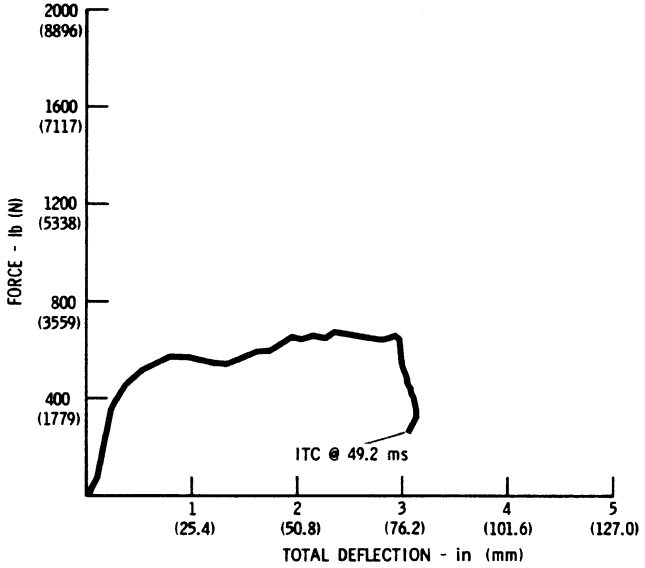

THORACO-ABDOMINAL NECROPSY

FRACTURES:
R2, R3, R4, L2, L4, L8, (6 TOTAL)

NO VISCERAL DAMAGE

AIS = 2

78029

Development of Driver/Vehicle Steering Interaction Models for Dynamic Analysis

Final Technical Report

for

The U. S. Army Tank Automotive Command

Contract Number DAAE07-85-C-R069

Report No. UMTRI-88-53

C. C. MacAdam

December 1988

UMTRI The University of Michigan Transportation Research Institute